The effect of various substrate pretreatment methods on the enzymatic degradability of a *Eucalyptus* sp. – a potential feedstock for producing fermentable sugars

A thesis submitted in fulfilment of the requirements for the degree of

DOCTOR OF PHILOSOPHY

In

BIOCHEMISTRY

At

RHODES UNIVERSITY

By

MARISKA THORESEN

June 2020

Plagiarism declaration

I, Mariska Thoresen, declare that this thesis is my own, original and unaided work. It is being submitted for the degree of Doctor of Philosophy at Rhodes University. It has not been submitted before, for any degree or examination, at any other university.

Signature 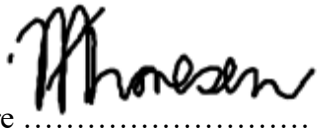

Date ……26 June 2020……..

ABSTRACT

Over the past few years, there has been a global urgency to make the transition from conventional fossil fuels to renewable energy in order to meet the world's increasing energy demands. Lignocellulosic biomass is currently at the forefront of intensive biofuel research due to its renewable nature. Lignocellulose valorisation into value added products such as bio-ethanol is a multistep process. The first step requires the biomass to go through a recalcitrance-reducing step (pretreatment), after which, enzymatic hydrolysis is required to break down the polysaccharides into simple sugars for fermentation. However, the recalcitrant structure of biomass and the low hydrolytic activities of the enzymes (glycoside hydrolases) on the substrate pose major technical and economic obstacles to the biomass conversion process. Since this process remains more expensive compared to petroleum-based fuels, lignocellulose has been intensively investigated in terms of its cost efficiency and effective decomposition.

Although improvements to this process are ongoing, with some of the first commercial facilities producing cellulosic ethanol in 2013 and 2014, there is still a deep sense of urgency to render the facilities more economically feasible. Some important factors that determine the yield and rate of enzymatic hydrolysis include the type of enzymes used, enzyme recognition with the substrate, substrate composition and crystallinity. In this context, the major focus of this study was to develop a deeper understanding of how enzymes co-operate (synergise) at a molecular level using model substrates. This knowledge was then used as a basis for understanding how these enzymes synergise on more natural, complex substrates. This study specifically focused on how different pretreatments affect the chemical and structural properties of *Eucalyptus.* Lastly, we wanted to develop an effective method of enzyme recycling as a means to reduce the high process costs in biomass saccharification.

Enhancing cellulose hydrolysis through enzyme synergy is essential for achieving higher hydrolysis rates, and numerous research efforts have focused on trying to elucidate the enzyme mechanisms required to design optimal enzyme cocktails. Despite the extensive amount of research carried out over the past few years, little is known about the enzymatic machinery underpinning the synergistic interactions between bacterial and fungal cellulases - neither is it understood why only a limited number of Cellobiohydrolases (CBHs) and Endoglucanases (EGs) exhibit synergism. Therefore, the first part of the study evaluated and compared the synergistic relationships between cellulases from different GH families and microbial sources (cross-synergism), i.e. cellobiohydrolase I (CBHI) from *Hypocrea jecorina* (Cel7A), CBHI from *Trichoderma longibrachiatum* (Cel7A), CBHI from *Clostridium stercorarium* (Cel48A), CBHII from a microbial source, CBHII from *Clostridium*

thermocellum (Cel5A), endoglucanases (EG) from *Bacillus amyloliquefaciens* (Cel5A), EG from *Thermotaga maritima* (Cel5A), EG from *Trichoderma reesei* and a β-glucosidase from *Aspergillus niger* (Novozyme 188). An aim of this study was to provide insights into how the molecular mechanisms of different GH families govern synergism. The results showed that cellulases from different GH families and microbial sources exhibit different substrate specificities, which influence their synergistic interactions with other enzymes. Based on these observations, this study agreed with evidence that not all endo- and exo-cellulase interactions are synergistic, and that the extent of synergism is dependent on the composition of the cellulase systems from various sources and their compatibility in the cellulase cocktail. From the enzymes assessed in this study, an optimal enzyme cocktail (CelMix) was formulated which was composed of Egl 68%, Cel7A 17%, Cel6A 6%, βgl 9%. This method of screening for maximal compatibility between exo- and endo-cellulases from different GH families constituted a critical step towards a better understanding of the specific interactions between the enzymes of interest and how they synergise at the molecular level. Consequently, this information may assist in the design of improved synergistic cellulose-degrading cocktails for industrial-scale biomass degradation.

The enzyme synergy studies provided a basis for the second part of this study, where it was assessed how these optimised enzyme cocktails would perform on complex substrates. It is well-known that lignocellulosic substrates are highly recalcitrant to microbial degradation, and although extensive research has been performed to understand biomass recalcitrance, the key features of biomass which hinder enzymatic hydrolysis are yet to be elucidated. In this study, we explored the effect of eight (8) different pretreatment methods on the enzymatic hydrolysis of a *Eucalyptus* sp. – a potential feedstock for biofuel production. This study was performed to increase our understanding of the relationship between biomass architecture and hydrolysis yield potential. Our results demonstrated that pretreatments induce changes at a micro- and macro-level in the cell walls of *Eucalyptus*, and that cellulose accessibility, cellulose crystallinity and the changes in the lignin S/G ratio played an important role in the enzymatic activity on the biomass. Thus, this study provided insight into important cellulose structural features related to biomass recalcitrance arising from various pretreatment methods, which may ultimately be used for the development of more efficient conversion technologies for better, more competitive bio-refineries.

Lastly, a simple and yet effective method for desorbing the adsorbed cellulases on lignocellulosic substrates was established for better understanding cellulase adsorption and desorption in order to develop an effective enzyme recycling strategy. Various reagents were assessed to determine how effective they were in promoting enzyme desorption. Tris-HCl buffer (pH 9.0; 0.05 M) was the most

effective method for promoting enzyme desorption and retained a substantial amount of hydrolytic activity after elution. However, minor activity loss was observed due to irreversible binding, which was further confirmed by SDS-PAGE analysis. With this information available, the feasibility of recovering the enzymes from the solid fraction after enzymatic hydrolysis of steam pretreated *Eucalyptus* was evaluated by two different approaches, i.e.: i) re-adsorption of the entire hydrolysed insoluble biomass fraction (no desorption) to fresh biomass (recycling approach 1 - RA1) and ii) re-adsorption of alkaline elution desorbed enzymes from hydrolysed biomass to fresh biomass (recycling approach 2 - RA2). The recycling performance of RA1 and RA2 achieved > 95% of the initial sugar liberation for three continuous rounds, whilst successfully reducing enzyme loadings by 50% and 40% for RA1 and RA2, respectively. This study presented a simple and effective pathway for improving the economic feasibility of fermentable sugar production for biofuels.

In conclusion, this study has contributed to expanding our knowledge and providing new insights into factors relating to the biomass conversion process, including enzyme synergism, pretreatment methods and enzyme recycling strategies. Ultimately, the knowledge and information gained from this study can be used as a platform for the development of more efficient conversion technologies for better, more competitive bio-refineries.

Table of Contents

Contents

Plagiarism declaration i

ABSTRACT ii

Table of Contents v

List of Figures ix

List of Tables xii

List of abbreviations and SI units xiii

Research outputs emanating from this study xvi

Acknowledgements xviii

Chapter 1: General Introduction and Literature Review 1

1.1. The bio-revolution - creating a sustainable future 1

1.2. Plant Biomass 2

1.2.1. Cellulose structure and properties 3

1.2.2. Hemicellulose 4

1.2.3. Lignin 7

1.2.4. Pectin polysaccharides 9

1.3. Enzymatic hydrolysis of plant biomass 10

1.3.1. Enzyme classification: Glycoside hydrolases 10

1.3.2. Enzymes required to degrade cellulose 11

1.3.3. Enzymes required to degrade hemicellulose 16

1.3.4. Enzymes required to degrade/modify lignin 16

1.3.5. Enzymes required to degrade pectin 17

1.4. Enzyme synergy 18

1.4.1. Degree(s) of synergy 18

1.4.2. Synergistic interactions 19

1.5.1 Pretreatment of lignocellulosic biomass 23

1.6. Addition of surfactants 27

Chapter 2: Project motivation and Research questions 31

2.1. Problem Identification 31

2.2. Research questions 32

2.3. Aims 32

2.4. Objectives 33

2.5. Outline of the Thesis 34

Chapter 3: Characterisation of Cellulolytic Enzymes 35

3.1. Introduction 35
3.2. Materials and methods 36
3.2.1. Materials 36
3.2.2. Protein determination 37
3.2.3. Bioinformatic characterisation of the cellulolytic enzymes 37
3.2.4. Enzyme characterisation studies 37
3.2.5. Optimal conditions for cellulases activity 38
3.3. Results 39
3.3.1. Protein determination 39
3.3.2. Bioinformatic characterisation of the cellulolytic enzymes 39
3.3.3. Substrate specificity determination 42
3.3.4. Optimum physico-chemical properties studies 43
3.4. Discussion 48
3.5 Conclusions 54
Chapter 4: Enzyme synergy between exo- and endo- acting cellulases on defined substrates 55
4.1. Introduction 55
4.2. Materials and methods 56
4.2.1. Materials 56
4.2.2. Synergy studies 56
4.2.3. Calculation of the degree of synergy (DS) 58
4.2.4. Data analysis 59
4.3. Results 59
4.3.1. Exo-exo synergy between CBHI (*Tl*Cel7A) and CBHII (microbial Cel6A) 59
4.3.2. Synergism between exo- and endo-glucanases 60
4.4. Discussion 68
4.5. Conclusions 74
Chapter 5: Unravelling the chemical and structural features of Eucalyptus sp. biomass pretreated by various technologies 75
5.1. Introduction 75
5.2. Materials and Methods 77
5.2.1. Enzymes 77
5.2.2. Raw material and pretreatment of *Eucalyptus* residues 77
5.2.3. Composition analysis 79
5.2.4. Pyrolysis Gas Chromatography Mass Spectrometry (Py-GC/MS) 79
5.2.5. Microscopic analysis of *Eucalyptus* samples 80

5.2.6. Fourier-transform infrared spectroscopy (FTIR) 80
5.2.7. Nuclear Magnetic Resonance (NMR) 81
5.2.8. X-Ray Diffraction (XRD) 81
5.2.9. Simons' staining 81
5.3. Results 82
5.3.1. Pretreatment of hardwood substrates 82
5.3.2. Chemical composition analysis 83
5.3.3. Py-GC/MS 85
5.3.4. Microscopy 85
5.3.5. FTIR 89
5.3.6. NMR 90
5.3.7. XRD Analysis 91
5.3.8. Simons' staining 92
5.4. Discussion 92
5.4.2. Py-GC/MS 94
5.4.3. Microscopy 95
5.4.4. FTIR analysis 97
5.4.5. NMR 98
5.4.6. XRD 99
5.4.7. Simons' staining 100
5.5. Conclusions 101
Chapter 6: Enzymatic degradation of Eucalyptus biomass by CelMix and accessory enzymes 102
6.1. Introduction 102
6.2 Methods 102
6.2.1. Enzymatic hydrolysis of *Eucalyptus* 102
6.3. Results 103
6.3.1. Enzymatic hydrolysis 103
6.4. Discussion 104
Chapter 7: Enzyme adsorption-desorption and evaluation of various cellulase recycling strategies for the enzymatic degradation of steam pretreated Eucalyptus 107
7.1. Introduction 107
7.2. Methods and materials 108
7.2.1. Enzymes and commercial substrates 108
7.2.2. *Eucalyptus* and its pretreatment via steam explosion 108
7.2.3. Preparation of isolated lignin samples 108

7.2.4. Analytical methods 109
7.2.5. Adsorption experiments 109
7.2.6. Desorption of cellulases by various surfactants and alkaline media 110
7.2.7. SDS-PAGE 110
7.2.8. Enzyme recycling strategies 111
7.3. Results 113
7.3.1. Enzyme adsorption and desorption studies 113
7.3.2. Individual cellulase activities and activity distribution profiles 116
7.3.4. Enzyme Recycling Strategies 117
7.4. Discussion 118
7.4.1. Enzyme adsorption 118
7.4.2. The effect of various reagents on cellulase desorption 120
7.4.3. Comparison between enzyme recycling systems: RA1 and RA2 121
7.5. Conclusions 123
Chapter 8: General Discussion and Future Recommendations 124
8.1. General discussion 124
8.2. Scope for future research 128
References 132
Appendices: 171
Appendix 1: Reagents list 172
Appendix 2: Standard Curves 175
Appendix 3: SDS-PAGE 179
Appendix 4A: Enzyme combinations 181
Appendix 5: Pretreatment ad substrate characterisation 184

List of Figures

Figure 1.1. The composition of lignocellulosic biomass.....2

Figure 1.2. The structure of cellulose.....4

Figure 1.3. The chemical structure of xylan…….....6

Figure 1.4. The chemical structure of: (a) mannan, (b) galactomannan, (c) glucomannan and (d) galactoglucomannan……..7

Figure 1.5. Chemical structures of phenylpropanoid monomers (A) guaiacyl (coniferyl alcohol, G) (B) syringyl (synapyl alcohol, S) and (C) *p*-hydroxyphenyl (p coumaryl alcohol, H)…….….8

Figure 1.6. Schematic illustration of the components in lignocellulosic biomass……....9

Figure 1.7. The proposed retaining (A) and inverting (B) mechanism of glycoside hydrolases……...11

Figure 1.8. Schematic representation of the enzymes required to degrade the cellulose chain……....15

Figure 1.9. The effect of pretreatment on lignocellulose.....24

Figure 3.1. The effect of temperature on cellulase activities……..…...44

Figure 3.2. The thermostability profiles of the cellulolytic enzymes……..…..45

Figure 3.3. The effect of pH on cellulase activities……..……46

Figure 4.1. Strategy for screening cellulases from different glycosyl hydrolases and microbial sources using a cellulase swapping approach to further our understanding of enzyme synergism……..…58

Figure 4.2. Synergistic degradation of Avicel by various ratios of: *Tl*Cel7A (CBHI) and (A): microbial Cel6A (CBHII) and (B): *Cs*Cel5A (CBHII)…….……59

Figure 4.3. Synergistic degradation of Avicel by various ratios of CmixA1 and: (A) *Ba*EG; (B) *Tm*EG; (C) *An*EG and (D)*Tr*EG……....61

Figure 4.4. Synergistic degradation of Avicel by various ratios of CmixA2 and: (A) *Ba*EG; (B) *Tm*EG; (C) *An*EG and (D)*Tr*EG…….……...62

Figure 4.5. Synergistic degradation of Avicel by various ratios of CmixB1 and: (A) *Ba*EG; (B) *Tm*EG; (C) *An*EG and (D)*Tr*EG……63

Figure 4.6. Synergistic degradation of Avicel by various ratios of CmixB2 and: (A) *Ba*EG; (B) *Tm*EG; (C) *An*EG and (D)*Tr*EG……..64

Figure 4.7. Synergistic degradation of Avicel by various ratios of CmixC1 and: (A) *Ba*EG; (B) *Tm*EG; (C) *An*EG and (D)*Tr*EG……...65

Figure 4.8. Synergistic degradation of Avicel by various ratios of CmixC2 and: (A) *Ba*EG; (B) *Tm*EG; (C) *An*EG and (D)*Tr*EG……..66

Figure 5.1. Visual presentation of: (A) untreated (B) sodium chlorite; (C) sodium carbonate; (D) steam explosion; (E) steam explosion + sodium chlorite; (F) steam explosion + sodium carbonate; (G) acid; (H) acid + sodium chlorite; (I) acid + sodium carbonate pretreated *Eucalptus* samples……82

Figure 5.2. Phloroglucinol staining of: (A) untreated; (B) sodium chlorite; (C) sodium carbonate; (D) steam explosion; (E) steam explosion + sodium chlorite; (F) steam explosion + sodium carbonate; (G) acid; (H) acid + sodium chlorite; (I) acid + sodium carbonate pretreated *Eucalyptus* samples……..86

Figure 5.3. SEM images of: (A) untreated *Eucalyptus*; (B) sodium chlorite; (C) sodium carbonate; (D) steam explosion; (E) steam explosion + sodium chlorite; (F) steam explosion + sodium carbonate; (G) acid; (H) acid + sodium chlorite; (I) acid + sodium carbonate pretreated samples. Bars: 20 µm, 1000x magnification……....87

Figure 5.4. Fluorescent microscopy images of: (A) untreated; (B) sodium chlorite; (C) sodium carbonate; (D) steam explosion; (E) steam explosion + sodium chlorite; (F) steam explosion + sodium carbonate; (G) acid; (H) acid + sodium chlorite; (I) acid + sodium carbonate pretreated *Eucalyptus* samples……88

Figure 5.5. FTIR images of: (A) untreated; (B) sodium chlorite; (C) sodium carbonate; (D) steam explosion; (E) steam explosion + sodium chlorite; (F) steam explosion + sodium carbonate; (G) acid; (H) acid + sodium chlorite; (I) acid + sodium carbonate pretreated *Eucalyptus* samples…….....89

Figure 5.6. NMR peak assignments for: (A) untreated; (B) sodium chlorite; (C) sodium carbonate; (D) steam explosion, steam explosion + sodium chlorite, steam explosion + sodium carbonate; acid and acid + sodium carbonate and (E) acid + sodium chlorite pretreated *Eucalyptus* samples……...90

Figure 5.7. XRD images of: (A) untreated; (B) sodium chlorite; (C) sodium carbonate; (D) steam explosion; (E) steam explosion + sodium chlorite; (F) steam explosion + sodium carbonate; (G) acid; (H) acid + sodium chlorite; (I) acid + sodium carbonate pretreated *Eucalyptus* samples……..91

Figure 5.8. Simons' staining of untreated and pretreated *Eucalyptus* samples……...……..…….92

Figure 6.1. Enzymatic hydrolysis of *Eucalyptus* by various pretreatments. (A) reducing sugars released and (B) glucose saccharification yield……..103

Figure 7.1. Schematic diagram of the two different recycling approaches investigated in this work. Approach 1 (RA1): re-adsorption of the entire un-hydrolysed insoluble solid fraction to fresh biomass and Approach 2 (RA2): enzyme desorption via alkaline elution (Tris-HCl, pH 9.0, 0.05 M) followed by re-adsorption of desorbed enzyme to fresh biomass……..…….112

Figure 7.2. Adsorption studies of CelMix to Avicel, lignin and steam pretreated *Eucalyptus* after 1-hour incubation. The Bradford assay was used to measure adsorbed enzymes. Data represent the mean value of triplicates (n=3, SD < 5%)……113

Figure 7.3. The desorption (recovery) of cellulases from Avicel, extracted lignin and steam pretreated *Eucalyptus.* (A): Precision Plus protein unstained standard; B: original CelMix (0.5 mg/mL); C, E and G: desorbed enzymes (supernatant wash) from Avicel, lignin and steam exploded *Eucalyptus*, respectively; D, F and H: solid residue (after enzyme desorption) of Avicel, lignin and steam exploded *Eucalyptus,* respectively……115

Figure 7.4. Adsorption studies of CelMix to Avicel, lignin and steam-pretreated *Eucalyptus* after 1-hour incubation. Activity (CMCase, *p*NPCase adglucosidase) assays were performed. Data represent the mean value of triplicates (n=3, SD < 5%).....116

Figure 7.5. The distribution profiles of the major cellulase enzyme activities of: (A) the complete CelMix preparation and un-adsorbed enzymes from the supernatants after 1-hour adsorption at 37°C on: (B) Avicel; (C) extracted lignin from steam pretreated *Eucalyptus* and (D) steam pretreated *Eucalyptus*...……..….117

Figure 7.6. Evaluation and comparison of the performance of two different recycling approaches (RA1 and RA2) for recycling the enzymes associated with the insoluble solid residue after the enzymatic hydrolysis of steam pretreated *Eucalyptus* (first round) (A): The effect of different fresh enzyme dosages on reducing sugar liberation (second round) for RA1 and RA2 and (B): The effect of fresh enzyme loading (50% for RA1; 60% for RA2) in the third hydrolysis cycles. Each cycle was performed for 24 hours, and fresh biomass (2%) was added to each hydrolysis cycle……...118

List of Tables

Table 1.1. An overview summary of the main enzymes required to degrade lignocellulose……..…18

Table 1.2. The advantages and disadvantages of various pretreatment methods……..…..….25

Table 1.3. Examples of various surfactants/proteins that have improved cellulase hydrolysis on different pretreated substrates……...……28

Table 1.4. The composition of different *Eucalyptus* sp. as reported by various studies……...30

Table 3.1. Protein determination of the cellulase enzymes as determined by the Bradford Assay…...39

Table 3.2. Summary of the data obtained from Uniprot and ProtParam for the cellulolytic enzymes...41

Table 3.3. Specific activities of cellulolytic enzymes on various cellulosic substrates…….……43

Table 3.4. Summary of comparison between the properties of different GH families used in this study……...…..……47

Table 4.1. Summary of the synergistic associations established between the different GH family enzymes, and the optimum ratios for each combination required for Avicel hydrolysis……..….67

Table 5.1. Chemical compositional analysis of untreated and pretreated *Eucalyptus* samples…….84

Table 5.2. Data obtained from Py-GC/MS analysis…….……..…….85

Table 7.1. The effect of various chemicals/washes on cellulase removal efficiency (%) from steam pretreated *Eucalyptus*…… 114

Table 7.2. The overall recovery of the initially adsorbed protein from lignocellulosic components after desorption using Tris-HCl (pH 9.0; 0.05 M)…….……..114

List of abbreviations and SI units

βgl - β-glucosidase

°C - degree Celsius

µg - microgram

µmol - micromole

µL - microliter

% - percentage

AA - auxiliary activity

AFM - atomic force microscopy

AIL - acid insoluble lignin

ASL - acid soluble lignin

ANOVA - analysis of variance

BC - bacterial cellulose

BCM - bacterial microcrystalline cellulose

BSA - bovine serum albumin

CBH - cellobiohydrolase

CBD - carbohydrate binding domain

CBM - carbohydrate binding module

CLEAs – cross-linked enzyme aggregates

CrI - crystallinity index

CMC - carboxymethylcellulase (endoglucanase)

DNS - 3, 5-dinitrosalicyclic acid

DP - degree of polymerisation

DS - degree of synergy

E.C. number - enzyme commission number

EG - endoglucanase

F-TIR - Fourier-transform infrared spectroscopy

g - gram

g – gravity

G - guiacyl lignin

GH - glycoside hydrolase

H - *p*-hydroxyphenyl

HG - homogalacturonan

Ha - hectare

HCl - hydrochloric acid

HPAEC – high performance anion exchange chromatography

HPLC - high performance liquid chromatography

kDa - kilodalton

LiP - lignin peroxidase

M - molar

mg - milligram

mg/ml - milligram per milliltre

mL - millilitre

mM - millimolar

MnP - manganese peroxidase

MW - molecular weight

nm - nanometer

NC-IUBMB - International Union of Biochemistry and Molecular Biology

NMR - nuclear magnetic resonance

NREL - National Renewable Energy Laboratory

PAGE - polyacrylamide gel electrophoresis

PEG - polyethylene glycol

pI - isolelectric point

*p*NPG - *p*-nitrophenol-α-D-glucopyranoside.

Py-GC/MS - pyrolysis gas chromatography mass spectroscopy

RA1 - recycling approach 1

RA2 - recycling approach 2

RBBR – Remazol Brilliant Blue R

RCF - relative centrifugal force

SD - standard deviation

SDS - sodium dodecyl sulfate

SEM - scanning electron microscopy

S - syringyl lignin

S/G - syringyl:guiacyl lignin ratio

TEM - transmission electron micrscopy

TEMED - tetramethylethylenediamine

TLC - thin layer chromatography

U - Enzymatic units - μmol of glucose produced min^{-1} in standard assay

U/mg - units per mg

v/v - volume per volume

w/v - weight per volume

XRD - X-ray Diffraction

Research outputs emanating from this study

i. Publications in peer reviewed journals and conference proceedings

Thoresen, M., Malgas, S., Pletschke, B.I. (2020). Enzyme adsorption-desorption and evaluation of various cellulase recycling strategies for steam pre-treated *Eucalyptus* enzymatic degradation. Biomass Conversion and Biorefinery. DOI: 10.1007/s13399-020-00670-9.

Malgas, S., **Thoresen, M**., van Dyk, J.S., Pletschke, B.I. (2017). Time dependence of enzyme synergism during the degradation of model and natural lignocellulosic substrates. Enzyme and Microbial Technology, 103, pp. 1-11. DOI: 10.1016/j.enzmictec.2017.04.007.

Pletschke, B.I., Malgas, S., Bhattacharya, A., Bhattacharya-Shrivastava., Clark, M.D., Mafa, M.S., Morake, S., **Thoresen, M**. (2016). Enzyme Synergism: A powerful tool for decreasing enzyme loading for efficient biomass conversion. 24th European Biomass Conference and Exhibition Proceedings, , Amsterdam, Netherlands. ISBN: 978-88-89407-165, Pages 68-82. DOI: 10.5071/24thEUBCE2016-1BO.5.4.

ii. Anticipated peer reviewed journal article publications (In preparation):

Thoresen, M., Malgas, S., Gandla, M.L., Jönsson, L.J., Sithole, B., Pletschke, B.I. The effect of chemical and structural factors on *Eucalyptus* sp. pretreated by various technologies on its enzymatic saccharification. In preparation for submisstion to Bioresource Technology.

Thoresen, M., Malgas, S., Mafa, M.S., Pletschke, B.I. Revisiting the mechanism of cellulase action: Not all endo- and exo-cellulase interactions are synergistic. In preparation for submission to Journal of Molecular Catalysis.

iii. Book chapters

Malgas, S., Mkabayi, L., Mathibe, B., **Thoresen, M**., Mafa, M., Le Roes-Hill, M., Van Zyl, W.H., Pletschke, B.I. (2020). Enzymatic path to bioconversion of lignocellulosic biomass In: Recent Advances in Bioconversion of Lignocellulose to Biofuels and Value Added Chemicals within the Biorefinery Concept. Ximenes Ferreira Filho, E., Rios de Souza Moreira, L., de Aquino Ximenes, E. and Sanchez Farinas, C. (Editors). ISBN: 978-0-12-818223-9.

iv. Conference presentations

Malgas, S., **Thoresen, M.,** Pletschke, B.I. An evaluation on the effects on the non-catalytic galactomannan binding affinity of β-mannosidases on their activity with a mannanase during

galactomannan hydrolysis. South African Society of Microbiology, 19th Biennial Congress 2016; Coastlands, Umhlanga, South Africa (Oral presentation).

Thoresen, M., Malgas, S., Chandra, R., Van Dyk, J.S., Saddler, J.N Pletschke, B.I. The effect of pretreatment on enzyme synergism between various lignocellulolytic enzymes on hardwoods - comparative evaluation of *Populus, Eucalyptus* and *Acacia* spp. as potential feedstocks for sugar release. 38th Symposiumm in Biotechnology for Fuels and Chemicals 2016; Hilton Camden Yards, Baltimore, MD, USA. (Oral presentation).

Acknowledgements

Successful completion of this project is the outcome of consistent guidance and assistance from many people, faculty and friends, and I am extremely fortunate to have got these all along the completion of this thesis.

I owe my profound gratitude and respect to my supervisor, Prof. B.I. Pletschke for his invaluable academic support, professional guidance and constant encouragement during the completion of this project. I would also like to deeply thank my co-supervisor, Dr. Samkelo Malgas for his selfless help, constructive advice and for being a source of inspiration and motivation. Their presence and assistance were fundamental in overcoming the struggles and issues that emerged throughout this project.

I place on record my sincere gratitude to Dr. B. Wilhelmi, Head Department of Biochemistry and Microbiology and Dr. Mpho Mafa for their constant encouragement.

To my parents; Ronnie and Ronel, and sister Yolandi, I cannot express how thankful I am for your love, patience, support and encouragement during this time. Thank you for always believing in me and reminding me that I could do this, especially when I felt like giving up so many times.

Chapter 1: General Introduction and Literature Review

1.1. The bio-revolution - creating a sustainable future

Fossil fuel (oil, coal and natural gas) refineries are the major sources of worldwide energy carriers, specifically in the transport sector (Balan, 2014; Cherubini, 2010). However, the on-going price increases in fossil resources, uncertainty regarding their availability and severe environmental effects, particularly greenhouse gas emissions, have become a major global concern (Balan, 2014; Cherubini, 2010). Therefore, developing clean and renewable alternatives that have the potential to mitigate climate change and reduce the consumption of fossil fuels has become a world-wide priority (De Bhowmick *et al.,* 2018; Vandenbrink *et al.,* 2012). Curent studies attempt to utilise non-conventional materials that can meet the criteria of being environmentally and economically sustainable (Anwar *et al.,* 2014; De Bhowmick *et al.,* 2018). Through technological innovation, particularly in the field of renewable energy, it is possible to enable this energy transition and help address the need for energy expansion in the future (Cherubini, 2010; Gielen *et al.,* 2019). According to Gielen *et al.* (2019), renewable energy can supply approximately 66% of the total global energy demand that is required between now and 2050. It has been stated that the cellulosic ethanol market will reach 27 billion gallons/year, this year (2020) (Adsul *et al.,* 2020; Valdivia *et al.,* 2016).

In this regard, lignocellulosic biomass, the most abundant carbon resource in nature, has emerged as a potential alternative for the sustainable production of renewable and clean energy, due to its abundance and feasibility (Anwar *et al.,* 2014; Srivastava *et al.,* 2019; De Bhowmick *et al.,* 2019). Herein, the concept of the biorefinery was created, whereby different classes of biofuels can be produced from various biomass feedstocks through jointly applied conversion technologies (Balan, 2014; Chandel *et al.,* 2018; Cherubini *et al.,* 2009). Sucrose and starch from sugarcane and maize (first generation biofuels), respectively, are currently the major sources for bio-ethanol production (Madadi *et al.,* 2017; Valentine *et al.,* 2012). Although first-generation ethanol from these resources has a lower impact on global climate change compared to petroleum-based fuels, there has been considerable debate about the food vs fuel dilemma; i.e. its competition with food production and its negative environmental impact (Kluts *et al.,* 2017; Kumar and Sharma, 2017; Valentine *et al.,* 2012). For this reason, attention has turned towards utilising lignocellulosic substrates (second-generation biofuels) in the form of forest residues, agricultural residues, dedicated energy crops, and municipal solid waste (Cherubini *et al.,* 2009; Madadi *et al.,* 2017; Sims *et al*., 2010). The dry mass of lignocellulosic biomass is composed of approximately 75% polysaccharides that can subsequently be broken down into fermentable sugars, which can then further be converted into bioethanol (Bayer *et al.,* 2007; Lynd *et al.,* 2002).

Although utilising lignocellulosic substrates for the commercial production of biofuels is considered an attractive option for creating a sustainable bioeconomy, success at an industrial level is yet to be achieved (Ahorsu *et al.,* 2018; Brennan and Owende, 2010). This is related to the recalcitrant structure of biomass, high operational costs, technical process immaturity and scale-up challenges (Chandel *et al.,* 2018; Van Zyl *et al.,* 2007). Therefore, in order to be sustainable and cost-competitive compared to conventional fuels, further research efforts are required to improve the efficiency of the biofuel production process (De Bhowmick *et al.,* 2018; Howard *et al.,* 2002).

1.2. Plant Biomass

The major structural constituents of lignocellulose include cellulose, hemicellulose and lignin, which are strongly bonded by non-covalent linkages (Figure 1.1) (Rongpipi *et al.,* 2019; Wang *et al.,* 2013). Minor quantities of pectin, proteins and ash may also be present (Gandolfi *et al.,* 2013; Rongpipi *et al.,* 2019). The composition of lignocellulosic biomass is generally made up of 30-50% cellulose, 20-30% hemicellulose and 10-25% lignin, but this may vary depending on the type of species, i.e. depending on whether it is derived from hardwood or softwood and/or grasses (Anwar *et al.,* 2014; Malgas *et al.,* 2020). All the aforementioned components of lignocellulosic biomass contribute to its mechanical recalcitrance and chemical durability (Madaj *et al.,* 2017; Shahzadi *et al.,* 2014).

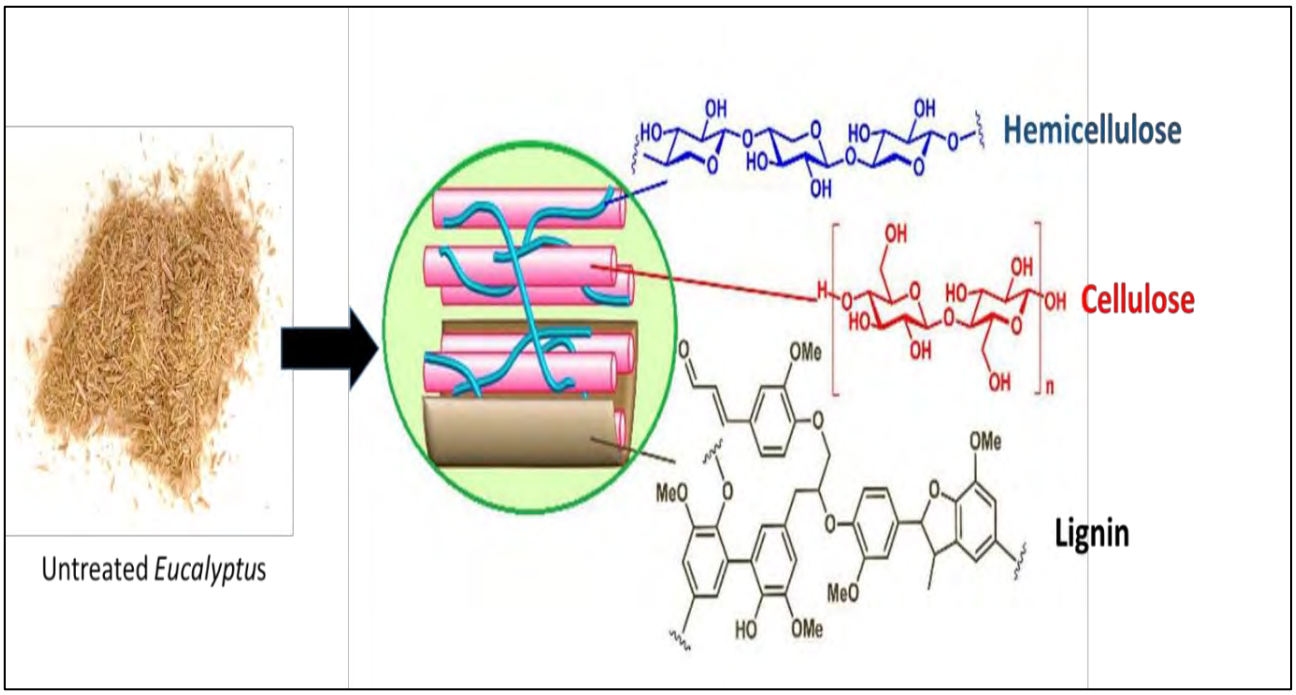

Figure 1.1. The composition of lignocellulosic biomass. Lignocellulose is composed of three major components: cellulose, (40-50%), hemicellulose (20-30%) and lignin (10-25%) (Adapted from Abo *et al.,* 2019).

1.2.1. Cellulose structure and properties

Cellulose, the most abundant carbon resource on earth, is the main constituent of lignocelluloses, making up approximately 30-50% of the total dry substance in most wood species (Kumar and Sharma, 2017; Malgas *et al.,* 2020). Although it is predominantly found in plant cell walls, it can also be produced by some animals (tunicates) and microorganisms (fungi and bacteria) (Jalak *et al.,* 2012; Lynd *et al.,* 2002).

Cellulose is a homo-polysaccharide composed of parallel and unbranched β-1,4-β-D-glucopyranosyl units (Figure 1.2) (Madadi *et al.,* 2017; Rongpipi *et al.,* 2019). Due to this linkage, the disaccharide cellobiose is the repeating unit for cellulose chains, whose degree of polymerisation (DP) ranges from 500 to 15 000 glucose molecules, depending on the cellulose source (Bayer *et al.*, 1998; Lynd *et al.,* 2002; George and Sabapathi, 2015). Because of its linear structure, cellulose is thought to be structurally simple, however, the arrangement of cellulose is typically in the form of tightly packed polysaccharide chains that form insoluble crystalline regions, interspersed with amorphous regions (i.e. paracrystalline in nature) (Anwar *et al.,* 2014; Bregado *et al.,* 2019; Malgas *et al.,* 2020). These tightly packed fibres, commonly known as microfibrils (rod-like structures) are stabilised by strong inter- and intra-molecular hydrogen bonds and van der Waals forces, which further aggregate into macrofibrils that form the framework of the cellulose fibre (Andlar *et al.,* 2018; Cocinero *et al.,* 2009; George and Sabapthi, 2015). Due to strong intermolecular interactions between polymer chains, cellulose is significantly more challenging to depolymerise compared to starch, which is a more accessible polymer of glucose that is utilised in the first-generation biofuels process (Horn *et al.,* 2012; Jørgensen *et al*., 2007).

Cellulose can be found in different crystalline forms (polymorphs), which differ in their physical and chemical characteristics (Moon *et al.,* 2011; George and Sabapathi, 2015). To date, seven crystal polymorphs have been identified for cellulose, which are designated as Iα, Iβ, II, IIII, IIIII, IVI, and IVII (Hindi, 2017; Simon *et al.,* 1988). Cellulose I and II are found in nature, of which cellulose I is the most abundant crystalline form (Horn *et al.,* 2012; Lee *et al*., 1997; Moon *et al.,* 2011). Cellulose I is further divided into allomorphs Iα (triclinic, less compact regions) and Iβ (monoclinic, compact regions) (Hindi, 2017; Miao and Hamad, 2019). Cellulose Iα is produced by microbial and algal sources and has one cellobiose residue per unit cell, whereas cellulose Iβ is the major allomorph in higher plant species and has two cellobiose residues per unit cell (Bregado *et al.,* 2019; Miao and Hamad, 2019). Two commercial examples of cellulose Iβ include medium length cellulose powder (C6288) and Avicel PH-101 from Sigma-Aldrich. Through various pretreatment methods, the structure

of type I polymorphs undergoes modification, forming cellulose II - IV. Carboxymethyl cellulose is a commercial example of modified cellulose, which possesses a carboxymethyl group on either the C-2 or the C-3 carbon.

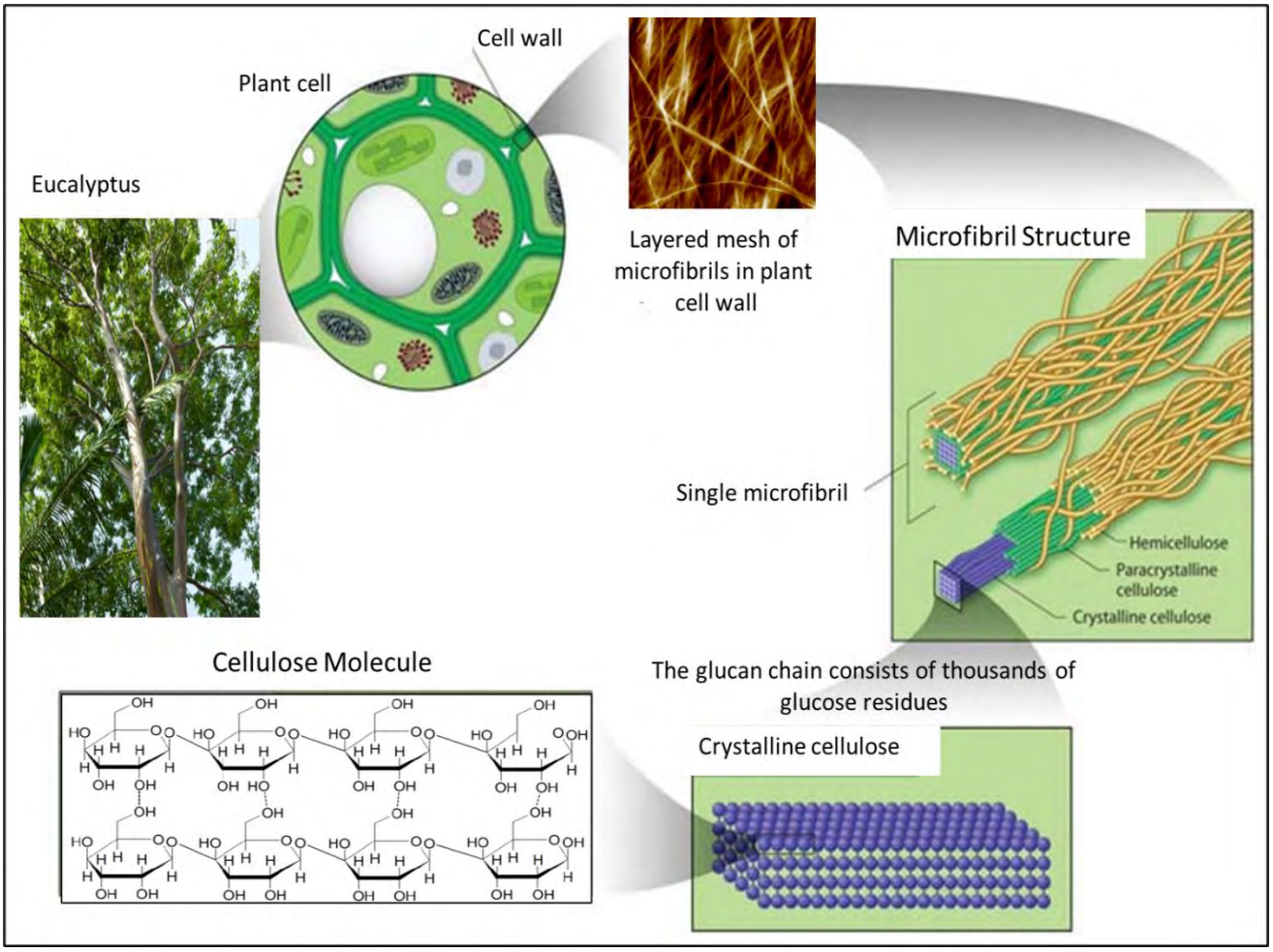

Figure 1.2. The structure of cellulose. Long chains of 1, 4-glycosidic linked glucose monomers pack in a parallel arrangement to form microfibrils. The microfibrils aggregate further to form macrofibrils, which form the framework for the cellulose fibre (Adapted from Quiroz-Castañeda and Folch-Mallol, 2013).

1.2.2. Hemicellulose

After cellulose, hemicellulose is the second most abundant terrestrial polysaccharide that accounts for 20-30% of lignocelluloses by dry weight (Anwar *et al.,* 2014; Shahzadi *et al.,* 2014). Hemicellulose is less crystalline than cellulose because its polymers are branched and are much shorter than those of cellulose (Zoghlami and Paës, 2019). Consequently, fewer hydrogen bonds are formed, which makes it easier to hydrolyse hemicellulose (as it has a weaker resistance to degradation) compared to cellulose (Sanchez, 2009; Zoghlami and Paës, 2019). Hemicellulose is said to be intertwined into the cellulose

structure and provides a connection between lignin and the cellulose fibres (Horn *et al*., 2012; Van Dyk and Pletschke, 2012). Hemicelluloses are generally branched, short lateral chain polysaccharides, with an average DP ranging from 80-200 (Andlar *et al.,* 2018; Sanchez*,* 2009). These polysaccharides can be classified as homopolymers (consisting of a single sugar repeat in their backbones) or most commonly, heteropolymers (consisting of more than one sugar in their backbones). A wide variety of building blocks can form the polysaccharide backbone, including pentoses (xylose and arabinose), hexoses (D-glucose, D-mannose and D-galactose) and uronic acids (4-O-methyl-glucuronic and galacturonic acids) (Andlar *et al.,* 2018; Madadi *et al.,* 2017). Generally, hemicelluloses are grouped according to various subclasses: (a) unbranched chains such as β-(1,4)-linked xylans or mannans; (b) helical chains such as (1,3)-linked xylans; (c) branched chains such as β-(1,4)-linked galactoglucomannans; and (d) pectin substances such as polyrhamnogalacturonans (Horn *et al*., 2012; Mohanram *et al.,* 2013; Van Dyk and Pletschke, 2012). Some hemicelluloses, particularly heteroxylans, also show a considerable degree of acetylation (Pawar *et al.,* 2017; Shahzadi *et al.,* 2014). According to Pan *et al.* (2005) and Pawar *et al.* (2017), acetyl groups can contribute to biomass recalcitrance by acting as a "protective layer" to prevent degradation by: i) changing surface hydrophobicity; ii) decreasing cellulose accessibility and iii) inhibiting productive binding of hydrolytic enzymes.

The two major hemicelluloses include xylan (the main component in hardwood and agricultural plants) and mannan (the main component in softwoods, plant seeds and fruits), which will now be discussed in further detail (Moreira and Filho, 2008; Yamabhai *et al*., 2014).

1.2.2.1. Xylan

Xylan is the predominant hemicellulose found in most plant cell walls, generally constituting 30% of the total plant biomass (Chakdar *et al.,* 2016; Zhang *et al.,* 2011). Xylan forms an overlaying sheath in the plant cell wall by forming hydrogen and covalent bonds with cellulose and lignin, respectively (Zeng *et al.,* 2017). Thus, it plays a major structural role in plants, contributing immensely to biomass recalcitrance (Beg *et al.,* 2001; Zeng *et al.,* 2017). Xylan is composed of branched β-1,4-linked D-xylopyranosyl residues which are modified by various substituents in their backbone (Beg *et al.,* 200; Zhang *et al*., 2011). The composition of the linkages of the side chains determines the specific type of xylan (Figure 1.3).

These substituted residues can be either: i) α-1,2-linked α-D-glucuronic acid or 4-O-methyl-α-D -glucuronic acid, which are predominantly found in hardwoods (such as beechwood or willow); or ii) α-1, 2- and α-1, 3-linked L-arabinoses, which are predominantly found in softwoods (such as spruce,

douglas fir and pine) (Sunna and Antranikian, 1997; Wagschal *et al.*, 2009). Acetylation at the C-2 or C-3 position may also occur, but this is predominantly found in hardwoods (Pawar *et al.,* 2017; Zhang *et al.*, 2011).

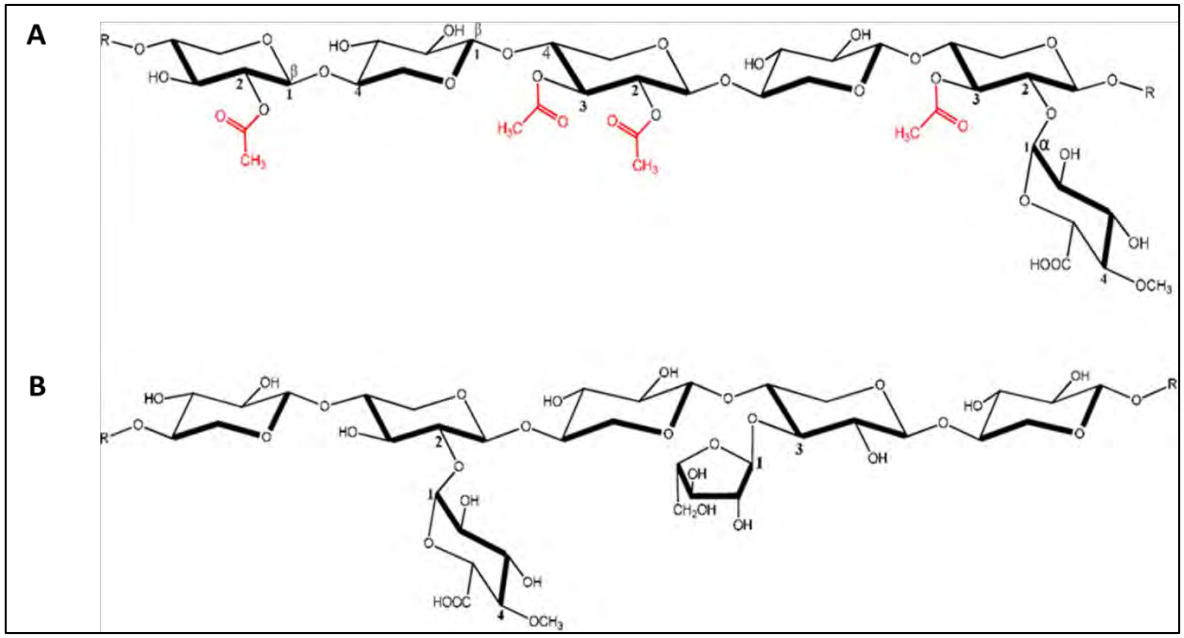

Figure 1.3. Representative structure of: (A) hardwood glucuronoxylan and (B) softwood arabinoglucuronoxylan (Adapted from Jansson, 2013).

1.2.2.2. Mannan and mannan derivatives

In addition to xylan, mannan is the other major hemicellulose polysaccharide (Moreira and Filho, 2008; Shahzadi *et al.,* 2014). The structure of mannan is analogous to cellulose, comprising of a linear polysaccharide composed of β-1,4-linked D-mannopyranose residues (which can sometimes be acetylated) (Malgas *et al.,* 2015; Moreira and Filho, 2008). However, mannan is only found in specific plants, particularly in softwoods and in endosperm seeds (Malgas *et al.*, 2015; Van Zyl *et al.,* 2010). Mannans may also exist as galactomannans, with the backbone composed of mannan residues; or glucomannans (hardwood) with the backbone composed of glucose and mannan residues to varying degrees (Moreira and Filho, 2008; Petkowicz *et al.*, 2001). The chains may be substituted with α-D-galactosyl residues, therefore, glucomannans (in hardwood) can, in turn, give rise to galactoglucomannans (in softwood) (Malgas *et al.*, 2015; Yamabhai *et al.*, 2014). The structure of mannans is shown in Figure 1.4 below.

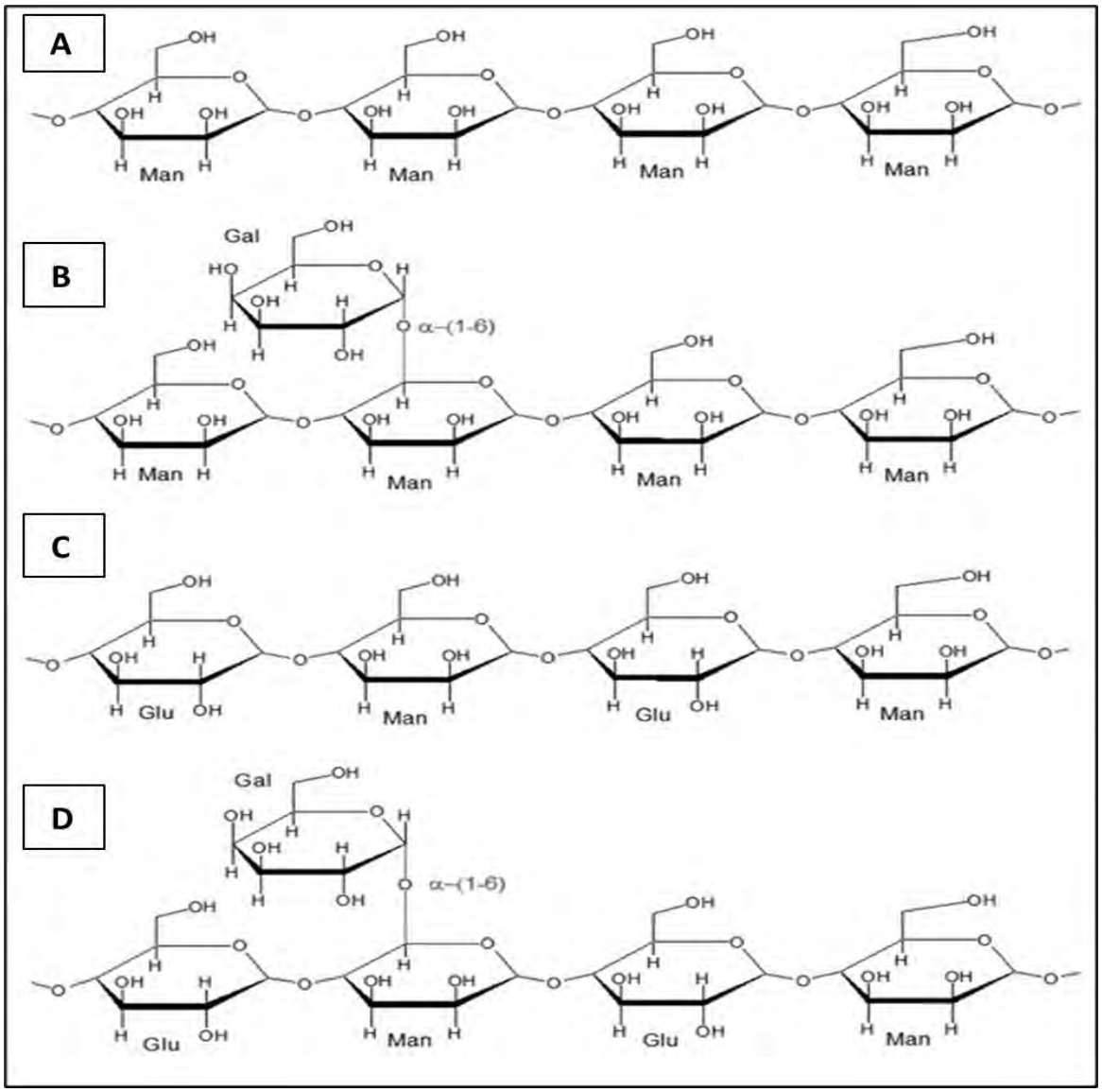

Figure 1.4. The chemical structure of: (a) mannan, (b) galactomannan, (c) glucomannan and (d) galactoglucomannan) (Adapted from Cruz, 2013).

1.2.3. Lignin

Lignin is the third major polymer making up 10-25% of the structural components in biomass (Madadi *et al.,* 2017; Mohanram *et al.,* 2013; Shahadzi *et al.,* 2014). Lignin is a hydrophobic, complex three-dimensional structure, made up of different phenylpropane units (produced through oxidative coupling) which create a protective sheath around the polysaccharides via various ester and ether linkages (Hendriks, 2009; Varnai *et al.,* 2011; Madadi *et al.,* 2017). Its primary role is to provide mechanical strength to the plant and it is therefore considered a primary source of biomass recalcitrance (Andlar *et al.,* 2018; Madadi *et al.,* 2017; Zeng *et al.,* 2017). There is extensive evidence implicating lignin as a major obstruction to achieving high cellulase efficiency in pretreated biomass

(Jørgensen *et al.,* 2007; Sammond *et al.,* 2014). Although its exact mechanism of action has not been fully elucidated, it has been proposed that lignin physically blocks the accessibility of cellulases to the cellulosic fibres, and that cellulases can unproductively bind to lignin, resulting in reduced cellulase efficiencies (Donohoe *et al.,* 2008; Li *et al.,* 2017).

Lignin is predominantly composed of three phenylpropanoids (monolignols) that contribute to lignin polymerisation (Andlar *et al.,* 2018; Karp *et al.*, 2013; Ramos, 2003). These include: i) *p*-coumaryl alcohol (precursor of *p*-hydroxyphenyl or H units, ii) sinapyl alcohol (precursor of syringyl or S units) and iii) coniferyl alcohol (precursor of guaiacyl or G units) (Figure 1.5) (Anderson *et al.,* 2019; Karp *et al.,* 2013). The relative abundance and arrangement of monolignols may vary, depending on the plant species (Ramos, 2003; Ragauskas *et al.,* 2013). Generally, small fractions of H units are found in both hard- and soft-woods, and in larger fractions in grasses (Rencoret *et al.,* 2011). G lignin is predominantly found in softwoods (gymnosperms or coniferous woods), whereas hardwoods (angiosperms or deciduous woods) contain a combination of both guaiacyl and syringyl lignin. All three monolignols are found in grasses (Horn *et al.*, 2012; Rencoret *et al.*. 2011).

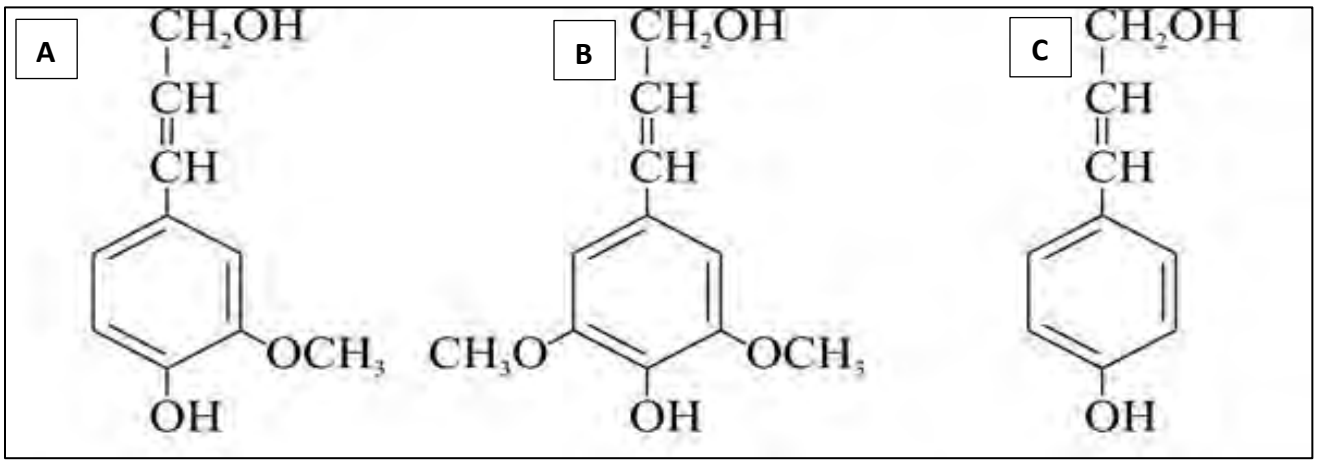

Figure 1.5. Chemical structures of phenylpropanoid monomers (A) guaiacyl (coniferyl alcohol, G) (B) syringyl (synapyl alcohol, S) and (C) p-hydroxyphenyl (p-coumaryl alcohol, H). (Adapted from Weng *et al.,* 2013).

Lignin is also composed of different types of inter-unit linkages (β-O-4; β-β; β-1; β-5; 4-O-5 and 5-5) depending on the biological origins of the wood (Gaudix-Montero and Sankar, 2018). The β-O-4 (β-aryl ether) (most common inter-linkage) is easier to cleave than β-5, β-β, 5-5, 4-O-5, and β-1 inter-linkages (Gaudix-Montero and Sankar, 2018). According to Ralph *et al.* (2004), softwoods contain more β-β, 5-5, and 4-O-5 linkages compared to hardwoods (more S units). Thus, softwood lignins are easier to depolymerise than hardwood lignins.

1.2.4. Pectin polysaccharides

Pectin is considered to be the most complex polysaccharide found in nature and plays an important role in the formation of higher plant cell walls (Malgas, 2017; Van Dyk and Pletschke, 2012; Voragen *et al.,* 2009). Pectins make up approximately 35% of the primary cell wall in dicotyledonous plants and nongraminaceous (nongrass) monocots, 2-10% of the primary walls in grasses and up to 5% of wood tissues (Malgas *et al.,* 2020; Wolf *et al.,* 2009). There are 5 different classes of pectin polysaccharides, which include: i) homogalacturonan (HG); ii) xylogalacturonan; iii) apiogalacturonan and iv) rhamnogalacturonan I and II (Malgas *et al.,* 2020; Pedrolli *et al.,* 2009; Wolf *et al.,* 2009). The major component in pectin is HG, which constitutes 60% of the pectin (depending on the source) (Malgas, 2017). Its structure is composed of a linear backbone of α-1,4-linked galactoronic acid residues, with a DP of approximately 100 units. Acetylation generally occurs at C-2 and/or C-3, whereas methyl-esterfication occurs at C-6 of the galactoronic acid residues (Pedrolli *et al.,* 2009; Wolf *et al.,* 2009)

An overview of the three main components in lignocellulose biomass (cellulose, hemicellulose and lignin) and all its components is provided in Figure. 1.6.

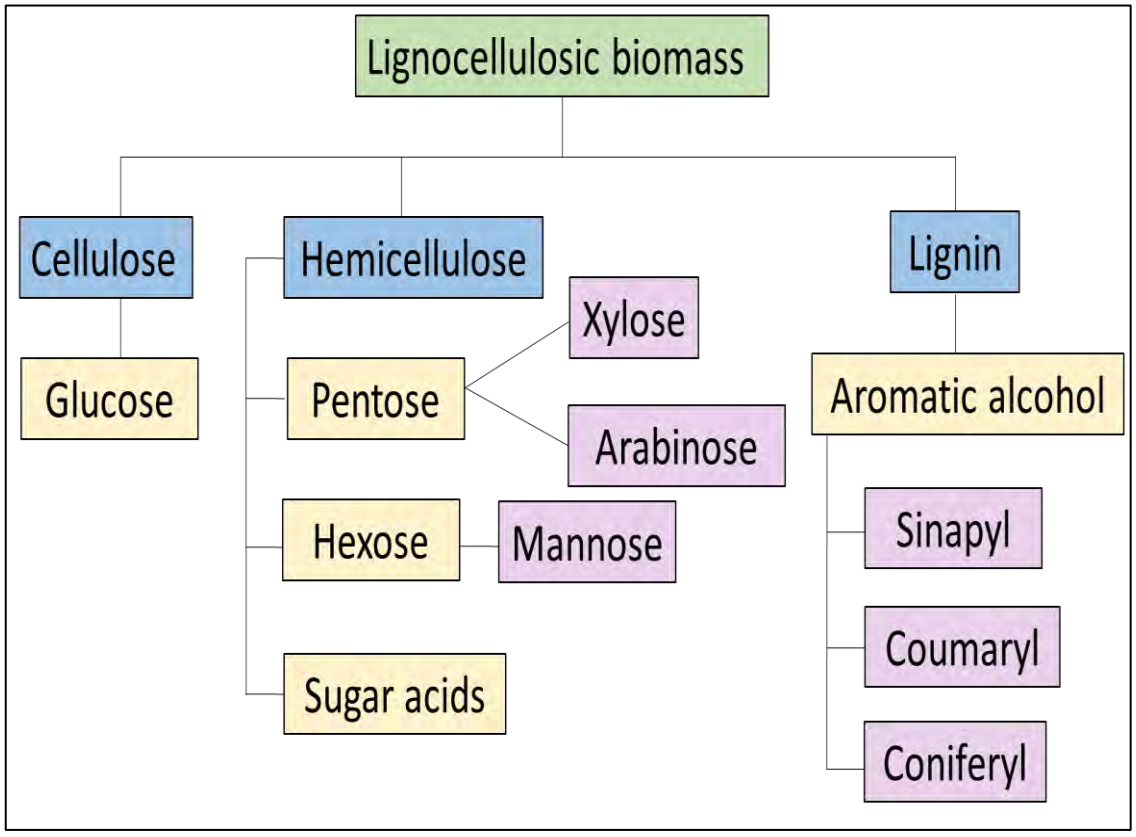

Figure 1.6. Schematic illustration of the components in lignocellulosic biomass (Adapted from Sajith *et al.,* 2016).

1.3. Enzymatic hydrolysis of plant biomass

1.3.1. Enzyme classification: Glycoside hydrolases

Cellulose is a heterogenous substrate which requires a consortium of enzymes to degrade it into its simple sugars (Den Haan *et al.,* 2013; Ganner *et al.,* 2012; Teeri *et al.,* 1997). These enzymes are known as glycoside hydrolases (GH), and are commonly produced by wood-degrading fungi and bacteria (Gupta *et al.,* 2019). These enzymes are classified as EC 3.2.1, and are responsible for catalysing the glycolytic cleavage of *O*-glycosidic bonds (Leis e*t al.,* 2017; Lynd *et al.,* 2002). An amino acid sequence-based classification system has been adapted for GHs, whereby 164 (to date – June 2020) different families have been identified based on protein sequences and folding similarities (http:/www.cazy.org/Glycoside-Hydrolases.html). Recent progress in glycosidase sequence analysis and 3D structure comparison has allowed the proposal of an extended GH hierarchical classification (Naumhoff, 2011). Consequently, these enzymes have been further grouped into clans (currently 14 clans), based on their three-dimensional (3D) structural similarities (Naumhoff, 2011). Enzymes that belong to the same clan have a common evolutionary origin of their genes, share similar functional characteristics (anomeric configuration of the glycosidic bonds cleaved, active site residues, possible substrates) and the molecular mechanism of their catalysed reaction (inverting/retaining) (Henrissat, 1991; Viborg *et al.,* 2019; Naumhoff, 2011). All of this information can be retrieved from an online database, known as the Carbohydrate-Active Enzymes (CAZy) database or server (Viborg *et al.,* 2019).

The mechanism by which GHs cleave glycosidic bonds is based on a general acid-base catalysis mechanism, whereby their stereochemical outcome of the hydrolysis reaction can either be: i) net retention (single displacement) or ii) net inversion (double displacement) of the anomeric carbon configuration, suggesting one or two transitional states (Figure 1.4) (Bayer *et al*., 1998; Dashtban *et al.*, 2009).

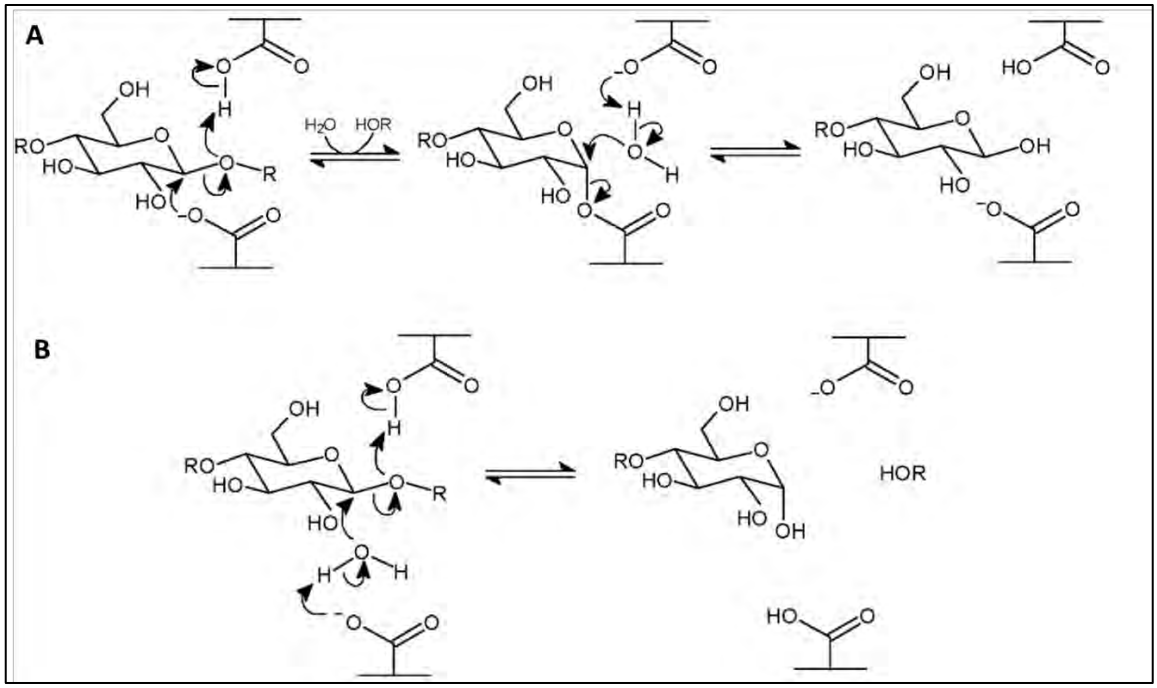

Figure 1.7. The proposed retaining (A) and inverting (B) mechanism of glycoside hydrolases (Adapted from Nerinckx *et al.,* 2005).

1.3.2. Enzymes required to degrade cellulose

The efficient degradation of cellulose requires the synergistic co-operation of at least three related biochemical enzymes, namely: i) cellobiohydrolases (CBHI, EC 3.2.1.176; CBHII, EC 3.2.1.91), ii) endoglucanases (EG, EC 3.2.1.4) and iii) β-glucosidases (EC 3.2.1.21) (Du *et al.,* 2020; Ganner *et al.*, 2012; Lynd *et al.,* 2002). Fungi are the most dynamic cellulose decomposers in nature, responsible for approximately 80% of cellulose degradation on earth (Cognilio *et al.,* 2017; Gupta *et al.,* 2019). The cellulose decomposing fungi include members of the Ascomycota, Basidiomycota, and Deuteromycota, as well as some Chytridiomycota that occur in the rumen of some animals (Sajith *et al.,* 2016). Efficient cellulolytic fungi are represented by the species of *Aspergillus, Penicillium, Chaetomium, Trichoderma, Fusarium, Stachybotrys, Cladosporium, Alternaria, Acremonium, Ceratocystis, Myrothecium* and *Humicola* (Sajith *et al.,* 2016; Mehrotra and Aneja, 1990). Various bacterial species may also produce cellulases, including *Bacillus, Clostridium, Cellulomonas, Thermomonospora* and *Thermobofida* sp. (Kuhad *et al.,* 2011; Sethi *et al.,* 2013).

1.3.2.1. Cellobiohydrolases/Exo-cellulases (CBHs, EC 3.2.1.91 and EC 3.2.1.176)

CBHs (also referred to as exo-cellulases) are the major components of most cellulolytic systems and are responsible for degrading highly crystalline cellulose (Boisset *et al.,* 2000; Den Haan *et al.,* 2013; Imai *et al.,* 1998). CBHs act in a processive manner on cellulose, liberating cellobiose from the chain

ends, but resulting in low polymer length reduction (Dashtban *et al*., 2009; Horn *et al*., 2012). However, it has been reported (but only in a limited amount of studies) that some CBHs have overlapping functions and can also degrade amorphous regions of cellulose (Ganner *et al.,* 2012). Therefore, they have been classified as bi-functional enzymes (Ganner *et al.,* 2012; Nidetzky *et al.,* 1994). CBHs have been grouped into two different classes (based on their sequence similarity and predicted structural and functional relationships). These include CBHI (GH family 7 and 48; EC 3.2.1.176) and CBHII (GH family 5 and 6; EC 3.2.1.91), which play key roles in liberating cellobiose from the reducing and non-reducing chain ends, respectively (Lynd *et al.,* 2002). Due to their specificities for opposite ends of the cellulose chain, the combined activities of CBHI and CBHII may enhance the overall degradation of cellulose (Barr *et al*., 1996; Nutt *et al.,* 1998; Wood and Mcrae 1979). CBHs also belong to families 5-7, 9, 48 and 74, where GH families 6 and 7 consists of aerobic fungal CBHs, GH families 6 and 48 consists of anaerobic fungal CBHs, whereas anaerobic bacterial CBHs may also belong to GH family 48, but are also grouped in family 9 (Lakhundi *et al.,* 2015).

CBHs are modular enzymes which possess enclosed tunnel-like active sites (channel-shaped cavities topped by several flexible loops) which allows them to initiate a processive mode of action on cellulose chain ends (Granum *et al.,* 2014; Segato *et al.,* 2012). The active sites are located on a catalytic domain (CD), and in some cases, fungal CBHs have a small carbohydrate-binding module (CBM) attached to the C-terminus (GH 7) or N-terminus (GH 6) via a flexible linker peptide (Erriksson *et al*., 2002; Lynd *et al.,* 2002; Segato *et al*., 2012). The presence of CBMs are essential for CBH activity as they are believed to bring the enzyme and substrate in close proximity with each other, leading to increased enzyme activity (Igarashi *et al*., 2009; Jalak *et al*., 2012; Teeri, 1997).

CBHs are monomeric proteins, with molecular weight (MW)'s ranging from 39-65 kDa (Cognilio *et al.,* 2017). These enzymes generally have low levels of glycosylation (approximately 12%), display a pH optimum of 4.0-6.0, and a temperature optimum ranging between 37 and 60°C, depending on the source of enzyme (Leis *et al.,* 2017; Takahashi *et al.,* 2010). Avicel, bacterial cellulose and filter paper (crystalline cellulose) are good substrates for CBH activity, due to the fact that they are crystalline and not amorphous substrates (Quiroz-Castañeda, 2013; Zhang and Lynd, 2004). However, some processive EGs can also hydrolyse Avicel and bacterial cellulose.

1.3.2.2. Endoglucanases (EGs, EC 3.2.1.4)

EGs are important members of the cellulases that assist CBHs in the cellulose degradation process. Endoglucanases are responsible for cleaving random sites in the amorphous regions of the cellulose chain, thus decreasing the DP of the substrate (Ganner *et al*., 2012; Lee, 1997; Nidetzky *et al*., 1994).

The ability of EGs to bind internally to the cellulose chain is due to their open active sites, which are in the form of clefts or grooves (Erriksson *et al.,* 2002; Teeri, 1997). Conversely, some studies have shown that EGs may possess a modular architecture like that of the CBHs, thus allowing them to act in a processive manner (Teeri, 1997; Zhang and Zhang, 2013). EGs belong to GH families 5-9, 12, 25, 44, 48, 51 and 74, where fungal EGs have a catalytic module (with or without a CBM). On the other hand, bacterial EGs can have multiple catalytic activities, CBMs, and other modules with unidentified functions (Forseberg *et al.,* 2014).

EGs are monomeric enzymes with a MW ranging from 22 to 45 kDa (Coniglio *et al.,* 2017). Generally, EGs are not glycosylated; however, they may contain relatively low amounts of carbohydrates (1-12%). The majority of EGs display a pH optimum between pH 4.0 and 5.0 and an optimum temperature ranging between 50 and 70°C (Busto *et al.,* 1996; Chokhawala *et al.,* 2015; Da Silva *et al.,* 2016). The most commonly used substrate to assess EG activity is carboxymethylcellulose (CMC), a soluble amorphous cellulose.

1.3.2.3. β-glucosidases (β-D-glucopyranoside glucohydrolase; EC 3.2.1.21)

β-Glucosidases (βgls) are a diverse group of enzymes (present in bacteria, eukaryotes and archaea) with great functional importance in biological systems (Singh *et al.,* 2016; Singhania *et al.,* 2013). They are the key enzymes accountable for catalysing the final step in cellulose hydrolysis (Lima *et al.,* 2013; Singh *et al.,* 2016; Singhania *et al.,* 2013). Although these enzymes don't show any activity on cellulose, they convert cellobiose and other short oligosaccharides into glucose monomers, which results in reduced product inhibition of upstream enzymes (Kostylev and Wilson, 2012; Li *et al.,* 2013; Sørensen *et al*., 2013). β-glucosidases are grouped into three classes (based on their substrate specificity), namely: (i) aryl-β-D-glucosidases (having strong affinity for aryl-β-D-glucosides), (ii) cellobiases (hydrolyse only disaccharides) and (iii) broad specificity glucosidases (exhibit activity on many substrate types and are the most commonly found β-glucosidases) (Rajan *et al.,* 2004; Singh *et al.,* 2016).

It has been proposed that βgls have pocket-like active sites that contain two glutamate residues and formed by large surface loops, surrounding the C termini of the barrel of β-strands (Singh *et al.,* 2016). This allows them to bind the nonreducing glucose unit and cleave glucose off from cellobiose (Xia *et al.,* 2016; Zhang and Zhang, 2013). They are proposed to possess no CBM and are classified mainly into GH1 (obtained from archaea, plants and mammals) and GH3 (obtained from bacteria, mould and yeast) families (Srivastava *et al.,* 2019). However, these enzymes are also classified into GH families 5, 9, 30 and 116 (Xia *et al.,* 2016).

These enzymes are generally glycosylated and can either be monomers or homo-oligomers, with molecular weights ranging from 35-64 kDa. Their pH optima range from pH 3.5-5.5, and their optimum temperatures range from 45-75°C (Narasimha *et al.,* 2016). Cellobiose or *p*-pitrophenyl glucopyranoside (*p*NPG) are the substrates used to measure β-D-glucosidase activities, which generally can't be hydrolysed by CBHs and EGs (Decker *et al.,* 2001; Larue *et al.,* 2016).

1.3.2.4. Other enzymes required for cellulose degradation

Although intensive research on cellulose-degrading enzymes for biomass degradation has mostly focused on the glycoside hydrolases i.e. CBHs, EGs and βgls (termed the classical enzyme system), other carbohydrate-active catalytic domains and proteins (non-hydrolytic) have been shown to contribute to the overall degradation of cellulose by means of increasing cellulose accessibility (Arfi *et al.,* 2014; Horn *et al*., 2012; Peciulyte *et al*., 2014). These include lytic polysaccharide monooxygenases (LPMOs) (previously classified as GH61 proteins), swollenins/expansins and CBMs.

1.3.2.4.1. Lytic Polysaccharide Mono-oxygenases (LPMOs)

LPMOs have gained significant attention in bioconversion studies, due to their boosting effect on enzymatic cellulose conversion (Andlar *et al.,* 2018; Johansen, 2016). They are classified as copper-dependent oxidases and exhibit enhanced activity in the presence of an external electron donor (cellobiose dehydrogenase or lignin and/or ascorbic acid) (Andlar *et al.,* 2018; Arfi *et al.,* 2014). They are believed to act on the surfaces of the insoluble substrate (catalysing the oxidative cleavage of glycosidic bonds), without the need of initially extracting individual chains from the crystalline matrix (Vaaje-Kolstad *et al.,* 2017). Consequently, this makes the cellulose polymer accessible to cellulases (Johansen, 2016). LPMOs are active towards a range of substrates, including: cellulose, xyloglucans, glucomannans, cello-oligosaccharides (fungal AA9 family); chitin and cellulose (bacterial/viral AA10 families and invertebrates AA15 family) (Filiatrault-Chastel *et al.,* 2019; Johansen, 2016).

1.3.2.4.2. Swollenins/Expansins/Loosenins

Proteins lacking any hydrolytic activity are believed to be key to solve problems associated with the slow process of enzymatic degradation. These proteins are classified into three related groups; swollenins, expansins and loosenins. Using different molecular mechanisms, these proteins disrupt hydrogen bonds within cellulose chains which result in the substrate loosening (Arantes and Saddler, 2010; Kang *et al.,* 2013). This causes an increase in substrate accessibility, enabling enzymes to perform hydrolysis leading to better decomposition of the lignocellulosic biomass (Kang *et al.,* 2013; Madaj *et al.,* 2017).

1.3.2.4.3. Carbohydrate Binding-Modules (CBMs)

Many microorganisms secrete multi-modular enzymes to assist them in cellulose hydrolysis, for example CBMs are attached to globular catalytic domains via a linker peptide (Kognole and Payne, 2018; Shoseyov *et al.,* 2006). The proposed functions of CBMs include: i) directing the cellulases to their specific substrate binding sites, ii) increasing the concentrations of enzyme onto the cellulose surface, and iii) loosening the substrate by disrupting the tightly packed cellulose chains (Duan *et al.,* 2016; Shoseyov *et al.,* 2006). These functions serve to increase the catalytic turn-over under substrate limited conditions, however, the way in which CBMs perform their function is still not yet fully understood (Duan *et al.,* 2016; Kognole and Payne, 2018). Since CBMS are structurally diverse proteins (with the ability to bind to many types of carbohydrate polymorphs and morphologies), they have been divided into different families (protein sequence similarity) and types (functionality similarity). Currently, there are 67 families, where CBMs from family 1 is the most commonly found type of CBM (Chen *et al*., 2014; Lombard *et al.,* 2014). Furthermore, they have been classified into: i) Type-A CBMs, which are specific for binding crystalline substrates, ii) Type-B CBMs, which bind to individual carbohydrate chains and (iii) Type-C CBMs, which are specific for binding oligosaccharides and non-crystalline substrates (Boraston *et al.,* 2000; Kognole and Payne, 2018; Malgas *et al.,* 2019).

An overview of all the enzymes required to degrade cellulose efficiently are shown in Figure 1.8.

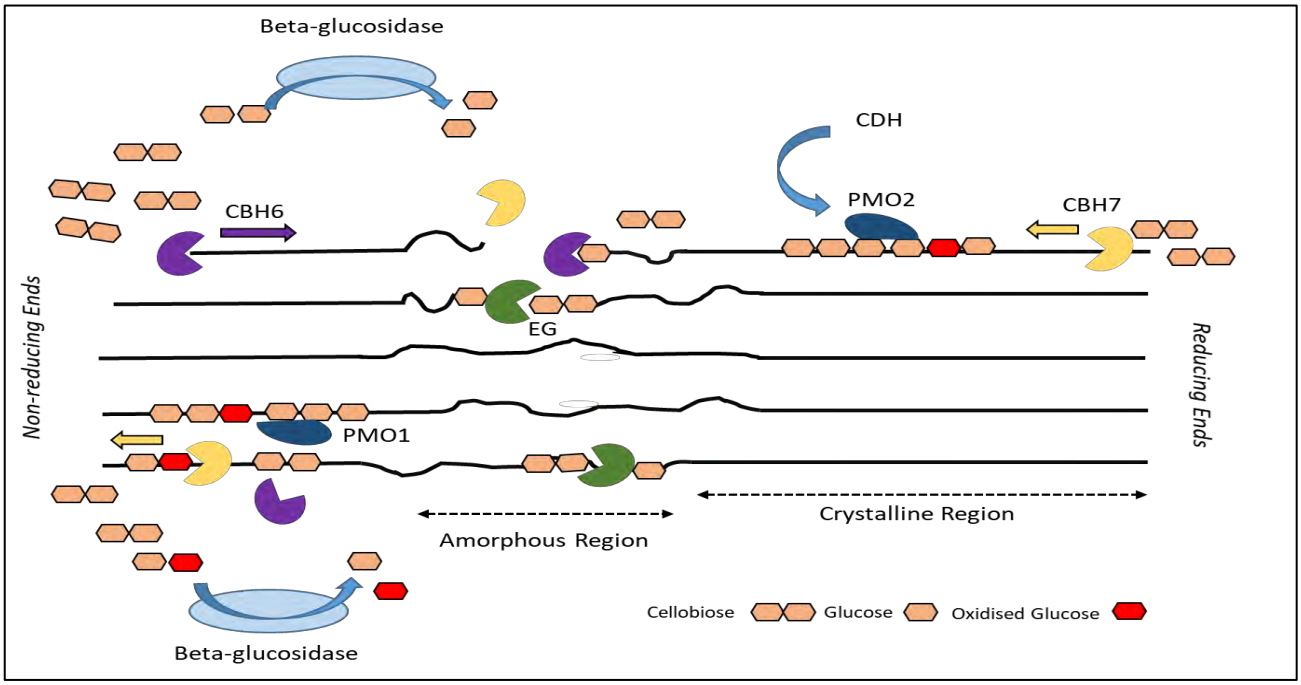

Figure 1.8. Schematic representation of the enzymes required to degrade the cellulose chain (Adapted from Dimarogona *et al.,* 2012).

1.3.3. Enzymes required to degrade hemicellulose

Several types of hemicellulose-degrading enzymes are required to achieve hemicellulose hydrolysis. According to Andlar *et al.* (2018), this synergistic activity is necessary, not only because of its complex structure, but also because it is intertwined with other plant cell components. The two major groups of enzymes required for hemicellulose degradation include xylanases and mannanases, which will be discussed in more detail.

1.3.3.1 Xylolytic enzymes

The degradation of xylan requires the co-operative activities of multiple xylanases and accessory enzymes (Hu *et al*., 2011; Zhang *et al*., 2011). Xylanases are hydrolytic enzymes responsible for randomly cleaving the polysaccharide xylan (Collins *et al.,* 2006). The two key xylanases are: i) endo-β-1,4-D-xylanases (EC 3.2.1.8), which are responsible for cleaving the xylan backbone to liberate shorter oligosaccharides, and ii) 1,4-β-D-xylosidases (EC 3.2.1.37) which are responsible for hydrolysing xylo-oligosaccharides to D-xylose from the non-reducing ends of the xylo-oligosaccharide chain (Sunna and Antranikian, 1997; Van Dyk and Pletschke, 2012). Additional enzymes such as arabinofuranosidases (EC 3.2.1.55), α-D-glucuronidases (EC 3.2.1.131) and phenolic esterases (EC 3.1.1.73) are required to liberate the substituted residues from the xylan backbone, thus contributing to the overall degradation of xylan (Meyer *et al*., 2009; Sweeney and Xu, 2012).

1.3.3.2 Mannanolytic enzymes

The degradation of mannan requires the co-operative activities of multiple mannanases (Malgas *et al*., 2015; Van Zyl *et al.*, 2010). The key mannanases are: i) β-1,4-D-mannanases (EC 3.2.1.78), which are responsible for randomly cleaving the mannan backbone to give rise to shorter manno-oligosaccharides, ii) β-mannosidases (EC 3.2.1.25), which are responsible for hydrolysing the manno-oligosaccharides into mannose monomers from the nonreducing ends of the mannan chain, and iii) β-glucosidase which are responsible for hydrolysing the glucomanno-oligosaccharides into glucose monomers (Malgas *et al.,* 2015; Shallom and Shoham, 2003). Additional enzymes, such as α-1,6-D-galactosidases galactohydrolase (EC 3.2.1.22) and acetyl-mannan esterases (EC 3.1.1.6) are required to liberate the substituted residues from the mannan backbone, thereby contributing to the overall degradation of mannan (Moreira and Filho, 2008; Yamabhai *et al*., 2014).

1.3.4. Enzymes required to degrade/modify lignin

Lignin-modifying enzymes are responsible for degrading lignin into low MW compounds and differ from the polysaccharide degrading enzymes (cellulases and hemicellulases) (Sajith *et al.,* 2016).

Ligninases are categorised into two groups: i) laccases or phenol oxidases and (ii) peroxidases (lignin peroxidases and manganese peroxidases). Laccases (EC 1.10.3.2; CAZy AA1) are multicopper containing glycoproteins, which may be monomeric, dimeric or tetrameric in nature (MW ranges of between 50 and 100 kDa). The mechanism of laccases includes the oxidation of nonphenolic and phenolic compounds to yield phenoxy radicals and quinines (Andlar *et al.,* 2018). The most common producers of laccases include *Aspergillus nidulans, Phanerochaete chrysosporium, Lentinula edodes, Phellinus ribis*, *Pleurotus pulmonarius*, *Trametes versicolor* and *Neurospora crassa* (Andlar *et al.,* 2018; Arora and Sharma, 2010; Sajith *et al.,* 2016).

Besides laccases, other important enzymes that can be used for delignification include peroxidases, responsible for catalysing the depolymerisation of lignin utilising H_2O_2 (Andlar *et al.,* 2018). Lignin peroxidase (EC 1.11.1.14; CAZy AA2) is a heme protein (MW ranging between 39 and 45 kDa) that possess high redox potential and can oxidise a wide range of phenolics (Arora and Sharma, 2010). Other enzymes, such as glucose oxidases (hydrogen-peroxidases) are also known to generate H_2O_2 from glucose. On the contrary, manganese peroxidase (MnP) (EC 1.11.1.13; CAZy AA2) utilises manganese as an intermediate in the transfer of electrons to lignin and oxidises phenolic structures to phenoxyl radicals (Lee, 1997; Wang *et al.,* 2013). The enzymes have MWs ranging between 38 and 62.5 kDa (Hofrichter, 2002; Sajith *et al.,* 2016).

Lignin degradation can further be boosted by the action of other enzymes, including (i) aryl alcohol oxidases (EC 1.1.3.7; CAZy AA3), (ii) pyranose 2-oxidase, including glucose 1-oxidase and cellobiose dehydrogense (EC 1.1.3.4; CAZy AA3), (iii) glyoxylate oxidase (EC 1.2.3.5), (iv) fungal aryl-alcohol dehydrogenase (EC 1.1.1.90), (v) quinone reductases (EC 1.6.99.2), (vi) tyrosinases (EC 1.14.18.1), and (vii) catechol oxidases (EC 1.10.3.1) (Andlar *et al.,* 2018; Kersten and Cullen, 2007).

1.3.5. Enzymes required to degrade pectin

In general, three types of pectinolytic enzymes are required for pectin degradation (Garg *et al.,* 2016; Pedrolli *et al,* 2009; Sharma *et al.,* 2012). These include: i) polygalacturonase (endo-polygalacturonases, EC 3.2.1.15 and exo-galacturonases, EC 3.2.1.67) which are responsible for hydrolysing the poly-galacturonic acid into monogalacturonic acid, ii) lyase/transe-elimases comprising of pectin lyase (EC 4.2.2.10) and pectate lyase (4.2.2.2), which are responsible for depolymerising pectic substances by a trans-eliminative split at C-4, and iii) pectin esterase (EC 3.1.1.11) which are responsible for the removal of methoxyl esters, resulting in polygalacturonic acid (Garg *et al.,* 2016; Sharma *et al.,* 2012).

A summary of the main enzymes required to degrade lignocellulose is provided in Table 1.1 below.

Table 1.1. An overview of the main enzymes required to degrade lignocellulose (Adapted from Andlar *et al.,* 2018 and Malgas *et al.,* 2017).

Polymer	**Enzymes**	**GH families**
Cellulose	Cellobiohydrolase, endoglucanase, β-glucosidase, lytic polysaccharide mono-oxygenase, carbohydrate binding module, expansin and swollenin	1, 2, 3, 5, 6, 7, 9, 12, 16, 30, 39, 45, 50, 55, 64, 74, 81, 86, 116, 118, 128
Hemicellulose	**Xylan:** Endo-xylanase, β-xylosidase, α-arabinofurosidase, α-glucoronosidase, α-galactosidase, acetyl xylan esterase, glucoronyl esterase, ferulolyl esterase **Mannan:** β-mannanase, β-mannosidase, acetyl mannan esterase, α-galactosidase	1, 2, 3, 5, 7, 8, 10, 11, 12, 15, 16, 26, 36, 39, 43, 51, 52, 54, 57, 62, 67, 113
Lignin	Laccase, peroxidase, phenol oxidase and esterase	(They are not classified as GH enzymes).
Pectin	Polygalacturonases, pectin esterases, pectate lyases	28

1.4. Enzyme synergy

A synergistic cocktail of hydrolytic enzymes tailored for a wide-range degree of substrate specificity is required for efficient and complete cellulose degradation (Van Dyk and Pletschke, 2012; Kognole and Payne, 2018). When the combined activities of two or more enzymes boost the rate of substrate depolymerisation, as opposed to the theoretical sum of their activities when acting independently on a substrate, they are said to be acting in synergy (Lynd *et al*., 2002; Olver *et al*., 2011; Van Dyk and Pletschke, 2012; Zhou *et al*., 2009).

1.4.1. Degree(s) of synergy

The degree of synergy (DS) is a quantitative measure used to determine whether enzymes interact synergistically to enhance the overall hydrolysis of a substrate (Jalak *et al*., 2012; Van Dyk and Pletschke, 2012). The DS is calculated by dividing the amount of product released by an enzyme cocktail divided by the theoretical sum of the products produced by their independent activities (Andersen *et al*., 2008; Van Dyk and Pletschke, 2012). The three possible outcomes for DS are: i) DS

> 1, when enzymes act synergistically to degrade a substrate, ii) DS = 1 or DS < 1, when the activity of one enzyme does not facilitate the activity of another enzyme (no synergy/anti-synergy), and iii) DS < 1, when enzymes do not interact synergistically, but could be a result of competitive behaviour (enzymes competing for the same binding sites) (Hu *et al.*, 2011; Van Dyk and Pletschke, 2012). The DS can be influenced by factors such as enzyme characteristics (enzyme ratios) and substrate characteristics (recalcitrance, DP and chemical composition) (Hu *et al.*, 2015; Jalak *et al.*, 2012).

1.4.2. Synergistic interactions

Investigating the synergistic interactions between lignocellulolytic enzymes has been the subject of extensive research in order to improve biomass hydrolysis and alleviate the high enzyme costs associated with biofuel production (Kallioinen *et al.*, 2014; Olver *et al.*, 2011). The most widely documented phenomenon is the synergy that occurs between cellulases (Boisset *et al.*, 2000; Moraïs *et al.*, 2010; Olver *et al.*, 2011). Interpolymer synergy (that which is between enzymes acting on different polymers within lignocellulose) between cellulases and xylanases, cellulases and mannanases, and xylanases and mannanases has also been reported, however, this type of synergy is not as extensively studied as the synergy between cellulases (Bura *et al.*, 2009; Hu *et al.,* 2011; Malgas *et al.,* 2017).

1.4.2.1. Intra-polymer synergy between cellulases

Numerous types of synergy between the various classes of cellulose-degrading enzymes have been investigated and are proposed in the literature. In particular, the most characterised cellulase synergism systems are: i) endo-exo synergism, whereby CBHs act on the new chain ends generated by the activities of the EGs and ii) exo–exo synergism, whereby CBHs degrade cellulose chains at opposite ends (Fägerstam and Pettersson, 1980; Henrissat *et al.*, 1985; Tang *et al.,* 2018; Väljamäe *et al.*, 1999). Furthermore, the addition of βgl is believed to prevent product inhibition of upstream enzymes by converting cellobiose into glucose, thus contributing to the overall degradation of cellulose (Kostylev and Wilson, 2012). Other types of synergism that have been reported include endo-endo synergism (EGs attacking different sites on the cellulose chain) and intramolecular synergy between catalytic domains and CBMs (Din *et al.,* 1994; Lamed *et al.*, 1991; Woodward, 1991). Some examples of intra-polymer synergy (that which is between enzymes acting on the same polymer within lignocellulose) systems that have been investigated and reported in literature include:

- Synergy between CBHI and CBHII (*T. reesei*) on Avicel and Whatman paper (Fägerstam and Pettersson, 1980);

- Synergy between cellulases from *C. thermocellum* and *Trichoderma koningii* on Avicel (Gow and Wood, 1988);
- Synergy between Cel6B, Cel9A and Cel5A from *Thermomonospora fusca* on BMCC and Avicel (Bothwell *et al.,* 1993; Jeoh *et al.,* 2006);
- Synergy between Cel7A (*T. reesei*) and Cel5A (*T. fusca*) on Avicel (Bothwell, 1993);
- Synergism between Cel6A and Cel7A (*T. reesei*) on filter paper (Nidetzky *et al.,* 1994);
- Synergy between a CBH and EG from *T. koningii* (Fujii *et al.,* 1995);
- Synergism between CBHI and EGII (*Humicola grisea*) on Avicel (Takashima *et al.,* 1997);
- Synergy between CBHI and EGI from *T. reesei* on BMCC (Väljamäe *et al.,* 1999);
- Synergism between Cel6A, Cel7A and Cel45A (*Humicola insolens*) in bacterial ribbons (Boisset *et al.,* 2000);
- Synergy between Cel7B and Cel6B (*Chaetomium lucknowense*) on cotton cellulose (Gusakov *et al.,* 2006);
- Synergy between Cel45A and Cel6A (*H. insolens*) and Cel3A (*Penicillium brasilianum*) on Avicel and PASC (Andersen *et al.,* 2008);
- Synergy between Cel6A and Cel45A from *H. insolens* on PASC (Andersen *et al.,* 2008);
- Synergy between Cel7A, Cel6A and Cel6B (*T. viride*) on steam exploded corn stover (Zhou *et al.,* 2009);
- Synergy between Cel7A and Cel6A (*T. reesei*) on crystalline cellulose (Igarashi *et al.,* 2011);
- Synergy between Cel7A, EG (*T. longibrachiatum*) and Cel6A (*T. reesei*) (Ganner *et al.,* 2012);
- Synergy between Cel6A and Cel45A (*Phialopora* sp.) on filter paper (Zhang *et al.,* 2012);
- Synergy between Cel7A (*Taloromyces emersonii*), Cel6A (*Chrysosporium lucknowense* and Cel5A (*T. reesei*) on Avicel (Den Haan *et al.,* 2013);
- Synergy between Cel7A, Cel6A and Cel5A (*T. reesei*) on steam pretreated wheat straw (Kallioinen *et al.,* 2014);
- Synergy between Cel6A and Cel7A from *H. jecorina* on Avicel (Badino *et al.,* 2017);
- Synergy between three cellulases (CBH, EG and βgl) from *A. niger* on filter paper and Avicel (Tang *et al.,* 2018).

For the past few decades, various hypotheses have been proposed to explain these synergistic interactions, however, the most widely accepted enzyme synergy model is based on the hypothesis that enzymes work on different regions within the substrate (crystalline or amorphous regions or reducing and non-reducing ends), thus exposing or creating new sites to facilitate the action of other enzymes

(Kosytlev and Wilson, 2014; Wood and Mcrae, 1979). It has been reported that this is an over-simplification of a far more complex process (Hu *et al*., 2015; Jalak *et al*., 2012; Kostylev and Wilson, 2012). During the last few years, some novel, alternative paradigms for enzyme synergy have appeared in literature, which are further discussed below.

1.4.2.1.1. Surface erosion model

Väljamäe *et al.* (1998) studied the hydrolysis of bacterial cellulose (BC) using two cellulases. A new model known as the surface erosion model was proposed, which is complementary to the endo-exo synergism model. This model is based on the hypothesis that the processive action of one enzyme (CBH) erodes the substrate structure, thereby creating solitary chains that hinder its own action (can no longer bind to the substrate). However, the eroded substrate is made more accessible for the activity of another enzyme (EGs), which enables further action of CBHs on cellulose chains. Kostylev and Wilson (2014) similarly proposed this synergism model, however, they hypothesised that the roles of the enzymes were reversed.

1.4.2.1.2. "Traffic jam" effect

Igarashi *et al.* (2011) used Atomic Force Microscopy (AFM) to study the co-operation between *Tr*Cel7A and *Tr*Cel6A and proposed that the resulting synergy was caused by a "traffic jam" effect. It was proposed that the obstacles present in the cellulose chain impede the activity of other enzymes. For example, CBHs may non-productively bind to the substrate making the overall hydrolysis rate slower. Therefore, when EG is present, it creates cuts in front of the obstruction, so that when CBH approaches the amorphous region, it has a dissociation site and may dissociate from the strand and seek a new catalysis site (Jalak *et al.,* 2012).

1.4.2.1.3. "Substrate polishing" effect

Ganner *et al.* (2012) studied the mechanistic actions of CBHI, CBHII and EG on a polymorphic cellulosic substrate, using AFM. Interestingly, their studies found the CBHII to display EG activity, due to its ability to degrade amorphous cellulose. It was, therefore, proposed that CBHII was a bi-functional enzyme. Furthermore, their results indicated that crystalline cellulose is covered by amorphous cellulose and that CBHII and EG are required to remove the amorphous regions. In so doing, they polish (expose) the crystalline regions in the cellulose chain, which ultimately require the activity of CBHI for their hydrolysis.

1.4.2.1.4. Microfibril swelling effect

Josefsson and colleagues proposed an extension of the typical endo-exo model of synergy. They suggested that cellulose microfibrils start swelling once the endo- and exo- acting enzymes have attached to the substrate. As a result of the swelling, it increases the availability of new sites for creating end attack points for more enzymes (Josefsson *et al.,* 2007).

1.4.2.2. Inter-polymer synergy between various lignocellulolytic enzymes

Various studies have reported that the synergistic interactions between cellulases and xylanases could enhance cellulose hydrolysis (Hu *et al*., 2011; Kumar and Wyman, 2009). Cellulose and hemicellulose are closely associated with each other through various covalent bonds (Moreira and Filho, 2008; Zhang *et al*., 2011). Therefore, xylanases may contribute to the overall hydrolysis of cellulose by removing the hemicellulosic component (xylan) in biomass that restricts the accessibility of cellulases to cellulose (Hu *et al*., 2011; Kumar and Wyman, 2009; Zhang *et al.,* 2011). Some examples of inter-polymer synergy systems that have been investigated and reported in the literature are listed below:

- Synergistic effect of cellulosomal xylanase and cellulase from *C. cellulovorans* on corn fibre (Murashima *et al.,* 2003);
- Synergy between cellulase, xylanase and feruloyl esterase on wheat straw (Tabka *et al.,* 2006);
- Synergy between a mannanase and xylanase on NH_4OH pretreated sugarcane bagasse (Beukes *et al.,* 2008);
- Synergy between Cel7A, Cel6A, Cel5A and Cel74A (xylanase) on wet oxidised corn stover (Benko *et al.,* 2008);
- Synergy between Celluclast (*T. reesei*) and XynA (*Thermomyces lanuginosus*) on pretreated corn stover (Selig *et al.,* 2008);
- Synergy between an α-galactosidase and mannanase on guar gum (Wang *et al.,* 2010);
- Synergy between cellulase and xylanase of (Hu *et al.,* 2011);
- Synergistic effect of three enzymes: endoglucanase (EngE), mannanase (ManA) and xylanase (XynA) on the degradation of corn stalk, grass, and pineapple fruit pulp (Olver *et al.,* 2011);
- Synergy between CBHI, EGII and Xyn (*T. aurantiacus*) on hydrothermally pretreated corn stover (Zhang *et al.,* 2011);
- Synergy between Accelerase 1500 and XynCnon steam pretreated wheat straw (Alvira *et al.,* 2012);
- Synergistic effect between a cellulase mixture (Primafast 200) and xylanase (Pentopan) on alkaline pretreated rice straw (Zou and Shao, 2012);

- Synergy between a cellulase and xylanase from *T. reesei* on steam pretreated corn stover (Pribowo *et al.,* 2012);
- Synergy between a Cel48A exoglucanase and a Cel5A endoglucanase, and two *T. fusca* xylanases, endoxylanases Xyn10B and Xyn11A (Moraïs *et al.,* 2013);
- Synergistic action between cellulases and pectinases on the hydrolysis of steam exploded and ensiled hemp (Zhang *et al.,* 2013);
- Synergy between a commercial cellulase (Accelerase) and a xylanase on pretreated rice straw (Choudhary *et al.,* 2014);
- Synergy between a cellulase mix (Egl, Cel7A, Cel6A, βgl) and a xylanase mix (Xyn2A, XT6, AguA and SxA) on pretreated *Poplar* and *Acacia* sp. (Malgas *et al.,* 2017);
- Synergy between a cellulase and xylanase on sugarcane bagasse (Huang *et al.,* 2018);
- Synergy between TrCel7A and a *Geobacillus stearothermophilus* xylanase, XT6, on cellulose-xylan complexes and steam exploded *Acacia* (Malgas *et al.,* 2019).

1.5.1. Pretreatment of lignocellulosic biomass

Although biomass is considered a potential feedstock for biorefineries that complement oil refineries as a source of fuels and chemicals, its efficient degradation presents several challenges which are mostly due to plant recalcitrance (Jönsson and Martin, 2016). Zhang and Lynd (2004) previously reported that hydrolysis of native lignocellulose resulted in less than 20% solubilisation of the orignal glucan. Thus, pretreatment is a vital process for efficient saccharification and utilisation of lignocellulose for its biological conversion into value-added products (Van Dyk and Pletschke, 2012; Jönsson and Martin, 2016; Wu *et al.,* 2019). The primary role of pretreatment is to simplify the biomass structure by altering or deconstructing the complex biomass structure, making the polysaccharides more accessible to enzymatic attack (Figure 1.9) (Karp *et al.,* 2013; Madaj *et al.,* 2017; Van Dyk and Pletschke, 2012). Hydrolysis of lignocellulose without any pretreatment generally results in low efficiencies, due to various structural properties, such as lignin content, acetylated hemicellulose, a limited surface area and crystallinity of cellulose.

There are also some drawbacks associated with various pretreatment methods. One of the major limitations of pretreatment is the generation of compounds which are known to inhibit enzyme activity (Malgas *et al.,* 2015; Wu *et al.,* 2019). These compounds include sugars (monomers, oligomers), organic acids (acetic, levulinic and formic acids), lignin derivatives (*p*-coumaric, vanillic and gallic acids), and furan deriatives (hydroxymethyl-furfural and furfural) (Brodeur *et al.,* 2011; Rahikainen *et al.,* 2013; Xiemenes *et al.,* 2011). Although various strategies (extraction and detoxification methods)

have been implemented to reduce the formation of these compounds, the effect of these inhibitors requires further investigation (Li *et al.,* 2013).

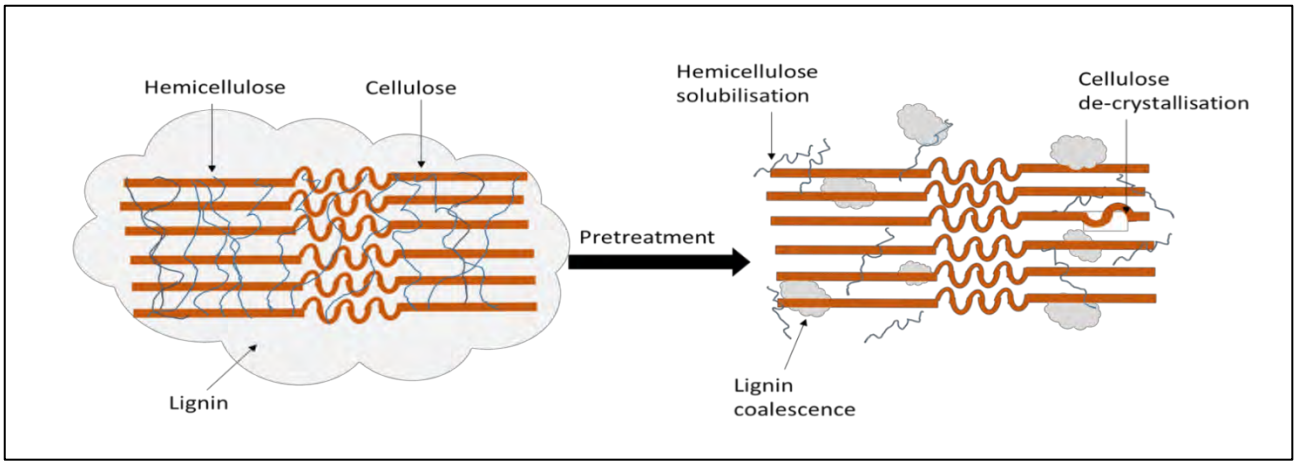

Figure 1.9. The effect of pretreatment on lignocellulose (Adapted from Mosier *et al.,* 2005).

1.5.2. Pretreatment methods

Various pretreatments have been developed and extensively investigated over the past few years, where researchers have devised hemicellulose-targeted, cellulose-targeted and lignin-targeted pretreatment approaches (Van Dyk and Pletschke, 2012; Zhang and Lynd, 2004). Various biological (bacteria, fungi), physical (grinding, milling, microwave), chemical (alkali, acids), thermo-chemical (pyrolysis, gasification), physico-chemical (steam explosion, wet oxidation, liquid hot water, ammonia fibre explosion), and multiple/combinatorial (bio-organosolvent) pretreatments have been developed and evaluated for different biomass feedstocks (Kumar and Sharma, 2017; Mood *et al.,* 2013). Each treatment imposes its own advantages and disadvantages, where its performance is also influenced by the structure and composition of the biomass (Table 1.2) (Alvira *et al.,* 2010; Hu *et al.,* 2015; Rico *et al.,* 2014). According to Alvira *et al.* (2010) and Romaní *et al.* (2014), the pretreatment method should aim to address as many of the following criteria listed below:

- Be simple and cost-effective;
- Minimise energy input;
- Avoid the loss or degradation of sugars;
- Minimise the use of hazardous chemicals;
- Avoid erosion effects on the biomass structure;
- Be able to recover valuable products from the polysaccharides;
- Minimise the formation of by-products/inhibitory compounds;
- Avoid large generation of waste products.

Table 1.2. The advantages and disadvantages of various pretreatment methods

Pretreatment	Example/s	Advantages	Disadvantages	References
Physical	Mechanical force	Reduction of particle size and cellulose crystallinity	Inability to remove lignin	Hendriks and Zeeman, 2009
Physico-chemical	Steam explosion	Cost-effective; Low energy input; High removal of hemicellulose; No hazardous chemicals required	Partial degradation of hemicellulose; Acid catalyst required; Not efficient for biomass with high lignin content; High formation of inhibitors	Brodeur *et al.,* 2011; Kumar *et al.,* 2009
	Liquid hot water	No catalysts required; Hydrolysis of hemicellulose; Low formation of inhibitors; Low degradation of sugars	High energy/water input; Limited disruption of lignin	Brodeur *et al.,* 2011; Wang *et al.,* 2012
	Ammonia fibre explosion	High removal of lignin; Low formation of inhibitors; Ammonia can be recycled; Higher accessibility of cellulose	High cost; Not efficient for biomass with high lignin content; Partial degradation of hemicellulose; Low lignin recovery	Kumar *et al.,* 2009
	Supercritical fluid	Cost effective; Low energy input; No degradation of sugars; Low formation of inhibitors	Low yield; Lignin and hemicellulose not modified	Brodeur *et al.,* 2011; Kumar *et al.,* 2009

	Acid hydrolysis	Hemicellulose removal; structural alterations of lignin		
Chemical	Organic solvent	Hydrolyses hemicelluloses and lignin; High lignin recovery	High cost; Need for solvent recovery and recycle; High formation of inhibitors;	Brodeur *et al.,* 2011; Kumar *et al.,* 2009
	Wet oxidation	High removal of lignin; Low formation of inhibitors;	High cost; Not efficient for biomass with high lignin content; Low lignin recovery;	Brodeur *et al.,* 2011
	Acid	High glucose yield; Solubilises hemicellulose and lignin; Limited formation of degradation products	High cost; High formation of inhibitors; Corrosive and toxic compounds	Brodeur *et al.,* 2011
Biological	Microorganisms Enzymes	Low energy input; Degrades lignin and hemicellulose; Environmentally friendly	Low hydrolysis rates	Kumar *et al.,* 2009

1.6. Addition of surfactants

Although various pretreatment methods have been employed to reduce plant recalcitrance and increase cellulose accessibility, large enzyme quantities or long hydrolysis times are still required to reach economically viable conversion levels (Kumar and Sharma, 2017; Zhang *et al.,* 2018). In addition, no pretreatment method has been developed that can sufficiently and economically remove lignin. Consequently, this presents a major obstacle for efficient enzymatic hydrolysis, as lignin physically blocks the accessibility of enzymes to the polymers, and non-productively binds enzymes (Qing *et al.,* 2010; Zheng *et al.,* 2013). One promising solution that can alleviate these challenges is to block the exposed lignin surfaces in the reaction medium by the addition of various compounds such as surfactants (non-ionic, anionic and cationic), proteins (bovine serum albumin (BSA), casein, corn steep liquor), polyhydric alcohols (PEG) and alkali media after biomass pretreatment (Alkaswari *et al.,* 2003; Kim *et al.,* 2019; Kristensen *et al.,* 2007; Qing *et al.,* 2010).

This assertion is based on the findings that surfactants/additives can: i) alter the substrate structure, resulting in increased substrate accessibility, (ii) increase the positive interactions between the enzyme and substrate, (iii) reduce non-productive adsorption, thus reduce the amount of enzymes and overall processing costs, and (iv) increase enzyme stability, thus prevent enzyme denaturation during hydrolysis (Du *et al.,* 2012; Yanfei *et al.,* 2016). Improved cellulase activity with different surfactants/additives has been reported for a wide range of pretreated substrates (Table 1.3).

Although numerous studies have demonstrated the potential of surfactants/proteins as lignin blockers for improved biomass saccharification, it has been established that some cellulase components are unable to desorb efficiently from various pretreated substrates. Moreover, the advantages of using surfactants/protein must always be balanced against its economic viability (Lindedam *et al.,* 2013). Alternatively, certain metal compounds such as $CaCl_2$, $CaSO_4$ and $MgSO_4$ can be used to efficiently decrease nonproductive adsorption of enzymes by lignin, through lignin–metal complexation (Liu *et al.,* 2010).

Table 1.3. Examples of various surfactants/proteins that have led to improved cellulase hydrolysis on different pretreated substrates

Surfactant	**Substrate**	**Pretreatment**	**Reference**
Tween 20	Mixed softwood	Steam pretreatment	Alkaswari *et al.,* 2003
	Wheat straw	Dilute acid	Qi *et al.,* 2010
Tween 80	Corn stover	Dilute-acid	Qing *et al.,* 2010
	Lodgepole pine	Steam explosion	Tu *et al.,* 2009
Casein	Corn stover	AFEX, dilute acid	Eckard *et al.,* 2013
BSA	Corn stover	AFEX	Kumar and Wyman, 2008
	Mixed hardwood chips	Liquid hot water	Ko *et al.,* 2015
PEG	Wheat straw	Steam, acid	Kristensen *et al.,* 2007
	Beechwood waste	Ionic liquid	Goshadrou and Lefsrud, 2017
	Corn stover	-	Lin *et al.,* 2015
	Fruit bundles	Hydrothermal	Kim *et al.,* 2019
Soybean protein	Sugar cane bagasse	Steam explosion	Brondi *et al.,* 2019
	Sugarcane bagasse	Hydrothermal	Florencio *et al.,* 2019
Triton X100	Rice straw	Ionic liquid	Chang *et al.,* 2017
Triton X100	Oil palm trunk	Dilute acid	Bukhari *et al.,* 2018
Sodium dodecyl sulfate (SDS)	Spruce	Steam	Erriksson *et al.,* 2002
	Water hyacinth	Ultrasound-assisted ionic liquid	Chang *et al.,* 2017

1.7. Motivation for using hardwoods as a feedstock for biofuel production

Hardwoods, which are composed of approximately 50% cellulose, 25% hemicellulose and 25% lignin (as well as traces of pectin, proteins and phenolics) are considered easier to delignify compared to softwoods as they have a much lower recalcitrance to enzymes (Ralph *et al.,* 2004). As a result of delignification, the polysaccharides become more accessible to the enzymes for efficient biomass saccharification (Malgas, 2017). The hardwood *Eucalyptus* was selected for the purpose of this study, and a detailed review of its chemical and ecological characteristics is provided below.

Eucalyptus is a hardwood belonging to the *Myrtaceae* family (Order Mytales) (Batish *et al.,* 2008; Crous *et al.,* 2006; Yoshida *et al.,* 2010). There are over 700 different species of *Eucalyptus* as well as three hybrids (Batish *et al.,* 2008; Crous *et al.,* 2006; Neiva *et al.,* 2015). Some of the most common species include *Eucalyptus camaldulensis, deglupta, globulis, grandis, robusta, saligna* and *urophylla.* This fast-growing tree is widely distributed throughout the world, including the tropical and subtropical regions of Asia, Australia, Africa and South America, as well as the temperate regions in Europe, and Australia (Cetinkol *et al.,* 2012; Grattapaglia *et al.,* 2012). *Eucalyptus* are the most widely cultivated commercial hardwoods globally, with over 20 million ha in cultivation (Bhalla *et al.,* 2019; Ledford, 2014). Generally, *Eucalyptus* is a valuable raw material for the papermaking and construction industries (Cetinkol *et al.,* 2012; Yu *et al.,* 2010). However, the residues (bark, crosscut ends, cork residues and black liquor) from the end processes are a major reservoir for unutilised polysaccharides, making it an ideal feedstock for bioenergy production (Howard *et al.,* 2002; Silva-Fernandes *et al.,* 2015; Yu *et al.,* 2010). In addition, *Eucalyptus* is a highly productive, fast-growing tree that has tolerance over a wide range of soils. It also has a lower pentose sugar content compared to other agricultural residues and its maintenance is also low in cost (Lima *et al.,* 2013; Wang *et al.,* 2012).

While hardwoods present many advantages as outlined above, *Eucalyptus* has a higher recalcitrant structure compared to grasses or cereal biomass because the wood and its barks are harder and denser (Lima *et al.,* 2013; Zhu *et al.,* 2009). For this reason, it presents additional challenges; it is more resistant to microbial and enzymatic degradation, and requires different pretreatment conditions compared to those used with other feedstocks (Bhalla *et al.,* 2019; Lima *et al.,* 2013; Zhu *et al.,* 2009). Several studies have determined the composition of *Eucalyptus* – these are presented in Table 1.4. Despite the recent focus on utilising *Eucalyptus* as a renewable source for biofuel production, no studies have been conducted on enzyme synergism for efficient *Eucalyptus* degradation, or how the composition and structural characteristics may influence these enzyme interactions (Alvira *et al.,* 2010).

Table 1.4. The composition of different *Eucalyptus* sp. Biomass (dry weight) as reported by various studies. "-" = not detected

Species	**Glucan (%)**	**Xylan (%)**	**Galactan (%)**	**Arabinan (%)**	**Mannan (%)**	**Klason Lignin (%)**	**Acid soluble lignin and ash (%)**	**Others* (%)**	**Reference**
Eucalyptus x urograndis	44.6	12.8	0.5	0.3	0.5	30.1		7.3	Gonzalez *et al.,* 2011
Grandis x urophylla	38.85	9.62	0.91	1.03	-	19.68	4.06	0.42	Lima *et al.,* 2013
Globulus	46	15.6	0.4	0.8	1.7	19.6	2.8	1.6	Martin-Sampedro *et al.,* 2014
	39.5	6.7	-	-	-	22.3		-	Rico *et al.,* 2014
	44.7	16	-	1.09	-	24.7	3.19	2.96	Romaní *et al.,* 2014
	36.1	13.9	1.3	2	1.7	26.7	2.4	14	Silva-Fernandez *et al.,* 2015
	69.1	17.7	-	-		4.9	2.2	-	Sun *et al.,* 2013
	42	13.4	-	-	-	24.4		-	Wang *et al.,* 2012
	42.6	15.4	2.3	1.9	-	28.3	3.3	3.3	Wei *et al.,* 2012
Grandis	43.4	18.8	1.2	0.3	-	28.5	3.2	2	Xiao *et al.,* 2014
	52.7	11.4	-	-	-	26.2	3.5	13.9	Yu *et al.,* 2010
	41.4	15.3	1.2	0.5	-	16.7	5.6	-	Vena *et al.,* 2013
	39.55	8.64	1.19	1.14	-	14.71	7.14	0.46	Lima *et al.,* 2013

*Pectin, extractives, waxes

Chapter 2: Project motivation and Research questions

2.1. Problem Identification

Bio-refineries for valorisation of lignocellulose has gained significant attention over the past few decades (Novy *et al.,* 2019; Thoresen *et al.,* 2020). The transition from conventional to non-conventional fuels has been motivated by an increase in environmental awareness (Novy *et al.,* 2019). Lignocellulose contains a large percentage of unutilised polysaccharides (75%) that can potentially be converted into different high-value products, including biofuels (Anwar *et al.,* 2014; Kumar and Wyman, 2009). While there have been major advancements in research regarding biomass-based fuels, the major technological and economical drawbacks that impede the development and commercialisation of biofuels include biomass recalcitrance, high operating enzyme costs and low conversion rates of the enzymes during substrate hydrolysis (Christopher *et al.,* 2015; Thoresen *et al.,* 2020; Limayem and Ricke, 2012). To address these challenges, ongoing research is required to improve the efficiency and the economics of this process. Potential ways to alleviate these inherent bottlenecks include: i) bioprospecting for novel enzymes with better stability and activity or improving enzymes used to depolymerise cellulose (engineering), ii) improving pretreatment conditions, iii) optimising cellulase mixtures (enzyme/substrate ratios, protein loading, enzyme synergy) to reduce enzyme loadings, and iv) immobilisation techniques to improve enzyme stability and reduce the cost of enzymes (enzyme recycling) (Bhattacharya *et al.,* 2014; Li *et al.,* 2009; Visser *et al.,* 2015).

Efficient biomass hydrolysis requires a mixture of cellulolytic, hemicellulolytic and accessory enzymes (Novy *et al.,* 2019). With regards to enzyme synergy, there are still major gaps in our understanding of enzyme mechanisms and the interactions that take place between various enzymes (Ganner *et al.,* 2012; Peciulyte *et al.,* 2015). An improved understanding of how enzymes completely hydrolyse biomass and the factors that influence enzyme-enzyme and enzyme-substrate interactions could potentially lead to breakthroughs that are important for further developments in bioethanol production (Hu *et al.,* 2015; Van Dyk and Pletschke, 2012; Yang *et al.,* 2011). Research has mainly focused on using model substrates to elucidate how their structures and compositions influence enzyme activity; however, using complex, heterogeneous substrates would allow for an improved understanding of enzyme synergy (Van Dyk and Pletschke, 2012; Yang *et al.,* 2011). As afore-mentioned, hardwoods have many advantages as biofuel feedstocks. Thus *Eucalyptus*, a viable feedstock for bio-ethanol production, will be investigated in this study, since limited or no studies (with respect to biomass hydrolysis and enzyme synergy) have been carried out on this substrate. The main objective of this research was to assist our understanding of how the structure and composition

of *Eucalyptus* (when subjected to various pretreatment methods) influences enzymatic hydrolysis/synergy which could provide us with novel information that is required to elucidate enzyme-substrate interactions. Furthermore, this knowledge could assist in developing better and more robust enzyme cocktails for efficient biomass hydrolysis.

In addition to the high cost of enzymes, another challenge that restricts feasible biomass conversion into value-added products is their single-use nature. Thus, researchers are exploring strategies to develop robust methods to recycle enzymes, which is another factor that will be addressed in this thesis.

2.2. Research questions

1. How do GH enzymes depolymerise the diverse portions of the woody substrate? Does synergy occur between the cellulases, or between the cellulases and hemicellulases? Do all endo- and exo-acting enzymes act synergistically, and if not, what are the factors that govern enzyme synergism between these enzymes?

2. How is lignin and hemicellulose associated with cellulose in lignocellulosic biomass? Does the structure and composition of *Eucalyptus* change when subjected to various pretreatment methods, and if so, how do these changes affect the interactions that are established between various enzymes for biomass saccharification?

3. Can the enzymes be re-used/recycled? If so, can this contribute towards the economic feasibility of the bioconversion process?

2.3. Aims

The initial aims of this study were to obtain an improved understanding of enzyme synergism and how the composition and structural characteristics of *Eucalyptus* influence the function of the GH enzymes that were used in this study [a cellobiohydrolase I from *H. jecorina* (Cel7A), CBHI from *T. longibrachiatum* (Cel7A), CBHI from *C. stercorarium* (Cel48A), CBHII from a microbial source (Cel6A), CBHII from *C. thermocellum* (Cel5A), a cellulase containing three endoglucanases (EglA (Cel9); EglB (Cel12) and EglC (Cel74)), as well as three other endoglucanases (EG); *B. amyloliquefaciens* (Cel5A), *T. maritima* (Cel5A) and *T. reesei* (Cel7B)] by:

- Investigating how the molecular mechanisms of cellulases from different GH families (i.e. GH 3, 5, 6, 7, 9, 12, 48 and 74) and various microbial sources govern synergism, by means of mapping various CBH to EG interactions;

- Unravelling the structure of *Eucalyptus* substrate (before and after the use of pretreatment methods) to determine the effects of different pretreatments on the chemical composition, morphology and enzymatic hydrolysis of the substrate;
- Assessing the performance of the optimal cellulase mixture (CelMix) on *Eucalyptus* saccharification with and without the addition of xylanase or laccase;
- Designing a robust method to recycle enzyme to reduce the high costs associated with the bioconversion process.

2.4. Objectives

- To characterise the enzymes (molecular, and physico-chemical characterisation);
- To determine the protein concentrations and substrate specificities of the GH enzymes used;
- To perform synergy studies between cellulases (CBHI, CBHII and EG) from different GH families and microbial sources;
- To formulate an optimal enzyme cocktail (from the synergy studies) that will be used in subsequent experiments;
- To perform various pretreatment methods on the *Eucalyptus* substrate;
- To characterise the pretreated *Eucalyptus* substrate in terms of chemical composition using a modified Klason method and sugar quantification kits;
- To determine the S/G ratio of *Eucalyptus* substrate before and after pretreatment using Py-GC/MS;
- To determine the morphological changes in the *Eucalyptus* substrate before and after pretreatment using various microscopic techniques: light microscopy, SEM and fluorescence microscopy;
- To analyse the physical/chemical characteristics of the substrate before and after pretreatment methods using methods such as the FTIR, NMR and XRD;
- To determine cellulose accessibility by the Simons' staining method using Direct Orange (DO) before and after pretreatment;
- To assess and compare the saccharification efficiency of the formulated cocktail on untreated and pretreated *Eucalyptus*;
- To assess and compare the reducing sugars released and the glucose saccharification efficiency of untreated and pretreated *Eucalyptus* substrate enzymatic hydrolysis;
- To assess the effect of xylanase and laccase addition on *Eucalyptus* substrate enzymatic hydrolysis;

- To develop an enzyme recycling strategy to reduce the cost of the bioconversion process.

2.5. Outline of the Thesis

Various cellulases from different GH families and microbial sources (which were used in this study) were characterised for their substrate specificities and physico-chemical properties in Chapter 3. These results were used as a knowledge base for establishing and understanding the synergistic behaviour between these enzymes using a cellulase swapping approach in Chapter 4. Chapter 5 of the thesis focused on various pretreatment technologies, where different pretreatment methods on *Eucalyptus* were explored, specifically focussing on how these pretreatments alter the morphological, structural and chemical properties in the substrate. Further investigation of enzyme synergy and hydrolysis yield potential with these pretreated substrates was conducted in Chapter 6, using the cellulase cocktail optimised in Chapter 4, in combination with accessory enzymes, including xylanase and laccase. Chapter 7 of the thesis constituted the last experimental chapter and assessed the effect of enzyme recycling on *Eucalyptus* hydrolysis potential. A general discussion, highlighting the conclusion and future perspectives regarding the study in this thesis is provided in Chapter 8.

Chapter 3: Characterisation of Cellulolytic Enzymes

3.1. Introduction

Cellulose is the major polysaccharide component of plant cell walls and has been recognised as a potential source of renewable energy (Muthuvelu *et al.,* 2019). However, cellulose is protected from degradation due to the presence of interlinked polymers (hemicellulose and lignin), which are known to form a physical barrier around cellulose. Cellulose is commonly degraded by enzymes called cellulases, which are generally produced by several fungi and bacteria (Kuhad *et al.,* 2011; Sethi *et al.,* 2013). Cellulases belong to numerous families of glycosyl hydrolases (GH), which are specific for cleaving the β-1,4-glycosidic bonds in the cellulose chain. Therefore, cellulases are the key enzymes required in the conversion of plant biomass to biofuels into sugar platform biorefineries (Lynd *et al.,* 2002; Zhang *et al.,* 2015). In this context, cellulases have attracted considerable attention, specifically for facilitating an understanding of the mechanisms underpinning enzymatic hydrolysis of plant polysaccharides (Bhat and Bhat, 1997; Leghlimi *et al.,* 2013).

Cellulolytic microorganisms produce an array of cellulases which act synergistically to degrade cellulose (Lynd *et al.*, 2002). The strategies in which cellulolytic microorganisms degrade lignocellulosic materials are classified into three broad categories: (i) the non-complexed or free cellulase system; (ii) the complexed or cellulosome system, and (iii) multimodular chimeric enzymes (Cheng *et al.,* 2012; Lynd *et al.,* 2002; Van Dyk and Pletschke, 2012). Cellulases are generally secreted as free enzymes in brown-rot fungi (*Coniophora puteana and Lanzites trabeum*), white rot fungi (*Phanerochaete chrysosporium* and *Trametes versicolor*) and soft rot fungi (*A. niger and T. reesei*), in actinomycetes (*T. fusca and Cellulomonas fimi*), anaerobic fungi (*Neocallimastix frontalis*) and aerobic bacteria (*Microbispora bispora* and *B. amyloliquefaciens*), whereas in certain anaerobic bacteria (*C. thermocellum* and *C. cellulolyticum*), they are generally secreted as complexed systems (cellulosomes) (Kuhad *et al.,* 2011; Lynd *et al.,* 2002; Matthew *et al.,* 2008).

Traditionally, three main enzymatic activities have been identified for cellulose hydrolysis (Du *et al.,* 2020; López-Mondéjar *et al.,* 2016). These include: (i) cellobiohydrolases, CBHs (EC 3.2.1.4 and EC 3.2.1.91), which processively cleave cellobiose units from one end (CBHI- reducing or CBHII- non-reducing) of the cellulase chain, (ii) endoglucanases, EGs (EC 3.2.1.4), which cleave at random internal regions of the cellulose chain to produce new chain oligosaccharides, and (iii) β-glucosidases, βgls (EC 3.2.1.21), which reduce the inhibitory effects of cellobiose and cellodextrans on enzyme activity (Den Haan *et al.,* 2013; Ganner *et al.,* 2012; Jalak *et al.,* 2012). On the basis of their amino

acid sequence and 3D structural similarities, the catalytic mechanisms of known cellulases has been classified into different GH families; 1, 3, 5, 6, 7, 8, 9, 12, 26, 44, 45, 48 and 74, as documented in the Carbohydrate-Active Enzymes database (CAZy; http://www.cazy.org). The major challenges associated with cellulases for their efficient deployment in the production of liquid fuels from lignocellulose include their low hydrolytic activities and their high production costs (Jørgensen *et al.,* 2007). Thus, there is a desperate need to develop strategies to reduce the cost of the hydrolysis process by improving our understanding of the process, and assessing cellulose hydrolysis under different conditions (temperature, pH, stability, enzyme/substrate ratios, enzyme combinations and protein loadings) to determine what the optimal conditions are for improved glucan saccharification (Herlet *et al.,* 2017). Thus, the first step in this process would be to investigate the biochemical and physico-chemical characteristics of the enzymes to be used in the saccharification of cellulose. This knowledge could provide a platform to better understand the conditions required for optimal enzyme activity, thus assisting the design of an ideal environment for future experiments (Nguyen and Quyen, 2010; Turon *et al*., 2008). Therefore, in the present study, a cellobiohydrolase I from *H. jecorina* (Cel7A), CBHI from *T. longibrachiatum* (Cel7A), CBHI from *C. stercorarium* (Cel48A), CBHII from a microbial source (Cel6A), CBHII from *C. thermocellum* (Cel5A), a cellulase containing three endoglucanases (EglA (Cel9); EglB (Cel12) and EglC (Cel74)), as well as three other endoglucanases (EG); *B. amyloliquefaciens* (Cel5A), *T. maritima* (Cel5A) and *T. reesei* (Cel7B) were subjected to detailed comparative biochemical characterisation studies and analysed for their substrate specificities.

3.2. Materials and methods

3.2.1. Materials

Avicel pH-101, carboxymethyl-cellulose (CMC), *para*-nitrophenyl substrates (4-nitrophenyl-β-D-cellobioside and -glucopyranoside), cellobiohydrolase I from *H. jecorina* (Cel7A) and cellulase containing three endoglucanases (EglA (Cel9); EglB (Cel12) and EglC (Cel74)) from *A. niger* were purchased from Sigma Aldrich (South Africa). The 1,4-β-D-cellopentaitol, CBHI from *T. longibrachiatum* (Cel7A), CBHII from a microbial source (Cel6A), and three endoglucanases (EG); *B. amyloliquefaciens* (Cel5A), *T. maritima* (Cel5A) and *T. reesei*. (Cel7B) were purchased from Megazyme™ (Ireland). CBHI from *C. stercorarium* (Cel48A) and CBHII from *C. thermocellum* (Cel5A) were purchased from NZYTech Ltd (Portugal). β-glucosidase (Nov 188) was purchased from Novozymes (Denmark).

The enzymes used in this study were selected according to their GH family affiliations, the source of the organism (fungal or bacterial) and their commercial availability.

3.2.2. Protein determination

The protein concentrations of the cellulases were determined by the Bradford method (Bradford, 1976). Bovine serum albumin (BSA) was used as a suitable protein standard. A standard curve was prepared using a concentration range between 0-1 mg/mL (Appendix 2). Protein samples (25 µL) were added to the Bradford reagent (230 µL) and incubated for 10 minutes at room temperature. Absorbance readings were measured at 595 nm in a microtiter plate reader (PowerWave$_X$ reader with KC Junior software, Biotek Instruments, U.S.A).

3.2.3. Bioinformatic characterisation of the cellulolytic enzymes

The protein sequences for the cellulases were retrieved from the Carbohydrate-Active Enzyme (CAZy) database, and their chemical and physical properties were determined using the ProtParam tool in the ExPASY bioinformatic portal (https://expasy.org/).

3.2.4. Enzyme characterisation studies

3.2.4.1. Substrate specificity determination

Avicelase and endo-glucanase activities were determined using the polymeric substrates; Avicel and CMC, whereas non-reducing end cellobiosidase activities were determined using cellopentaitol – a modified oligosaccharide. For Avicelase and endo-glucanase activities, the reaction mixtures contained 300 µL of the substrate (2.66% w/v) dissolved in sodium citrate buffer (50 mM, pH 5.0) and 100 µL of enzyme solution to make the final protein loading in the reaction 1.375 mg/g of Avicel. The reactions were conducted at 37°C for 24 hours and 1 hour for the Avicelase and CMCase assays, respectively. For the determination of cellopentaose activity, the reaction mixture contained 50 µL of enzyme, 50 µL of substrate (2% w/v) and 100 µL sodium citrate buffer (50 mM, pH 5.0). The assay was run at 37°C for 24 hours after which the sample was centrifuged for 5 minutes (16, 060 × *g*). The supernatant was used to measure the amount of reducing sugars released (as glucose equivalents) using a modified 3,4-dinitrosalicylic acid (DNS) method (Miller, 1959). The supernatant (150 µL) was added to 300 µl of DNS solution and incubated at 100ºC (Labnet AccuBlock digital dry bath) for 7 minutes, followed by cooling of the samples on ice for 10 minutes. The sample (supernatant + DNS solution) (250 µL) was pipetted into a 96 well plate and the absorbance was measured at 540 nm using the PowerWave$_X$ reader. The reducing sugars released were determined from a glucose standard curve (Appendix 2). The amount of glucose was measured by the glucose/peroxidase (GOPOD) method (K-GLUC, Megazyme, Ireland). The assay was performed in a 96 well plate and readings were taken at

340 nm, after incubating the assay at 37°C for 20 minutes. The glucose released was determined using a glucose standard curve (Appendix 2).

Glucosidase and cellobiosidase activities were assayed using 100 mM *p*-nitrophenyl-β-D-galactopyranoside (*p*NPG) and *p*-nitrophenyl-β-D-cellobioside (*p*NPC), respectively. The reaction mixture contained 25 µL enzyme, 5 µL *p*-nitrophenyl substrate (0.05 mM) and 220 µL sodium citrate buffer (50 mM, pH 5.0). The assay was conducted at 37°C for 15 and 30 minutes for *p*NPG and *p*NPC, respectively, and terminated by the addition of 250 µL sodium carbonate (2 M). The released *p*-nitrophenyl product was measured at 405 nm (Appendix 2). All enzyme assays were peformed in triplicate. One unit of enzyme activity was defined as the amount of enzyme required to liberate 1 µmol of product per minute, under the assay conditions specified.

3.2.5. Optimal conditions for cellulases activity

3.2.5.1. Temperature optimum and temperature stability

The temperature optima of the cellulolytic enzymes were determined using a range of temperatures (30-90°C) (Labnet AccuBlock™ digital dry bath) at pH 5.0 (50 mM sodium citrate buffer). The enzyme activities were set up as described in Section 3.2.4.1.

The thermostabilities of the individual cellulolytic enzymes were investigated in triplicate over time at 37 and 50ºC (Labnet AccuBlock™ digital dry bath) at pH 5.0 (50 mM sodium citrate buffer). Each enzyme was incubated at these two temperatures for different time intervals, up to 48 hours, and the residual activity was then determined. The enzyme activities were set up as described in Section 3.2.4.1.

3.2.5.2. pH optimum

A range of pH values (pH 3.0-9.0) was used to determine the optimal pH of the individual cellulolytic enzymes. The buffers used to generate this pH range were 50 mM sodium citrate (pH 3.0 - 6.0), 50 mM potassium phosphate (pH 6.0-8.0) and 50 mM Tris-HCl (pH 9.0). The enzyme assays were performed in triplicate at 37°C (Labnet AccuBlock™ digital dry bath) using the protocols described in Section 3.2.4.1.

3.3. Results

3.3.1. Protein determination

The protein concentrations of the individual enzymes were determined by the Bradford assay and are shown in Table 3.1 below. For this study, all the enzyme concentrations were standardised at 0.5 mg/mL. As can be seen in Table 3.1, *Hj*Cel7A, *Tl*Cel7A, *Cs*Cel48A, *Ct*Cel5A, microbial Cel6A, *Ba*Cel5A, *Tm*Cel5A, *Tr*Cel7B, *An*EG (Cel9, 12, 74) and βgl all had protein concentrations ranging between 1 and 66 mg/mL. Using the Bradford assay, the protein concentration of each cellulolytic enzyme (Table 3.1) was found to be similar to the amount reported by the suppliers in their product specification sheets.

Table 3.1. Protein determination of the cellulase enzymes as determined by the Bradford Assay (Bradford, 1976)

Enzyme	Protein Concentration (mg/mL)
*Hj*CBHI (Cel7A)	2.17
*Tl*CBHI (Cel7A)	3.18
*Cs*CBHI (Cel48A)	1
*Ct*CBHII (Cel5A)	1
Microbial CBHII (Cel6A)	5
*Ba*EG (Cel5A)	15.62
*Tm*EG (Cel5A)	2.37
*Tr*EG (Cel7B)	4
*An*EG (Cel9, 12, 74)	2.7 (in 100 mg powder)
βgl (Cel3A)	66

3.3.2. Bioinformatic characterisation of the cellulolytic enzymes

In silico characterisation of various physical and chemical parameters of the enzymes was assessed using the ProtParam tool in the ExPasy Bioinformatics Resource Portal (Gasteiger *et al.*, 2005). Table

3.2 describes the biochemical, physical and molecular properties derived from the predicted amino acid sequences of each cellulolytic enzyme investigated in this study.

All the GH family 5 cellulases (*Ct*Cel5A, *Ba*Cel5A and *Tm*Cel5A) belong to clan A and exhibit a retaining mechanism and share the same $(\beta/\alpha)_8$ structure. The CBHII (*Ct*Cel5A) has the higher MW (75.2 kDa), followed by *Ba*Cel5A (55.13 kDa) and then *Tm*Cel5A (37.84 kDa). The GH family 7 cellulases (*Hj*Cel7A, *Tl*Cel7A and *Tr*Cel7B) belong to clan A and B, exhibit a retaining mechanism and have a β-jelly roll structure (http://www.cazy.org/). *Tl*Cel7A has the highest MW of 65 kDa, whereas *Hj*Cel7A and *Tr*Cel7B have MWs of 54.07 and 42.30 kDa, respectively. The three GH 7 cellulases display a pI between 5.0 and 6.0. βgl also exhibits a retaining mechanism, has an α/β barrel structure, a molecular mass of 93.30 kDa and a pI of 4.66. The Cel6A from a microbial source and *Cs*Cel48A exhibit an inverting mechanism (http://www.cazy.org/). Cel6A has an (α/β) fold structure, whereas *Cs*Cel48A (belonging to GH-M) has an α/α 3D structure. Both enzymes have similar MWs (i.e. 42.30 kDa for Cel6A and 40.02 kDa for *Cs*Cel48A). *An*EG contains 3 families, including GH families 9, 12 and 74. The families 9 (Clan A) and 74 (Clan: not yet assigned) both display inverting mechanisms. GH 9 displays an α/α_6 3D structure, has a MW of 36.6 kDa and a pI of 4.36, whereas GH 74 displays a fold β-propeller structure, has a MW of 90.97 kDa and a pI of 4.35. On the other hand, the GH family 12 (ClanC) from *An*EG has a retaining mechanism, displays a β-jelly roll structure, has a MW of 25.87 kDa and a pI of 4.49.

Table 3.2. Summary of the data obtained from Uniprot, Protein Data Bank and ProtParam for the cellulolytic enzymes

Enzyme	Family	Clan	Mechanism	Structure	Mass (kDa)	pI	Uniprot ID	Amino acids
				Cellobiohydrolase (I/II)				
*Hj*Cel7A	7	B	Retaining	β-Jelly Roll	54.07	5.05	P62694	513
*Tl*Cel7A	7	B	Retaining	β-Jelly Roll	65	5.05	-	-
*Cs*Cel48A	48	GH-M	Inverting	(α/α)	40.02	5.12	D4N2U9	354
Cel6A	6	A	Inverting	(α/β) Barrel Fold	42.30	4.7		-
*Ct*Cel5A	5	A	Retaining	$(\beta/\alpha)_8$	75.2	-	-	-
				Endoglucanses				
*Ba*Cel5A	5	A	Retaining	$(\beta/\alpha)_8$	55.13	6.1	Q8RPQ6	499
*Tm*Cel5A	5	A	Retaining	$(\beta/\alpha)_8$	37.84	5.99	Q9X273	317
*Tr*Cel7B	7	B	Retaining	β-Jelly Roll	42.30	5.9	P07981	459
*An*EG	9, 12, 74	1. A 2. C 3. -	1. Inverting 2. Retaining 3. Inverting	1. $(\alpha/\alpha)_6$ 2. β Jelly Roll 3. 3. 7-Fold β-Propeller	1. 36.6 2. 25.87 3. 90.97	1. 4.36 2. 4.49 3. 4.35	1. O74706 2. A2R322 3. A2Q7T5	1. 331 2. 239 3. 861
				Beta-glucosidases				
βglC	3		Retaining		93.30	4.66	A8WE01	860

Any annotated post-translational modifications were not taken into account

3.3.3. Substrate specificity determination

The substrate specificities of the enzymes were determined according to the methods described in Section 3.2.4.1 and are summarised in Table 3.3. Among the CBHIs, *Tl*Cel7A displayed the highest activity on CMC (0.70 U/mg^{-1}) and Avicel (0.35 U/mg^{-1}). *Cs*Cel48A also displayed high CMCase activity (0.70 U/mg^{-1}), but very minimal Avicelase activity at 0.028 U/mg^{-1}. *Hj*Cel7A exhibited low Avicelase and CMCase activity of 0.35 and 0.10 U/mg^{-1}, respectively. *Hj*Cel7A also exhibited the highest *p*NPCase activity of 0.25 U/mg^{-1}, followed by *Tl*Cel7A (0.15 U/mg^{-1}) and then *Cs*Cel48A (0.02 U/mg^{-1}. All three CBHs displayed low activities on *p*NPG; 0.06 U/mg^{-1} (*Hj*Cel7A), 0.03 U/mg^{-1} (*Tl*Cel7A) and 0.09 U/mg^{-1} (*Cs*Cel48A), and displayed no cellopentaitol activity. Among the CBHIIs, *Ct*Cel5A displayed the highest CMCase and cellopentaitol activity of 4.90 U/mg^{-1} and 0.5 U/mg^{-1}, respectively, whereas the microbial Cel6A displayed very low activity on CMC (0.08 U/mg^{-1}), but higher cellopentaitol activity of 0.48 U/mg^{-1}. Both CBHIIs displayed very low activities on Avicel, *p*NPC, and *p*NPG.

Among the EGs assessed, *An*EG displayed the highest CMCase, Avicelase, glucosidase and cellopentaitol activity of 42.6 U/mg^{-1}, 0.41 U/mg^{-1}, 4.90 U/mg^{-1} and 2.05 U/mg^{-1}, respectively. *Ba*EG displayed the highest *p*NPC activity at 5.59 U/mg^{-1}, whereas *Tm*EG, *Tr*EG and *An*EG exhibited 0.85 U/mg^{-1}, 2.02 U/mg^{-1}, and 0.80 U/mg^{-1} activity on *p*NPC, respectively. *Ba*EG, *Tm*EG and *Tr*EG displayed similar CMCase activity at 21.3 U/mg^{-1}, 22.01 U/mg^{-1}and 20.16 U/mg^{-1}, respectively and displayed little to no activity on Avicel. *Ba*EG, *Tm*EG and *Tr*EG displayed 0.15 U/mg^{-1}, 0.20 U/mg^{-1} and 0.05 U/mg^{-1} glucosidase activity, respectively, and displayed 0.55 U/mg^{-1}, 1.04 U/mg^{-1} and 1.39 U/mg^{-1} cellopentoase, respectively.

βgl exhibited high glucosidase activity at 53.2 U/mg^{-1} and 0.30 U/mg^{-1} activity on CMC and *p*NPC, respectively. No detectable activity was observed on Avicel or cellopentaitol by the enzyme.

Table 3.3. Specific activities of cellulolytic enzymes on various cellulosic substrates. Values are presented as means ± S.D. (n=3). "Nd" = not detected

Enzyme	Specific Activity (U/mg^{-1})				
	CMC	**Avicel**	***p*NPC**	***p*NPG**	**Cellopentaitol**
			Cellobiohydrolase I (CBHI)		
*Hj*Cel7A	0.35	0.10	0.25	0.06	Nd
*Tl*Cel7A	0.70	0.35	0.15	0.03	Nd
*Cs*Cel48A	0.70	0.028	0.02	0.09	Nd
			Cellobiohydrolase II (CBHII)		
*Ct*Cel5A	4.90	0.026	0.017	0.08	0.50
Microbial Cel6A	0.08	0.05	0.023	0.03	0.48
			Endo-glucanase (EG)		
*Ba*EG (Cel5A)	21.30	0.062	5.59	0.15	0.55
*Tm*EG (Cel5A)	22.01	Nd	0.85	0.20	1.04
*Tr*EG (Cel7B)	20.16	0.16	2.02	0.05	1.39
*An*EG (Cel 9, 12, 74)	42.60	0.41	0.80	4.90	2.05
			Glucosidase		
βgl (Cel3A)	0.30	Nd	0.30	53.2	Nd

1 U is defined as the amount of enzyme releasing 1 µmol of product per minute unless stated otherwise

3.3.4. Optimum physico-chemical properties studies

3.3.4.1. Temperature optimum and stability studies

For determing the optimal temperature, the activities of the individual enzymes were determined at different temperatures ranging from 30°C to 90°C in 50 mM sodium citrate buffer (pH 5.0) containing 1% (w/v) of the substrate (Avicel, CMC or *p*NPC). The reducing sugars released at different temperatures were measured and the relative activity was calculated (defined as percentage of the maximal activity obtained). The thermostability of the enzymes was investigated by incubating the enzymes at 37 and 50°C for 48 hours in sodium citrate buffer (pH 5.0; 50 mM), containing 1% (w/v) of the substrate (Avicel, CMC or *p*NPC). The residual activity (measured in %) of the enzyme was determined under standard assay conditions and a blank/control was included. Figures 3.1 and 3.2 illustrate the temperature optima and thermal stability of each enzyme.

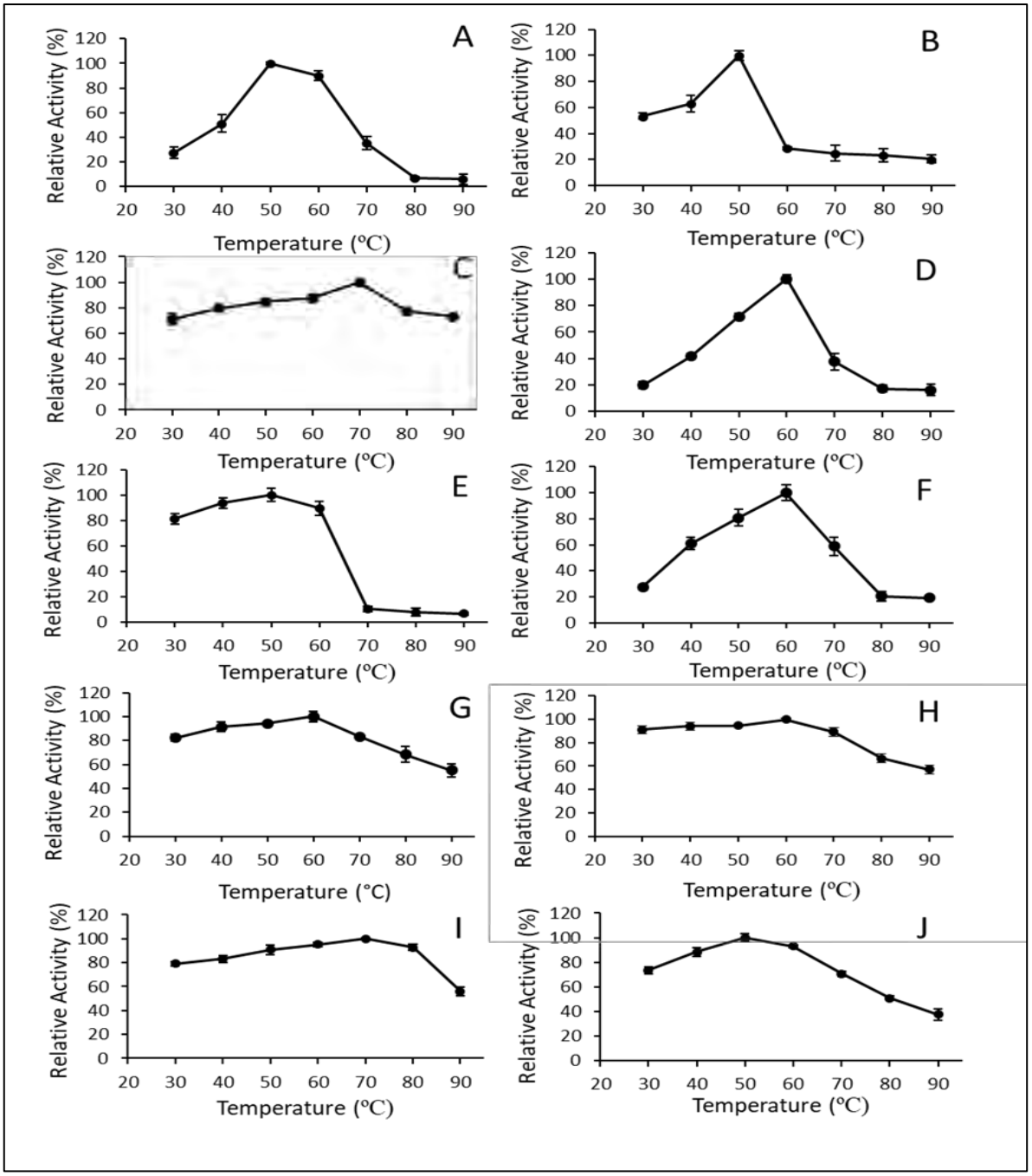

Figure 3.1. The effect of temperature on cellulase activities. Activities were measured against their respective substrates (Avicel, CMC or *p*NPG) in sodium citrate buffer (pH 5.0; 50 mM) at different temperatures (30°C - 90°C). (A) *Hj*Cel7A; (B) *Tl*Cel7A; (C) *Cs*Cel48A; (D) βgl; (E) microbial Cel6A; (F) *Ct*Cel5A; (G) *An*EG; (H) *Ba*Cel5A; (I) *Tm*Cel5A; and (J) *Tr*Cel7B. Values are presented as mean values ± Standard Deviation (SD) (n=3).

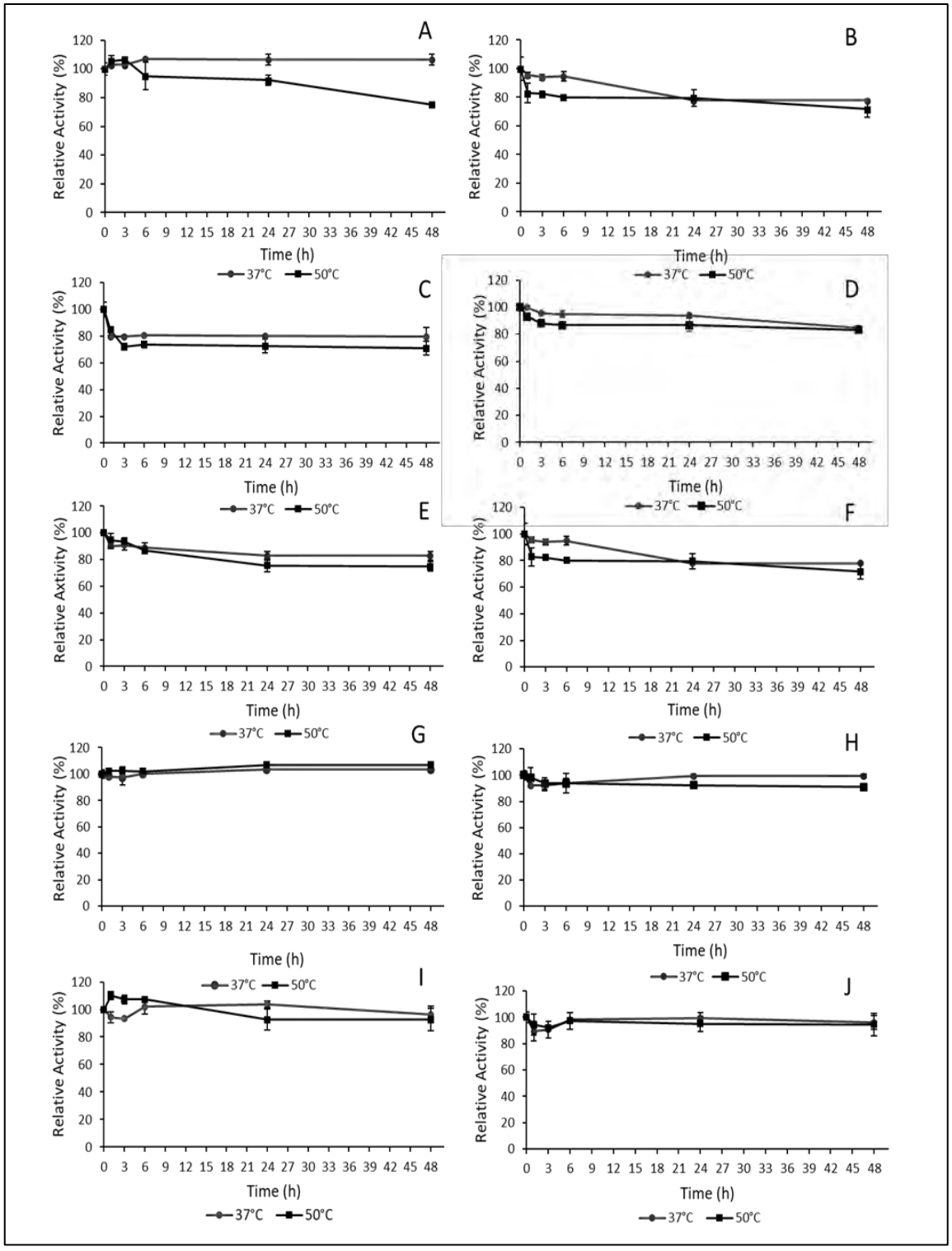

Figure 3.2. The thermostability profiles of the cellulolytic enzymes. Activities were measured against their respective substrates (Avicel, CMC or *p*NPG) in sodium citrate buffer (pH 5.0; 50 mM) at 37°C and 50°C. (A) *Hj*Cel7A; (B) *Tl*Cel7A; (C) *Cs*Cel48A; (D) βgl; (E) microbial Cel6A; (F) *Ct*Cel5A; (G) *An*EG; (H) *Ba*Cel5A; (I) *Tm*Cel5A; and (J) *Tr*Cel7B. Values are presented as mean values ± SD (n=3).

As can be seen in Figure 3.1, the enzymes had a temperature optimum between 50 and 70°C, where *Hj*Cel7A, *Tl*Cel7A, microbial Cel6A and *Tr*Cel7B exhibited a temperature optimum of 50°C, βgl, *Ct*Cel5A, *An*EG and *Ba*Cel5A displayed a temperature optimum of 60°C and *Cs*Cel48A and *Tm*Cel5A a temperature optimum of 70C°. All the enzymes were relatively stable at both 37°C and 50°C as seen in Figure 3.2.

3.3.4.2. pH optimum studies

Figure. 3.3 represents the pH optimum profiles of the enzymes used in this study.

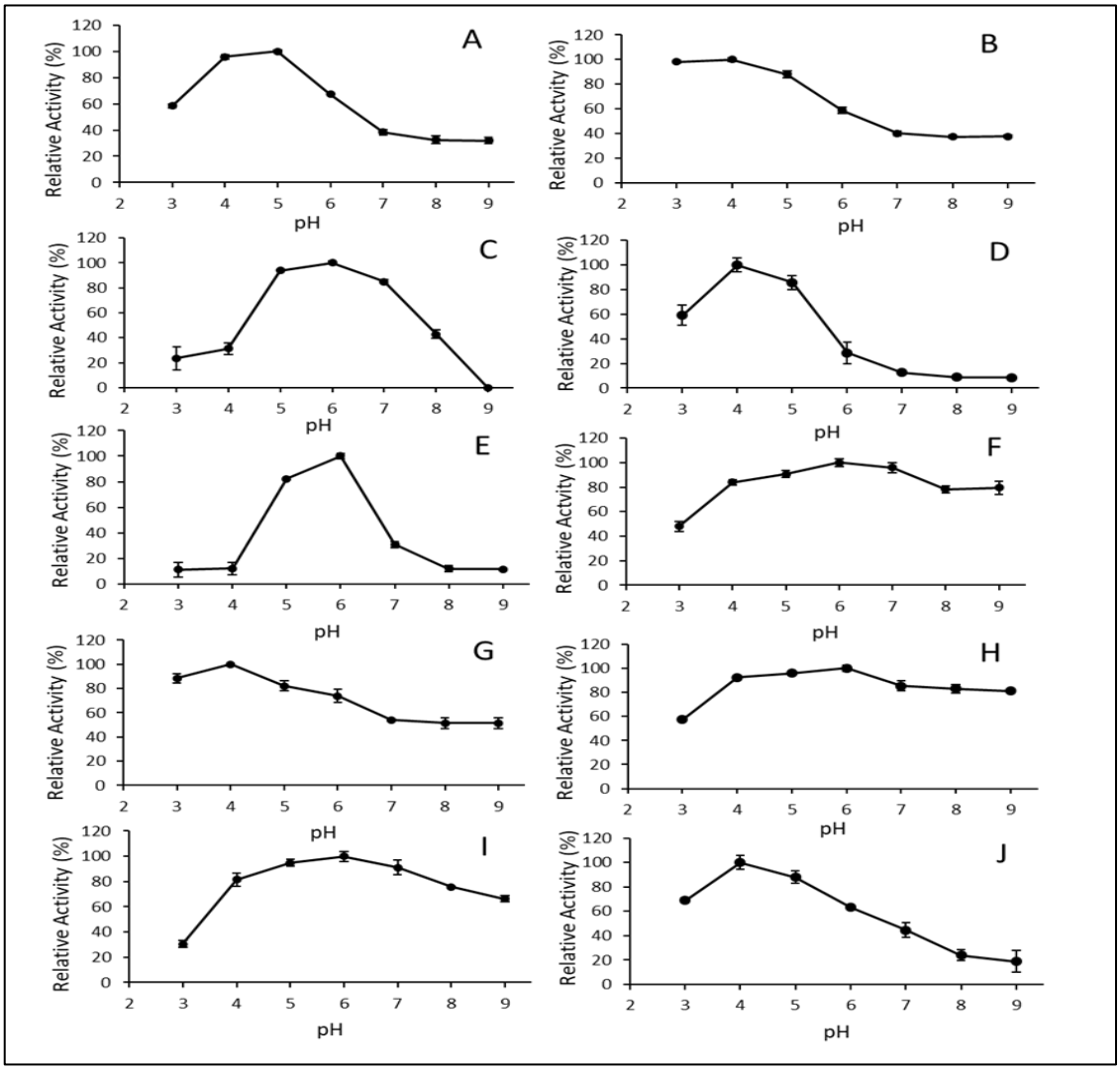

Figure 3.3. The effect of pH on cellulase activities. Activities were measured against the enzymes' respective substrates (Avicel, CMC or *p*NPG) in sodium citrate buffer (pH 3.0-6.0; 50 mM), phosphate buffer (pH 6.0-8.0; 50 mM) and Tris buffer (pH 9.0; 50 mM) at 50ºC. (A) *Hj*Cel7A; (B) *Tl*Cel7A; (C) *Cs*Cel48A; (D) βgl; (E) microbial Cel6A; (F) *Ct*Cel5A; (G) *An*EG; (H) *Ba*Cel5A; (I) *Tm*Cel5A; and (J) *Tr*Cel5A. Values are presented as mean values ± SD (n=3).

As can be seen in Figure 3.3, the enzymes exhibited a pH optimum range of 4.0-6.0 and retained more than 80% of their activity in this pH range. *Tl*Cel7A, βgl, *An*EG and *Tr*Cel7B displayed a pH optimum of 4.0, *Hj*Cel7A displayed a pH optimum of 5.0 and *Cs*Cel48A, microbial Cel6A, *Ct*Cel5A, *Ba*Cel5A and *Tm*Cel5A displayed a pH optimum of 6.0.

The results regarding the physico-chemical properties of the cellulases evaluated in this study are summarised in Table 3.4 below.

Table 3.4. Summary and comparison of the properties/characteristics of different GH family enzymes used in this study

Origin	Enzyme name	pH_{opt} [a]	T_{opt} [b] (°C)	Thermal stability$_{\tau}$ [c]	Family (GH)
H. jecorina	CBHI	5.0	50	48 h, 37 °C	7
				48 h, 50 °C	
T. longibrachiatum	CBHI	4.0	50	48 h, 37 °C	7
				48 h, 50 °C	
C. stercorarium	CBHI	6.0	70	48 h, 37 °C	48
				48 h, 50 °C	
A. niger	βgl	4.0	60	48 h, 37 °C	3
				48 h, 50 °C	
Microbial source	CBHII	6.0	50	48 h, 37 °C	6
				48 h, 50 °C	
C. thermocellum	CBHII	6.0	60	48 h, 37 °C	5
				48 h, 50 °C	
A. niger	EG	4.0	60	48 h, 37 °C	9, 12, 74
				48 h, 50 °C	
B. amyloliquefaciens	EG	6.0	60	48 h, 37 °C	5
				48 h, 50 °C	
T. maritima	EG	6.0	70	48 h, 37 °C	5
				48 h, 50 °C	
T. reesei	EG	4.0	50	48 h, 37 °C	5
				48 h, 50 °C	

[a] pH_{opt} – *pH optimum*
[b] T_{opt} (°C) – *Temperature optimum*
[c] $_{\tau}$ – *Thermal Stability*

3.4. Discussion

Various biochemical and physico-chemical properties, such as temperature and pH, influence the activities displayed by cellulases (Turon *et al.,* 2008). Therefore, it was essential to investigate these factors to understand the conditions required for optimal activity of the cellulases used in this study.

3.4.1. Substrate Specificity

To provide an indication of the mechanisms of individual enzymes during cellulose hydrolysis, the cellulases were evaluated for their endo- and/or exo-activity, using polysaccharide substrates (Avicel and CMC), modified oligosaccharides (cellopentaitol), as well as chromogenic substrates (*p*NPG and *p*NPC). From the characterisisation of the CBHs, *Hj*Cel7A and *Tl*Cel7A, both belonging to GH family 7, displayed the highest Avicelase activity of 0.10 and 0.35 U/mg, respectively. Cel7A (CBHI) is the major component of the cellulolytic system and is considered to be a highly processive exo-glucanase that initiates degradation from the reducing cellulose chain ends (Borisova *et al.,* 2015; Kipper *et al.,* 2005; Teeri, 1997). Structurally, CBHs within GH family 7 are multi-modular in nature, distinguished by tunnel-enclosed active sites with a roof consisting of elongated flexible loops (Borisova *et al.,* 2015; Boisset *et al.,* 2000; Taylor *et al.,* 2018). This feature enables the enzyme to initiate a processive mode of action along the cellulose chain, while cleaving numerous cellobiose units in a proccesive manner (Boisset *et al.,* 2000; Borisova *et al.,* 2015). Although Cel7A (CBHI) is considered to be a highly processive exo-glucanase, due to its inactivity towards substituted cellulose derivatives (CMC) (Bronnenmeier *et al.,* 1990), the results from this study revealed that these enzymes exhibited CMCase activity of 0.36 U/mg and 0.70 U/mg, respectively. These results infer that these enzymes could display minor endoglucanase activity, due to their ability to bind to soluble cellulose. However, this is a good indication that the CBHs used in this study only displayed residual CMC activity, since true CMC-ase enzymes (EGs) display a higher activity (2-100 U/mg) on the CMC substrate. Therefore, these results confirm that these enzymes are, in fact, true CBHs. Overall, *Tl*Cel7A exhibited 100% or greater performance on Avicel and CMC compared to *Hj*Cel7A. These findings were comparable to a study by Taylor *et al.* (2018), who compared the activities of CBHs from *T. reesei* and *Penicillium funiculosum* and found that *Pf*Cel7A exhibited 60% greater performance on biomass than *Tr*Cel7A. The majority of the reported differences were observed with differences in length and sequence of loops around substrate-binding paths, catalytic centres or product binding sites, ultimately affecting the accessibility of the active site, processivity, product inhibition, endo-activity initiation and the release of non-productively bound enzyme (Borisova *et al.,* 2015; Ogunmolu *et al.,* 2017; Payne *et al.,* 2015).

On the other hand, *Cs*CBHI (Cel48A) exhibited low Avicelase activity (0.028 U/mg). The low Avicelase activity of Cel48A observed in this study was in agreement with previous studies, which reported low or no activity of GH family 48 enzymes on crystalline cellulose (10 times less than Cel7A cellulases) (Berger *et al.,* 2007; Irwin *et al.,* 2000; Kostylev and Wilson, 2014; Sánchez *et al.,* 2004). Interestingly, Cel48A exhibited high CMCase activity (0.70 U/mg). According to Guimarães *et al.* (2002) and Parsiegla *et al.* (1998), the catalytic domains of *C. thermocellum* (Cel48S) and *C. cellulolyticum* (Cel48F), which have 54-56% amino acid sequence identity to Cel48A, have previously been solved and found to be structurally different from other processive cellulases. Their 3D structures consist of an $(\alpha/\alpha)_6$ helix barrel fold, where the active site is situated at a junction between a tunnel (7 subsites) and a cleft (3 subsites) (Arai *et al.,* 2003). It has been proposed that the flexible loops forming the tunnel of Cel48 starts as an open tunnel, allowing the enzyme to initiate an endo-cleavage attack on an exposed cellulose chain, followed by the processive hydrolysis of the cellulose chain (Irwin *et al.,* 2000; Reverbel-Leroy *et al.,* 1997).

Furthermore, the exo-mode of action of the CBHIs towards *p*NPC – a synthetic substrate conjugated with chromogenic *p*-nitrophenol at the reducing end of the cellulose chain was measured. The specific activities of *Hj*CBHI (Cel7A) and *Tl*CBHI (Cel7A) were 0.25 U/mg and 0.15 U/mg, respectively. Thus, demonstrating catalytic properties representative of GH family 7 cellobiohydrolases (Kipper *et al.,* 2005; Woon *et al.,* 2017). *Cs*Cel48 showed minimal activity towards *p*NPC (0.02 U/mg), which was in accordance with a study by Sánchez *et al.* (2004), who reported that the GH48 enzymes show very low and restricted activity on most common cellulosic substrates.

In contrast to Cel7A, which initiates cellulose degradation from the reducing end of the cellulose chain, Cel6A (a CBHII) is known for its specific preference for the non-reducing ends of the cellulose chain (Boisset *et al.,* 2000; Borisova *et al.,* 2015). In this study, a CBHII (Cel5A) was used. Although the activity indicated for most characterised GH5 enzymes is endo-β-1,4-glucanase activity, it has been reported that *C. thermocellum* exhibits exo-acting cellobiohydrolase activity (Aspeborg *et al.,* 2012; Zverlov *et al.,* 2003).

Although CBHI and CBHII both possess enclosed active sites, CBHII exhibits a different 3D structure compared to CBHI, whereby the catalytic core of CBHII is half as long (20 Å) as CBHI (50 Å) and has four distinct binding sites (A-D) (Harjanpaa *et al.,* 1996; Igarashi *et al.,* 2009). Generally, the activities of CBHIIs are detected with soluble oligosaccharides (chromogenic substrates), where the chromogenic aryl residue is liberated from the reducing end of the cellulose chain (Harjanpaa *et al.,* 1996; Zverlov *et al.,* 2003). The specific activities of microbial CBHII (Cel6A) and *Ct*CBHII (Cel5A)

towards cellopentaitol were 0.48 and 0.50 U/mg, respectively. As expected, the microbial CBHII (Cel6A) and *Ct*CBHII (Cel5A) displayed no *p*NPCase activity since they are not reducing-end dependent processive enzymes, and also exhibited low Avicelase activities of 0.05 U/mg and 0.026 U/mg, respectively. This was similar to what has previously been reported in the literature for CBHII; 0.016 U/mg (Poidevin *et al.,* 2013) and 0.027 U/mg of Avicelase activity (Billard *et al.,* 2012*;* Tomme *et al.,* 1988). Cel6A also exhibited minor endoglucanase (CMC) activity (0.08 U/mg) compared to Cel5A (4.90 U/mg), probably due to differences in their active site tunnels. Studies have reported that this enzyme (GH5) behaves as an endo-glucanolytic cellobiohydrolase (multi-functional enzyme). This may be attributable to its typical $(\alpha/\beta)_8$-barrel structure, with an open active cleft topology (Boisset *et al.,* 2000; Boer and Koivula *et al.,* 2003; Kostylev and Wilson, 2012; Igarashi *et al.,* 2009). Another noteworthy feature of many GH5 family proteins is that their protein sequence may include additional modules with different functions (particulary CBMs) (Aspeborg *et al.,* 2012). According to Aspeborg *et al.* (2012), depending on the location (N- or C- terminal) of the CBM of the GH5 module, the catalytic domains may target different tissue components.

In contrast to the tunnel structures of CBHs, the catalytic sites of EGs exhibit extended open substrate-binding clefts, offering an easier entry to the cellulose chain (Kleywegt *et al.,* 1997). Thus, CMC is the preferred substrate for determining EG activity, since CMC contains carboxymethyl substituents that can only enter active sites with an open conformation (Leis *et al.,* 2017; Varrot *et al.,* 1999; Zverlov *et al.,* 2003). As expected, CMC was cleaved by the EGs (*Ba*EG, *Tm*EG, *Tr*EG and *An*Eg), which randomly hydrolyse internal β-1,4-linkages of the cellulose chain (Leis *et al.,* 2017). The activities of *Ba*EG, *Tm*EG, *Tr*EG and *An*Eg towards CMC were 21.3, 22.01, 20.16 and 42.6 U/mg, respectively.

*Ba*EG, *Tr*EG and *An*EG also exhibited Avicelase activity of 0.062, 0.16 and 0.41 U/mg, respectively. These enzymes displayed higher Avicelase activity compared to the CBHI enzymes assessed (excluding *Tl*Cel7A), as well as all the CBHII enzymes assessed in this study, thus, suggesting that these EGs exhibit exo-glucanase activity on micro-crystalline cellulose (Teeri, 1997). In addition, Kim *et al.* (1995) reported that endoglucanases from a *Bacillus* sp., and also various fungi, may exhibit Avicelase activity in addition to CMCase activity with the help of an exo-activity resident in the same molecule. Studies have revealed that EGs may exhibit processive behaviour due to a CBM attached to the catalytic domain, and have performed studies to support the critical role of CBM for EG processivity (Aspeborg *et al.,* 2012; Zheng and Ding, 2013). Structural data has also revealed that subtle changes in the loop extensions surrounding the active site can result in exo-glucanase activity by EGs (Leis *et al.,* 2017). However, structural data is required to confirm this statement.

All four endoglucanases exhibited CBHI (*p*NPC) and CBHII (cellopentaitol) activities. Their specific activities on *p*NPC were 5.59 U/mg, 0.85 U/mg, 2.02 U/mg and 0.40 U/mg for *Ba*EG, *Tm*EG, *Tr*EG and *An*EG, respectively and 0.55 U/mg, 1.04 U/mg, 1.39 U/mg and 2.05 U/mg for *Ba*EG, *Tm*EG, *Tr*EG and *An*EG on cellopentaitol, respectively. Although the mode of processivity seems to be more common in CBHIs, studies have reported that EGs can change their character to facilitate a processive mode of action on recalcitrant substrates (Jeon *et al.,* 2012; Zheng and Ding, 2013). Their ability to cleave internal sites of the cellulose chain, and to release soluble oligosaccharides prior to separating from the cellulose chain has resulted in the introduction of a subclass of cellulases, referred to as processive endo-cellulases (Kostylev and Wilson, 2014; Reverbel-Leroy *et al.,* 1997; Yang *et al.,* 2016). To further confirm the processive behaviour of the EGs in this study, thin-layer chromatography (TLC) or high-performance liquid chromatography (HPLC) could have been performed to assess whether cellobiose and cellotriose were products of cellopentaitol hydrolysis.

As expected, βgl displayed high specific activity towards *p*NPG (53.2 U/mg). This is because *p*NPG is specific for βgl, since *p*-nitrophenol is a good leaving group and the hydrolysis of this substrate does not require the enzyme to be specific to the β-1,4-glycosidic bonds (Decker *et al.,* 2001; Larue *et al.,* 2008).

Although enzymes are substrate specific, it is apparent that the division into endo- and exo-glucanases in many cases is not absolute, and that enzymes can use different catalytic mecahnisms within the same active site. This emphasises the central role of divergent evolution among enzymes (O'Brien and Herschlag, 1999; Rauwerdink and Kazlauskas, 2015).

3.4.2. Physico-chemical characterisation of the cellulolytic enzymes

According to Boer and Koivula (2003), the activity profile of an enzyme is dependent on its temperature and pH, therefore, these are the major factors that need to be considered when performing enzyme studies so that we can beter understand how enzymes function under different physico-chemical conditions. This information is fundamental to assess whether an enzyme is suitable for application in a biotechnological process (Antov *et al.,* 2017; Herlet *et al.,* 2017). As cellulose requires multiple cellulases for its efficient hydrolysis, it is crucial that all enzymes in this "one-pot" reaction are compatible with one another and under the employed process conditions (pH and temperature) (Herlet *et al.,* 2017). According to Herlet *et al.* (2017), applying the most suitable conditions for all enzymes in a "one-pot" reaction can ultimately reduce the amount of enzymes required. This is important for improving the feasibility of enzymatic bioconversion (Antov *et al.,* 2017). The pH

temperature and pH optimum of the cellulases used in this study were assessed and are described below.

_Hj_Cel7A

The temperature optimum of *Hj*Cel7A (CBHI) used in this study (Figure 3.1A) was similar to that (50°C) exhibited by the same enzyme in a report by Bülbül and Karakuş (2013). Thermal stability studies (Figure 3.2A) revealed that *Hj*Cel7A retained 100% activity at 37°C for 48 hours, but wasn't as stable at 50°C. This was in agreement with to Goedegebuur and colleagues (2017), who reported thar *H. jecorina* generally does not have enough stability beyond 50°C. pH studies (Figure 3.3A) showed that *Hj*Cel7A displayed optimal activity at pH 5.0, which was in agreement with previous studies (Boer and Koivula, 2003; Busto *et al.,* 1996; Pingali *et al.,* 2011).

_Tl_Cel7A

Similar to our *T. longibranchiatum* Cel7A, Cel7A from *H. grisea* var. *thermoidea* exhibited temperature and pH optima of 50°C (Figure 3.1B) and 4.0 (Figure 3.3B), respectively (Takashima *et al.,* 1999), while Cel7A from *T. emersonii* displayed a temperature optimum of 60 - 65°C (Voutilainen *et al.,* 2010). *Tl*Cel7A showed good thermal stability at 37°C and 50°C (Figure 3.3B), which was in agreement with Leghlimi *et al.* (2013).

_Cs_Cel48A

The thermophilic bacterium *C. stercorarium* Cel48A used in this study displayed temperature and pH optima of 70°C (Figure 3.1C) and 6.0 (Figure 3.3C), respectively. These results were similar to the findings of Broeker *et al.* (2018), who reported this enzyme to be most active at 60-70°C and at pH 5.0-6.5.

βgl

The temperature optima of the *A. niger* βgl used in this study (Figure 3.1D) was similar to that (60°C) reported for the same enzyme by Chauve and co-workers (Chauve *et al.,* 2010) and Le Traon-Masson and Pellerin (1998). The βgl in our study was more thermo-stable (Figure 3.2D) than the solid-state fermentation expressed and purified version described by Junior *et al.* (2014). Possible reasons for the lowered stability of their βgl could be due to the fact that, upon purification, the protein concentration was lowered and did not contain other proteins and preservatives which may have been found in the βgl containing Novozyme 188 commercial preparation (Junior *et al.,* 2014; Malgas, 2017). Similar to the findings of Le Traon-Masson and Pellerin (1998), the βgl used in this study displayed a pH

optimum of 4.0 (Figure 3.3D), while Narasimha and colleagues (Narasimha *et al.,* 2016) reported a pH optimum of 5.0, for βgl from *A. niger.*

Microbial Cel6A

Contrary to other findings for Cel6A homologs, the microbial Cel6A characterised in this study exhibited temperature and pH optima values of 50°C (Figure 3.1E) and pH 6.0 (Figure 3.3E), respectively, while Bukhtojarov and co-workers reported temperature and pH optima values of 60°C and 5.0, respectively, for *Chrysosporium lucknowense* Cel6A (Bukhtojarov *et al.,* 2004); whereas Takahashi *et al.* (2010) reported that Cel6A from *Magnaporthe oryzae* displayed a temperature and pH optimum of 40°C and 4.0, respectively.

***Ct*Cel5A**

Similar to our Cel5A from *C. thermocellum*, Fierobe *et al.* (1991) and Leis *et al.* (2017) reported that *C. thermocellum* exhibited a temperature and pH optima of 60°C and pH 5.5-5.8, respectively (see Figures 3.1F and 3.3F).

***An*EG**

The temperature optimum (50-60°C) exhibited by the Egl preparation used in our study (Figure 3.1G) coincided well with the optimal temperature for EglA (50-65°C) reported by Quay *et al.* (2011) and Dobrev and Zhekova (2012), respectively, and EglB (60°C) reported by Li *et al.* (2012). In this study, Egl displayed a pH optimum of 4.0 (Figure 3.3G), and this was similar to that of a recombinant EglB reported by Li *et al.* (2012).

***Ba*Cel5A**

The temperature optimum (60°C) (Figure 3.1H) and pH optimum (pH 6.0) (Figure 3.3H) of the *B. amyloquefaciens* EG (Cel5A) used in this study was similar to that exhibited by the same enzyme reported by Deb *et al.* (2013), El-tayeb *et al.* (2007) and Ye *et al.* (2017). However, Nusrat and Rahman (2007) found the pH optimum for this enzyme to be at pH 7.0.

***Tm*Cel5A**

The hyperthermophilic bacteria *T. maritima* characterised in this study exhibited a temperature optimum of 70°C (Figure 3.1I), while a temperature optimum of 80°C has been reported for the same enzyme by numerous studies (Hong *et al.,* 2007; Kim *et al.,* 2010; Wang *et al.,* 2018). Our pH optimum data (pH 6.0) (Figure 3.3I) coincided well with the pH optimum for EG (Cel5A) from *T. maritima* reported by Basit and Akhtar (2018), as well as Kim *et al.* (2010).

***Tr*Cel7B**

There was a slight difference between our temperature optimum (50°C) for *Tr*Cel7B used in this study (Figure 3.1J) compared to that of Chokhawala *et al.* (2015), who determined that EG from *T. reesei* displayed optimal activity at 60°C. However, Busto and co-workers (Busto *et al.,* 1996) reported that the optimal temperature for *T. reesei* cellulases was between 50 and 70°C, and reported maximal activity at 60°C. The pH optimum (4.0) (Figure 3.3J) coincided well with those studies performed by Boer and Koivula (2003), and Busto *et al.* (1996), who reported that cellulases from *T. reesi* exhibited maximal activity between pH 4.0 and 5.0

3.5. Conclusions

Glycoside hydrolases are important for various industrial and scientific applications (Herlet *et al.*. 2017). The aim of this chapter was to assess characteristics of the different cellulases (*Hj*Cel7A, *Tl*Cel7A, *Cs*Cel48A, microbial Cel6A, *Ct*Cel5A, *Ba*Cel5A, *Tm*Cel5A, *Tr*Cel7B, *β*gl and *An*EG) to better understand their behaviour (substrate specificities), as well as determine the optimal conditions required for their cellulolytic activities.

To better understand the mechanisms of the individual enzymes during cellulose hydrolysis, the cellulases were evaluated for their endo-activity and/or exo-activity, using polysaccharide substrates (Avicel and CMC), a modified oligosaccharide (cellopentaitol), as well as the chromogenic substrates (*p*NPG and *p*NPC) (Table 3.3). Although enzymes are substrate specific, it is apparent that the division into endo- and exo-glucanases in many cases is not always absolute (cross activity was observed), and that enzymes can use different catalytic mechanisms within the same active site (O'Brien and Herschlag, 1999; Rauwerdink and Kazlauskas, 2015).

In most cases, similar conclusions were drawn from our physico-chemical data compared to that previously reported in literature. Based on their physico-chemical properties, all the cellulases assessed in this study performed reasonably well under the standard operating conditions of pH 5.0 and 50°C. Thus, it is possible to use these enzymes together (or various combinations of these enzymes) under the same reaction conditions (at the standard industrial conditions), as all the enzymes were active and stable at these conditions (pH 5.0; 50°C). The data in this chapter provided information on the conditions that was used in subsequent experiments and served to facilitate a better understanding and interpretation of the synergistic interactions that occured between these enzymes on model (defined) cellulose substrates in the next chapter, Chapter 4.

Chapter 4: Enzyme synergy between exo- and endo- acting cellulases on defined substrates

4.1. Introduction

Cellulolytic organisms produce an array of cellulases that work synergistically to depolymerise cellulose. As discussed previously, the three main enzymatic activities that have been identified for cellulose hydrolysis include CBHs, EGs and βgls (Den Haan *et al.,* 2013; Ganner *et al.,* 2012; Teeri *et al.,* 1997). Although each individual component of the cellulase system plays a pivotal role in cellulose depolymerisation, it is important to understand that the activity of a single enzyme cannot effectively hydrolyse the tightly packed crystalline polymer chains (Jalak *et al.,* 2012; Horn *et al.,* 2012; Murashima *et al.,* 2003). Efficient enzymatic hydrolysis of cellulose can only be achieved by a complete and balanced composition of cellulases which cooperate with each other to depolymerise the substrate (Fang *et al.,* 2019). The model generally used to describe this type of collaboration is referred to as enzyme synergism (Lynd *et al.,* 2002; Malgas *et al.,* 2017; Van Dyk and Pletschke, 2012).

Synergy between cellulolytic enzymes has been documented previously, including: i) exo-exo synergism, ii) processive endo-endo synergism, iii) endo-exo synergism, and iv) intramolecular synergy between catalytic domains and cellulose binding domains (CBMs) (Boisset *et al.,* 2000; Henrissat *et al.*, 1985; Jalak *et al.,* 2012). Synergy between endo- and exo-cellulases is the most extensively studied type of synergism, whereby EGs are believed to stimulate the activity of CBH by exposing or generating new chain ends for their processive action (Jalak *et al.,* 2012; Kosytlev and Wilson, 2014; Kurašin and Väljamäe, 2011). Although this phenomenon holds true to a large degree, this is an over-simplification of a much more complicated process (Kostylev and Wilson, 2012). Despite the numerous research efforts and various hypotheses made towards elucidating the synergism between cellulases on crystalline cellulose, the synergistic mechanisms by which cellulases hydrolyse cellulose are not yet fully complete or comprehensive (Jalak *et al.,* 2012; Kostylev and Wilson, 2012). Due to the overlapping functions and conflicting natures of endo- and exo-glucanases, the questions as to how these enzyme synergise at a molecular level, or why only a limited number of CBHs and EGs exhibit synergism, remain a constant challenge (Adsul *et al.,* 2020; Kurašin and Väljamäe, 2011; Yang *et al.,* 2016). Moreover, only a few studies have investigated the synergistic relationships between fungal and bacterial enzymes, thus there is a lack of understanding of how the structural and mechanistic features of various GH families affect the synergistic relationship of a given cellulase cocktail for efficient cellulose hydrolysis. Despite the extensive amount of research carried out over

the past few years, little is known about the enzymatic mechanisms underpinning the nature of synergistic interactions between bacterial and fungal cellulases, i.e. how these enzymes function to depolymerise the diversity of the substrate - also, do all endo- and exo-acting enzymes act synergistically, and what are the factors that govern enzyme synergism? Furthermore, optimising the composition of cellulase mixtures is an effective method to increase/improve their hydrolytic ability and reducing protein loading during lignocellulose degradation.

The aim of this study was to provide insights into how the molecular mechanisms of cellulases from different GH families (i.e. GH 3, 5, 6, 7, 9, 12, 48 and 74) and various microbial sources govern synergism, by means of mapping various CBH to EG interactions. This rational approach of screening for maximal compatibility between different GH families could ultimately provide a platform for a better understanding of the specific interactions between the enzymes of interest and how the complex synergistic activities of different enzymes assist each other in degrading cellulose. Consequently, this can shed light on designing synergistic enzyme cocktails which are tailored to effectively convert biomass into fermentable sugars, thus reducing the overall cellulase loadings required to achieve efficient biomass conversion.

4.2. Materials and methods

4.2.1. Materials

The enzymes used in this study were selected according to their GH family affiliations, the source of organism (fungal or bacterial) and their commercial availability. All the enzymes showed > 95% purity on SDS-PAGE. The preparation on SDS materials are provided in Appendix 3.

4.2.2. Synergy studies

The relationships between the enzymes were determined by setting up various reactions containing different protein mass ratios of exo/endo- and exo-cellulases. The total protein loading for all enzyme cocktail experiments was kept consistent at 1.375 mg protein/g of Avicel and was supplemented with βgl (at a 10% mass ratio of the total protein loading) to ensure complete hydrolysis of cellobiose. The reactions were carried out in 400 µL reaction volumes, containing 2% (w/v) substrate (Avicel) suspended in sodium citrate buffer (50 mM; pH 5.0). The reactions were conducted at 37°C with mixing at 25 rpm for 24 hours.

The hydrolysis was terminated by heat-deactivating the enzymes at 100°C for 5 minutes. Hydrolysis controls consisted of the substrate without the enzyme, and enzyme controls consisted of enzyme

without the substrate. The samples were stored at 4°C for further analysis. Analyses of reducing sugars and glucose released were conducted according to the methods described in Section 3.2.4.1. All enzyme hydrolysis assays were performed in triplicate.

4.2.2.1. Determination of the optimal CBH1: CBHII ratio (exo-exo synergy) and the effect of CBHII swapping on synergy

We investigated the exo-exo synergy between CBHI (*Tl*Cel7A) and CBHII (microbial Cel6A) to determine the optimal CBH (CBHI + CBHII) cocktail required for cellulose hydrolysis. CBHII (microbial Cel6A) was swapped with a CBHII from a different GH family and enzyme source (*Ct*Cel5A) in order to compare their hydrolysis and synergistic profiles. Analyses for reducing sugars and glucose released were conducted according to the methods described in Section 2.4.3.1. The CBHI:CBHII combination that resulted in increased cellulose hydrolysis and a good degree of synergy was chosen as the benchmark Cmix for subsequent experiments.

4.2.2.2. Synergistic interactions between endo- and exo- acting cellulases from different GH families

The benchmark Cmix CBHI (*Tl*Cel7A):CBHII (microbial Cel6A or *Ct*Cel5A) was swapped with the activities of four different EGs (*Ba*Cel5A, *Tm*Cel5A, *Tr*Cel7B, and mixture of *An*Cel9, 12 and 74) at different protein ratios, and assessed for their capacity to liberate reducing sugars and glucose (individually, and in combination) from Avicel as described in Section 3.2.4.1 (see Appendix 4A for the specific enzyme combinations).

4.2.2.3. CBHI swapping

The CBHI (*Tl*Cel7A) in the benchmark mix was swapped with CBHIs from different GH families or microbial sources (*Hj*Cel7A or *Cs*Cel48A) to assess whether this approach of CBHI swapping had any influence on the synergism established between endo- and exo-cellulases. Analyses for reducing sugars and glucose released were conducted according to the methods described in Section 3.2.4.1. All enzyme hydrolysis assays were run in triplicate. The ratio of 3:1 between CBHI: CBHII was kept consistent throughout all the experiments (this ratio was selected based on the data obtained from the first set of experiments performed between CBHI and CBHII, which also agreed well with literature). Figure 4.1 illustrates a simplification of the synergy approach used in this study.

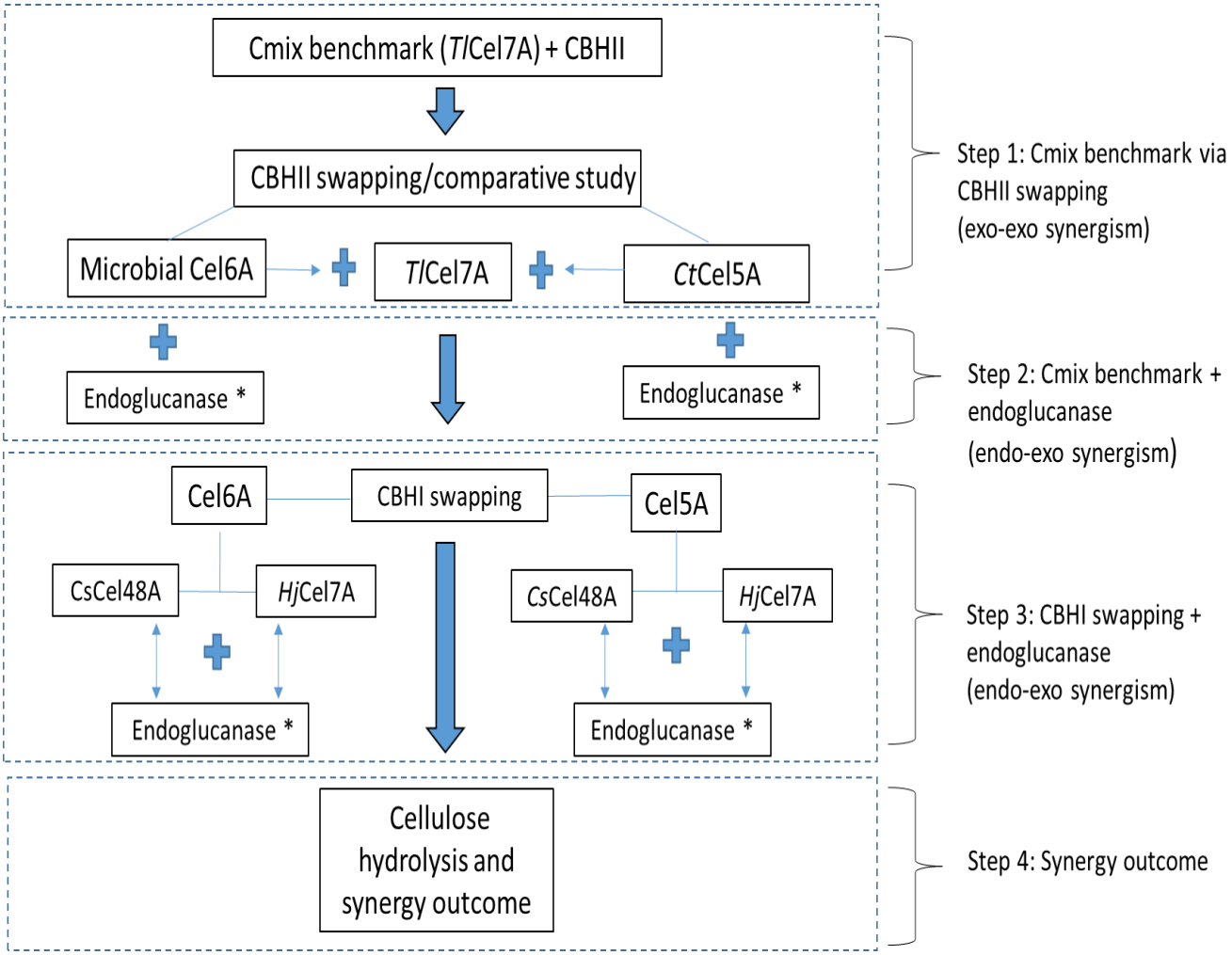

*Endoglucanases: *Ba*EG (Cel5A); *Tm*EG(Cel5A); *An*EG (Cel9, 12, 74); *Tr*EG (Cel7B)

Figure 4.1: Strategy for screening cellulases from different glycosyl hydrolases and microbial sources using a cellulase swapping approach to further our understanding of enzyme synergism.

4.2.3. Calculation of the degree of synergy (DS)

The degree of synergy was calculated as the ratio between the activity that was observed to be produced by the combination of enzymes performing in synergism and the theoretical sum of the activities produced by the individual enzymes (Jalak *et al.,* 2012; Van Dyk and Pletschke, 2012).

$$DS = (total\ activity\ of\ enzyme\ 1\ and\ 2) / (activity\ of\ enzyme\ 1) + (activity\ of\ enzyme\ 2)$$

The degree of synergy assists in determining whether one enzyme renders the substrate more accessible for another enzyme (Van Dyk and Pletschke, 2012). The three outcomes for DS are: i) DS > 1, when enzymes act synergistically to degrade a substrate; ii) DS = 1, when the activity of one enzyme does not facilitate the activity of another enzyme: i.e. no synergy, and iii) DS < 1, when

enzymes do not interact synergistically but rather display competitive behaviour (enzymes competing for the same binding sites) (Van Dyk and Pletschke, 2012).

4.2.4. Data analysis

One-way analysis of variance (ANOVA) was used for the evaluation of significant activity increases exhibited by enzyme combinations (with respect to reducing sugars and glucose released) compared to those displayed by 100% protein loading of the most active single enzyme cocktail. All pairwise comparison procedures were based at 95% or 99% confidence level ($p = 0.01$ or $p = 0.05$) and conducted using the Data analysis feature in Microsoft Excel.

4.3. Results

4.3.1. Exo-exo synergy between CBHI (*Tl*Cel7A) and CBHII (microbial Cel6A)

Exo-exo synergy between CBHI (*Tl*Cel7A) and CBHII (microbial Cel6A) was investigated to determine the optimal CBH mixture (CBHI + CBHII) cocktail required for cellulose hydrolysis (Figure 4.2A). We then further performed a comparative study by swapping CBHII (microbial Cel6A) with a CBHII from a different GH family and source (*Ct*Cel5A) in order to compare their hydrolysis and synergistic profiles with one another (Figure 4.2B).

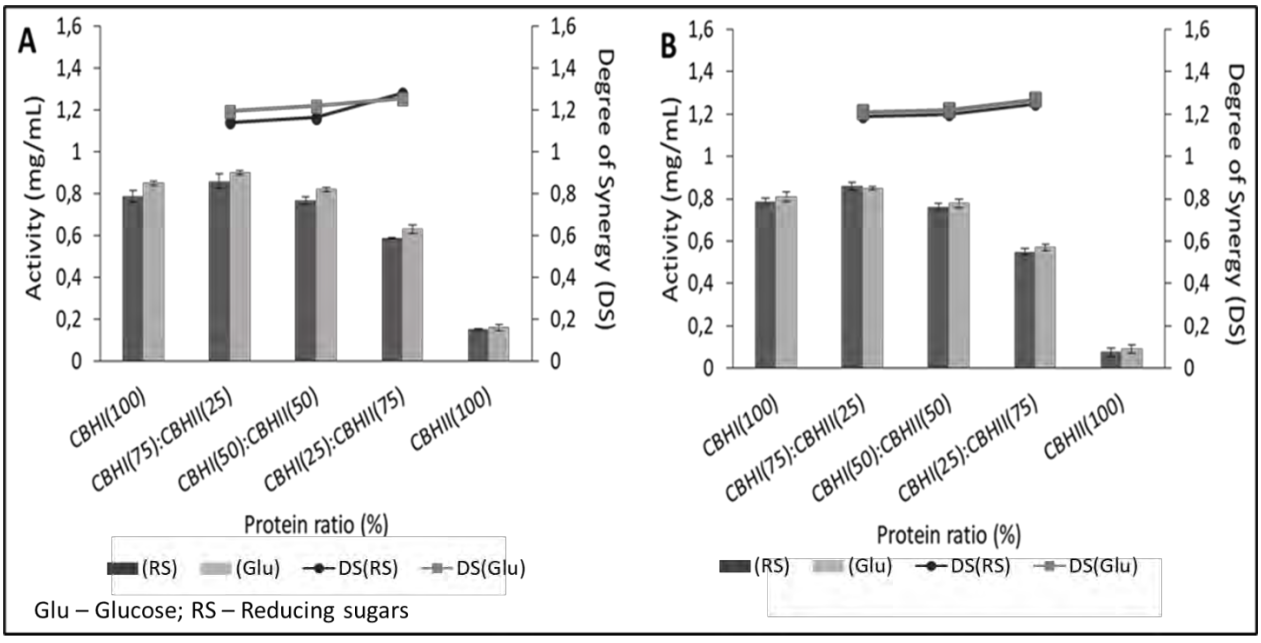

Figure 4.2. Synergistic degradation of Avicel by various ratios of *Tl*Cel7A (CBHI) and microbial Cel6A (CBHII) **(A)**, and *Tl*Cel7A (CBHI) and *Ct*Cel5A (CBHII) **(B)**. Assays were performed in sodium citrate buffer (0.05 M; pH 5.0) and incubated at 37°C for 24 h. Values represented as mean values ± SD. ($n = 3$).

The results show that the concerted action of CBHI (*Tl*Cel7A) and CBHII (microbial Cel6A) resulted in a synergistic effect, and that the combination of CBHI and CBHII at a protein ratio of 75% to 25%, respectively, was significantly ($p < 0.01$) better at releasing sugars during Avicel hydrolysis compared to when the enzymes were used individually (100% protein loading). Figure 4.2B revealed that the hydrolysis and synergistic profiles were not significantly influenced by swapping CBHII (Cel6A) with CBHII (Cel5A). This is evident by the similar synergy and activity profiles observed in Figure 4.2A (using microbial Cel6A + *Tl*Cel7A) and 4.2B (using *Ct*Cel5A + *Tl*Cel7A). As expected, the βgl enzyme played an important role by hydrolysing the CBHI and CBHII products into glucose, which reduced potential product inhibition (as seen by the glucose amounts that are shown in both Figures 4.2A and B).

4.3.2. Synergism between exo- and endo-glucanases

4.3.2.1. Synergy between CmixA1 (*Tl*Cel7A and microbial Cel6A) and various endoglucanases

The synergistic relationships between CmixA1 (*Tl*Cel7A and microbial Cel6A) and various EG (*Ba*EG, *Tm*EG, *An*EG and *Tr*EG) combinations were assessed to determine which combination released the highest quantity of reducing sugars or glucose and displayed the highest DS (Figure 4.3).

CmixA1 and *Ba*EG displayed the highest degree of synergy (DS) at the ratio of 75%:25% followed by 50%:50%, respectively. The largest amounts of total reducing sugars and glucose released from Avicel by this enzyme combinations were 1.2 mg/mL and 1.1 mg/mL, respectively (Figure 4.3A). The highest DS of around 1.4 also demonstrated that the CmixA1 and *Ba*EG enzymes were co-operating during the reactions. In contrast, there was no co-operattion between **CmixA1 and *Tm*EG**. Figure 4.3B shows that the CmixA1 and *Tm*EG had a DS of about 1.0 – in addition, the total reducing sugars and glucose released were not higher than that of the CmixA1 (100%). The DS of around 1.0 suggests that only the CmixA1 was hydrolysing the Avicel to produce the total reducing sugars.

CmixA1 and *An*EG synergy was interesting because the highest amout of total reducing sugars were produced by a 25% CmixA1: 75% *An*EG combination. This combination was unique, because the *An*EG enzyme (at 100%) in this case displayed the higher activity compared to the optimised CmixA1 (at 100%). Also, at 50% CmixA1:50% *An*EG combination, the synergy displays significantly high amounts of the total reducing sugars, suggesting that both the CmixA1 and *An*EG enzyme were cooperating in hydrolysing the Avicel substrate (Figure 4.3C). **For CmixA1 and *Tr*EG** there was no synergy between the enzymes and this observation was supported by the DS values which were below 1.0 (Figure 4.3D).

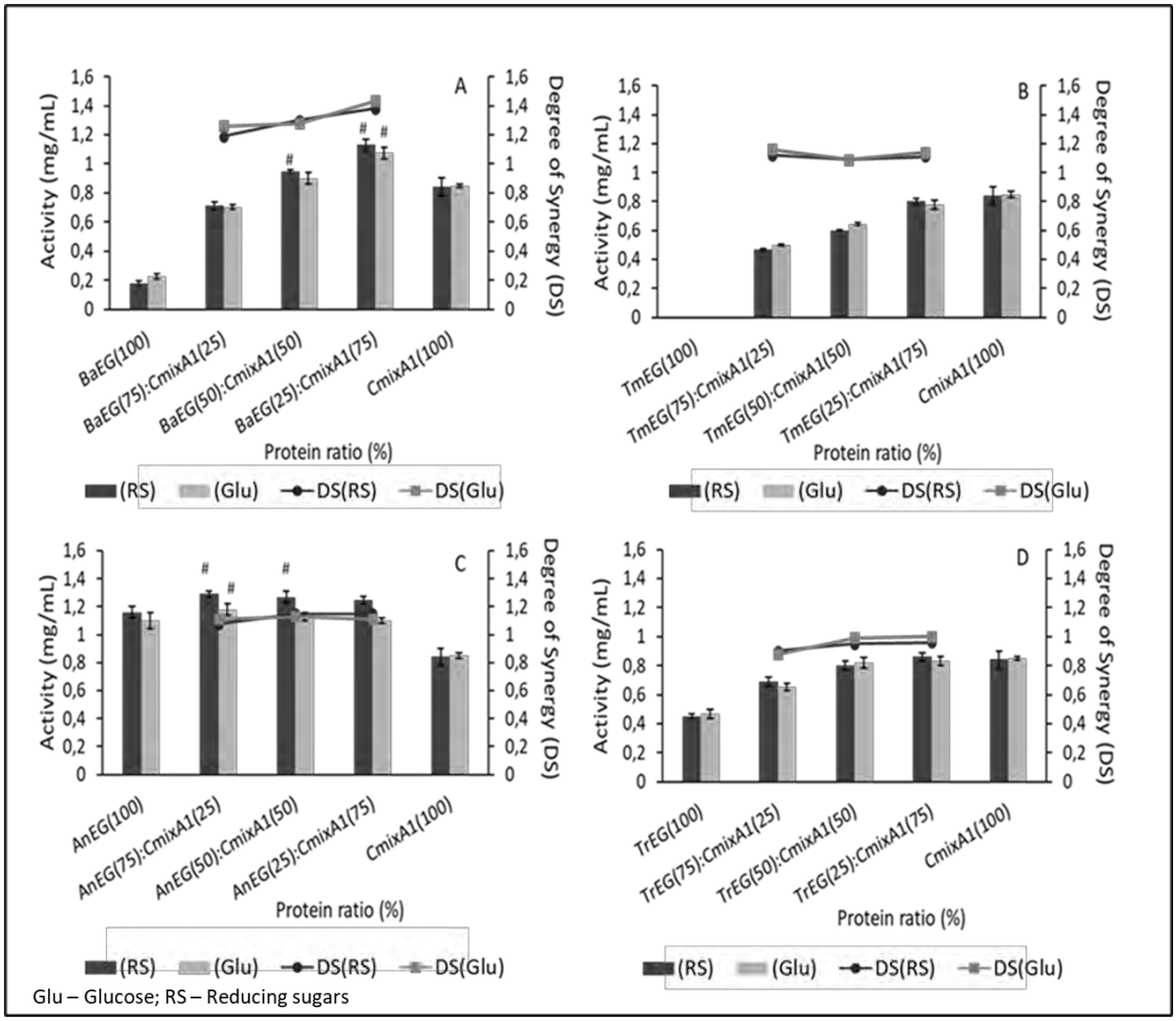

Figure 4.3. Synergistic degradation of Avicel by various ratios of CmixA1 and (A) *Ba*EG; (B) *Tm*EG; (C) *An*EG or (D) *Tr*EG. Assays were performed in sodium citrate buffer (0.05 M; pH 5.0) and incubated at 37°C for 24 h. Values are presented as mean values ± SD. (n = 3).

4.3.2.2. Synergy between CmixA2 (*Tl*Cel7A and *Ct*Cel5A) and various endoglucanases

The synergistic relationships between CmixA2 (*Tl*Cel7A and *Ct*Cel5A) and various EG (*Ba*EG, *Tm*EG, *An*EG and *Tr*EG) combinations were assessed to determine which combination released the highest quantity of reducing sugars, and displayed the highest DS (Figure 4.4).

The results obtained were similar to the synergistic relations established with CmixA1 (Figure 4.3). Figure 4.4 shows that CmixA2 displayed the highest synergistic effect (DS: 1.47) with *Ba*EG (reducing sugars: 1.47; glucose: 1.38) at a protein ratio of 75% to 25%. This enzyme combination also produced significantly more ($p < 0.01$) soluble sugars (reducing sugars: 1.21 mg/mL; glucose: 1.12 mg/mL) than the total amount produced by these enzymes individually at 100% protein loading. The highest quantity of sugars (reducing sugars: 1.43 mg/mL; glucose: 1.35 mg/mL) was liberated by the combined

activities of *An*EG and CmixA2 at a protein ratio of 75% to 25%, respectively (DS: 1.19 for reducing sugars and 1.29 for glucose), which was also significantly higher ($p < 0.0.1$) than their separate, individual activities at 100% protein loading (Figure 4.4C).

Figure 4.4 B and D showed that there was no synergy between CmixA2 and the EGs (*Tm*EG and *Tr*EG), which was supported by the low DS values (< 1). We therefore propose that *Trichoderma* endoglucanases do not synergise with CmixA (both CmixA1 and CmixA2).

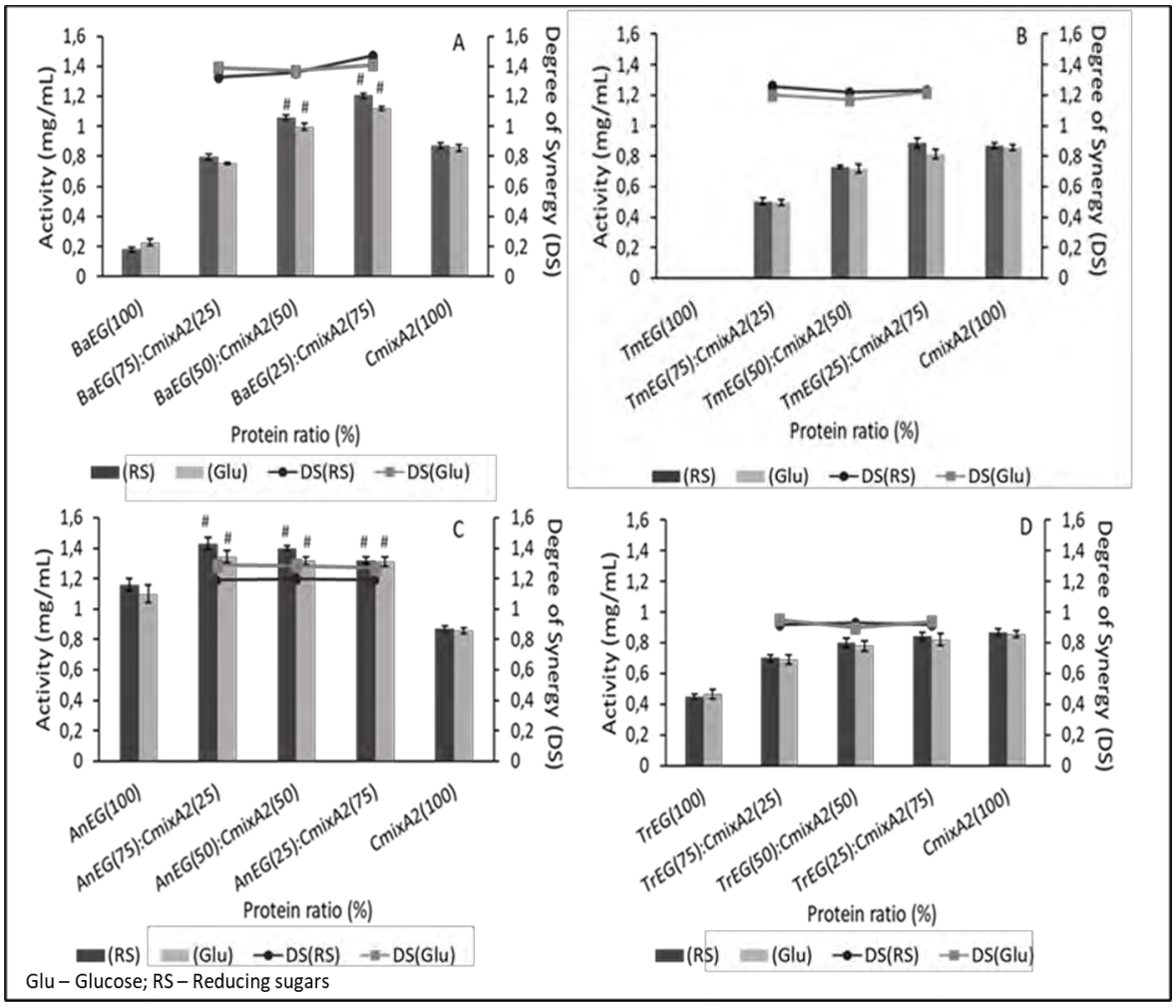

Figure 4.4. Synergistic degradation of Avicel by various ratios of CmixA2 and (A) *Ba*EG; (B) *Tm*EG; (C) *An*EG or (D)*Tr*EG. Assays were performed in sodium citrate buffer (0.05 M, pH 5.0) and incubated at 37°C for 24 h. Values are presented as mean values ± SD. ($n = 3$).

4.3.2.3. Synergy between CmixB1 (*Hj*Cel7A and microbial Cel6A) and various endoglucanases

The synergistic relationships between CmixB1 (*Hj*Cel7A and microbial Cel6A) and various EG (*Ba*EG, *Tm*EG, *An*EG and *Tr*EG) combinations were assessed to determine which combination released the highest quantity of reducing sugars and displayed the highest DS (Figure 4.5).

As can be seen in Figure 4.5, no synergism was detected between CmixB1 and any of the EGs, and did not improve the overall cellulose hydrolysis. At 100% protein loading, CmixB1 produced 0.397 mg/mL of reducing sugars and 0.414 mg/mL of glucose, which was higher than the sugars liberated by all the tested combinations.

Figure 4.5C shows that as the *An*EG amounts (%) decreased, the total amount of reducing sugars and glucose also decreased. This was a clear indication that there was no cooperation between CmixB1 and *An*EG during the hydrolysis of Avicel. In Figure 4.5A and B, a similar trend was observed in an opposite direction, whereby the enzyme in CmixB1 resulted in the increased sugar release from the Avicel, indicating that there was still no interaction/cooperation observed between the enzymes.

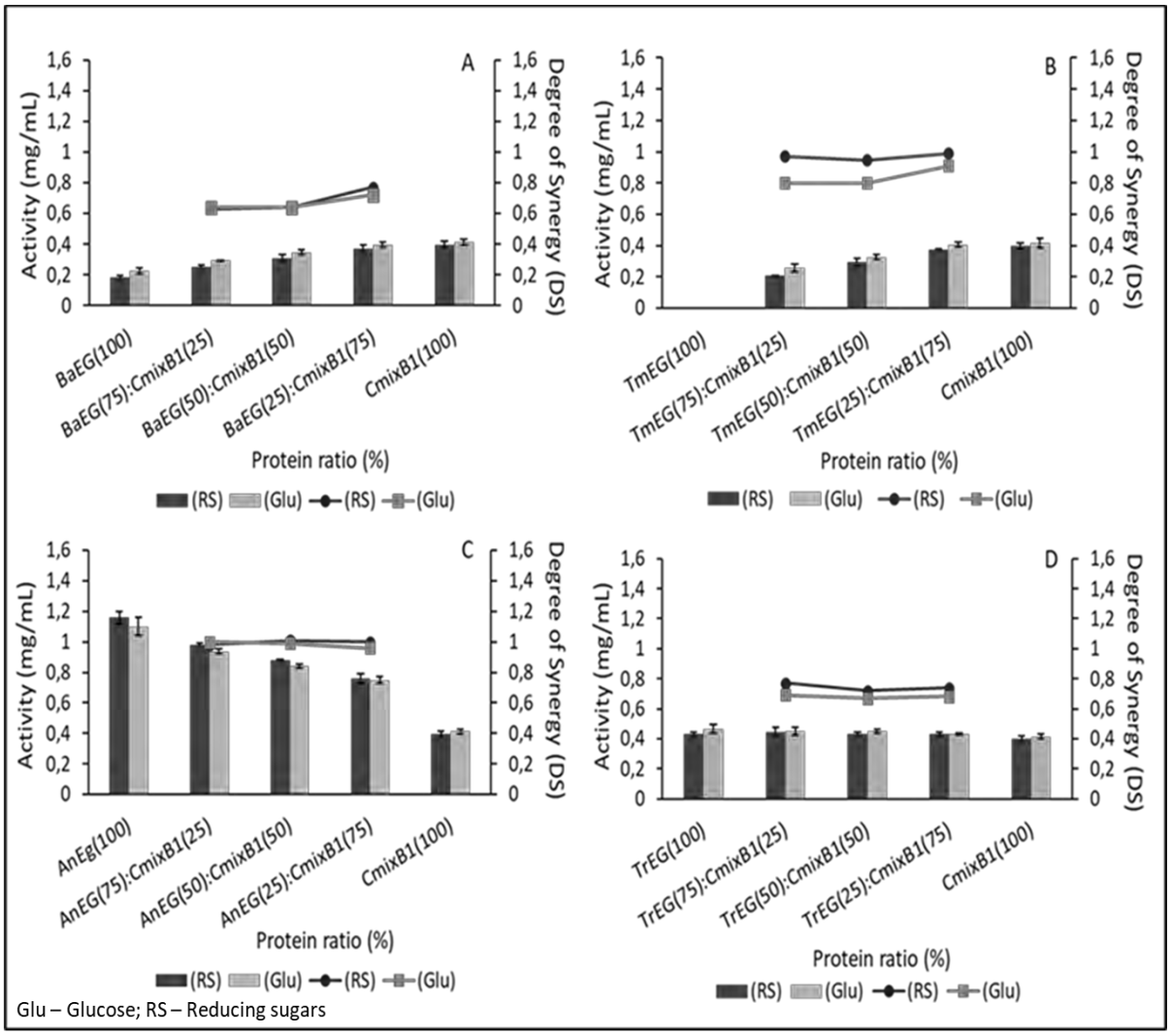

Figure 4.5. Synergistic degradation of Avicel by various ratios of CmixB1 and (A) *Ba*EG; (B) *Tm*EG; (C) *An*EG or (D)*Tr*EG. Assays were performed in sodium citrate buffer (0.05 M, pH 5.0) and incubated at 37°C for 24 h. Values are presented as mean values ± SD. (n = 3).

4.3.2.4. Synergy between CmixB2 (*Hj*Cel7A and *Ct*Cel5A) and various endoglucanases

The synergistic relationships between CmixB2 and various EG combinations (*Ba*EG, *Tm*EG, *An*EG and *Tr*EG) were assessed to determine which combination released the highest quantity of reducing sugars and displayed the highest DS (Figure 4.6).

The results observed in Figure 4.6 were similar to the findings between CmixB1 and EGs (Figure 4.5). No synergism was detected between CmixB2 and any of the EGs, and the overall cellulose hydrolysis was not improved. When CmixB2 was used individually (100% protein loading), it liberated 0.40 mg/mL of reducing sugars and 0.43 mg/mL of glucose.

Based on these results (Figure 4.5 and 4.6) we propose that that CmixB does not interact with any endoglucanase (bacterial and fungal), and therefore, it can not be used to form the enzyme cocktail for effective biomass hydrolysis.

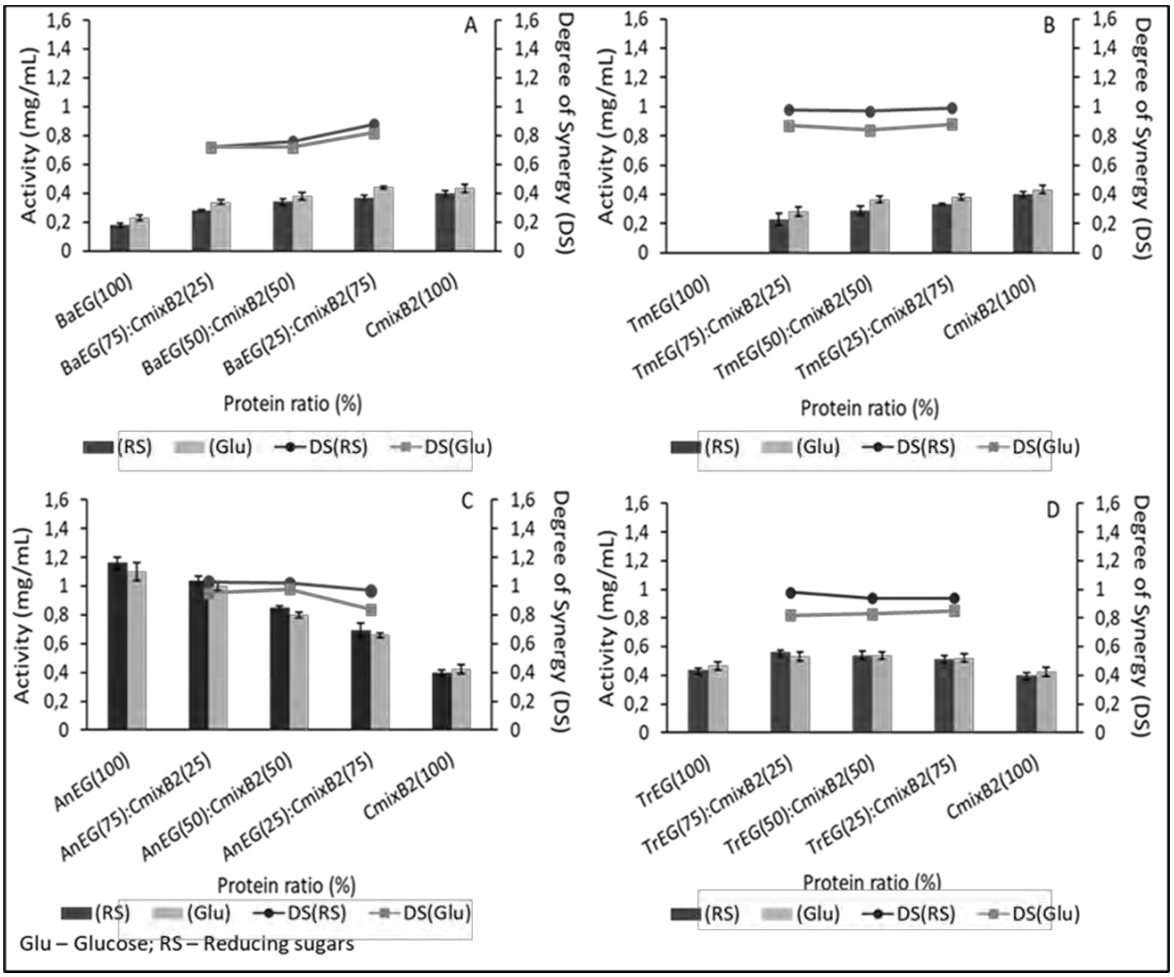

Figure 4.6. Synergistic degradation of Avicel by various ratios of CmixB2 and (A) *Ba*EG; (B) *Tm*EG; (C) *An*EG or (D)*Tr*EG. Assays were performed in sodium citrate buffer (0.05 M, pH 5.0) and incubated at 37°C for 24 h. Values are presented as mean values ± SD. (n = 3).

4.3.2.5. Synergy between CmixC1 (*Cs*Cel48A and microbial Cel6A) and various endoglucanases

The synergistic relationships between CmixC1 and various EG combinations (*Ba*EG, *Tm*EG, *An*EG and *Tr*EG were assessed to determine which combination released the highest quantity of reducing sugars and displayed the highest DS (Figure 4.7).

It can be seen that seen that CmixC1 (*Cs*Cel48A + microbial Cel6A) or EG alone at a 100% protein mass loading released the same quantity or even more sugars than the combinations assessed (Figure 4.7A-D). No synergistic relationships were therefore established established between Cmix1 and any of the EGs assessed in this study.

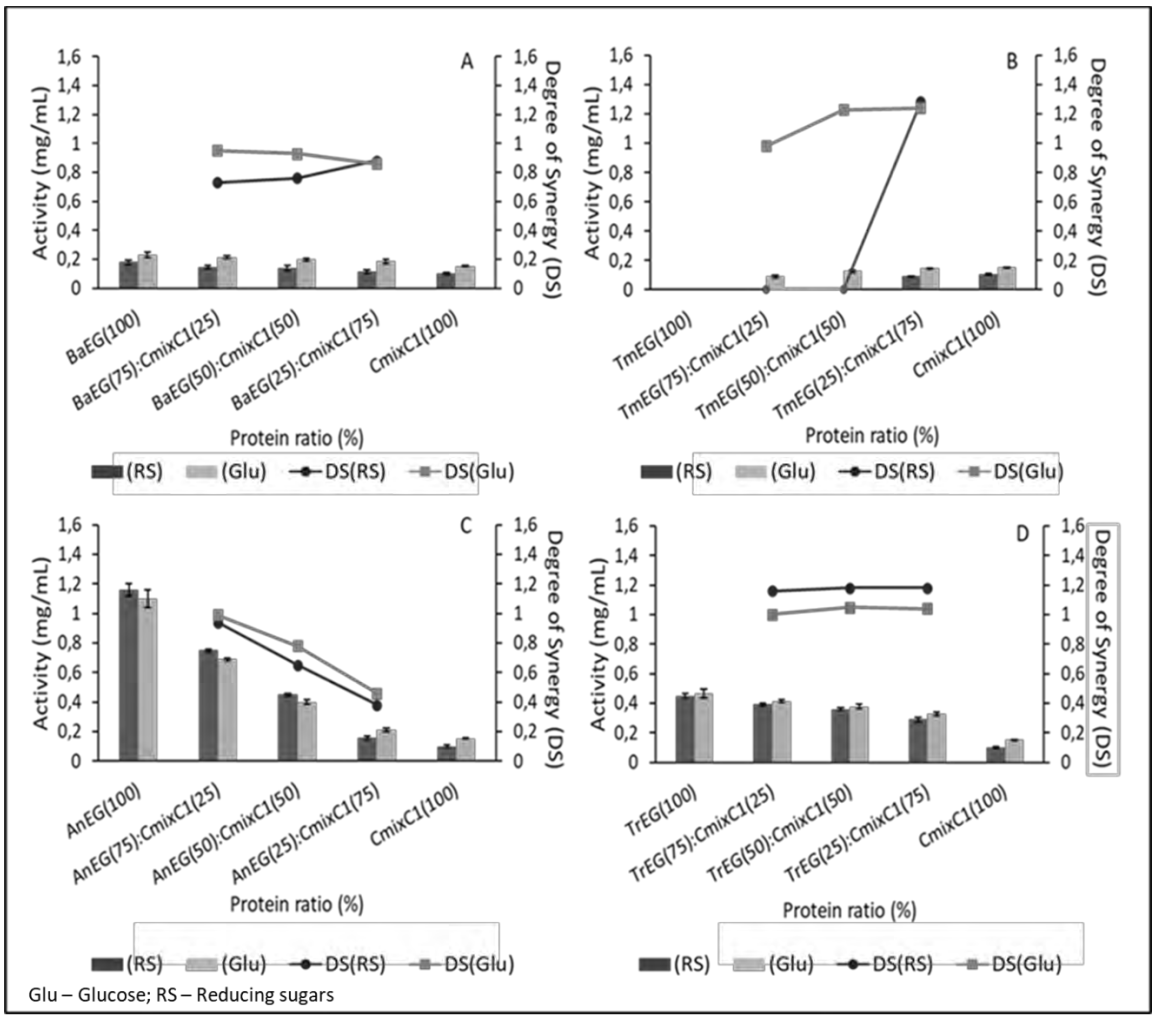

Figure 4.7. Synergistic degradation of Avicel by various ratios of CmixC1 and (A) *Ba*EG; (B) *Tm*EG; (C) *An*EG or (D) *Tr*EG. Assays were performed in sodium citrate buffer (0.05 M, pH 5.0) and incubated at 37°C for 24 h. Values are presented as mean values ± SD. (n = 3).

4.3.2.6. Synergy between CmixC2 (*Cs*Cel48A and *Ct*Cel5A) and various endoglucanases

The synergistic relationships between CmixC2 and various EG combinations (*Ba*EG, *Tm*EG, *An*EG or *Tr*EG) were assessed to determine which combination released the highest quantity of reducing sugars and displayed the highest DS (Figure 4.8).

Similar results to that obtained between Cmix 1 and EGs (Figure 4.7) were observed when assessing the synergistic relationships between Cmix2 (*Cs*Cel48A + *Ct*Cel5A) and the EGs (Figure 4.8) It can be seen that seen that CmixC2 (*Cs*Cel48A + *Ct*Cel5A) or EG alone at a 100% protein mass loading released the same quantity or even more sugars than any of the combinations tested (Figure 4.8). Again, no synergistic relationships were established between Cmix2 and any of the EGs.

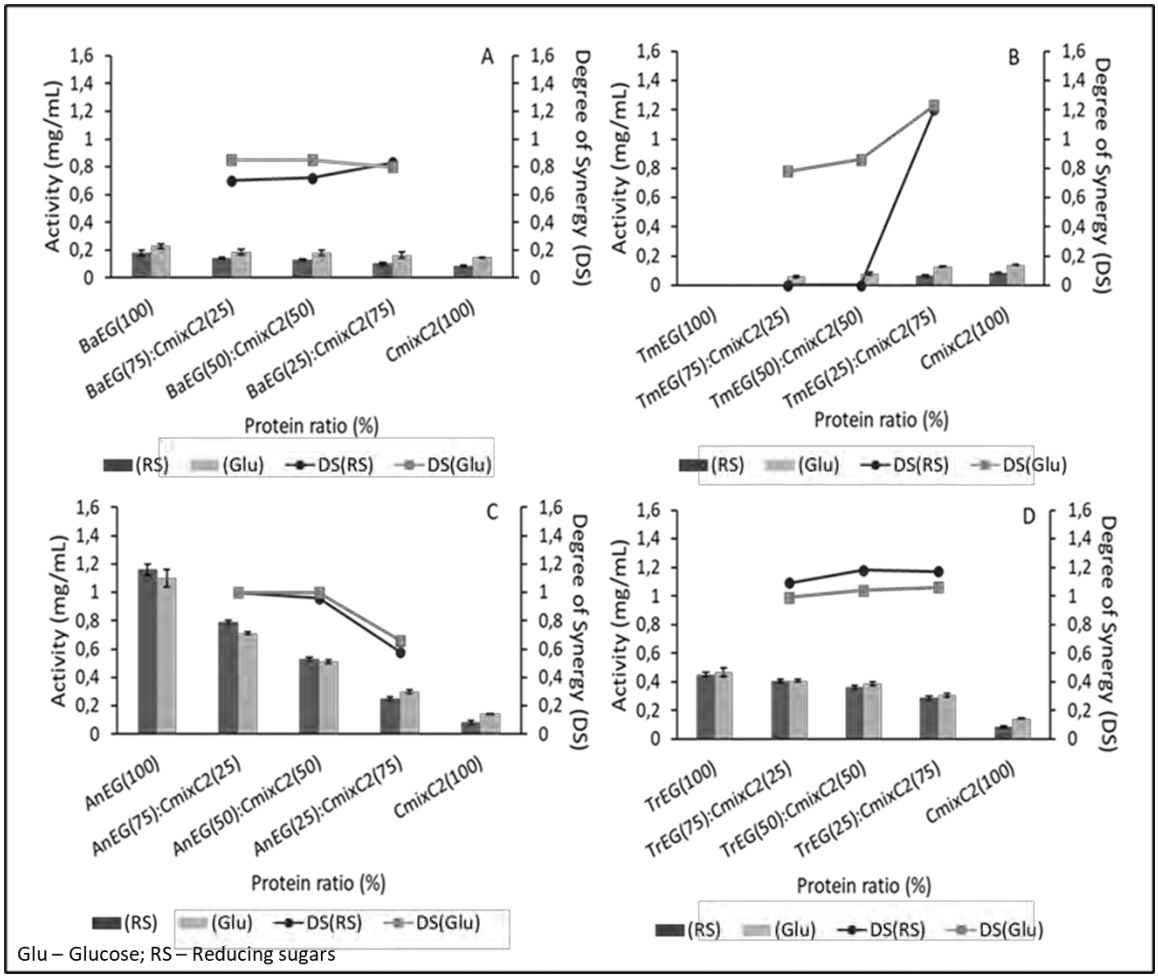

Figure 4.8. Synergistic degradation of Avicel by various ratios of CmixC2 and (A) *Ba*EG; (B) *Tm*EG; (C) *An*EG or (D)*Tr*EG. Assays were performed in sodium citrate buffer (0.05 M, pH 5.0) and incubated at 37°C for 24 h. Values are presented as mean values ± SD. (n = 3).

A summary of all the synergy results (Figures 4.1 - 4.8) obtained during Avicel hydrolysis by the various binary and ternary combinations of CBHI, CBHII and EG is shown in Table 4.1 below.

Table 4.1. Summary of the synergistic associations established between the different GH family enzymes, and the optimum ratios for each combination required for Avicel hydrolysis.

	***Ba*EG**		***Tm*EG**		***Tr*EG**		***An*EG**	
	Synergy result	**Optimum ratio**	**Synergy result**	**Optimum ratio**	**Synergy result**	**Optimum ratio**	**Synergy result**	**Optimum ratio**
CmixA1	✕	**mixture 75:25%**	✕	CmixA1: 100%	✕	CmixA1: 100%	✕	**mixture 25:75%**
CmixA2	✓	**mixture 75:25%**	✓	CmixA2: 100%	✕	CmixA2: 100%	✓	**mixture 25:75%**
CmixB1	✕	CmixB1: 100%	✓	CmixB1: 100%	✕	*Tr*EG: 100%	✕	*An*EG: 100%
CmixB2	✕	CmixB2: 100%	✕	CmixB2: 100%	✕	*Tr*EG: 100%	✕	*An*EG: 100%
CmixC1	✓	**mixture 75:25%**	✓	CmixC1: 100%	✕	*Tr*EG: 100%	✓	*An*EG: 100%
CmixC2	✕	*Ba*EG: 100%	✓	CmixC2: 100%	✓	*Tr*EG: 100%	✕	*An*EG:100 %

Where CmixA1 is (*Tl*Cel7A + microbial Cel6A), CmixA2 is (*Tl*Cel7A + *Ct*Cel5A), CmixB1 is (*Hj*Cel7A + microbial Cel6A), CmixB2 is (*Hj*Cel7A + *Ct*Cel5A), CmixC1 is (*Cs*Cel48A + microbial Cel6A) and CmixC2 is (*Cs*Cel48A + *Ct*Cel5A), a tick means generally synergy observed, while a cross generally means no synergy or anti-synergy observe

4.4. Discussion

Synergy studies

When mixtures of hydrolytic enzymes interact synergistically, the total effect is greater than the theoretical sum of the individual enzymes, commonly referred to as synergy (Van Dyk and Pletschke, 2012; Kostylev and Wilson, 2012; Malgas *et al.,* 2017). This study investigated the potential synergistic relationships between cellulases from different GH families and microbial sources via a cellulase swapping approach. Quantification of the reducing sugars and glucose released during Avicel hydrolysis allowed the degree of synergy (DS) to be calculated, in an attempt to gain an overall understanding of synergistic degradation of cellulose by cellulolytic enzymes.

Determination of the optimal CBH1: CBHII ratio (exo-exo synergy)

We investigated exo-exo synergy between CBHI (*Tl*Cel7A) and CBHII (microbial Cel6A) to determine the optimal CBH (CBHI + CBHII) cocktail required for cellulose hydrolysis (Figure 4.2A). The results show that the concerted action of CBHI (*Tl*Cel7A) and CBHII (microbial Cel6A) resulted in a synergistic effect, and that the combination of CBHI and CBHII in a protein ratio of 75% to 25%, respectively, was significantly ($p < 0.01$) better at releasing sugars during Avicel hydrolysis compared to when the enzymes were used individually (100% protein loading). This exo-exo synergism is a phenomenon that was first proven by Fagerstam and Pettersson in 1980 and has since then been confirmed by other researchers (Den Haan *et al*., 2013; Badino *et al.,* 2017; Henrissat *et al*. 1985; Nidetzky *et al.,* 1994). According to the exo-exo synergy model, it has been hypothesised that CBHI and CBHII prefer to hydrolyse cello-oligosaccharides from opposing sides of the cellulose chain (CBHI- reducing and CBHII- non-reducing end). Consequently, this renders a strong synergistic relationship between the two different CBHs (Kurašin and Väljamäe, 2011).

The effect of CBHII swapping on cellulose hydrolysis and synergy profiles

We performed a comparative study by swapping CBHII (microbial Cel6A) with a CBHII from a different GH family and source (*Ct*Cel5A) in order to compare their hydrolysis and synergistic profiles with CBHI (Figure 4.2). Figure 4.2B shows that the hydrolysis and synergistic profiles were not significantly influenced by swapping CBHII (Cel6A) to CBHII (Cel5A). Similarly, the 75%: 25% combination between CBHI (*Tl*Cel7A) and CBHII (*Ct*Cel5A) significantly ($p < 0.01$) increased the quantity of sugars during Avicel hydrolysis, compared to when the enzymes were used individually (100% protein loading). Based on these results, the ratio of 75% CBHI (*Tl*Cel7A): 25% CBHII (microbial Cel6A or *Ct*Cel5A) was selected as the benchmark (optimal ratio) CBH mix (Cmix) for

subsequent experiments. This ratio is in agreement with the CBHI (70%): CBHII (30%) ratio reported by Den Haan *et al.* (2013) and Nidetzky *et al.* (1994).

Synergy between CmixA1/CmixA2 and various endoglucanases

It is well documented that the synergistic co-operation between endo- and exo-acting enzymes is a pre-requisite for efficient cellulose degradation (Brás *et al.,* 2011; Den Haan *et al.,* 2013; Malgas *et al.,* 2017). The synergistic relationships between CmixA1 (*Tl*Cel7A and microbial Cel6A) and various EG combinations were assessed. The *Ba*EG and CmixA1 enzyme combination (i.e. at a protein ratio of *Ba*EG to CmixA1 of 25%: 75%) displayed the greatest synergistic effect (DS) of 1.39 mg/mL (reducing sugars) and 1.43 mg/mL (glucose), indicating that the concerted action of the two enzymes produced substantially more soluble sugars than the total amounts produced by these enzymes individually. This observation agreed with previous studies by Den Haan *et al.* (2013); Henrissat *et al.* (1985) and Woodward *et al.* (1988), who determined that the optimum synergistic effect is achieved when a higher ratio of CBH to EG is used in the reaction. However, this is dependent on the nature and characteristics of the EG and the substrate used (Andersen *et al.,* 2008; Van Dyk and Pletschke, 2012). In our case, the CmixA1 and *Ba*EG combination stimulated cellulose hydrolysis and released significantly higher ($p < 0.01$) sugars (reducing sugars: 1.13 mg/mL; glucose: 1.074 mg/mL) compared to when *Ba*EG (reducing sugars: 0.18 mg/mL; glucose: 0.228 mg/mL) or CmixA1 (reducing sugars: 0.842 mg/mL; glucose: 0.849 mg/mL) were used alone at 100% protein loading. Due to the high synergistic effect exhibited by this enzyme combination and the significant increase in soluble sugars released, we propose that CmixA1 (CBHI and CBHII) was the main contributor to Avicel hydrolysis and that the presence of EG induced the synergistic efficiency shearing the β-1,4 glycosidic bonds from internal filaments, and releasing smaller fragments of cellulose to provide new sites for CBH binding (Henrissat *et al.,* 1985; Jalak *et al.,* 2012; Tang *et al.,* 2018). An alternative explanation for endo-exo synergism has been proposed by Väljamäe *et al.* (1999), known as the surface erosion model. This model is based on the hypothesis that CBHI modifies the substrate structure, thereby generating obstacles that results in slow dissociation as well as stalling of CBHI, leading to an overall loss in catalytic efficiency. However, the eroded substrate is more accessible for EG activity, which then cleaves the substrate into smaller fragments to release the trapped CBHs (Kurašin and Väljamäe, 2011; Jalak *et al.,* 2012) As a result, the synergistic interaction of endo- and exo- cellulases results in the acceleration of cellulose hydrolysis (Nidetzky *et al.,* 1994; Väljamäe *et al.,* 1999).

From all the enzyme combinations tested, the concerted action of *An*EG and CmixA1 (i.e. in a protein ratio of 75% *An*EG to 25% CmixB) produced the highest quantity of sugars (reducing sugars: 1.29

mg/mL; glucose: 1.22 mg/mL), which performed significantly ($p < 0.01$) better compared to when *An*EG and CmixB1 were used individually at 100% protein loading. At this point, the degree of synergy was 1.08 (reducing sugars) and 1.11 (glucose), which was lower than that exhibited by the *Ba*EG (25%) and CmixA1 (75%) combination, but which is still a good indication that these enzymes were acting in synergism. It must be noted though, that the DS remained consistent for all the *An*EG and CmixA1 combinations assessed and that the concerted action of the two enzymes always produced substantially more soluble sugars than the total amounts produced by these enzymes individually, with no significant ($p > 0.5$) differences observed between the different enzyme combinations (with respect to the quantity of sugars produced). This observation was similar to Karlsson *et al.* (1999), who found that the ratio between CBH and EG was not that important, since the ratio of 95% CBH: 5% EG showed similar synergism/hydrolysis profiles to the 60% CBH: 40% EG ratio. This was in contrast to what we observed with the *Ba*EG + CmixA1 combination (a higher ratio of *Ba*EG to CmixA1 resulted in decreased cellulose hydrolysis and synergism), as a higher ratio of *An*EG to CmixA1 liberated higher quantities of soluble sugars compared to when a higher ratio of CmixA1: *An*EG was used. We need to consider that these discrepancies could be attributable to the nature of the EG used (Van Dyk and Pletschke, 2012). Moreover, the evolution of the overlapping functions between CBHs and EGs has also been recognised as a major contributor to the discrepancies that have been reported in the literature, since the exact roles of single enzymes displaying different degrees of processivity and endo-activity remain unclear (Kurašin and Väljamäe, 2011; Teeri, 1997).

Furthermore, CmixA1 also showed a consistent synergistic relationship with *Tm*EG for all the combinations assessed (DS: 1.12 - 1.16), however, the concerted action of CmixA1 and *Tm*EG did not liberate more sugars compared to the individual activities of CmixA1 or *Tm*EG at 100% protein loading. These results did not agree with what was previously reported by Klyosov (1990), who indicated that the amount of soluble sugars produced was enhanced when enzymes were acting synergistically. However, Andersen *et al.* (2008) reported contradictory results and reported that the degree of synergy and the highest quantity of sugars don't necessarily go hand in hand (i.e. cellulases may display synergistic behaviour, but not lead to increased product formation). We postulate that this may be attributable to the inability of *Tm*EG to hydrolyse Avicel efficiently, thus the synergistic effect is unable to result in enhanced cellulose hydrolysis. The observed synergy between CmixA1 + *Ba*EG/*An*EG/*Tm*EG is consistent with previous studies, displaying a synergistic association between exo- and endo-glucanases (Brás *et al.,* 2011; Den Haan *et al.,* 2013; Jalak *et al.,* 2012). However, no synergistic association ($DS < 1$) were established when CmixA1 was combined with *Tr*EG. These results were interesting, as they clearly highlight that CmixA1 displayed pronounced synergism with

all the other EGs, except when combined with *Tr*EG. With regards to the favored endo-exo synergism model, Brás *et al.* (2011) stated that this model does not explain the low degree of synergy observed between some combinations of CBHs and EGs, thus it does not provide a comprehensive understanding of how enzymes hydrolyse cellulose completely. They suggested that the free chain ends (oligosaccharides) generated by some types of EGs are not always accessible as a substrate for CBH activity. In addition, we propose that the enzymes had overlapping functions (i.e. high Avicelase activity, as seen in Table 3.1), and therefore competed with each other for the same target sites on the substrate (DS = 0.88) or that the enzymes were not associated with each other, therefore worked independently to degrade Avicel (DS = 0.99 or 1) (Andersen *et al.,* 2008; Malgas *et al.,* 2015).

Similarly, CmixA2 (*Tl*Cel7A and *Ct*Cel5A) displayed the highest synergistic effect/DS with *Ba*EG (reducing sugars: 1.47; glucose: 1.38) at a protein ratio of 75% to 25%, respectively. This enzyme combination also produced significantly more ($p < 0.01$) soluble sugars (reducing sugars: 1.21 mg/mL; glucose: 1.12 mg/mL) than the total amount produced by these enzymes individually at 100% protein loading. The highest quantity of sugars (reducing sugars: 1.43 mg/mL; glucose: 1.345 mg/mL) was liberated by the combined activities of *An*EG and CmixA2 in a protein ratio of 75% to 25%, respectively (DS: 1.19 for reducing sugars and 1.29 for glucose), which was also significantly higher ($p < 0.0.1$) than their separate individual activities at 100% protein loading. These results further confirm that a higher ratio of CBH to EG does not always lead to a higher degree of synergy or enhanced cellulose hydrolysis, as the nature and substrate promiscuity of EG does indeed influence the expected synergism outcome. Combining CmixA2 with *Tm*EG resulted in no improvement in the amount of sugars released, compared to when CmixA2 was used individually to degrade Avicel. However, a synergistic effect was observed between all the combinations tested. Once again, CmixB2 did not act synergistically (DS < 1) with *Tr*EG, which further confirms the suggestion of Brás *et al.* (2011), who stated that the free chain ends produced by *Tr*EG are not always accessible to CBHI, or that overlapping functions or competition for the same binding sites on the substrate result in anti-synergy (Converse and Optekar, 1993). As described in Chapter 1, when the activity of one enzyme does not facilitate the activity of another enzyme then, anti-synergy is observed (DS < or =1), whereas this phenomena may also occur when competitive behaviour between the enzymes is observed (enzymes competing for the same binding sites; DS < 1) (Van Dyk and Pletschke, 2012).

Although *Ba*EG and *Tm*EG are bacterial cellulases and originate from GH family 5, it was assumed that *Ba*EG was able to potentiate a higher degree of synergy with CmixA1 and CmixA2, as well as an overall increase in sugar release compared to that of *Tm*EG, due to their differences in specific activities. *Ba*EG exhibited higher processivity (5.59 U/mg on *p*NPC) than *Tm*EG (0.85 U/mg), and

higher Avicelase activity of 0.062 U/mg compared to 0 U/mg exhibited by *Tm*EG (Table 3.3). Therefore, the ability of *Ba*EG to be more efficient at hydrolysing crystalline cellulose may have led to the observed differences between the cellulose hydrolysis and synergistic profiles of the two cellulases. On the other hand, *Tr*EG, a fungal enzyme belonging to GH family 7 resulted in no synergistic interactions with CmixA1 and CmixA2. We postulate that this may be a result of competitive binding with CBHI (Cel7A), as it exhibited higher Avicelase activity (0.16 U/mg) than both *Ba*EG and *Tm*EG. In addition, one may ask why synergy and enhanced cellulose hydrolysis was observed when CmixA1/CmixA2 was combined with *An*EG and not with *Tr*EG, since they both exhibited Avicelase and CMCase activity. The only plausible explanation for these observed differences could be that *An*EG showed much higher substrate promiscuity than *Tr*EG, resulting in positive synergism and cellulose hydrolysis.

Synergy between CmixB1/CmixB2 and various endoglucanases

Although the CmixA1 (*Tl*Cel7A + microbial Cel6A) and CmixA2 (*Tl*Cel7A + *Ct*Cel5A) combinations displayed a high degree of synergism with various EGs, CmixB1 (*Hj*Cel7A + microbial Cel6A) and CmixB2 (*Hj*Cel7A + *Ct*Cel5A) exhibited no synergistic relationship (i.e. exhibiting a DS not greater than 1) with any of the EGs, and did not offer any advantages to enhancing overall cellulose hydrolysis. At 100% protein loading, CmixB1 produced 0.397 mg/mL of reducing sugars and 0.414 mg/mL of glucose. Similarly, when CmixB2 was used individually (100% protein loading) it liberated 0.40 mg/mL of reducing sugars and 0.434 mg/mL of glucose, indicating that the source of CBHII had no significant effect on the observed hydrolysis and synergy profiles. On the contrary, all of the combinations that were tested between CmixB1/CmixB2 and *An*EG exhibited significantly higher activities ($p < 0.01$) to that released by CmixB1 or Cmix B2 alone at 100% protein loading, however, they exhibited lower activity than that released by *An*EG alone (reducing sugars: 1.16 mg/mL; glucose: 1.10 mg/mL). These results provide clear evidence that not all endo- and exo- cellulases act synergistically. One may ask why pronounced synergism was established between various combinations of EGs and *Tl*Cel7A, but not with *Hj*Cel7A? What differentiates these CBHs from the same glycoside hydrolase family (7) from each other? Various studies have reported that observed synergism could be related to their adsorption capacities. If both enzymes are weakly bound to the substrate, synergism will be shown at a much lesser degree (Wood *et al.,* 1989). Furthermore, we assume that these discrepancies in our results are likely due to their specific activities on the substrate. As mentioned previously, *Tl*Cel7A had 3-fold higher activity on Avicel and CMC (Table 3.3), compared to *Hj*Cel7A. Here, we propose that the low Avicelase activity of *Hj*Cel7A cannot effectively access the individual chains in the cellulose provided by EGs and is therefore considered rate-limiting

in effective cellulose hydrolysis. This makes *Hj*Cel7A an un-suitable candidate in designing an optimal cellulase cocktail.

Synergy between CmixC1/CmixC2 and various endoglucanases

Studies have reported that, despite the low specific activity of Cel48 on crystalline cellulose, it plays an integral role in the bacterial cellulose-degrading system and has a high synergistic effect with other enzymes (specifically Cel9 EG) from the same enzyme source (i.e. *Clostridium* sp. or *Thermobofida* sp.), resulting in an overall increase in cellulose hydrolysis (Berger *et al.,* 2007; Irwin *et al.,* 2000). However, using either CmixC1 (*Cs*Cel48A + microbial Cel6A)/CmixC2 (*Cs*Cel48A + *Ct*Cel6A) or EG alone, at a 100% protein mass loading, released the same quantity or even more sugars than the combinations tested. This phenomenon has been reported by Väljamäe *et al.* (2001), who similarly found that a combination of CBH and EG yielded less activity as opposed to when CBH was used independently, at 100% protein dosage. However, they hypothesised that this may have been attributable to substrate related factors. In the case of CmixC1/CmixC2 and *Tm*EG or *Tr*EG, combining these enzymes resulted in more rapid cellulose hydrolysis than either using enzyme acting alone (DS >1) - but their ability to overcome Avicel recalcitrance was equal to or less than that of the enzymes acting independently at 100% protein dosage. We suggest that, although the endo- and exo- cellulases behaved synergistically, the overall hydrolysis was not enhanced due to the insufficient exo-cellulase activity exhibited by *Cs*Cel48A, thereby restricting the activity of the EGs to completely hydrolyse the substrate. Similar findings were reported by Irwin *et al.* (1993), however, their study assessed the synergistic relationship between fungal exo-glucanases and bacterial endo-glucanases on filter paper. The highest synergistic association (DS 1.24 for reducing sugars and glucose) was established when CmixC1/CmixC2 and *Tm*EG were combined in a protein ratio of 75% to 25%. Interestingly, CmixC1/CmixC2 also synergised with *Tr*EG with the highest degree of synergy (reducing sugars: 1.18; glucose: 1.04) observed at a protein ratio of 75% to 25%, respectively. We postulate that the ability of *Tr*EG to synergistically interact with *Cs*Cel48A, and not with *Tl*Cel7A, is due to the low specific activity exhibited by *Cs*Cel48A on Avicel (0.028 U/mg), which agreed with a study conducted by Kostylev and Wilson (2014). They suggested that the low activity of Cel48A makes it incompatible with the conventional role of exo-cellulases, as it cannot effectively gain access in the individual chains of cellulose during cellulose hydrolysis. Thus, it is not clear whether the mechanism by which Cel7A and Cel48A synergise with other enzymes is the same. Furthermore, they found that Cel48A from *T. fusca* synergises well with Cel9A from *T. fusca* and that these two enzymes play similar roles to that of *Tr*Cel7B and *Tr*Cel7A, respectively. Thus, we assume that *Tr*EG, a processive endo-cellulase, with relatively high activity on Avicel (0.16 U/mg) played the role of Cel48A, leading to noticeable synergy,

but no enhanced cellulose hydrolysis. These results support the evidence that synergy and high product formation do not always go hand-hand (Andersen *et al.,* 2008).

In contrast to the synergistic behaviour observed between CmixA1/CmixA2 and *Ba*EG, as well as with *An*EG, these EGs displayed anti-synergistic behaviour with CmixC1 and CmixC2. Although we postulate that this is attributable to the insufficient degree of cellulose hydrolysis displayed by *Cs*Cel48A, it remains unclear as to why a synergistic relationship would be established when *Cs*Cel48A was combined with processive enzymes *Tr*EG or *Tm*EG, but not with the processive enzymes *An*EG and *Ba*EG. These results support the evidence that the relationships between enzymes are highly complex and are highly dependent on the type of enzymes and the degree to which their activities complement each other. Therefore, there is no "guaranteed" optimal ratio of endo-cellulase/exo-cellulase for maximum degree of synergy, since the phenomena that cause the synergistic effect depend not only on the particular enzyme class, but also on the nature of the substrate and enzymes involved.

A summary of the comparison between the key results is provided in Appendix 4B.

4.5. Conclusions

The results showed that swapping CBHII had little effect on the synergistic and hydrolysis patterns observed for the Cmix, suggesting that microbial Cel6A and *Ct*Cel5A enzymes may share similar catalytic mechanisms, because they displayed similar synergistic patterns. The major conclusion drawn from this study is that that synergies between endo and exo-glucanases are not necessarily effective in any given situation, since the phenomena that underpin the synergistic effect depend not only on the particular enzyme class, but also on the nature of the involved substrate and enzymes. We therefore postulate that, due to the different substrate specificities exhibited by cellulases from different GH family affiliations and microbial sources, enzymes are not always compatible with each other for efficient cellulose degradation. The only plausible explanation for this phenomenon is that there is not always a distinct difference between the CBHs and EGs (as some of these enzymes display cross-activity), but if one enzyme renders the substrate more accessible for the action of another enzyme, synergism will most likely occur. Only by examining the specific activities of an enzyme (individually and in combination) can we substantiate whether an enzyme/enzyme cocktail will offer any advantages towards enhancing cellulose hydrolysis. The information gained from this study can be used to compare cellulases from different GH families and enzyme sources, to ultimately provide a better understanding of their behaviour in synergistic mixtures.

Chapter 5: Unravelling the chemical and structural features of Eucalyptus sp. biomass pretreated by various technologies

5.1. Introduction

Lignocellulosic biomass is amongst the most promising alternative energy resources for producing biofuels (Srivastava *et al.,* 2019; De Bhowmick *et al.,* 2019; Wang *et al.,* 2017). Lignocellulose is the major structural component of the plant cell wall and is composed of three major constituents; cellulose, hemicellulose and lignin, which are in close association with each other (Chandel *et al.,* 2018; Mohaptra *et al.,* 2017; Wang *et al.,* 2017). The high complexity in the component organisation and interaction in the cell wall makes biomass naturally resistant to microbial degradation, which is the primary obstacle impeding the cost-efficient production of biofuels (Auxenfans *et al.,* 2017; Melati *et al.,* 2019). Although several factors such as crystallinity, degree of polymerisation, the presence of acetyl groups, lignification and available surface area are said to contribute to biomass recalcitrance, a greater understanding of the underlying factors behind highly recalcitrant biomass is critical in overcoming the high costs associated with the commercialisation of biofuels (Auxenfans *et al.,* 2017; Li *et al.,* 2017; Madadi *et al.,* 2017).

Reducing biomass recalcitrance can be achieved by altering the cell wall structure, i.e. by pretreatment (Du *et al.,* 2020; Muthuvelu *et al.,* 2019). Thus, the success of cellulosic ethanol production relies on the development of an effective pretreatment method, which can ultimately reduce biomass recalcitrance and increase the susceptibility of cellulose to enzymatic saccharification (Bernardinelli *et al.,* 2015; Kumar and Sharma, 2017; Wu *et al.,* 2019). Various pretreatments, including biological, chemical, physical, physico-chemical and combinatorial methods, have been investigated and developed in order to disrupt the recalcitrant native structure of different biomass feedstocks (Wang *et al.,* 2017; Zhang *et al.,* 2019). Although the mechanisms for biomass deconstruction vary between the different pretreatment technologies, the common goal for any pretreatment is to remove or redistribute lignin, but preserve hemicellulose (as it also required to produce value-added products) and increase cellulose accessibility (Kumar *et al.,* 2009; Zhang *et al.,* 2019). As much as it is known that the various pretreatment methods can improve the efficiency of enzymatic hydrolysis, more information is required on how pretreatments affect the macro-, micro- and nano-structures of plant cell walls. This information will provide a better understanding of the pretreatment mechanisms and how these processes could be optimised for improved enzymatic hydrolysis. Furthermore, different lignocellulosic materials and methods have been evaluated in different studies, and the effects of

different feedstock traits (crystallinity, degree of polymerisation, accessible surface area and particle size) on cell wall deconstruction is very complex (Lupoi *et al.,* 2014; Mittal *et al.,* 2015). According to Bhalla *et al.* (2019) and Mittal *et al.* (2015), it is difficult to make comparisons and draw conclusions between different pretreatments, specifically when trying to elucidate which of the key features greatly impact efficient enzymatic degradation. This is because, feedstock variability, even when the same plant species are utilised, can contribute to differences in pretreatment results, as the properties (i.e. genotype, growth, harvest conditions, particle size and storage history) can result in considerable differences in different plant species.

It has been confirmed that lignin removal can improve cellulose accessibility, thus delignifaction by oxidation (sodium chlorite-acetic or acid/sodium carbonate-acetic acid) was selected as a form of pretreatment in this study (Han *et al.,* 2020). According to Siquera *et al.* (2013), delignification can remove up to 60% lignin from the lignocellulosic biomass, but may also to some extent degrade the polysaccharides, and affect cellulose reactivity through oxidation and structural changes (Malgas, 2017). The second pretreatment that was selected for this study was steam explosion (a physico-chemical pretreatment). Steam explosion involves subjecting the biomass to high-pressure steam, followed by reducing the pressure so that the materials undergo an explosive decompression which causes lignin redistribution, partial hemicellulose hydrolysis/solubilisation and increased cellulose accessibility (Auxenfans *et al.,* 2017). Sulfuric acid (chemical pretreatment), similar to steam explosion, results in lignin redistribution, partial hemicellulose hydrolysis/solubilisation and increased cellulose accessibility, was selected as the third pretreatment in this study.

Replacing fossil fuels with biofuels requires the correct selection of lignocellulosic plant species with great sustainability (Muthuvelu *et al.,* 2019). In this study, *Eucalyptus*, a highly productive, fast-growing tree, which has a high tolerance and adaptability to various environmental conditions, was selected as the lignocellulosic substrate (Bhalla *et al.,* 2019; Lima *et al.,* 2013). Despite the recent focus on utilising *Eucalyptus* as a renewable source for biofuel production, there are limited studies that have specifically focused on how the structural features of *Eucalyptus* (including chemical composition and physical structure) are affected by various pretreatment methods (Alvira *et al.,* 2010). In the present study, the objective was to unravel the structure of *Eucalyptus* and assess how the chemical and ultrastructural organisation of cell walls of this biomass are modified by various pretreatments (including the design of novel pretreatment methods, i.e. pretreatments were applied in combination to determine whether they would optimise lignocellulose utilisation) using various microscopic, spectroscopic and chemical characterisation techniques.

5.2. Materials and Methods

5.2.1. Enzymes

The enzyme cocktail, CelMix, used in this study was developed by Malgas and co-workers in a previous study (Malgas *et al.,* 2017). The enzyme cocktail was composed of Egl 68%, Cel7A 17%, Cel6A 6%, βgl 9%. It must be noted though, that although Poplar and Acacia were the hardwood substrates used in the study conducted by Malgas *et al.* (2017), the enzyme synergy studies (cellulase swapping studies in Chapter 4) confirmed that the same enzyme cocktail was required for optimal *Eucalyptus* hydrolysis.

5.2.2. Raw material and pretreatment of *Eucalyptus* residues

Wood chips of a *Eucalyptus* sp. were generously supplied by Mondi Limited, Durban (South Africa). The wood chips were dried in an oven at 80ºC for approximately 18 hours. The chips were cooled down and then placed in air-tight, sealed bags, which were stored in a dry and dark place until further use. Prior to pretreatment, the wood chips were passed three times through a Trimtech garden vacuum blower (vacuum/mulch speed set at 6). The chips were then processed into fine residues using a Waring Commercial Blender (spin speed set to high). Three cycles were performed for 2 minutes per run. Once the process was complete, the fine residues were considered as the "untreated" substrate for pretreatment methods.

5.2.2.1. Sodium chlorite/acetic acid (delignification) pretreatment

Eucalyptus sp. wood chips (10 g) were treated with sodium chlorite/acetic acid for 4 hours according to a modified method by Siqueira *et al.* (2013). Sodium chlorite (0.3 g), anhydrous acetic acid (0.1 mL) and water (32 mL) were added to a gram of substrate. The flasks (in duplicate) were incubated in a water bath at 70ºC, with intermittent mixing taking place every 15 - 20 minutes. After 2 hours, a fresh charge of sodium chlorite and acetic acid (same quantity) was added to the reaction and incubated for another 2 hours. After the incubation process, the flasks were removed from the water bath and cooled down to room temperature. The samples were filtered through a cheese cloth to separate the liquid from the solids and the solids were washed with water until a pH of 7.0 was reached.

5.2.2.2. Sodium carbonate pretreatment

Eucalyptus sp. wood chips (10 g) were treated with sodium carbonate for 4 hours. Sodium carbonate (0.263 g) and water (10 mL) were added to a gram of substrate. The flasks (in duplicate) were incubated in a water bath at 70ºC, with intermittent mixing taking place every 15-20 minutes. After 2 hours, a fresh charge of sodium carbonate (same quantity) was added to the reaction and incubated for another

2 hours. After the incubation process, the flasks were removed from the water bath and cooled down to room temperature. The samples were filtered through a cheese cloth to separate the liquid from the solids and the solids were washed with water until a pH of 7.0 was reached.

5.2.2.3. Steam explosion

Upon passing the Trimtech garden vacuum blower, the *Eucalyptus* sp. wood chips were subjected to steam explosion at the Forest Products Biotechnology/Bioenergy Laboratory at the University of British Columbia, Vancouver (Canada), based on the conditions described by Bura and co-workers (2009). The substrate was pretreated in a 2 L StakeTech III steam gun (Stake Technologies, Norvall, ON, Canada) at a temperature of 210°C for a residence time of 5 min.

5.2.2.4. Sulfuric acid pretreatment

Eucalyptus sp. wood chips (10 g) were treated with 2% (v/v) sulfuric acid (10 mL/g) and left to stand at room temperature for 10 minutes. Thereafter, the samples (in duplicate) were autoclaved at 120ºC for 2 hours and then centrifuged at 2136 × *g* for 5 minutes. The samples were filtered through a cheese cloth to separate the liquid from the solids and the solids were washed with water until a pH of 7.0 was reached.

5.2.2.5. Steam explosion + sodium chlorite pretreatment

Dry steam exploded wood chips as described in 5.2.2.3 were subjected to sodium chlorite pretreatment as described in 5.2.2.1.

5.2.2.6. Steam explosion + sodium carbonate pretreatment

Dry steam exploded wood chips as described in 5.2.2.3 were subjected to sodium carbonate pretreatment as described 5.2.2.2.

5.2.2.7. Acid + sodium chlorite pretreatment

Dry acid pretreated wood chips as described in 5.2.2.4 were subjected to sodium chlorite pretreatment as described in 5.2.2.1.

5.2.2.8. Acid + sodium carbonate pretreatment

Dry acid pretreated wood chips as described in 5.2.2.4 were subjected to sodium carbonate pretreatment as described in 5.2.2.2.

5.2.3. Composition analysis

5.2.3.1. Carbohydrate and lignin compositional analysis

The wood biomass was characterised according to a modified NREL/TP-510-42618 protocol at the Plant Cell Wall and Carbohydrate Analytical Facility at the Umeå Plant Science Centre (UPSC) (Umeå, Sweden). Briefly stated, 3 mL of 72% (v/v) sulfuric acid was added to 100 mg of dry extractive-free wood and then kept at 30ºC for 1 hour. Samples were then diluted to 4% (v/v) sulfuric acid and autoclaved at 121ºC for 1 hour. Thereafter, the samples were filtered to separate the solid residue and the filtrate. The Klason lignin (KL) content was determined by measuring the mass of the solid residue after overnight drying at 105ºC. The acid-soluble lignin (ASL) and monosaccharide content were analysed using the filtrate, where ASL was determined by measuring the absorbance at 205 nm and 280 nm, and the monosaccharides (glucose, xylose, arabinose, galactose and mannose) were analysed using high-performance anion exchange chromatography (HPAEC) with an ICS-5000 ion-chromatography system (Dionex, Sunnyvale, CA) equipped with an electrochemical detector following the procedure described by Normark *et al.* (2014).

5.2.3.2. Ash content

Following EN14755:2004, dry wood powder (100 mg) was transferred to a pre-weighed dry crucible (crucible was pre-heated at 550°C for 1 hour). The samples were heated to 550°C with a ramping temperature of 5°C per min and then charred at 550°C for 3 hours. After cooling, the sample was weighed along with the crucible. The ash content of the samples were reported as the difference in mass between the initial and the final mass.

5.2.3.3. Extractives

Following the TAPPI T 264 (preparation of wood for chemical analysis) procedure, 200 mg of dry wood powder of a particle size between 100 and 500 µm were used for extraction, with 1) ethanol:toluene 1:2 (v/v) for 15 cycles, 2) ethanol 95% (v/v) for 10 cycles, and 3) distilled water (two cycles). After extraction, the wood powder was dried overnight in an oven (105°C). The content of extractives was reported as the difference between the initial and the final mass.

5.2.4. Pyrolysis Gas Chromatography Mass Spectrometry (Py-GC/MS)

Py-GC/MS was used to determine the ratio of lignin subunits of the *Eucalyptus* samples. The analysis was performed at the Plant Cell Wall and Carbohydrate Analytical Facility of the Umeå Plant Science Centre (UPSC) (Sweden). Briefly stated, 50 µg ball-milled wood powder was applied to a pyrolyser

(PY-2020iD and AS-1020E, Frontier Lab, Japan) connected to a GC/MS (7890A/5975C; Agilent Technologies AB) and analysed according to the method described by Gerber *et al.* (2012).

5.2.5. Microscopic analysis of *Eucalyptus* samples

Various microscopic techniques were used to assess the morphological changes and lignin distribution of the *Eucalyptus* sp. wood biomass before and after pretreatment.

5.2.5.1. Light Microscopy (Wiesner histochemical assay for lignin)

The samples were stained with a solution of phloroglucinol in strong hydrochloric acid. The ratio consisted of 2 parts of 5% (w/v) phloroglucinol (mixed with 95% (v/v) ethanol) to 1 part of concentrated HCl. The images were visualised with an Olympus BX40 light microscope and photographed with an Olympus DP72 digital camera.

5.2.5.2. Scanning electron microscopy (SEM)

Prior to electron microscopy, the samples were fixed on a metal stub, dried using a critical point-drying process and coated with gold under vacuum to ensure image quality during SEM analysis. Images were acquired using a TESCAN Vega TS 5136LM Scanning Electron Microscope (Cross, 2001). SEM images were taken at different magnifications between 500x to 2000x.

5.2.5.3. Fluorescence microscopy

Following the protocol described by Wang *et al.* (2017), the samples were embedded in 2% (w/v) agar and fixed with 1% (w/v) glutaraldehyde dissolved in 100 mM phosphate buffer (pH 7.0). The samples trapped in the agar matrix were dehydrated in a series of ethanol solutions ranging from 50 to 100% (10% step increments). The samples were then sectioned (2 µm) in epoxy-resin and visualised by excitation using a Zeiss LSM510 Meta Confocal Microscopy System, Germany. Within the broad fluorescence emission range, spectra were acquired by excitation at 420 - 480 nm and emission at 500 -550 nm.

5.2.6. Fourier-transform infrared spectroscopy (FTIR)

FTIR was performed at the Forestry and Forest Products Research Centre, Natural Resources and the Environment, Council for Scientific and Industrial Research (CSIR), Durban (South Africa). An FTIR spectrometer was used in the attenuated reflectance mode (Frontier Universal, PerkinElmer). Each sample had an average of 4 scans recorded at a resolution of 4 cm^{-1} in the range of 400–4000 cm^{-1}.

5.2.7. Nuclear Magnetic Resonance (NMR)

NMR analysis was performed at the Plant Cell Wall and Carbohydrate Analytical Facility of the Umeå Plant Science Centre (UPSC) (Sweden). Briefly stated, fine wood powder (50-80 mg) was packed into 4 mm ZrO2 rotors and ^{13}C Cross-Polarisation Magic Angle Spinning (CPMAS) spectra were recorded on a 500 MHz Bruker Advanced III spectrometer equipped with a 4 mm MAS probe. The settings used were 1 ms contact time, 8 k scans and 10 kHz spinning rate at ambient temperature.

5.2.8. X-Ray Diffraction (XRD)

XRD analysis of the samples was recorded with a D8 ADVANCE diffractometer (Bruker, German) equipped with a proportional counter using Nickel-filtered Cu/Ka_1 radiation (X= 0.1541 841 nm). The scattering angle (2θ) ranged from 10-40° with a scanning speed of 0.2 s and step size of 0.02° s. The operating voltage and current value were 40 kV and 40 mA, respectively. The crystallinity index (CrI) was determined as the percentage of the crystalline material in biomass as shown below.

$$CrI = \left[\frac{I002 - Iam}{I002}\right] X\ 100$$

Where I_{002} is the intensity of the diffraction from the 002 plane at 2θ = 22.6°and I_{am} is the intensity of the background scatter at diffraction intensities at 2θ = 18.9° (Brienzo *et al.,* 2017).

5.2.9. Simons' staining

Direct Orange (DO, Pontamine Fast Sky Orange 6RN) dye was used for the Simons' stain analysis. The modified Simons' staining procedure developed by Chandra *et al.* (2008) was applied with a slight modification of the incubation temperature (50°C was used instead of 70°C). The concentrations for the substrate and Direct Orange were prepared at 10 mg/mL and 1 mg/mL, respectively. For the reaction, 100 µL of the substrate mixture, 500 µL of DO and 400 µl of citrate/phosphate buffer (pH 5.0) were added to the Eppendorf tube. The reactions were carried out for 6 hours at 50°C, mixing at 25 rpm. Thereafter, the samples were centrifuged for 3 minutes (7-9k rpm) and 250 µL of the sample supernatant was added to a 96 well plate and absorbance readings were taken at 625 nm (Appendix 2). The controls included a blank (1000 µL citrate/phosphate buffer), negative control (500 µL of 1 mg/mL DO and 500 µL buffer) and substrate control (100 µL of 10 mg/mL substrate and 900 µL buffer).

5.3. Results

5.3.1. Pretreatment of hardwood substrates

Eucalyptus was subjected to various pretreatments, including sodium chlorite, sodium carbonate, steam explosion, steam explosion + sodium chlorite, steam explosion + sodium carbonate, acid, acid + sodium chlorite and acid + sodium carbonate. Figure 5.1 below shows a naked eye visual presentation of the untreated and pretreated substrates.

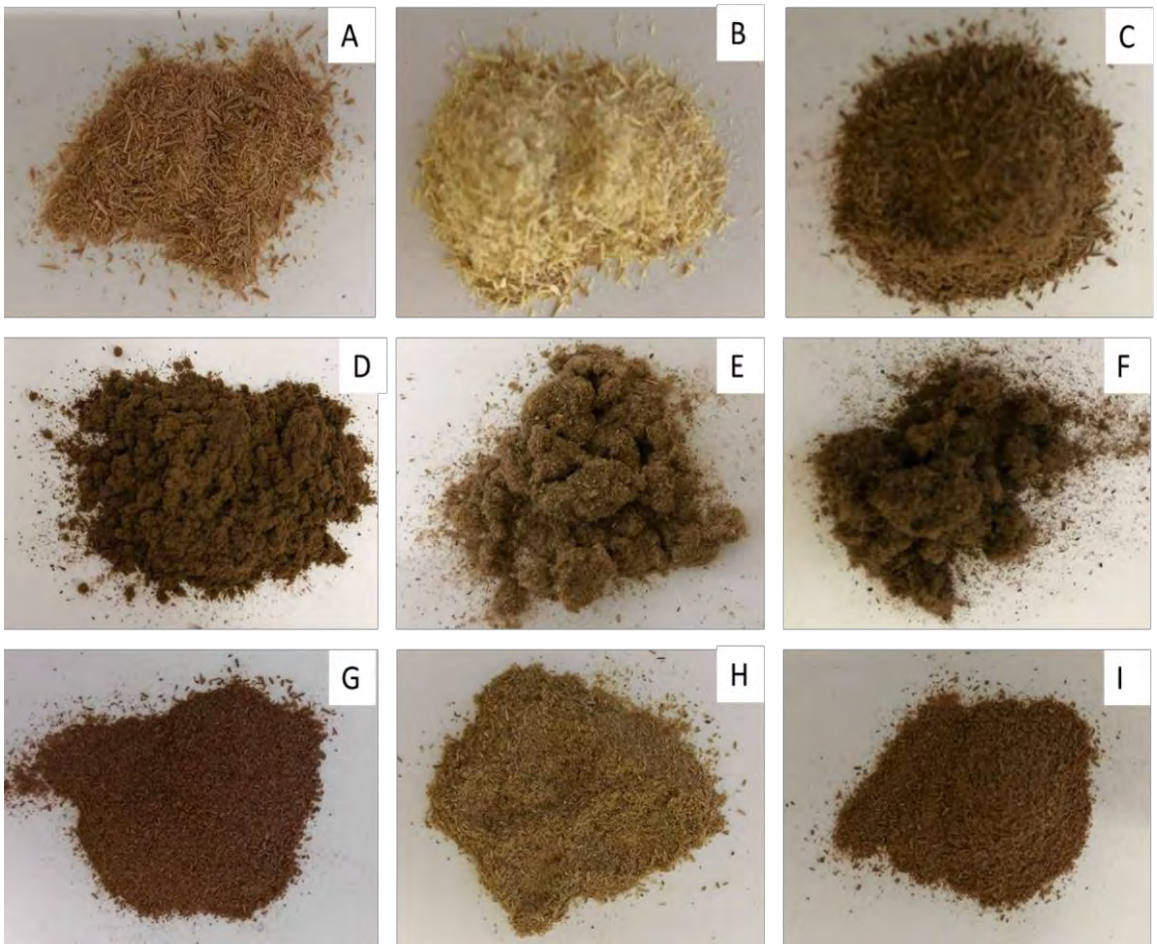

Figure 5.1. Visual presentation of (A) untreated *Eucalyptus*; (B) sodium chlorite; (C) sodium carbonate; (D) steam explosion; (E) steam explosion + sodium chlorite; (F) steam explosion + sodium carbonate; (G) acid; (H) acid + sodium chlorite; and (I) acid + sodium carbonate pretreated samples.

From Figure 5.1, it was evident that the different treatments induced textural changes to the substrate. The untreated substrate (Figure 5.1A) had a typical appearance of sawdust and was light-brown in colour. The sodium chlorite (Figure 5.1B) and sodium carbonate (Figure 5.1C) treated wood samples displayed similar textural characteristics to the untreated substrate (slightly fluffy) but had a lighter brown (almost white) and darker brown appearance compared to the untreated samples, respectively.

The white colour in the delignified sample is attributable to the removal of lignin. The substrates treated with steam explosion (Figure 5.1D), steam explosion + sodium chlorite (Figure 5.1E), and steam explosion + sodium carbonate (Figure 5.1F) displayed a "fluffier" and softer textural appearance compared to the untreated samples. There were also clear colour changes in the substrates (darker colour is attributable to the presence of lignin). For the acid-treated substrates: i.e. acid (Figure 5.1G), acid + sodium chlorite (Figure 5.1H) and acid + sodium carbonate (Figure 5.1I), the substrates appeared to have a less compact texture compared to the untreated substrate, but not as "fluffy" as the samples that had been subjected to steam explosion.

5.3.2. Chemical composition analysis

The effects of pretreatment on *Eucalyptus* were assessed by detailed chemical composition analysis (NREL protocol) and the data is/are shown in Table 5.1. The samples were analysed to quantify their components, such as cellulose, hemicellulose, lignin, extractives and ash (all expressed as relative %). The native *Eucalyptus* sample was found to contain 38.5% glucose, 10% xylose, 28.8% lignin and small amounts of arabinose, galactose and mannose (>2%). From all the pretreatments assessed, steam explosion + sodium chlorite displayed the highest relative glucan content (67.2%), followed by acid + sodium chlorite (62.8%), acid + sodium carbonate (54.9%), steam explosion + sodium carbonate (53.1%), acid (50.7%), sodium chlorite (48%), steam explosion (47%) and lastly sodium carbonate treatment had the lowest glucan content (44%). The relative Klason lignin content was highest in the acid treated sample (36.9%), followed by steam explosion + sodium carbonate (32.9%), steam explosion (32.3%), acid + sodium carbonate (30.4%), whereas sodium carbonate (24.2%), acid + sodium chlorite (21.7%), steam explosion + sodium chlorite (19.3%) and sodium chlorite (14.9%), all showed lower relative lignin contents than the untreated sample (24.7%). The observed trends were that delignification methods, i.e. sodium chlorite and sodium carbonate, led to an increase in the relative (%) carbohydrate and hemicellulose content while the relative (%) content of lignin decreased upon these pretreatments. On the other hand, steam explosion and acid pretreatments led to an increase in relative glucan and lignin content, while the relative content of xylan decreased (< 2%). Furthermore, delignifying these samples (with acid or steam) led to a further boost in relative glucan content and decrease in relative lignin content, resulting them to be highly cellulosic in nature.

The extractives and ash contents present in the untreated and treated samples are also shown in Table 5.1 below. The untreated sample contained 8.1% extractives and 0.3% ash. Differences in these contents were observed for all the pretreatments assessed, where the samples treated with steam explosion contained the highest amount of extractives, ranging from 12.1 – 15.6%.

Table 5.1. Chemical compositional analysis of untreated and pretreated *Eucalyptus* samples (expressed as relative weight percentage, %)

	Untreated	Sodium Chlorite	Sodium carbonate	Steam Explosion	Steam explosion + sodium chlorite	Steam explosion + sodium carbonate	Acid	Acid + sodium chlorite	Acid + sodium carbonate
Klason lignin	24.7 ± 0.7	14.9 ± 0.2	24.2 ± 0.6	32.3 ± 1.7	19.3 ± 1.6	32.9 ± 0.8	36.9 ± 1.9	21.7 ± 0.5	30.4 ± 0.3
ASL	4.1 ± 0.2	7.8 ± 0.2	3.9 ± 0.1	1.4 ± 0.1	1.5 ± 0.1	1.5 ± 0.1	3.3 ± 0.1	3.3 ± 0.1	2.1 ± 0.1
Glucose	38.5 ± 1.4	48.0 ± 2.0	44.0 ± 2.7	47.0 ± 4.0	67.2 ± 0.1	53.1 ± 1.4	50.7 ± 0.3	62.8 ± 1.2	54.9 ± 1.4
Xylose	10.0 ± 0.5	12.8 ± 0.5	11.5 ± 0.7	1.7 ± 0.1	1.8 ± 0.1	1.8 ± 0.1	2.6 ± 0.1	1.1 ± 0.1	1.7 ± 0.1
Mannose	0.5 ± 0.1	0.7 ± 0.1	0.6 ± 0.2	ND	ND	ND	0.4 ± 0.1	ND	0.3 ± 0.1
Galactose	1.4 ± 0.1	1.6 ± 0.1	1.5 ± 0.1	0.2 ± 0.1	ND	0.2 ± 0.1	ND	ND	ND
Arabinose	0.3 ± 0.1	0.3 ± 0.1	0.3 ± 0.1	ND	ND	ND	ND	ND	ND
Extractives	8.1 ± 0.3	6.6 ± 0.2	7.7 ± 0.7	15.6 ± 1.5	13.9 ± 0.4	12.1 ± 1.5	6.7 ± 0.3	11.1 ± 0.9	8.9 ± 0.1
Ash	0.3	0.9	1.7	0.5	0.9	3.7	ND	0.1	ND

[a]Values are given as mass fraction (dry mass) × 100. Error estimates indicate standard deviation based on two replicates. ND: Not detected

5.3.3. Py-GC/MS

Py-GC/MS was used to determine the relative ratios of lignin units in G type, S type and the P type in the untreated and pretreated samples, as well the C/L (ratio carbohydrate and lignin), the S:G:H (ratio of lignin units) and carbohydrates (pseudo-lignin formation) in the samples (Table 5.2). P lignin significantly changed (decreased) upon biomass pretreatment, while the other components were not significantly altered. As seen in Table 5.2, the untreated sample had an S/G ratio of 1.9, which decreased partly upon most of the pretreatments. In contrast, this ratio increased to 2.4 for sodium carbonate pretreatment. There was also an increase in the carbohydrate to lignin (C/L) ratio for all the pretreated substrates (excluding sodium carbonate and acid + sodium carbonate) compared to the untreated sampled (1.8), where acid + sodium chlorite had the highest C/L ratio of 12.8 and sodium carbonate had the lowest C/L ratio of 1.2.

Table 5.2. Py-GC/MS analysis of the untreated and pretreated *Eucalyptus* samples

	C	G	S	H	P	O	SG	CL	L
Untreated	61.3 ± 5.8	10.4 ± 1.5	19.7 ± 2.7	1.0 ± 0.1	4.7 ± 0.1	2.8 ± 0.3	1.9 ± 0.1	1.8 ± 0.4	35.9 ± 6.1
Sodium chlorite	66.8 ± 1.7	7.4 ± 0.4	11.6 ± 0.9	0.7 ± 0.1	0.3 ± 0.1	13.1 ± 0.9	1.6 ± 0.1	3.3 ± 0.3	20.1 ± 1.3
Sodium carbonate	53.5 ± 0.7	12.5 ± 0.2	30.7 ± 0.5	1.0 ± 0.1	0.2 ± 0.1	2.1 ± 0.3	2.4 ± 0.1	1.2 ± 0.1	44.4 ± 0.7
Steam explosion (SE)	67.3 ± 1.4	10.3 ± 0.4	19.0 ± 0.9	1.0 ± 0.1	0.05 ± 0.1	2.2 ± 0.1	1.8 ± 0.1	2.2 ± 0.1	30.5 ± 1.3
SE + sodium carbonate	67.7 ± 1.5	11.1 ± 0.5	15.5 ± 1.0	1.4 ± 0.1	0.4 ± 0.1	3.9 ± 0.1	1.4 ± 0.1	2.4 ± 0.2	28.4 ± 1.5
SE + sodium chlorite	62.4 ± 0.9	12.8 ± 0.2	21.0 ± 0.6	1.8 ± 0.1	0.3 ± 0.1	1.6 ± 0.1	1.6 ± 0.1	1.7 ± 0.1	36.0 ± 0.9
Acid	75.2 ± 2.6	8.6 ± 1.0	13.3 ± 1.4	0.9 ± 0.1	0.1 ± 0.1	1.9 ± 0.1	1.5 ± 0.1	3.3 ± 0.5	22.9 ± 2.5
Acid + sodium chlorite	84.7 ± 2.2	2.9 ± 0.3	3.3 ± 0.4	0.5 ± 0.1	0.03 ± 0.01	8.6 ± 1.6	1.1 ± 0.1	12.8 ± 1.9	6.7 ± 0.8
Acid + sodium carbonate	77.9 ± 1.8	7.4 ± 0.5	11.7 ± 1.0	0.7 ± 0.1	0.04 ± 0.01	2.2 ± 0.3	1.6 ± 0.1	4.0 ± 0.4	19.8 ± 1.5

[a] *C, carbohydrate related; G, Guaiacyl; S, Syringyl; H, p-hydroxyphenyl; P, Generic benzene derivatives (without phenolic hydroxyl groups) (probably generated from lignin, and therefore included in L); O, unknown spectra (neither lignin nor carbohydrate); SG, S/G ratio; CL, C/L ratio; L, total lignin, G+S+H+P.*

[b] *C, G, S, H, P, U, O are expressed as % of total (C+G+S+H+P+U+O).*

5.3.4. Microscopy

Various microscopic techniques, including light microscopy (histochemical assay), SEM and fluorescent microscopy were performed.

5.3.4.1. Wiesner Staining (Histohemical staining)

The presence of lignin distribution in the untreated and pretreated wood samples was determined histochemically using the Weisner (phloroglucinol) stain. As seen from Figure 5.2, lignin was present in almost all the substrates (as seen by the red/magenta colour), however, there was no evidence of the presence of lignin in the samples pretreated with sodium chlorite (Figure 5.2B) and acid + sodium chlorite (Figure 5.2H) (as seen by the lack of red/magenta colour). The steam explosion + sodium chlorite substrate (Figure 5.2E) also contained less lignin compared to all the other substrates, however, the presence of lignin was still observable.

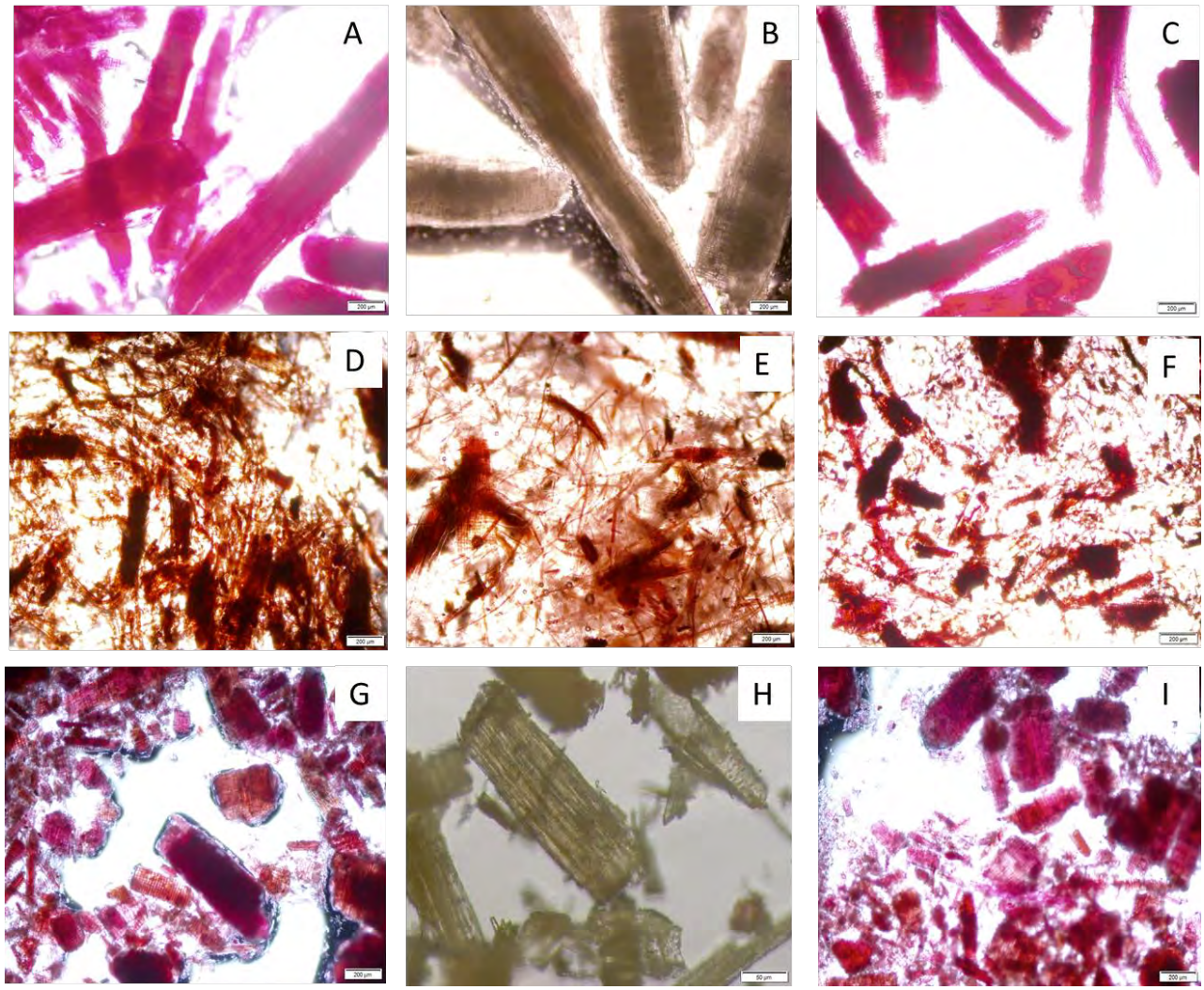

Figure 5.2. Phloroglucinol staining of (A) untreated; (B) sodium chlorite; (C) sodium carbonate; (D) steam explosion; (E) steam explosion + sodium chlorite; (F) steam explosion + sodium carbonate; (G) acid; (H) acid + sodium chlorite; and (I) acid + sodium carbonate pretreated *Eucalyptus* samples.

5.3.4.2. SEM

SEM was performed to assess the modifications and structural changes caused at nano-resolution upon pretreatment. The SEM micrographs are shown in Figure 5.3.

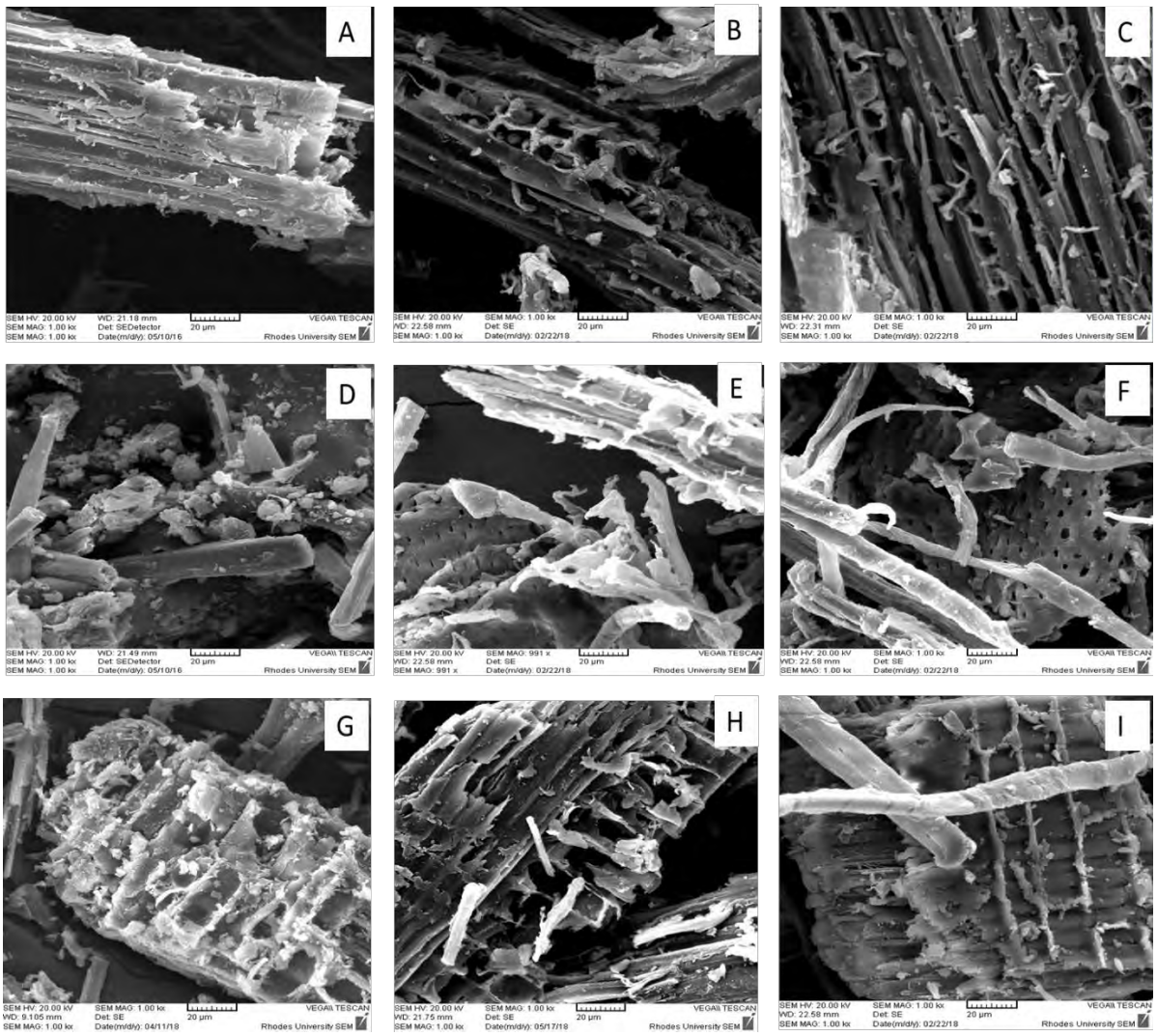

Figure 5.3. SEM images of (A) untreated *Eucalyptus*; (B) sodium chlorite; (C) sodium carbonate; (D) steam explosion; (E) steam explosion + sodium chlorite; (F) steam explosion + sodium carbonate; (G) acid; (H) acid + sodium chlorite; and (I) acid + sodium carbonate pretreated samples. Bars: 20 µm, 1000x magnification.

The SEM micrographs of the cell wall structure of the native (untreated) *Eucalyptus* sample showed that it was tight, orderly and had fluffly matrices coating the fibrils (Figure. 5.3A). After pretreatment, clear differences in the surface structure were observed, such as irregular, rough and defibrillated characteristics. It was also apparent that some of the external fibres had coalesced in the samples

pretreated with sodium chlorite (Figure 5.3B), sodium carbonate (Figure 5.3C), acid (Figure 5.3G), acid + sodium chlorite (Figure 5.3H) and acid + sodium carbonate (Figure 5.3I). However, it was evident that the fibres were still compact and not fully exposed after these treatments. Steam explosion (Figure 5.3D), steam explosion + sodium chlorite (Figure 5.3E) and steam explosion + sodium carbonate (Figure 5.3F) all showed greater disruption of the cell wall architecture, where the samples possessed loose fibrils, coated by droplet like particles.

5.3.4.3. Fluorescence microscopy

The lignin distribution in the untreated and pretreated wood samples (as shown by autofluorescence) was determined by fluorescent microscopy and is presented in Figure 5.4 below.

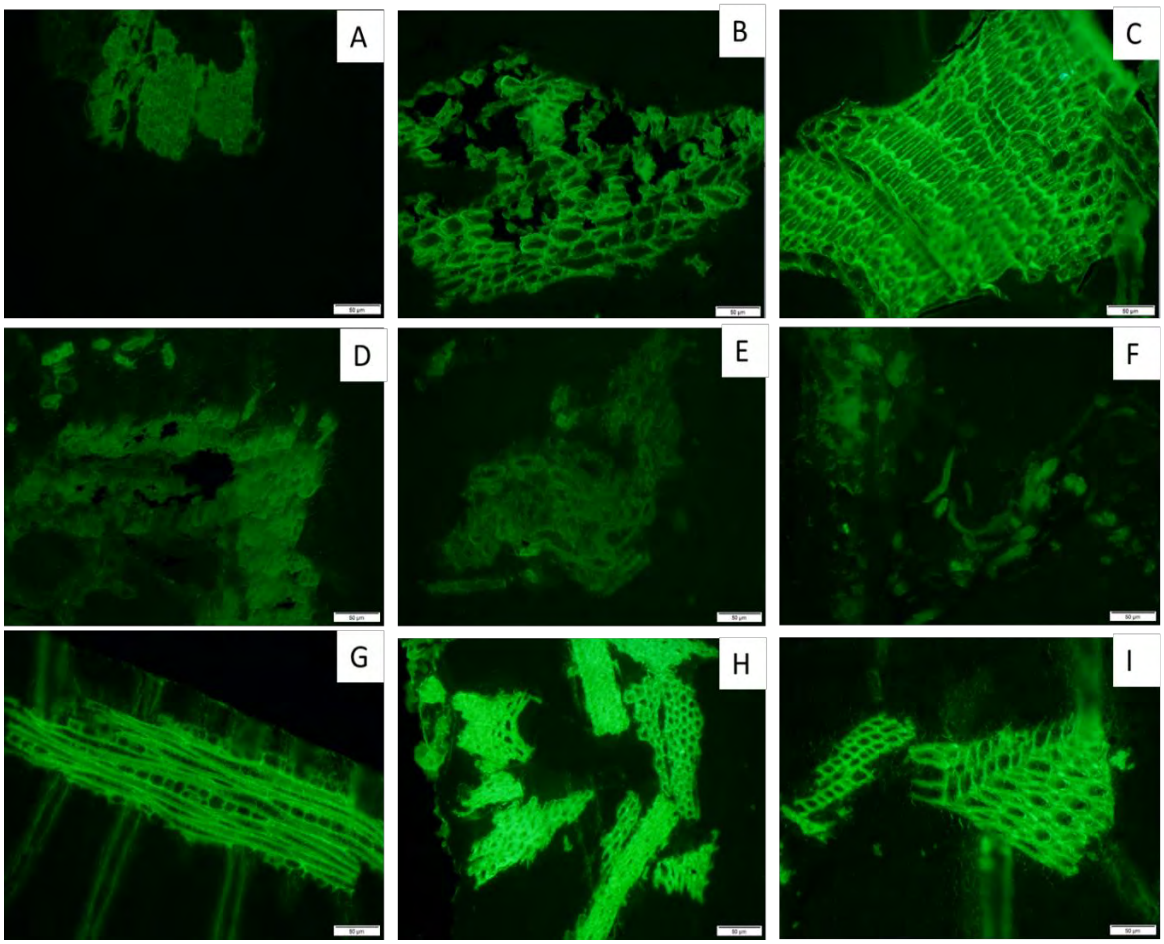

Figure 5.4. Fluorescence microscopy images of (A) untreated; (B) sodium chlorite; (C) sodium carbonate; (D) steam explosion; (E) steam explosion + sodium chlorite; (F) steam explosion + sodium carbonate; (G) acid; (H) acid + sodium chlorite; and (I) acid + sodium carbonate pretreated *Eucalyptus* samples.

Examination of the samples with fluorescence microscopy indicated that the untreated *Eucalyptus* sample had a very thick cell wall and a small lumen diameter. It was evident that after pretreatment, some changes in the wood structure had occured. After delignification (Figure 5.4B and 5.4C), the images showed that the cell wall fragments were still present, but the lumen diameter had increased. Similar observations were made for the acid pretreated samples (Figure 5.4G - 5.4I). For the steam explosion samples (Figure 5.4D – 5.4E), the cell walls appeared deformed and collapsed and a few distinct cell walls were present.

5.3.5. FTIR

FTIR was performed to analyse the chemical and structural changes in untreated and pretreated *Eucalyptus* samples and the spectra (400–4000 cm^{-1}) of the samples are presented in Figure 5.5 below.

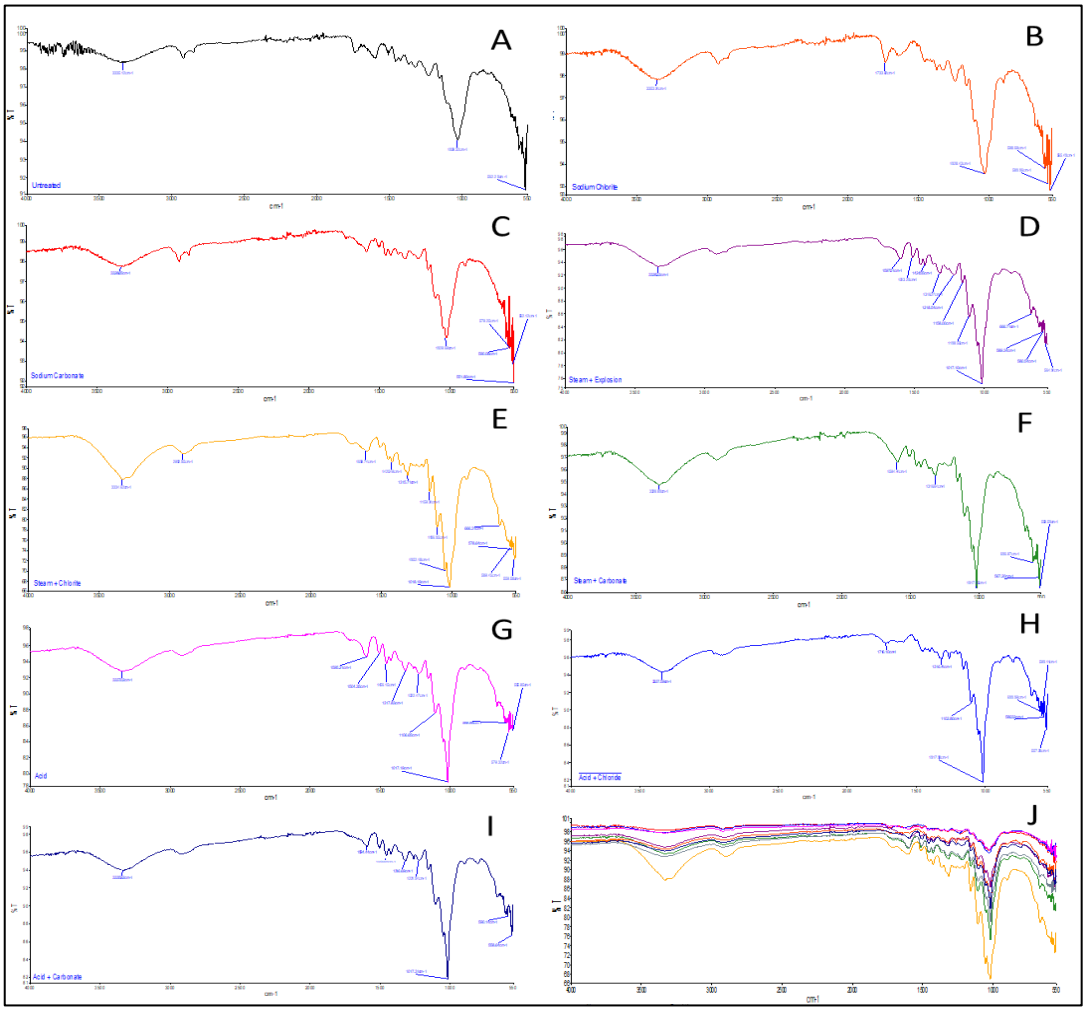

Figure 5.5. FTIR images of (A) untreated; (B) sodium chlorite; (C) sodium carbonate; (D) steam explosion; (E) steam explosion + sodium chlorite; (F) steam explosion + sodium carbonate; (G) acid; (H) acid + sodium chlorite; and (I) acid + sodium carbonate pretreated *Eucalyptus* samples.

When observing the main bands, it was evident that the FTIR spectra between the untreated and pretreated *Eucalyptus* samples (Figure 5.5) displayed differences with respect to the intensity and shape of their peaks. The peaks between 1234 and 1594 cm^{-1}, which represent lignin (aromatic skeletal vibrations and other lignin related bands) didn't change for the delignified samples (sodium chlorite and sodium carbonate) whereas the intensity increased for all the other samples. Characteristic assignment of cellulose at 896 cm^{-1} and 1430 cm^{-1} increased in intensity for all the pretreated samples, excluding the delignified samples, whereas the characteristic assignment of hemicellulose at 1730 cm^{-1} was only present in the delignified samples and had disappeared for all the other pretreated samples.

5.3.6. NMR

NMR is a powerful tool for analysing structural changes in the major constituents of plant biomass (cellulose, lignin and hemicellulose). NMR analysis was performed on the untreated and pretreated samples as described in Section 5.2.7. The NMR graphs are depicted in Figure 5.6 below.

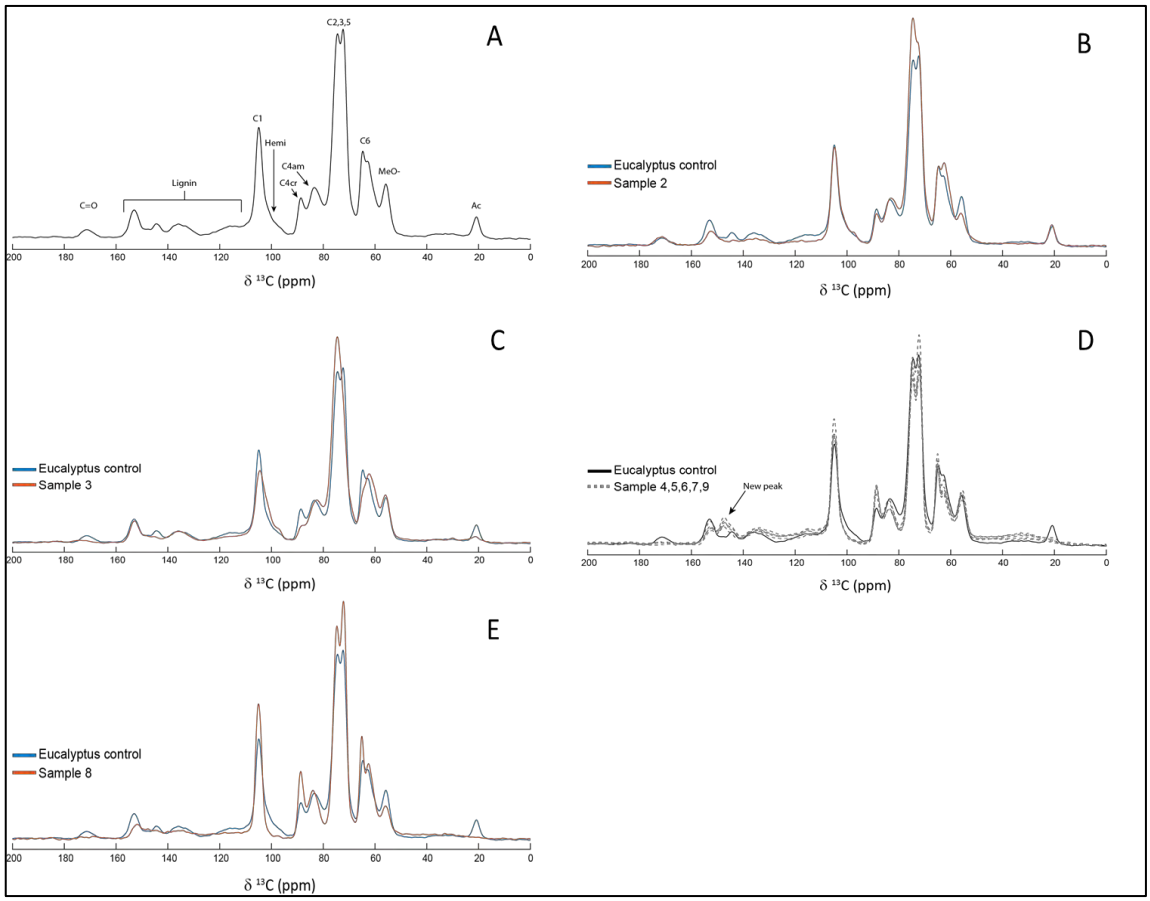

Figure 5.6. NMR peak assignments for (A) untreated; (B) sodium chlorite; (C) sodium carbonate; (D) steam explosion, steam explosion + sodium chlorite, steam explosion + sodium carbonate; acid and acid + sodium carbonate; and (E) acid + sodium chlorite pretreated *Eucalyptus* samples.

NMR (Figure 5.6) revealed that the pretreatment of *Eucalyptus* resulted in structural changes in the main constituents in plant biomass. As seen in Figure 5.6B (sodium chlorite) and Figure 5.6C (sodium carbonate), the samples contained less lignin and hemicellulose (110-160 ppm) compared to the native *Eucaylptus* sample (Figure 5.6A). Steam explosion (Figure 5.6D), steam explosion + sodium chlorite (Figure 5.6D), steam explosion + sodium carbonate (Figure 5.6D), acid (Figure 5.6D) and acid + sodium carbonate (Figure 5.6D) pretreated samples were similar to each other, whereby hemicellulose was removed (100 ppm) and some modifications in the lignin structure occurred (100-160 ppm). For the acid + sodium chlorite (Figure 5.6E) pretreated sample, the hemicellulose was completely removed (100 ppm) from the sample and there was also a reduction in the lignin content (110-160 ppm).

5.3.7. XRD Analysis

XRD analysis was performed on the untreated and pretretaed *Eucalyptus* samples, as described in Section 5.2.8. This was done to determine the exposure of the crystalline fraction of the biomass surface. The reflections at 2θ around 22.6° and 18.9° represent the crystalline and amorphous components, respectively (Phitsuwan *et al.,* 2017). The data is summarised in Appendix 5.

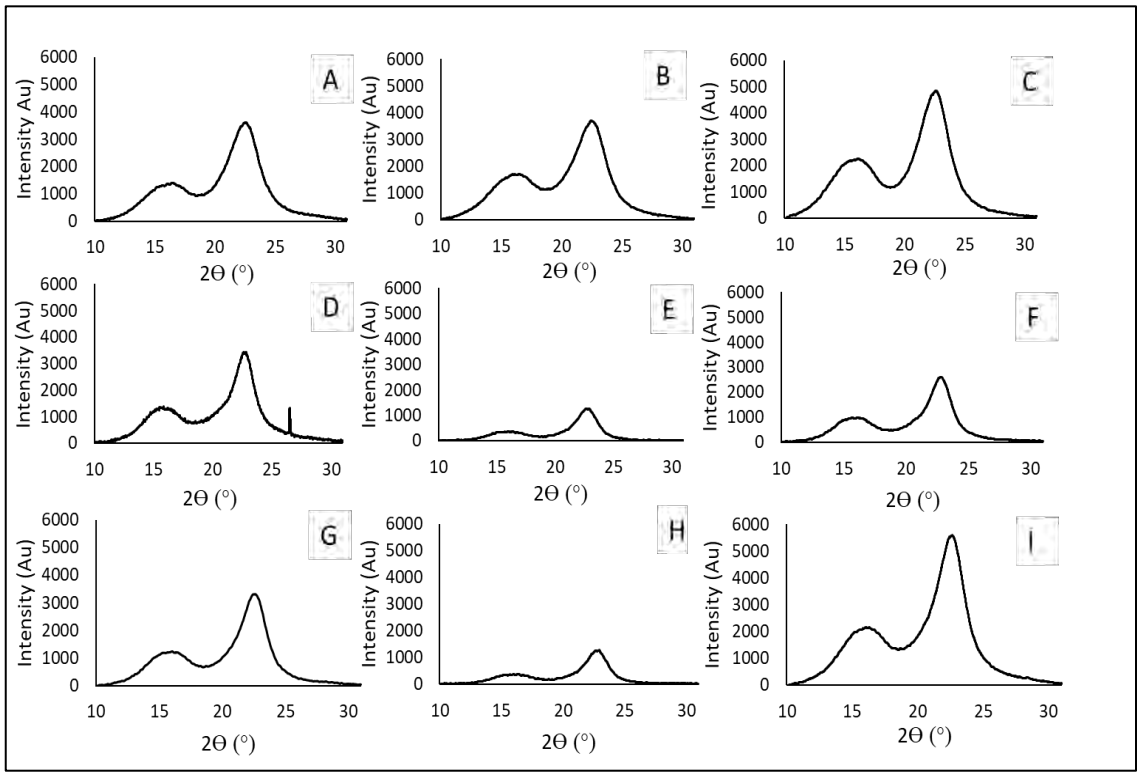

Figure 5.7. XRD images of (A) untreated; (B) sodium chlorite; (C) sodium carbonate; (D) steam explosion; (E) steam explosion + sodium chlorite; (F) steam explosion + sodium carbonate; (G) acid; (H) acid + sodium chlorite; and (I) acid + sodium carbonate pretreated *Eucalyptus* samples.

The CrI for the untreated *Eucalptus* was determined to be 74.44% (Figure 5.7A). The CrI decreased to 72.77% and 68.61% for the sodium chlorite (Figure 5.7B) and sodium carbonate (Figure 5.7C) pretreatments, respectively. The CrI increased to 77.19, 87.85, 80.59, 77.97, 87,85 and 75.24% for steam explosion (Figure 5.7D), steam explosion + sodium chlorite (Figure 5.7E), steam explosion + sodium carbonate (Figure 5.7F), acid (Figure 5.7G), acid + sodium chlorite (Figure 5.7H) and acid + sodium carbonate (Figure 5.7I), respectively. The increase in CrI indicates that these pretreatments led to fiber collapse and entanglement, resulting in a greater exposure of the cellulose fibres.

5.3.8. Simons' staining

Simons' staining was performed to measure the cellulose accessibility, as described in Section 5.2.9.

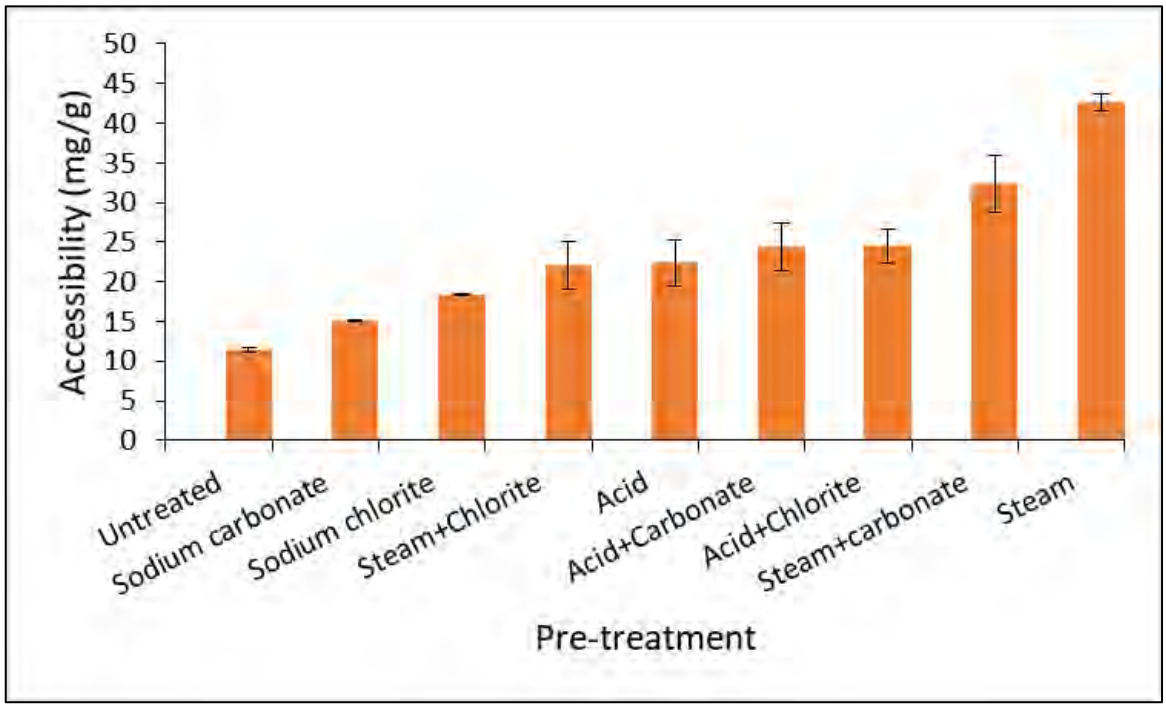

Figure 5.8. Simons' staining of untreated and pretreated *Eucalyptus* samples

As seen in Figure 5.8, steam explosion adsorbed the highest amount of dye (42.70 mg/g), followed by steam explosion + carbonate (32.38 mg/g), acid + chlorite (24.52 mg/g), acid + carbonate (24.38 mg/g), acid (22. 41 mg/g), steam + chlorite (22 mg/g), sodium chlorite (18.34 mg/g), sodium carbonate (15.11 mg/g) and untreated (7.5 mg/g).

5.4. Discussion

The absence of low-cost technology for overcoming biomass recalcitrance is the primary hurdle to the commercialisation of energy production from biomass feedstocks (Brodeur *et al.,* 2011). Thus, a

greater understanding of the underlying factors behind biomass recalcitrance is key to overcoming this problem. This chapter focused on investigating key factors that influence biomass recalcitrance, by subjecting the *Eucalyptus* biomass to various pretreatments. Delignification (sodium chlorite-acetic acid and sodium carbonate-acetic acid) was selected as the first pretreatment method. According to Malgas *et al.* (2017), this method is an oxidative pretreatment that can selectively remove lignin and leaves a larger proportion of hemicellulose in the substrate (Han *et al.,* 2020). Steam explosion (a form of physico-chemical pretreatment) and sulfuric acid (chemical pretreatment) were selected as the other pretreatments in this study. These pretreatments are best known to partially remove hemicellulose and cause lignin re-distribution (Malgas *et al.,* 2017; Meng and Ragauskas, 2017). Selecting these different pretreatment methods could potentially assist in understanding the complex structure of *Eucalyptus* biomass (Malgas *et al.,* 2017).

5.4.1. Chemical composition of the wood samples prior to and after pretreatment

According to Li *et al.* (2017), the chemical composition of biomass is an important factor for biomass utilisation and its digestibility, thus the chemical composition of *Eucalyptus* before and after pretreatment were determined in this study (as reported in Table 5.1). When compared with the previously reported composition for untreated *Eucalyptus*, similar results were obtained (Lima *et al.,* 2013; Wang *et al.,* 2017; Yu *et al.,* 2012). Compared to the untreated samples, the pretreated substrates showed various changes in their composition. As expected, delignification (sodium chlorite and sodium carbonate) resulted in decreased relative lignin composition and increased relative hemicellulose composition. Our results were similar to that reported by Troncoso *et al*. (2017) for delignified *Eucalyptus*, who reported glucan, xylan and lignin contents of 39.9%, 11% and 16.1%, respectively. On the other hand, samples that were pretreated with steam explosion or acid resulted in a higher relative lignin composition and lower relative hemicellulose composition which is consistent with findings by other researchers (Chiarello *et al.,* 2016; Chen *et al.,* 2020; Troncoso *et al.,* 2016). As mentioned previously, both steam explosion and acid pretreatments are ineffective at removing lignin, but instead alter lignin distribution that leads to increased cell wall porosity and enzyme accessibility (Meng and Ragauskas, 2017; Sun *et al.,* 2014). According to Meng and Ragauskas (2017), the lignin content generally increases after pretreatment with steam explosion and acid, due to a partial loss of carbohydrates or from pseudo-lignin formation. The mechanisms leading to the pseudo-lignin formation are yet to be elucidated, due to its complex structure and the heterogeneity of reaction sources and media (Hu *et al.,* 2012; Meng and Ragauskas, 2017).

The composition analysis data for the acid pretreated substrate in this study was similar to the findings by Lima *et al.* (2013), who reported a glucan, lignin and xylose content of 54.8%, 32% and 3.3%, respectively. However Chen *et al.* (2020) reported a glucan and lignin content of 38.09% and 23.36%, respectively, which was lower than what was reported in this study. The differences in the results may be attributable to different pretreatment conditions (i.e. severity and residence time of the pretreatments). Currently, there is no compositional analysis data for samples pretreated with a hybrid of steam or acid + delignification (with sodium chlorite or sodium carbonate). However, Lima *et al.* (2013) performed a combinatorial pretreatment (acid + NaOH) on *Eucalyptus* and the results were similar to our combinatorial pretreatment (acid + sodium chlorite). They reported a glucan, lignin and xylose content of 66.5%, 23.9% and 1.6%, respectively.

The extractives and ash content present in the untreated and treated samples were determined (Table 5.1). The untreated sample contained 8.1% extractives and 0.3% ash. Differences in these contents were observed for all the treatments tested (with higher or lower contents observed), where steam explosion contained the highest amount of extractives (15.6%) and sodium chlorite pretreatment the least (6.6%) of all the treatments assessed. According to Chiarello *et al.* (2016), the high content of extractives is attributable to the presence of larger quantities of waxes, cinnamic, acid derivatives, terpenes, lipids and other extractable materials (Jönsson and Martin, 2016).

5.4.2. Py-GC/MS

Plants have varying cell wall compositions (Davison *et al.,* 2006). Although total lignin content is of interest, the composition of lignin should also be considered when evaluating biomass recalcitrance (Davison *et al.,* 2006). One measure of lignin composition is the guaiacyl (G) and syringyl (S) components (Anderson *et al.,* 2019; Davison *et al.,* 2006). Py-GC/MS was performed, and monomeric composition analysis showed that *Eucalyptus* contained both G and S lignin monomers, as well as minor amounts of *p*-hydroxyphenyl (H) (Table 5.2). The higher S/G ratio in *Eucalyptus* was expected, since hardwoods contain a higher amount of S lignin monomers compared to G lignin monomers (Lima *et al.,* 2013; Lupoi *et al.,* 2014). In our study, the untreated *Eucalyptus* sample had an S/G ratio of 1.9 (Table 5.2), which was in accordance with previously published data for *Eucalyptus* spp. (S/G: 1.8 - 3.6) (Lupoi *et al.,* 2014; Ramadevi *et al.,* 2016). Our data showed that the S/G ratio decreased (< 1.9) for all of the pretreatments assessed (except for sodium carbonate pretreatment where the S/G ratio increased to 2.4). The decrease in S/G ratio suggests that the S-type lignin was more easily degraded compared to the G-type lignin for all the pretreatments assessed (Auxenfans *et al.,* 2017; Wang *et al.,* 2018). A similar observation was made by Auxenfans *et al.* (2017) for pretreated miscanthus and wheat

straw. They proposed that this may be attributable to a higher content of condensed structures in lignin of pretreated substrates, as G-lignin was determined to be more reactive towards condenstation. Additionally, a decrease in the S/G ratio is also indicative that hemicellulose has successfully been removed from the substrate and that some changes in lignin composition have occurred (Lima *et al.,* 2013; Studer *et al.,* 2011; Wang *et al.,* 2018).

Although the ratio of S/G lignin moieties has typically been used as a quantification method to evaluate biomass recalcitrance, many discrepancies have been reported in the literature (Anderson *et al.,* 2019; Davison *et al.,* 2006; Guo *et al.,* 2001). Various studies have reported that higher saccharification yields were achieved when the S/G ratio was higher, as branched G-lignin gives rise to a more physical barrier and is more resistant to chemical and biological degradation (Li *et al.,* 2010, Mansfield *et al.,* 2012; Studer *et al.,* 2011). Controversially, other studies have found degradability to be optimal at a lower S/G ratio, since S-lignin (non-condensed lignin) is said to be linear in shape, resulting in a higher coverage over cellulose fibres, thus protecting the secondary structure from degradation (Davison *et al.,* 2006; He *et al.,* 2018; Xu *et al.,* 2012). Jung and Deetz (1993) also hypothesised that S-rich lignin would be more inhibitory to cell wall degradation, as S mono-lignols have fewer potential polymerisation sites. Thus, in all likelihood, the influence of the S/G ratio on cell wall degradability should not be explained by the nature of the S or G unit itself.

Another important observation made from the Py-GCMS data was the increase in the C/L ratio for all the pretreatments assessed (excluding sodium carbonate and steam explosion + sodium carbonate). It is likely that this increase could be due to lignin removal that leads proportionally to more carbohydrates in the pyrogram. This is consistent with the chemical composition analysis data in this study (Rouches *et al.,* 2016).

5.4.3. Microscopy

5.4.3.1. Light microscopy

Staining biomass with dyes such as phloroglucinol and observing the samples under a light microscope is a simple and effective approach to qualitatively identify and localise the presence of lignin in samples (Mitra and Loqué, 2014; Trabucco *et al.,* 2013). Phloroglucinol stains reacts with cinnamaldehyde end-groups of lignin to give a magenta/red colour, and the intensity of the colour generally correlates with the level of lignification (Pradham and Loque, 2014; Stange *et al.,* 2011). The presence of the deep magenta colour in the untreated sample and the samples pretreated with sodium carbonate, steam explosion, steam explosion + sodium chlorite, steam explosion + sodium carbonate, acid and acid + sodium chlorite indicated that these samples contained lignin, whereas the

lack of this colour in the sodium chlorite and acid + sodium chlorite pretreated samples indicated that these samples contain no detectable lignin. These results were in accordance with the composition analysis results reported in Table 5.1.

5.4.3.2. SEM

SEM analysis revealed that morphological and structural changes took place on the surface of the wood samples after pretreatment methods. After delignification with sodium chlorite and sodium carbonate, the surface of *Eucalyptus* fibres exhibited a less compact and more defibrillated structure compared to the untreated sample. It seemed as if the outer matrix (which was observed in the untreated sample) had been removed, which may be be related to the delignification in the cell walls. Consequently, this disruption in the micro-structure led to an increased surface area of delignified *Eucalyptus.* Similar observations were made by Li *et al.* (2016), who reported a distorted and disintegrated structure of *Eucalyptus* after delignification with ionic liquids and alkali.

The samples that had been treated with acid resulted in surfaces with decreased amounts of residues, where no other significant morphological changes could be observed. These results were similar to the findings reported by Lima *et al.* (2013), who reported that these observations are consistent with the concept that acid pretreatment mainly removes the hemicellulose portion (of which *Eucalyptus* has a low content). Another observation made for the acid pretreated substrates (similar to the delignified substrates) was that fibre coalescence had occurred, which would lead to increased cellulose crystallinity.

Samples that had been exposed to steam explosion showed greater disruption of the cell wall architecture, resulting in a higher surface area compared to the other pretreatments. This was characterised by the loose fibrous network, which appeared as large fibrous tissue aggregates with a cylindrical shape. According to Auxenfans *et al.* (2017), this may be attributed to the solubilisation of cell wall components, where this exposed structure generally allows increased cellulose accessibility for the enzymes. These observations were similar to what has been previously reported in literature (Auxenfans *et al.,* 2017; Troncoso *et al.,* 2017).

5.4.3.3. Fluorescence microscopy

Fluorescence microscopy is a method that can be used to observe plant cell wall architecture, which is specifically useful when visualising the effect of pretreatment methods, aimed at lignin transformation. The fluorophores of the specimen absorb the specific wavelengths that are generated by the light source with an excitation filter, causing the emission of light with a longer wavelength (Wang *et al.,* 2017). Fluorescent microscopy was performed on the transverse sections of all the samples to evaluate the

spatial distribution and spectral properties of lignin (predominant fluorophore in plant cell walls) before and after pretreatment. The structure of the delignified and acid pretreated samples were similar to that of the untreated sample, although the lumen diameter had slightly increased after these pretreatments. These results were similar to the findings of Wang *et al.* (2017), who reported that small changes observed after these pretreatments may have been a result of partial hemicellulose or lignin removal. The collapsed lignin structure (few distinct cell wall fragments were present) observed after steam explosion indicates that steam explosion had the highest capacity to disrupt the cell wall structure (Wang *et al.,* 2017).

5.4.4. FTIR analysis

The structural changes in *Eucalyptus* due to the various pretreatments were investigated by FTIR analysis (Figure 5.5). Characteristic assignment of carbohydrate was observed at position 3335.12 cm^{-1} for the untreated *Eucalyptus* sample. Minor chemical shifts at this position were observed for all the pretreated samples, however, it was observed that, after pretreatment, the width of the peaks became narrower compared to the untreated sample. According to Wang *et al.* (2012), narrowing of these peaks indicates that these pretreatments cause breaking of intermolecular hydrogen bonds in cellulose. Two other bands of prime importance with respect to cellulose characteristics analysis by FTIR include the bands at 1425 cm^{-1} (cellulose I) and 896 cm^{-1} (cellulose II) (Chen *et al.,* 2020; Noori and Karimi, 2016; Troncoso *et al.,* 2017). These absorbance bands were observed in all the hardwood biomass substrates assessed in this study. Similar to the findings by Chen *et al.* (2020), a slight increase in the band at 1425 cm^{-1} was observed, indicating an increase in cellulose crystallinity for all the pretreated samples (excluding sodium chlorite and sodium carbonate) (Chen *et al.,* 2020). This was in agreement with composition analysis and XRD data that showed that these two pretreatments had similar relative glucan content and a lower CrI compared to the untreated substrate, respectively.

After pretreatment, the absence of the 1730 cm^{-1} band in the pretreated samples (steam explosion, steam explosion + sodium chlorite, steam explosion + sodium carbonate, acid and acid + carbonate) was observed, indicating a large removal of acetyl groups. Therefore, these results confirm the effectiveness of xylan removal by these pretreatment techniques (Lima *et al.,* 2013; Mohaptra *et al.,* 2017; Pandey and Pitan, 2003). These findings were similar to the findings by Troncoso *et al.* (2017) and were also supported by the composition analysis performed in this study. Interestingly, the peak at 1716.10 cm^{-1} for acid + sodium chlorite was unexpected, since the composition analysis data (Table 5.1) revealed that it was an effective pretreatment for xylan removal. The shift from 1733.92 cm^{-1} to 1716.10 cm^{-1} does, however, indicate that the acid + sodium chlorite sample contains less acetyl groups

compared to those in untreated, sodium chlorite and sodium carbonate samples (Colom *et al.,* 2003). A plausible explanation for these results could be that these groups migrated to other biomass polymers upon xylan solubilsation.

The bands at 1595 cm^{-1} and 1504 cm^{-1}, corresponding to aromatic skeletal vibration and stretching of the benzene ring in lignin, respectively, were not observed after pretreatment with sodium chlorite and acid + sodium chlorite, suggesting that these treatments were successful at removing lignin from the substrate. On the other hand, the other pretreatments resulted in an increase in this characteristic band, suggesting that part of the lignin was released and coprecipitated (Chen *et al.,* 2020; Wang *et al.,* 2019). These results were similar to the findings reported by Troncoso *et al.* (2017), who pretreated *Eucalyptus* by autohydrolysis and steam explosion. They reported that the increased intensities of the bands at 1595 cm^{-1} and 1504 cm^{-1} is attributable to the incorporation of new aromatic systems, coupled to the splitting of the lignin aliphatic side chains and the formation of new covalent bonds by condensation reactions. Interestingly, the disappearance of these bands was also expected for the steam explosion + sodium chlorite pretreated sample, since there was a decrease in relative lignin observed (similar to the acid + sodium chlorite sample). Although the characteristic band at 1504 cm^{-1} did not decrease in intensity after this pretreatment, the 1595 cm^{-1} band broadened to 1609 cm^{-1}, suggesting that there was an increase in structural diversity around the aromatic rings (Esteves *et al.,* 2013). In addition, the peak at 1220 cm^{-1} (corresponding to aromatic C-H stretching in lignin), disappeared after pretreatment with sodium chlorite, steam explosion + sodium chlorite and acid + sodium chlorite, further confirming the removal of lignin from the substrate with these pretreatments (Huang *et al.,* 2013).

5.4.5. NMR

NMR results revealed that sodium chlorite-pretreated *Eucalyptus* sample contained less lignin than the control (native or untreated sample), whereas the carbohydrates were largely unaffected. Sodium carbonate pretreatment, on the other hand, resulted in the deacetylation of hemicellulose (lower intensities of peaks at 173 and 22 ppm) and a drastic reduction in crystalline cellulose (89 ppm). When comparing the steam explosion, steam explosion + chlorite, steam explosion + sodium carbonate, acid and acid + sodium carbonate pretreated samples to the control (untreated *Eucalyptus* sample), it was found that the samples were similar to each other. There was a removal of hemicelluloses and some modifications to the structure of lignin. For all these pretreatments, a new peak appeared around 147 ppm and the intensity of the peak at 153 ppm decreased. The peak at 153 ppm is, at least in part, originating from aromatic carbons connected to a methoxy group. For the acid + sodium chlorite

pretreated sample, the hemicellulose was completely removed (100 ppm) from the sample and there was also a reduction in the lignin content (110-160 ppm).

5.4.6. XRD

Previous studies have reported that pretreatment changes the biomass crystallinity by: (i) opening crystal hydrogen bonding; (ii) degrading amorphous constituents and (iii) increasing crystal regions (Peciulyte *et al.,* 2015; Zhang *et al.,* 2018). Biomass crystallinity is considered to have a major influence on enzymatic hydrolysis; however, many discrepancies have been reported in the literature - therefore, no consensus has been reached regarding the effect of crystallinity on enzymatic hydrolysis. For example, studies performed by Goshadrou *et al.* (2011), Hall *et al.* (2010), Jeihanipour *et al.* (2010) and Poornejad *et al.* (2013) reported that higher conversion rates were achieved with a lower crystallinity, whereas some studies found the opposite effect - higher conversion rates were achieved with a higher crystallinity (Bali *et al.,* 2014; Sun *et al.,* 2014). Therefore, for us to better understand the relationship between crystallinity and biomass degradability of *Eucalyptus,* XRD was performed on the untreated and pretreated residues in this study. After substrate pretreatment, the height of the XRD peak changed as a result of the O-H bonds breaking, causing alteration of the cellulosic structure (Feng and Chen, 2008; Sangian *et al.,* 2018). After treatment with sodium chlorite and sodium carbonate, the CrI decreased suggesting that a certain amount of crystalline cellulose was removed. Acccording to Malgas *et al.* (2019), an increase in the non-cellulosic component (hemicellulose) should result in lowered CrI values in lignocellulosic biomass. Since both pretreatments resulted in a decrease in lignin and increase in hemicellulose (as seen in the composition analysis), we hypothesise that the removal of hemicellulose has a greater influence on crystallinity compared to lignin removal. Moreover, the CrI increased after treatment with steam explosion (77.19%), steam explosion + sodium chlorite (87.85%), steam explosion + sodium carbonate (80.59%), acid (77.97%), acid + sodium chlorite (87.85%) and acid + sodium carbonate (75.24%). This is in line with previous studies that observed increases in the *Cr*I after pretreatment in sorghum (Vandenbrink *et al.,* 2012), switch grass (Li *et al.,* 2010), corn stover (Kim and Lee, 2005) and miscanthus (Yoshida *et al.,* 2008). According to Bernardinelli *et al.* (2015) and Vandenbrink *et al.* (2012), the increase in CrI is attributed to the removal of lignin and hemicellulose, due to a proportional reduction in the amorphous halo of the XRD diffractogram (Zhang *et al.,* 2018), which was supported by the FTIR data (Figure 5.6). Since there was evidence that steam explosion and acid pretreatments resulted in hemicellulose reduction, we can further confirm the assumption that was made previously, i.e. that the removal of hemicellulose has a greater influence on the crystallinity compared to lignin removal. Another plausible explanation for the increased CrI (after pretreatments) is a result of fibre

entanglement and coalescence. According to Karp *et al.* (2014), high severity pretreatment can cause lignin to coalesce into discrete structures (with surrounding areas without lignin), which would result in increased cellulose crystallinity. This waas supported by the SEM images (Figure 5.3), where fibre coalescence after pretreatment was observed.

Interestingly, when comparing the results with the compositional data (Table 5.1), we also observed that *Cr*I was positively correlated with cellulose content. Samples that had a higher cellulose content exhibited higher crystallinity. These findings were similar to what was reported previously by Thygesen *et al*. (2005) and Vandenbrink *et al*. (2006), who found a positive correlation between *Cr*I and cellulose content. Thus, we confirm that cellulose content is another important factor in the increase of biomass CrI.

5.4.7. Simons' staining

One of the main outcomes of pretreatment is an increase in accessible surface area, which is one of the main features for enzymatic hydrolysis (Herbaut *et al.,* 2018; Sun and Cheng, 2002). The two accessible areas include the internal (porosity and capillary structure of cellulose fibres) and external surface areas (size and shape of the particles) (Taherzadeh and Karimi, 2008). The pretreated samples adsorbed more dye compared to the untreated sample, which was similar to the results reported by Wang *et al.* (2018). However, the observations made in this study were that the cellulosic accessible surface was not affected by the lignin content in the pretreated samples, i.e. the cellulosic accessible surface was higher in samples with a higher lignin content (steam explosion) compared to the samples with lower lignin. This was in line with the findings of Bali *et al.* (2014), who found that samples pretreated with ammonia had the highest lignin content (compared to lime pretreatment) but still showed high cellulose accessibility. Thus, it is plausible to assume that lignin is not the main contributing factor that limits the access of enzymes to cellulose. According to Sun *et al.* (2014), cellulose accessibility is attributable to hemicellulose removal, lignin-hemicellulose phase separation, and/or lignin redistribution due to the pretreatments.

In conclusion, it was difficult to establish the relationship between enzymatic hydrolysis and accessibility by Simons' staining, as the results obtained for each pretreatment were quite similar. Therefore, additional experiments such as congo red staining, water swelling capacity studies, nitrogen adsorption or electron topography would be required to correlate biomass accessibility to hydrolysability (Herbaut *et al.,* 2018).

5.5. Conclusions

The structural changes of the components of lignocellulosic materials during pretreatment is critical for explaining pretreatment chemistry and progressing the bioeconomy (Li *et al.,* 2017). In this study, *Eucalyptus* was used to better understand biomass recalcitrance. Eight different pretreatments were the subject of parallel comparisons, to test their impact on cell well solubilisation and lignin properties of their substrates. Samples that had undergone severe pretreatment (high lignin and hemicellulose removal) exhibited higher crystallinity compared to the milder pretreatments, which had a higher lignin and hemicellulose content. Microscopy images showed that pretreatment caused structural changes to the biomass, whereby cellulose coalescence was observed for most of the substrates. For steam explosion, it was evident that the cell walls were "loosened", which allowed for increased cellulose accessibility. This was further confirmed by Simons' staining. In conclusion, this study provides insight into important cellulose structural features responsible for biomass recalcitrance and how these could potentially influence enzymatic digestibility and saccharification of the biomass (which is the subject of the next chapter).

Chapter 6: Enzymatic degradation of Eucalyptus biomass by CelMix and accessory enzymes

6.1. Introduction

Bioconversion is generally achieved in two stages: (i) pretreatment, to reduce biomass recalcitrance, and (ii) enzymatic cellulose hydrolysis for fermentable sugar production (Adsul *et al.,* 2020; Kucharska *et al.,* 2019). In Chapter 5, *Eucalyptus* was subjected to various pretreatment processes and the effect of these treatments on the chemical and structural features of lignocellulose materials were assessed. This chapter specifically focused on the second stage of the bioconversion process, enzymatic cellulose hydrolysis. Enzymatic hydrolysis is the process in which cellulases are added to hydrolyse and convert the pretreated substrate into glucose (Du *et al.,* 2020). The main steps involved in the enzymatic hydrolysis process includes: i) the shift of enzymes from the liquid phase to the cellulose surface, ii) enzyme adsorption (formation of enzyme-substrate complex), iii) cellulose hydrolysis, (iv) transfer of the hydrolysis products from the cellulose surface to the liquid phase, and (v) hydrolysis of cellobiose and cellodextrins in the liquid phase (Fan, 2014). Although this seems like a relatively straightforward process, many structural features, and the composition and source of the cellulases play a major role in the overall rate of enzymatic hydrolysis. Thus, the interactions that occur between enzyme complexes and the substrate are not fully understood (Mansfield *et al.,* 1999).

Furthermore, research has mainly focused on using model substrates to elucidate how biomass structure and composition influences enzyme activity. However, using complex, heterogeneous substrates allows for an improved understanding of enzyme synergy and how these interactions are influenced by the chemical and structural features of biomass before and after pretreatment (Yang *et al.,* 2011). Therefore, the aim of this chapter was to examine the effect of chemical composition and structural features of the pretreated substrates (Chapter 5) on the synergistic enzymatic hydrolysis of *Eucalyptus* biomass. Another aim of this study was to provide valuable insights and differences into biomass pretreatment/recalcitrance and how this influences enzyme synergism.

6.2. Methods

6.2.1. Enzymatic hydrolysis of *Eucalyptus*

Reactions were carried out in 400 µL reaction volumes, containing 2% (w/v) substrate suspended in sodium citrate buffer (50 mM; pH 5.0) and a CelMix loading of 6.875 mg/g of substrate at 50°C, mixing at 25 rpm for 24 hours and then terminated by heat-deactivation at 100°C for 5 minutes. The

CelMix was also dosed with 1 mg/g of substrate of a GH11 endo-β-1,4-xylanase (*Neocallimastix patriciarum*, supplied by Megazyme) or a laccase (*Agaricus bisporus*, from Sigma Aldrich) to determine their effect on cellulose conversion. The reducing sugar and glucose concentrations were determined after hydrolysis using the protocols described in Section 3.2.4.1. Saccharification yield (%) was then calculated using the equation:

$$Saccharification\ yield\ (\%) = \frac{Glucose\ \left(\frac{mg}{ml}\right)\times 0.9}{Glucan\ \left(\frac{mg}{ml}\right)} \times 100\%.$$

Calculated on basis of initial cellulose content of 200 mg of untreated wood used for the experiments. Results obtained after 48 h enzymatic hydrolysis.

6.3. Results

6.3.1. Enzymatic hydrolysis

Enzymatic hydrolysis was performed as described in Section 6.2.1. The reducing sugars released and saccharification yields were determined and are shown in Figure 6.1.

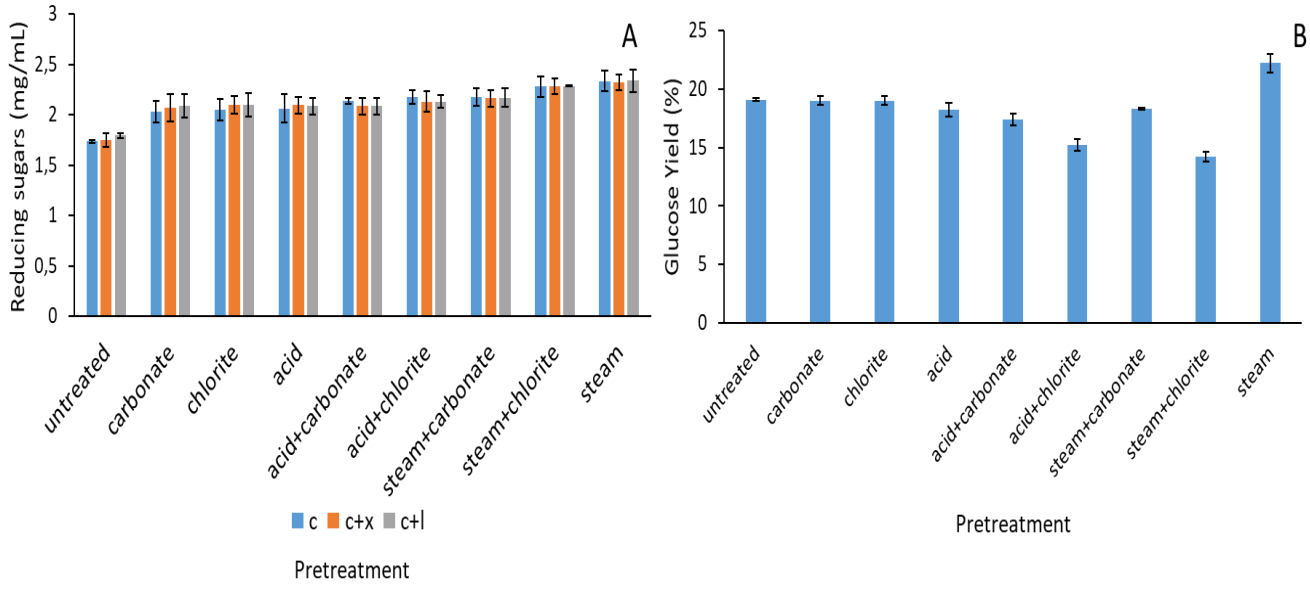

Figure 6.1. Enzymatic hydrolysis of pretreated *Eucalyptus*. All enzymes (c = CelMix, c+x = CelMix + xylanase and c+l = CelMix + laccase) were evaluated at the same protein loading (6.875 mg protein/g biomass) for 24 h. **(A)** reducing sugars released and **(B)** glucose saccharification yield. Datapoints represent the means of triplicate values (n=3, SD < 5%).

As seen in Figure 6.1A, there was an increase in reducing sugars released after the various pretreatments were performed. It was also evident that the addition of xylanase and laccase did not

significantly increase the amounts of reducing sugars released. In Figure 6.1B it is evident that the hydrolysis yield potential only increased after subjecting *Eucalyptus* to steam explosion and that the other pretreatmets did not improve saccharification yields, and that some pretreatments (acid, acid + carbonate, acid + chlorite, steam + carbonate and steam + chlorite) actually caused inhibition (lower saccharification yields compared to the untreated sample).

6.4. Discussion

Efficient saccharification of cellulose to fermentable sugars is a fundamental challenge in the bioconversion process. In this study, enzymatic saccharification of *Eucalyptus* samples was conducted for 24 hours, and the reducing sugars and glucose yield were determined (Figure 6.1). As expected, the amount of reducing sugars (Figure 6.1A) was lower for the untreated sample compared to pretreated samples. The addition of laccase or xylanase did not statistically improve enzymatic hydrolysis. Previous studies have shown that the addition of laccase (Deng *et al.,* 2019; Moilanen *et al.,* 2014) or xylanase (Hu *et al.,* 2011; Huang *et al.,* 2018; Murashima *et al.,* 2003; Zou and Shao, 2012) enhances enzymatic hydrolysis of the biomass. For example, Hu *et al.* (2011) proposed that xylanase improves cellulose hydrolysis as a result of increased cellulose accessibility to the cellulase enzymes, due to xylan removal from the pulp fibres. However, they also suggested that the observed improvement in hydrolysis yields were highly substrate and enzyme-dependent (Hu *et al.,* 2013). Therefore, we would not expect xylanase to statistically boost enzymatic hydrolysis, as the pretreatments were already efficient at removing xylan. In addition, pretreatment studies support the swapping of cellulases (in Chapter 4), since the pretreated substrates contained little hemicellulose. We did, however, expect an improvement with laccase addition, due to the high amounts of lignin present in the substrates. It must be noted though that a mediator is generally added to facilitate laccase-mediated delignification. Since this study was limited to only one laccase (without a mediator), we cannot positively confirm that this enzyme does not improve hydrolysis yields. Hence, we propose that future studies should assess the effect of various laccases (including a mediator), lignin modifying enzymes and LPMOs from different AA families and sources on cellulose hydrolysis, as this may present different results.

Enzymatic hydrolysis of *Eucalyptus* samples that had been treated by steam or acid (or their combined treatment with sodium chlorite or sodium carbonate) released similar concentrations of reducing sugars, however, steam pretreatment produced slightly more reducing sugars compared to samples that had been treated with acid. Their similar enzymatic hydrolysis rates may be attributable to the fact that

steam explosion and acid pretreatments both resulted in lignin redistribution and removal of hemicellulose that, in turn, increases cellulose accessibility (Donaldson and Vaidya, 2017).

Furthermore, the saccharification yield potential was established (Figure 6.1B), and provided a different overall picture compared to the data obtained for the reducing sugar release (Figure 6.1A). The saccharification potential of the untreated sample was 19.1%, which remained consistent for sodium chlorite and sodium carbonate pretreatment (19.0%). However, the saccharification decreased slightly for steam + sodium carbonate (18.3%), acid (18.2%) and acid + sodium carbonate (17.4%), whereas a higher decrease was observed for acid + sodium chlorite (15.5%) and steam + sodium chlorite (15.2%). The steam explosion was the only pretreatment that showed an increase in saccharification yield (22.2%), indicating that the steam explosion was the most effective pretreatment. It is important to note though, that the ratio of cellulase to to cellulose is not the same for these substrates, i.e. the substrates that had been exposed to steam explosion or acid + delignification with sodium chlorite had approximately 33% more glucan than the untreated and steam exploded biomass. Therefore, the mg protein/g glucan will be less than that of untreated and steam exploded substrates, which may explain why the yield didn't increase and yet the activity of reducing sugars did.

When comparing the reducing sugar release to the saccharification yield, it was evident that enzymatic hydrolysis failed to release a big fraction of the available sugar, indicating that the readily available substrate was all that was released. However, it is difficult to ascertain whether the efficiency of the pretreatment or the enzymatic mixture limited the overall yield. A study performed by Pawar *et al.* (2017) reported that hardwoods have enormous potential as renewable sources of sugars (due to their high carbohydrate content), however, saccharification is hampered by xylan acetylation. Although pretreatments such as acid pretreatment are said to remove a high portion of acetyl groups, acetyl groups are converted to acetic acid – a potent inhibitor of microorganisms (Jönsson *et al.,* 2013; Pawar *et al.,* 2017). Several studies have found that removing the acetyl groups prior to, or blocking upon pretreatment is a promising strategy for improving the economic viability of hardwood biorefining (Chen *et al.,* 2012; Pawar *et al.,* 2017). Pawar and colleagues (2017) introduced a fungal gene, acetyl xylan eseterase, into aspen wood, and found that deactylation had a positive effect on saccharification. This study did not assess the effect of de-branching enzymes on cellulose hydrolysis, which may have benefited the saccharification yields. Another factor that may have led to lower saccharification yields may be attributable to the collapse and aggregation of the cellulose microfibril network (Zeng *et al.,* 2017). This may have resulted in a significant reduction in enzyme digestibility, which would ultimately have reduced efficient enzyme penetration and rapid digestion (Zeng *et al.,* 2017).

6.5. Conclusions

When integrating the results from Chapter 5 and Chapter 6, we can propose various conclusions regarding biomass recalcitrance and enzymatic hydrolysis. The results revealed that a relationship between the S/G ratio and enzymatic saccharification existed and that a lower S/G ratio resulted in higher crystallinity, which led to a reduction in glucose saccharification yield. According to Davison *et al.* (2006), a lower S/G ratio implies more potential for covalent crosslinking and thus lower hydrolysis yields would be expected. Moreover, the results revealed that saccharification was higher when the S/G ratio was higher and that an increase in cellulose crystallinity seems to have a negative effect on enzymatic hydrolysis. This may be attributable to the removal of more amophous cellulosic layers (and the presence of more crystalline cellulose), which could be a hindrance to enzymatic hydrolysis. This study provided insight into important cellulose structural features responsible for biomass recalcitrance and how it influences enzymatic digestibility. Ultimately this information can be used as a platform for the development of more efficient conversion technologies for new competitive bio-refineries.

Chapter 7: Enzyme adsorption-desorption and evaluation of various cellulase recycling strategies for the enzymatic degradation of steam-pretreated Eucalyptus

7.1. Introduction

Enzymes play a critical role in the conversion of lignocellulosic biomass into sugar platforms, however, the high cost of enzymes associated with the hydrolysis step remains a major impediment to successful commercialisation of bio-refinery technologies (Leis *et al.,* 2017; Visser *et al.,* 2015; Yuan *et al.,* 2018). Although various pretreatment methods are used to reduce biomass recalcitrance and increase cellulose accessibility, large enzyme quantities or long hydrolysis times are still required to reach economically viable conversion levels (Kumar and Sharma, 2017; Lu *et al.,* 2002; Zhang *et al.,* 2018). It is, therefore, crucial to develop cost-effective processes that can increase the catalytic efficicency of enzymes, while reducing the enzyme loadings required to achieve efficient cellulose saccharification (Thoresen *et al.,* 2020; Weiss *et al.,* 2013).

As part of research efforts to develop a commercial process that reduces enzyme costs and improves the profitability of the bioconversion process of hardwoods, this study explored strategies for enzyme recycling (Thoresen *et al.,* 2020; Visser *et al.,* 2015; Weiss *et al.,* 2013). Theoretically, if enzymes are still active after hydrolysing a substrate, it should be possible to recover and re-utilise their remaining activities in multiple rounds of hydrolysis (Xue *et al.,* 2011). As enzymes are constantly adsorbing, desorbing and re-adsorbing on to the substrate during hydrolysis, enzymes can be recovered from both the solid and liquid phase (Van Dyk and Pletschke, 2012; Weiss *et al.,* 2013; Yuan *et al.,* 2018).

Although enzyme recycling may seem to be a relatively simple approach to reduce the economic costs of lignocellulosic biofuels, it is a complex process that requires in-depth knowledge of enzyme-substrate interactions and the different factors that may influence these interactions (Thoresen *et al.,* 2020). Although notable efforts have been made to try and better understand these enzyme-substrate interactions, the exact mechanisms of adsorption-desorption are yet to be elucidated (Hu *et al.,* 2018; Shang *et al.,* 2014). Most studies have used model substrates and purified enzymes to try and better understand these interactions, which unfortunately is not a true representation of the real interactions that take place between complex enzyme mixtures and lignocellulosic substrates (Pribowo *et al.,* 2012; Thoresen *et al.,* 2020). In addition, recycling the enzymes adsorbed to the solid residue of various pretreated lignocellulosic substrates has not been well studied, and the results reported in the literature are often contradictory and elusive (Lindedam *et al.,* 2013; Qi *et al.,* 2011; Yuan *et al.,* 2018).

Thus, using this information as our starting point, we developed two different strategies for recycling the enzymes associated with the insoluble solid residue, after enzymatic hydrolysis of the steam pretreated *Eucalyptus* samples, i.e. i) recycling the entire insoluble solid fraction (no desorption) (recycling approach 1- RA1) and ii) recycling the desorbed enzymes via elution (recycling approach 2 – RA2). The recycling performance of these two approaches was evaluated and compared by re-using a significant amount of hydrolytic activity from the insoluble solid fraction after hydrolysis to successfully reduce the enzyme loading (to reach a given level of sugar production). This study presents a potential approach for improving the economic feasibility of biofuel production at a commercial scale.

7.2. Materials and methods

7.2.1. Enzymes and commercial substrates

The enzyme cocktail, CelMix, used in this study was developed by Malgas and co-workers in a previous study (Malgas *et al.*, 2017). Please refer to Section 5.2.1 for the enzyme cocktail combination used in this study.

Protease from *Bacillus licheniformis,* Avicel PH-101, carboxymethyl-cellulose (CMC), *para*-nitrophenyl substrates; *p*-nitrophenyl-β-D-galactopyranoside (*p*NPG) and *p*-nitrophenyl-β-D-cellobioside (*p*NPC), Tris base (molecular biology grade – CAS 77-86-1- Calbiochem), PEG400, TritonX, Tween 20 and Tween 80 were purchased from Sigma-Aldrich (South Africa).

7.2.2. *Eucalyptus* and its pretreatment via steam explosion

The lignocellulosic substrate used in this study was *Eucalyptus* sp. which was kindly supplied by Mondi Ltd, Durban (South Africa). Prior to pretreatment, the wood chips were prepared as described in Section 5.2.2. Steam explosion was performed as described in Section 5.2.2.3.

7.2.3. Preparation of isolated lignin samples

Lignin was obtained from extensively enzymatically hydrolysed steam exploded *Eucalyptus* (800 mg, dry weight). The hydrolysis was conducted using a mixture of Novozyme Cellic® CTec2 and Novozyme Cellic® HTec (in a 4:1 protein ratio) at a total enzyme loading of 3 mg/mL in sodium citrate buffer (pH 5.0, 0.1 M) and incubated at 37°C (the temperature of 37°C was chosen throughout the study for consistency and lower energy imput). After a 48-hour hydrolysis period, the mixture was centrifuged (5488 × *g* for 10 minutes), the supernatant was decanted and the solid substrate was

washed with distilled water to remove any unbound enzymes and sugars. This was repeated until no sugar was detected. The residual solid was further treated with a protease (0.5 mg/mL) in sodium citrate buffer (pH 5.0; 0.1 M) and incubated at 37°C, mixing at 25 rpm for 24 hours. Thereafter, the mixture containing the protease was heat de-activated by incubating the sample at 100°C for 10 minutes, followed by centrifugation (5488 ×*g*, 10 minutes) and decanting of the supernatant. The remaining solid residue was washed and alkaline treated with Tris-HCl (pH 9.0; 0.05 M) for 2 hours, followed by the addition of 15% HCl in order to precipitate the dissolved lignin. The obtained lignin was washed with distilled water to remove residual proteins and sugars. After drying the residue at 50°C for 18 hours, the resulting material had a low protein content and was assumed to be a pure lignin fraction.

7.2.4. Analytical methods

7.2.4.1. Compositional analysis of steam pretreated *Eucalyptus*

The wood biomass was characterised using a modified sulphuric acid method of the National Renewable Energy Laboratory (NREL) at the Forest Products Biotechnology Group, University of British Columbia, Canada. Please refer to Section 5.2.2.3.

7.2.4.2. Protein determination

Total protein in solution was measured by the Bradford method (Bradford, 1976). Bovine serum albumin (BSA) was used as a suitable protein standard (Section 3.2.2). The amount of protein adsorbed to the substrate was determined as the difference between the protein concentration of the cellulases in solution before and after incubation with the substrate (Siquera *et al.,* 2017). The interference of the surfactants was accounted for by having controls in place, i.e. (supernatant + Bradford reagent) – (surfactant + Bradford reagent).

7.2.4.3. Determination of cellulase activity

CMCase, Avicelase and glucosidase activities were determined using CMC, *p*NPC and *p*NPG as described in Section 3.2.4.1.

7.2.5. Adsorption experiments

Cellulase adsorption was performed by allowing the CelMix to interact with the various lignocellulosic components (Avicel, extracted lignin from steam pretreated *Eucalyptus* and the whole biomass from steam pretreated *Eucalyptus*). These different materials were selected to assess the difference in the adsorption dynamics of CelMix on various lignocellulosic biomass components. Incubations were

performed with 2% (w/v) of the substrate, with CelMix loaded at 6.875 mg/g of biomass. The reactions were conducted at 50°C, with mixing at 25 rpm for 1 hour so that a stable adsorption equilibrium was reached (Hu *et al.,* 2010; Zheng *et al.,* 2013). After incubation, the samples were centrifuged at 5488 $\times g$ for 10 minutes and the liquid containing the unbound enzymes was collected and stored at 4°C for SDS-PAGE analysis, quantification of enzymatic activity and protein estimation. All experiments were performed in triplicate and were repeated twice for more accurate results. Samples lacking enzyme or substrate were used as enzyme and substrate controls, respectively.

7.2.6. Desorption of cellulases by various surfactants and alkaline media

Upon separation of the liquid fractions from biomass residues, various chemicals (Triton X100, PEG 2000, Tween 20 and Tween 80) and Tris-HCl (pH 9.0; 0.05 M) were added to the biomass (individually) to determine the most effective method for desorbing cellulases from the solid residues. The desorption efficiency was determined using the Bradford assay (Section 3.2.2) and then calculated using the equation:

$$Desorption\ efficiency\ \% : \frac{Bound\ enzyme - Unbound\ enzyme}{Bound\ enzyme}\ x\ 100$$

Tris-HCl (pH 9.0; 0.05 M) was determined to be the most effective desorption treatment and was selected for subsequent experiments. Therefore, after enzyme adsorption, the solid residue was subjected to an alkaline wash treatment (Tris-HCl pH 9.0; 0.05 M) at room temperature, mixing at 25 rpm for 3 hours. After incubation, the samples were centrifuged at 5488 $\times g$ for 10 minutes and the supernatants were collected and stored at 4°C for SDS-PAGE analysis, quantification of enzymatic assays and protein estimation. The solid fractions were obtained after alkaline elution and were then re-suspended in the same volume of the supernatant (that was recovered after desorption) in 0.1 M sodium citrate buffer (pH 5.0).

7.2.7. SDS-PAGE

Sodium dodecyl sulfate-polyacrylamide gel electrophoresis (SDS-PAGE) was performed using an 8% resolving gel and a 4% stacking gel as described by Laemmli (1976). The supernatant and solid samples (Avicel, lignin and steam exploded *Eucalyptus*) after enzyme desorption with Tris-HCl, as well as the control (complete cellulase mixture), were mixed with sample buffer and boiled for 5 minutes before being loaded into the wells of the gel.

7.2.8. Enzyme recycling strategies

Two different enzyme recycling approaches were performed (as illustrated in Figure 7.1) in order to assess their efficiencies at recycling the enzymes adsorbed onto the solid residue, after enzymatic hydrolysis of steam pretreated *Eucalyptus,* as described by Lindedam *et al.* (2013). Enzyme reusability was assessed by measuring the amount of enzyme activity adsorbed onto the insoluble solid residue and the ability of the enzymes to hydrolyse fresh steam pretreated *Eucalyptus* for multiple hydrolysis cycles.

7.2.8.1. Enzymatic hydrolysis

Hydrolysis experiments were performed in 400 µl reaction volumes, containing 2% (w/v) biomass suspended in sodium citrate buffer (pH 5.0; 0.1 M). After 24 hours of hydrolysis at 50°C, the supernatant was removed to measure the amount of reducing sugars (as glucose equivalents) using a modified 3,4-dinitrosalicylic acid (DNS) protocol (Miller, 1959).

7.2.8.2. Enzyme recycling of the solid residue by re-adsorption onto fresh substrate (RA1 approach)

Enzyme recycling was performed by recycling the solid residue after enzymatic hydrolysis of steam pretreated *Eucalyptus* (1st round) to the next round of hydrolysis (Figure 7.1, RA1 approach) to make sure that the unhydrolysed solids containing adsorbed enzymes could be recycled at the same time (Yuan *et al.,* 2018). After 24 hours, the samples were centrifuged (5488 × *g*; 10 minutes) and the unhydrolysed solids with adsorbed enzymes were mixed with fresh biomass, using the same 2% (w/v) solid loading. Various concentrations of fresh CelMix (0%; 40%, 50%, 60% v/v of the original protein loading) were supplemented to the reaction mixture for the next round of hydrolysis in order to achieve constant production of sugars during enzyme recycling. These concentrations were selected and optimised according to a study by Yuan *et al.* (2018), which was based on the amount/concentration of enzyme that was lost from the bulk adsorbed protein during hydrolysis rounds (i.e. approximately 40-50% of enzyme remains bound to the substrate, thus we added a minimum of 40% fresh enzyme to the next hydrolysis round).

7.2.8.3. Enzyme recycling of the solid residue by alkaline washing and adding the desorbed enzymes onto fresh substrate (RA2 approach)

Enzyme recycling was performed by recycling the desorbed enzymes (by Tris-HCl, pH 9.0; 0.05 M) from the solid residue after enzymatic hydrolysis (1st round) to the next round of hydrolysis (Figure 7.1, RA2 approach). After 24 hours, the samples were centrifuged (5488 × *g*; 10 minutes) and Tris-

HCl (pH 9.0; 0.05 M) was added to the recycled solid residue and incubated for 3 hours in order to remove any adsorbed enzymes. After alkaline elution, the samples were centrifuged (5488 ×*g;* 10 minutes) and the supernatants (desorbed enzymes) were added to fresh biomass, using the same 2% (w/v) solid loading. Various concentrations of fresh CelMix (0%; 40%, 50%, 60% v/v) were supplemented to the reaction mixture for the next round of hydrolysis in order to achieve constant production of sugars during enzyme recycling. Figure 7.1 provides a schematic representation of how the adsorption experiments were performed using both recycling procedures, RA1and RA2.

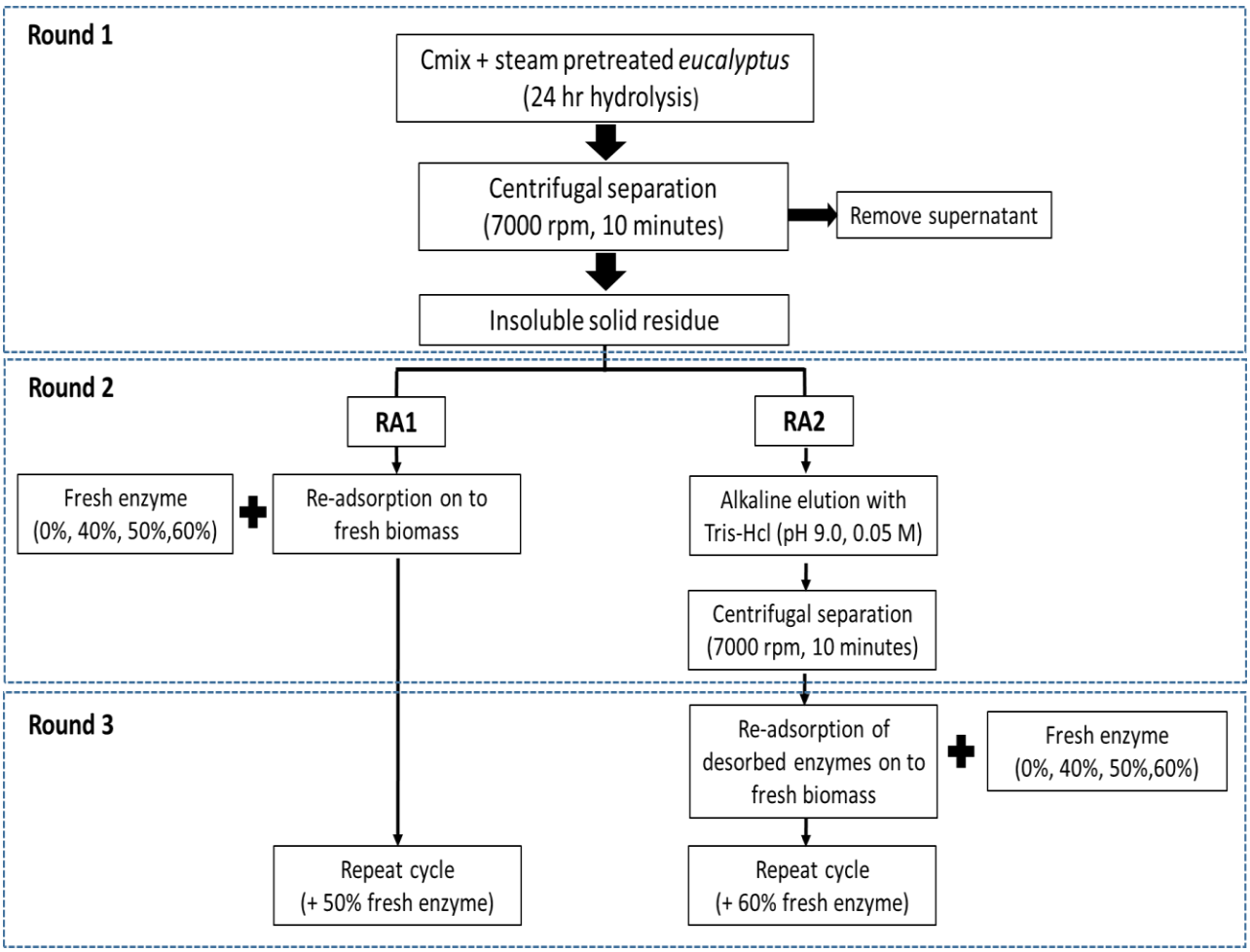

Figure 7.1. Schematic diagram of the two different recycling approaches investigated in study: Approach 1 (RA1): re-adsorption of the entire un-hydrolysed insoluble solid fraction (enzymes + biomass from the previous recycling round) to fresh biomass, and Approach 2 (RA2): enzyme desorption from insoluble fraction via alkaline elution (Tris-HCl, pH 9.0, 0.05 M) followed by re-adsorption of the desorbed enzymes to fresh biomass. In each cycle, fresh steam pretreated *Eucalyptus* biomass was added at 2% (w/v). The enzyme loading in cycle 1 was 6.875 mg/g substrate. Different enzyme dosages were added (0%, 40%, 50% and 60% v of the original protein loading) in cycle 2. In cycle 3, RA1 and RA2 were supplemented with 50% and 60% fresh enzyme, respectively.

7.3. Results

7.3.1. Enzyme adsorption and desorption studies

7.3.1.1. Enzyme adsorption studies

Cellulase adsorption was performed by allowing the CelMix to interact with the various lignocellulosic components (Avicel cellulose, extracted lignin from steam pretreated *Eucalyptus* and the whole insoluble fraction of steam pretreated *Eucalyptus*). The results depicted in Figure 7.2 show that 15.56%, 37.65% and 38.73% of CelMix adsorbed to Avicel, lignin and steam pretreated *Eucalyptus,* respectively.

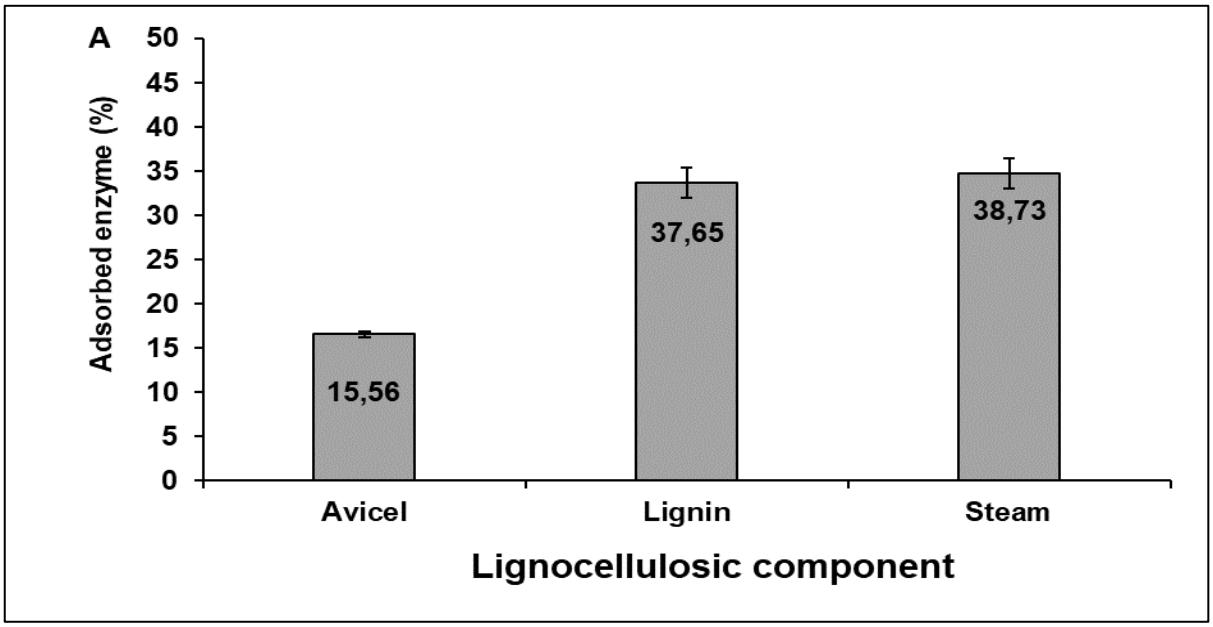

Figure 7.2. Adsorption studies of CelMix to Avicel, lignin and steam pretreated *Eucalyptus* after 1-hour incubation. The Bradford assay was used to measure adsorbed enzymes. Data represent the means of triplicate values (n=3, SD < 5%).

The data in Figure 7.2 illustrates that the cellulase components of CelMix have a higher binding affinity for lignin compared to cellulose as higher degree of adsorption was observed on the isolated lignin and the whole woody biomass containing both lignin and cellulose, with minor quantities of xylan.

7.3.1.2. Enzyme desorption studies

The efficiency of cellulase desorption was assessed using different surfactans or buffers, i.e. sodium citrate buffer (pH 5.0; 0.05 M), Tween 20, Tween 80, Triton X100, PEG and Tris HCl (pH 9.0; 0.05 M). For this study the supernatant was used. As seen in Table 7.1, Tris HCl (pH 9.0) exhibited the highest cellulase desorption efficiency of 90.67%, followed by PEG (81.37%), Triton X (36.36%), Tween 80 (30.60%), Tween 20 (30.20%) and lastly sodium citrate buffer (12.3%).

Since Tris HCl (pH 9.0) exhibited the highest desorption efficiency from all the washes assessed, it was used for the remainder of the study. The overall recovery of the initially adsorbed protein from lignocellulosic components after desorption using Tris-HCl (pH 9.0; 0.05 M) was assessed. Table 7.2 shows that the recovery of the initial protein was 86.8%, 93.94% and 94.62% for Avicel, lignin and steam exploded *Eucalyptus,* respectively.

Table 7.1. The effect of various chemicals/washes on cellulase removal efficiency (%) from steam pretreated *Eucalyptus*

Washing condition	Cellulase desorption efficiency (%)
Citrate (pH 5.0)	12.3 ± 0.96
Tween 20 (T20)	30.20 ± 3.1
Tween 80 (T80)	30.60 ± 3.99
Triton X	36.36 ± 2.23
Polyethylene glycol (PEG)	81.37 ± 2.9
Tris HCl (pH 9.0)	90.67 ± 12

Data represent the means of triplicate values (n=3, SD < 5%).

$$Desorption\ efficiency\ \% \frac{Bound\ enzyme\ -unbound\ enzyme}{Bound\ enzyme}\ x\ 100\%$$

Table 7.2. The overall recovery of the initially adsorbed protein from lignocellulosic components after desorption using Tris-HCl (pH 9.0; 0.05 M).

	Avicel	Lignin	Steam
Adsorbed enzyme on residue (% of initial protein)	16 ± 1.5	37.65 ± 2.1	38.73 ± 2.0
Washable enzyme (% of adsorbed protein)	19.23 ± 2.3	82.94 ± 3.5	84.04 ± 2.1
Overall recovery potential (of initial protein)	86.8 ± 2.3	93.94 ± 3	94.62 ± 3.3

Data represent the means of triplicate values (n=3, SD < 5%).

7.3.1.3. SDS-PAGE

The initial (control) enzyme and recovered enzymes from Tris-HCl desorption were further analysed using SDS-PAGE by visualising the protein (protein bands) in the supernatants after alkaline desorption from the substrates (Figure 7.3).

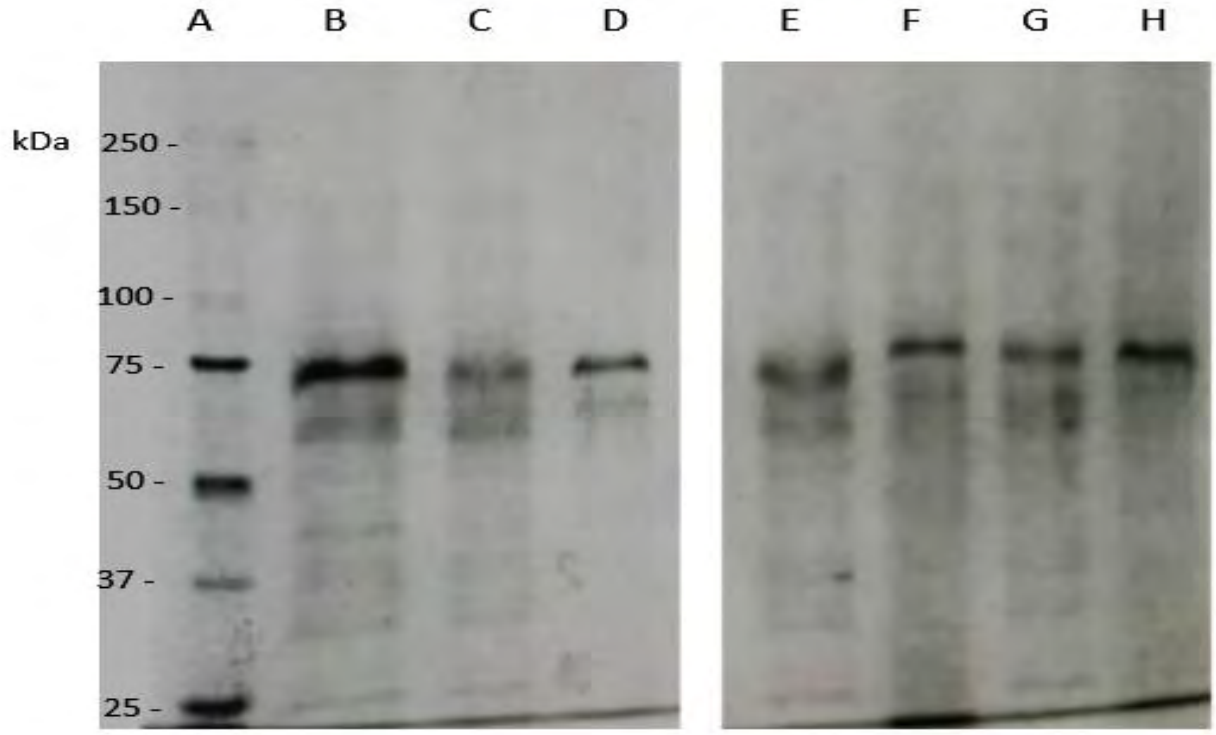

Figure 7.3. The desorption (recovery) of cellulases from Avicel, extracted lignin and steam pretreated *Eucalyptus.* Desorption was performed by washing the solid residues with Tris-HCl (pH 9.0; 0.05 M) at 25°C for 3 hours. A: Precision Plus protein unstained standard; B: control CelMix (0.5 mg/mL); C, E and G: desorbed enzymes (supernatant washes) from Avicel, lignin and steam exploded *Eucalyptus*, respectively; D, F and H: solid residues (after enzyme desorption) of Avicel, lignin and steam exploded *Eucalyptus,* respectively.

The high intensity of the bands in lane B represents the control (100% CelMix). In lanes C, E and G, bands were observed in the supernatants containing the desorbed enzymes (Figure 7.3). By observing the differences in band intensities between the control solution (CelMix), and recovered protein after alkaline elution, the effectiveness of alkaline desorption with Tris-HCl could further be evaluated. The bands in lanes C, E, G (desorbed enzymes) had lower intensities compared to the CelMix control (lane B). The presence of these bands confirmed that Tris-HCl was effective at facilitating cellulase desorption from all three substrates. However, the presence of the bands in lanes D, F and H, indicated that bound enzymes were still present after desorption.

7.3.2. Individual cellulase activities and activity distribution profiles

CMCase, Avicelase and β-glucosidase activities were determined using CMC, *p*NPC and *p*NPG as described in Section 3.2.4.1. Activity assays were performed to determine whether enzyme activity could be recovered from the desorbed enzyme after treatment with Tris HCl (pH 9.0; 0.05 M).

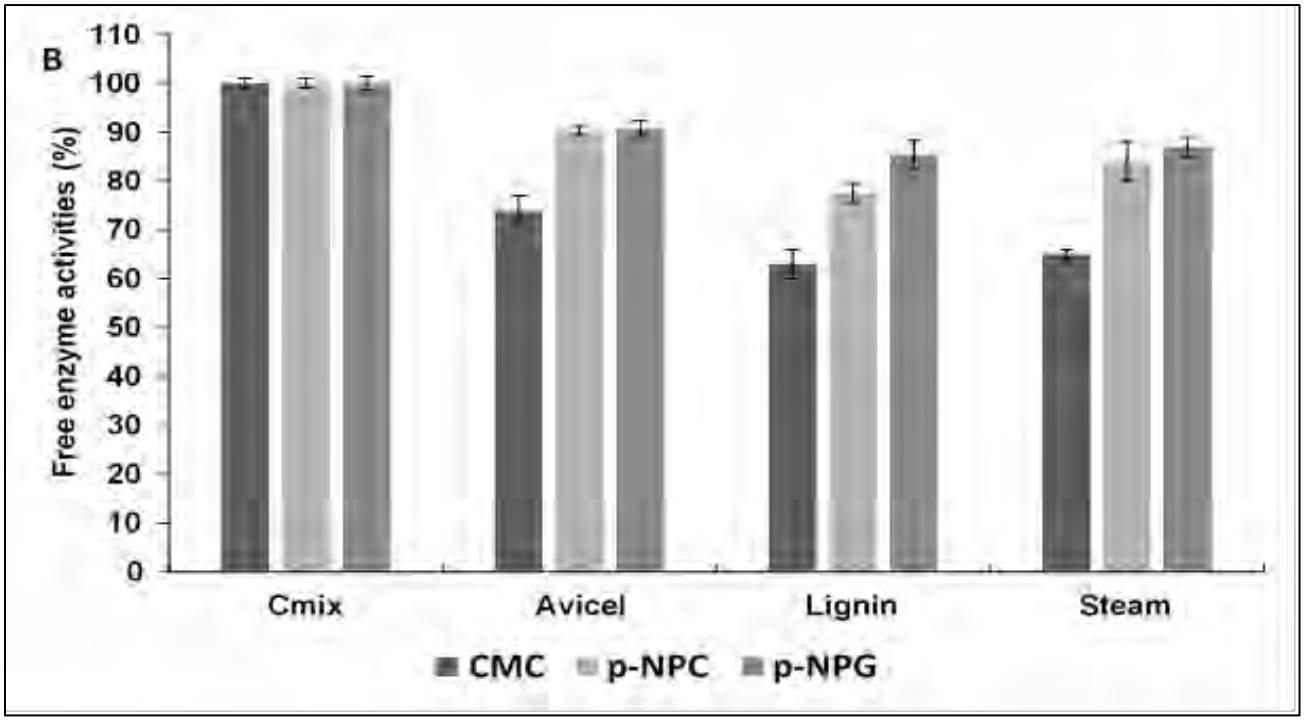

Figure 7.4. Adsorption studies of CelMix to Avicel, lignin and steam-pretreated *Eucalyptus* after 1-hour incubation. Activity (CMCase, *p*NPCase and β-glucosidase) assays were performed. Data represent the means of triplicate values (n=3, SD < 5%).

From the results in Figure 7.4, it was observed that 74.0% (Avicel), 63% (lignin) and 65% (steam exploded *Eucalyptus*) of CMC-ase activity could be recovered after alkaline elution. For *p*NPC activity, 90.4% (Avicel), 77.6 (lignin) and 85.4% (steam-exploded *Eucalyptus*) could be recovered, whereas for *p*NPG activity, 90.7% (Avicel), 84% (lignin) and 87% (steam exploded *Eucalyptus*) could be recovered from the solid residues.

Subsequently, we also evaluated the distribution of CelMix activities in the supernatant upon its adsorption to the lignocellulosic biomass components (see Figure 7.5 below). This was calculated by determining the individual activities (*p*NPC, *p*NPG and CMC as described in Section 3.2.4.1) of the unbound enzymes in the supernatants after 1 hour desorption compared to the activities in the complete Celmix preparation (expressed as relative activity %).

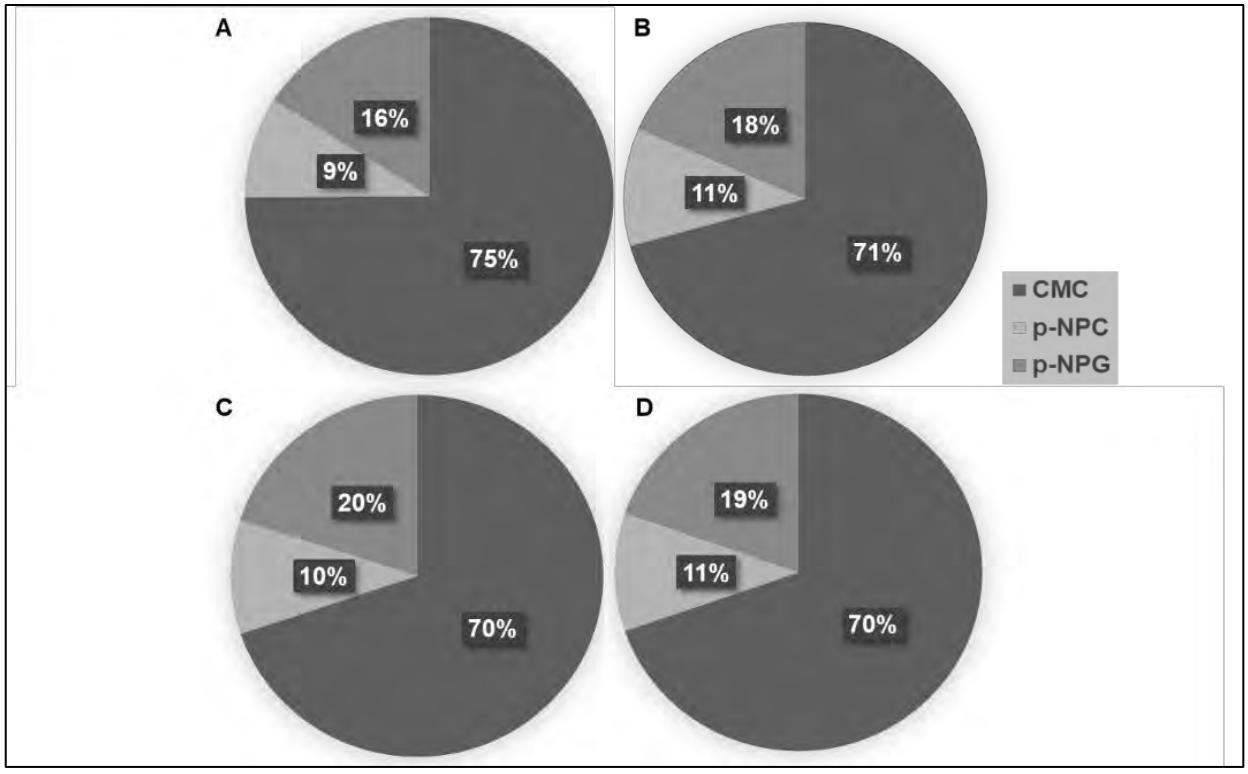

Figure 7.5. The distribution profiles of the major cellulase enzyme activities (A) in the complete CelMix preparation, and unbound enzymes in the supernatants after 1-hour adsorption at 37°C on (B) Avicel; (C) extracted lignin from steam pretreated *Eucalyptus* and (D) steam pretreated *Eucalyptus.*

From the distribution profiles in Figure 7.5, it was evident that after the enzymes had interacted with the different lignocellulosic components, the enzyme activity profiles in the supernatants (after binding) were different compared to that of the complete CelMix (100%). The original CelMix mixture (no adsorption) contained the major enzyme activities i.e. 75% EG (CMC) activity, 16% β-glucosidase (*p*-NPC) activity and 9% CBH (*p*-NPG) activity (Figure 7.5A). After enzyme adsorption, the supernatant displayed a slight decrease in EG activity (71%) and an increase in both β-glucosidase (18%) and CBH activity (11%) for Avicel (Figure 7.5B). The same pattern was observed after enzyme adsorption to extracted lignin - containing 70% EG activity, 20% β-glucosidase activity and 10% CBH activity (Figure 7.5C). Only 70% EG activity, 19% β-glucosidase activity and 11% CBH activity remained after adsorption to steam pretreated *Eucalyptus* (Figure 7.5D).

7.3.4. Enzyme Recycling Strategies

Two different enzyme recycling approaches were performed as described in Section 7.2.8 in order to assess their efficiency at recycling the enzymes adsorbed onto the solid residues after enzymatic hydrolysis of steam pretreated *Eucalyptus.* The results are presented in Figure 7.6.

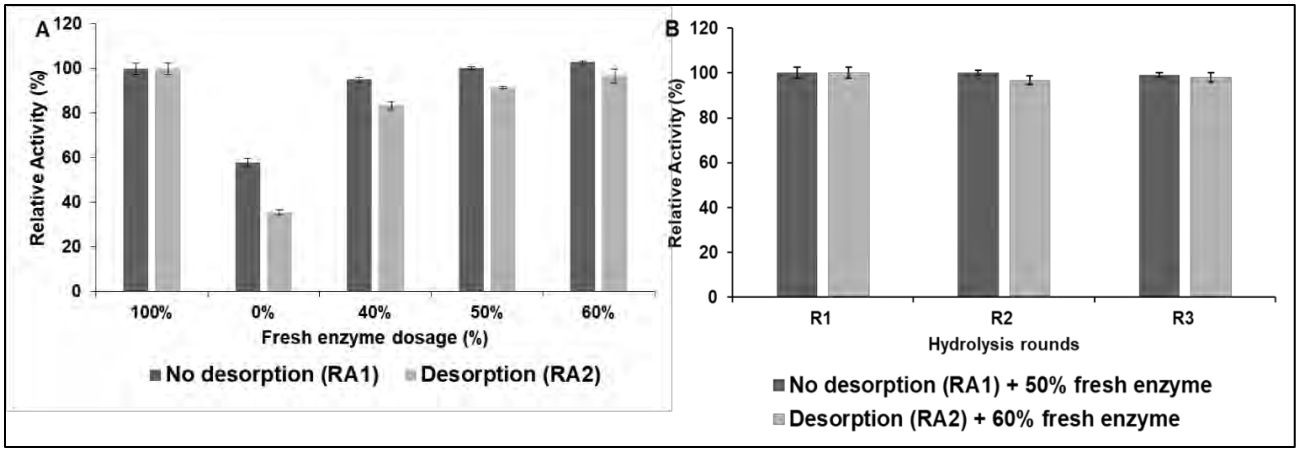

Figure 7.6. Evaluation and comparison of the performance of two different recycling approaches (RA1 and RA2) for recycling the enzymes associated with the insoluble solid residue after the enzymatic hydrolysis of steam pretreated *Eucalyptus* (first round). (A), The effect of different fresh enzyme dosages on reducing sugar release (second round) for RA1 and RA2, and (B), the effect of fresh enzyme loading (50% for RA1; 60% for RA2) in the third hydrolysis cycles. Each cycle was performed for 24 hours, and fresh biomass (2% w/v) was added to each hydrolysis cycle.

The results in Figure. 7.6A showed that without the supplementation of fresh CelMix in the 1st round, the amount of reducing sugars decreased to 58% and 37.2% for RA1 and RA2, respectively. The addition of fresh enzyme was required in the 2nd round for both recycling approaches, where RA1 needed 40-50% fresh enzyme and RA2 required 60% fresh enzyme. Figure 7.6B revealed that the enzymes could be recycled for at least 3 times using both RA1 and RA2.

7.4. Discussion

Developing a cost-effective processes that can increase the catalytic efficiency of enzymes, while reducing the enzyme loading is critical for achieving efficient cellulose saccharification (Thoresen *et al.,* 2020; Weiss *et al.,* 2013). An enzyme recycling strategy was therefore developed in this study.

7.4.1. Enzyme adsorption

Enzyme adsorption on to solid surfaces is a critical step in the enzymatic hydrolysis of lignocellulose, during which cellulases can productively bind to cellulose or non-productively bind to other cell wall polymers (Gomes *et al.,* 2015; Hu *et al.,* 2010; Machado *et al.,* 2015). Different pretreated substrates possess different binding accessible sites for various cellulase components, which affect their adsorption-desorption characteristics (Baig *et al.,* 2016; Van Dyk and Pletschke, 2012). Consequently, this has resulted in many controversial results with respect to enzyme recycling, making it important

for us to understand the enzyme adsorption-desorption characteristics of a pretreated substrate prior to designing a recycling system (Jørgensen, 2017; Machado *et al.,* 2015; Thoresen *et al.,* 2020).

Adsorption studies (Figure 7.2) showed that CelMix bound more extensively to lignin containing substrates compared to Avicel cellulose. High cellulase adsorption on lignin has been reported in numerous studies (Palonen *et al*., 2004; Seo *et al.,* 2011; Zheng *et al.,* 2013). It has been proposed that cellulases adsorb non-productively to lignin due to the presence of a CBM, since the aromatic amino acids (tryptophan and tyrosine) that are essential in CBM-cellulose interactions have also been shown to contribute to lignin-binding via hydrophobic interactions (Vermaas *et al.,* 2015; Yanfei *et al.,* 2016). A study performed by Malgas *et al.* (2019) reported that Douglas fir had a higher ligin content compared to Black wattle, and the higher lignin content in the softwood led to more non-specific binding of the Cel7A CBM (compared to the hardwood) on the biomass fraction. Studies have reported that CBMs are responsible for the adsorption of cellulases via electrostatic, hydrophobic and hydrogen bonds (Malgas *et al.,* 2019; Jørgensen *et al*, 2017; Zheng *et al.,* 2013). As a result, the presence of lignin in lignocellulose is believed to be detrimental for efficient cellulose hydrolysis and is not ideal when recycling the enzymes in a liquid phase.

Since these adsorption studies are representative of the total CelMix containing different cellulases, it is impossible to confirm which enzymes in the CelMix were predominantly bound to the various substrates and which enzymes were free in the supernatant. As mentioned previously, different enzymes have different binding affinities for different substrates, which play a major role in their adsorption behaviour (Baig *et al.,* 2016; Van Dyk and Pletschke, 2012). Thus, specific cellulase activity assays (CMC-ase, *p*NPG-ase, and *p*NPC-ase) were performed in order to assess the adsorption characteristics of the individual enzymes in the cellulase mixture. The percentage of bound activity for each cellulase component was measured by the difference in the activity levels in the CelMix control and the unbound (i.e. free) fraction as described previously (Hu *et al.,* 2010). The results (Figure 7.4) showed that EG bound more extensively onto all three substrates (CMC-ase activity). According to MacKenzie *et al.* (1998) and Palonen *et al.* (2004), EG has a higher affinity for lignin compared to CBH, due to its open conformation active site, rendering more aromatic residues to lignin that results in a hydrophobic interaction between the enzyme and lignin. Our results agreed with those of Mackenzie *et al.* (1998) and Palonen *et al.* (2004). CBHs bound to a lesser degree than EG to the other three substrates, as determined by the *p*NPC activity present in the supernatant, whereas the β-glucosidase bound to a lesser extent than both cellulases, CBH and EG. These results were in accordance with studies performed by Pareek *et al.* (2013), Sipos *et al.* (2010) and Varnai *et al.* (2011), who reported that β-glucosidase adsorbed to biomass to a lesser extent during the hydrolysis of Avicel

and different lignocellulosic substrates. They proposed that the low affinity of β-glucosidase for lignocellulosic substrates is because it lacks a CBM, which facilitates adsorption to the insoluble substrate. Since the enzymes displayed different binding affinities for the different lignocellulosic components, their enzyme activity distribution profiles (required to synergistically hydrolyse cellulose) after adsorption were expected to be different to that of the complete CelMix (100%). After enzyme adsorption, the supernatants for all the substrates assessed displayed a slight decrease in EG activity and a slight increase in CBH and glucosidase activity. Although only slight differences were observed with respect to the original CelMix mixture, compared to unadsorbed enzymes in the supernatant (after enzyme adsorption), it is evident that EG had a higher binding affinity for the substrates (manifesting in decreased CMCase activity in the supernantant), compared to the CBH and β-glucosidase.

7.4.2. The effect of various reagents on cellulase desorption

By taking advantage of the high adsorption affinity of CelMix to the substrate and considering that the bound enzymes are the key enzymes required for cellulose hydrolysis, recycling the adsorbed enzymes by re-adsorption onto fresh substrate would be a promising approach for reducing enzyme costs (Qi *et al.,* 2011). Thus, an alternative effective approach for recycling the adsorbed enzymes is through desorption and reuse of cellulases, which requires an understanding of the adsorption characteristics of cellulases (Baig *et al.,* 2016; Rodrigues *et al.,* 2014). Tris-HCl (pH 9.0; 0.05 M) was identified to be the most effective at facilitating enzyme desorption (90.67%) desorption efficienc. This was similar to the results reported by Zhu *et al.* (2009), who found that desorption was highly favoured at pH 7.0-10.0, indicating the potential of using *in situ* pH adjustment to monitor cellulase adsorption-desorption. According to Lou *et al.* (2013), at elevated pH values the electrostatic forces between enzymes and lignocellulosic substrates are increased, and hence the adsorption of enzymes onto the substrate is decreased (i.e. amino acids become negatively charged at a higher pH because they are operating above their isoelectric point, thus resulting in desorption from the substrate). Significant desorption was also found with PEG, which had a desorption efficiency of 81.37%, while TritonX, Tween20, Tween80 had minor effects on cellulase desorption (< 40% desorption efficiency) (Table 7.1).

We then determined how much initial protein could be recovered from the solid residues, after alkaline elution with Tris-HCl (pH 9.0; 0.05 M). Since high levels of protein could be desorbed from the substrates with Tris-HCl, it was selected for all subsequent experiments. The initial (control) and recovered enzymes from Tris-HCl desorption were further analysed using SDS-PAGE, by visualising the amount of protein in the supernatant after alkaline desorption from the substrates (Figure 7.3). The

high intensity of the bands in lane 2 represents the control (100% CelMix). Lanes C, E and G bands represent the supernatants containing the desorbed enzymes. By observing the differences in band intensities between the initial solution (CelMix), and recovered protein after alkaline elution, the effectiveness of alkaline desorption with Tris-HCl could further be evaluated. As expected, the bands present in lanes C, E and G (desorbed enzymes) had a lower intensity compared to CelMix control (lane B), due to the fact that CelMix is representative of the initial enzyme dosage (100%). However, the presence of these bands (lanes 3, 5, 7) confirmed that Tris-HCl was effective at facilitating cellulase desorption from all three substrates. It must be noted though that minor quantities of CelMix remained bound onto the solid residue (more so for lignin and steam pretreated *Eucalyptus* than Avicel) after alkaline elution (Lanes D, F and H in Figure 7.3). This may be attributable to the non-reversible binding of some cellulases to lignin (Jørgensen, 2017).

7.4.3. Comparison between enzyme recycling systems: RA1 and RA2

The enzymes adsorbed to the solid substrate are generally the key enzymes required for efficient saccharification (Hu *et al.,* 2018; Yuan *et al.,* 2018). In addition, a large fraction of the enzymes remains bound to the residual biomass after enzymatic hydrolysis (Lu e*t al.,* 2002). For this reason, the objective of this study was to study the adsorption-desorption characteristics of CelMix to various lignocellulosic components. This information provided an approach for developing a viable recycling system(s) (for the enzymes adsorbed to the solid residue) for steam pretreated *Eucalyptus* enzymatic hydrolysis. Based on the adsorption and desorption studies, two different recycling approaches were proposed for this study and their recycling performances were evaluated and compared (Figure 7.1). Enzyme reusability was determined by measuring the amount of enzyme adsorbed to the insoluble solid residue and the ability of the enzymes to hydrolyse fresh, steam pretreated *Eucalyptus* for multiple hydrolysis cycles as described elsewhere (Lindedam *et al.,* 2013).

Both recycling approaches were performed by hydrolysing steam pretreated *Eucalyptus* for 24 hours (1st hydrolysis round). Generally, most of the biomass was hydrolysed within the first 24-hour hydrolysis period and a significant portion of enzymes adsorbed to the substrate during this time. In addition, the advantages of performing hydrolysis for only 24 hours is that it allows for shorter hydrolysis periods which ultimately minimises loss of enzyme activities (Yuan e*t al.,* 2018). For each hydrolysis round, the same amount of fresh biomass and buffer as that used in the first hydrolysis cycle was added to each recycling approach. In addition, various CelMix protein mass loadings were added to the reaction mixture for each hydrolysis round (0%, 40%, 50% and 60%) in order to replenish enzyme activities. According to Xue *et al.* (2011), if the original enzyme dosage is used in each

hydrolysis cycle, the amount of sugars produced will increase as a result of enzyme accumulation. Thus, we supplemented various enzyme dosages to each cycle, in an attempt to make up the same initial enzyme loading as the original CelMix, in order to produce similar quantities of sugar as those attained in the first hydrolysis round.

As shown in Figure 7.6A, the reducing sugars released after the first round of hydrolysis is represented as 100% (based on relative activity), and the amount of reducing sugars released in the second hydrolysis round was compared to the 100% relative activity in round 1. The results showed that without the supplementation of fresh CelMix, the amount of reducing sugars decreased by 65.1% and 42.2% for the mixture containing desorbed enzymes (RA2) and unhydrolysed solids (no desorption) (RA1) achieved in the first round, respectively. It was evident that in the second hydrolysis round, both recycling approaches required the addition of fresh CelMix. In order to statistically ($p > 0.05$) achieve similar amounts of reducing sugars to that attained in the first round of hydrolysis (100% enzyme loading), supplementing the solid residue (RA1) with approximately 40-50% fresh enzyme was sufficient for the second hydrolysis rounds, whereas, a higher dosage (60%) of fresh enzyme was required when recycling the desorbed enzymes (RA2). Since our adsorption studies show that approximately 40% of enzymes adsorbed to steam pretreated *Eucalyptus* after 1 hour (Figure 7.6A), it would make sense that the 2nd cycle would require fresh enzyme dosages in order to achieve similar amounts of reducing sugars to that attained in the first hydrolysis round. Moreover, based on the assumption that the enzyme loading for the first hydrolysis round is 100%, we postulated that approximately 60% fresh enzyme supplementation would be required for the unhydrolysed solids. Our results deviated slightly from this assumption, as only 40-50% fresh enzyme was required to achieve similar amounts of reducing sugars to that obtained in round 1. According to Yuan *et al.* (2018), more adsorption sites on lignin become accessible during the course of hydrolysis. Thus, a plausible explanation for the slight deviations observed in this study could be that more enzymes adsorbed to the substrate (>40%) during the 24-hour hydrolysis course compared to that adsorbed to the substrate after 1 hour, thus less fresh enzyme was required. With respect to the desorbed enzymes, the higher dosage of fresh enzyme (60%) compared to the enzyme dosage required for unhydrolysed solids may be attributable to enzyme loss during alkaline elution, or from irreversibly binding to the solid residue after alkaline elution (Du *et al.,* 2012; Palonen *et al.,* 2004). The results in Table 7.1 confirm that some enzyme activities were lost during the alkaline wash process. Another round of hydrolysis (24 hours) and enzyme recycling cycle (round 3) was performed, where 50% and 60% fresh enzyme was supplemented to the unhydrolysed solid (no desorption) and supernatant containing the desorbed enzymes, respectively. Figure 7.6 shows that both recycling approaches could liberate similar amounts

of reducing sugars in the 2nd and 3rd cycle compared to that attained in the 1st hydrolysis cycle, and that both recycling approaches were capable of reducing the enzyme dosage for steam pretreated *Eucalyptus* degradation i.e. 50% (RA2) and 40% (RA1). With respect to conversion rates and reduction in enzyme dosage, RA1 performed slightly better than RA2, indicating that increasing the solid loading in each cycle did not have adverse effects on enzyme hydrolysis efficiency - although we expected that lignin accumulation and the increase in solid loading in each cycle would have a negative effect on hydrolysis (Kim *et al.,* 2019). Kristensen *et al.* (2009) and Visser *et al.* (2015) reported that these negative effects are generally only observed at solid loadings above 8%. Because only three (3) cycles were performed in this study, the solid loading could not have exceeded 8%. Thus, we would only be able to confidently confirm the adverse effects of lignin build-up on cellulase performance if additional hydrolysis/recycling cycles were performed. It must be noted though that high solid concentrations (>20%) are required in an industrial situation, thus additional experiments using high solid loadings would be critical for substantiating the concept of enzyme recycling.

7.5. Conclusions

This study studied the adsorption-desorption characteristics of a cellulase mixture (CelMix) on various lignocellulosic components to better understand enzyme-substrate interactions. The results revealed that lignin rich residues had a higher adsorption capacity compared to Avicel cellulose and that alkaline washing (Tris-HCl) had the greatest effect on enzyme desorption (90.67% efficiency). Based on these findings, two recycling strategies were developed in order to recover enzymes associated with the insoluble solid residue after steam exploded *Eucalyptus* hydrolysis. An evaluation on the recycling performance of the two different approaches: 1) recycling the entire un-hydrolysed solid residue (no desorption) and 2) recycling the desorbed enzymes (via alkaline elution) for three consecutive hydrolysis rounds showed that both approaches produced good recycling efficiencies (>95% of the initial hydrolysis yield was retained after 3 cycles) and reduced the enzyme loadings by 50% and 40%, respectively, in successive hydrolysis cycles. Enzyme usage was decreased by 50% (RA1) and 40% (RA2), while maintaining similar glucose yields, in successive hydrolysis rounds. These results clearly indicate that it is possible to recover and recycle the insoluble solid substrate associated enzymes after hydrolysis of steam pretreated *Eucalyptus*. Therefore, this approach presents a simple and effective way for reducing enzyme requirement for biomass hydrolysis, thereby contributing to the overall improvement in the economic feasibility of biofuel production. However, results may vary between different substrates and pretreatments, and the enzyme-substrate interactions may be influenced at high substrate consistency. It is therefore recommended tha future studies should be continued for its industrial application.

Chapter 8: General Discussion and Future Recommendations

8.1. General discussion

Global energy and environmental crises are driving the efficient utilisation of renewable sources of energy using green technologies (Anwar *et al.,* 2014; Balan *et al.,* 2014). Bioconversion of plant biomass to biofuels and value-added products is considered a promising solution to meet these demands. However, second generation biofuels are still finding their way towards development for commercialisation. The major challenges that hinder this process include biomass recalcitrance, the high cost of enzymes and the inability of any single microorganism to produce all the cellulases required for hydrolysis of feedstocks in sufficiently high quantities (Adsul *et al.,* 2020; Jørgensen *et al.,* 2007). Thus, numerous research efforts have focused on developing strategies to reduce enzyme costs during cellulosic ethanol production. These include designing optimal cellulase cocktails through enzyme synergy, assessing and optimising various pretreatment methods to increase hydrolysis efficiency and developing strategies to recycle enzymes (Adsul *et al.,* 2020; Bhattacharya *et al.,* 2014; Visser *et al.,* 2015).

In this context, the aims of this study were to: (i) gain a deeper understanding of the molecular mechanisms of glycoside hydrolases with respect to their substrate specificities and synergistic interactions in order to design an optimised enzyme cocktail, (ii) to understand the factors that significantly contribute to biomass recalcitrance and how this may potentially influence enzymatic hydrolysis, and (iii) gain an understanding of the enzymes' adsorption and desorption characteristics to develop an effective recycling strategy.

Synergy between various enzymes remains a subject of discussion since a full understanding of enzyme synergism is yet to be elucidated in order to develop a productive and cheap enzyme cocktail for efficient cellulose hydrolysis for biomass conversion into value added products (Adsul *et al.,* 2020; Du *et al.,* 2020). Therefore, the first objective of this study was to better understand how enzymes synergise at a molecular level, with the aim of formulating more effective enzyme cocktails for efficient biomass hydrolysis. To investigate the synergistic relationships between cellulolytic enzymes, 10 cellulolytic enzymes from different GH families and microbial sources were selected for this study. These included a cellobiohydrolase I from *H. jecorina* (Cel7A), CBHI from *T. longibrachiatum* (Cel7A), CBHI from *C. stercorarium* (Cel48A), CBHII from a microbial source (Cel6A), CBHII from *C. thermocellum* (Cel5A), a cellulase containing three endoglucanases (EglA (Cel9); EglB (Cel12)

and EglC (Cel74)), as well as three other endoglucanases (EG); *B. amyloliquefaciens* (Cel5A), *T. maritima* (Cel5A) and *T. reesei* (Cel7B). Prior to the synergy studies, the enzymes were first subjected to detailed comparative biochemical characterisation and analysed for their substrate specificities. The observations made with regards to their physico-chemical characteristics were similar to previously published results. All the enzymes were relatively stable at both 37 and 50°C and had a pH optimum range between 4.0 and 6.0. Thus, it was possible to use the enzymes together (or various enzyme combinations of these enzymes) in a single reaction at the standard industrial conditions (pH 5.0; 50°C). Substrate specificity studies revealed that the division into endo- and exo-glucanases in many cases are not absolute, and that enzymes can use different catalytic mechanisms within the same active site (O'Brien and Herschlag, 1999; Rauwerdink and Kazlauskas, 2015).

The characterisation of each cellulolytic enzyme led to an improved understanding of their substrate specificities (mechanistic behaviour) and the optimal conditions required for maximal activity. With this as a basis, we could delve deeper into gaining a better understanding of cellulase synergism. By means of mapping various CBH to EG interactions we designed a rational approach of screening for maximal compatibility between different GH families (cross-synergism), which provided an approach for a better understanding of the specific interactions between the enzymes of interest and how the complex synergistic activities of different enzymes assist each other in degrading cellulose. The results showed that swapping CBHII had minor effects on the synergistic and hydrolysis patterns observed between the CelMix (Egl 68%, Cel7A 17%, Cel6A 6%, βgl 9%), suggesting that microbial Cel6A and *Ct*Cel5A may share similar catalytic mechanisms because they showed similar synergistic patterns. Most importantly, this study captured the synergistic behaviour of endo- and exo-cellulases from different GH families and microbial sources. The major conclusion drawn from this part of the study was that synergies between endo and exo-glucanases are not necessarily effective in any given situation and there is no "guaranteed" optimal ratio of endo-cellulase/exo-cellulase for maximum degree of synergy, since the phenomena that cause the synergistic effect depends not only on the particular enzyme class, but also on the nature of the substrate and enzymes involved. We therefore postulated that, due to the different substrate specificities exhibited by cellulases from different GH family affiliations and microbial sources, enzymes are not always compatible with each other for efficient cellulose degradation. The only plausible explanation for this phenomenon is that the differences between CBHs and EGs are not always absolutely clear (as they may display cross-activity), but if one enzyme renders the substrate more accessible for the action of another enzyme, synergism will most likely occur. Only by examining the specific activities of an enzyme (individually, and in combination), can we substantiate whether an enzyme/enzyme cocktail will offer any

advantages towards enhancing cellulose hydrolysis. Information from this study can be used to compare cellulases from different GH families and microbial sources, to ultimately provide a better understanding of their behaviour in synergistic mixtures. This knowledge on how enzymes best work together synergistically provides a novel perspective to formulate better synergistic models to produce more economically viable enzyme cocktails, by promoting the synergistic actions among key enzymes to maximise the hydrolysis efficiency on various cellulosic substrates.

As mentioned previously, the heterogenous nature of lignocellulose makes it challenging to completely understand the interactions that take place between the enzymes and substrate. However, evidence suggests that the structural characteristics of the substrate and/or the modifications that occur as hydrolysis proceeds, are key factors that contribute to hydrolysis efficiency. Therefore, this thesis also investigated the use of pretreatments to achieve higher yields of reducing sugars from *Eucalyptus* sp. – a potential feedstock for biofuel production. Pretreatment is the first essential step required in the biomass conversion process, as it reduces biomass recalcitrance and increases cellulose accessibility (Karp *et al.,* 2013; Madaj *et al.,* 2017; Van Dyk and Pletschke, 2012). In this context, we wanted to gain a greater understanding of the underlying factors behind highly recalcitrant biomass. Eight different pretreatment methods were assessed in this study, upon which, various techniques were used to evaluate the chemical and structural changes that occured during pretreatment, including chemical composition analysis, Py-GC/MS, FTIR, NMR, XRD and various microscopic techniques, i.e. light microscopy, SEM and fluorescence microscopy. In evaluating their effectiveness towards the substrates, several observations were made. Composition analysis, FTIR, NMR and XRD studies showed that pretreatment leads to compositional and chemical changes in the principal components of wood, i.e. lignin and cellulose content (Popescu *et al.,* 2007). It was shown that lignin was not a major player in biomass recalcitrance and that the effects arising from lignin composition are probably masked by the complexities of the biomass species and other structural cell wall modifications that arise from pretreatment methods. Samples that had undergone severe pretreatment (high lignin and hemicellulose removal) exhibited higher crystallinity compared to the milder pretreatments, which had a higher lignin and hemicellulose content. Microscopy images revealed that pretreatment led to structural changes to the biomass, where cellulose coalescence was observed for most of the substrates. For steam explosion, it was evident that the cell walls were “loosened” which allowed for increased cellulose accessibility, which was further confirmed by Simons' staining.

Thereafter, synergy studies were performed on all the pretreated substrates using the enzyme cocktail formulated in Chapter 4. Since a model substrate (Avicel) was used in Chapter 4, it was uncertain as

to whether the enzymes would act in a similar manner on *Eucalptus*, a more complex natural substrate. The amount of reducing sugars released by enzymatic action increased after pretreatment, however, the addition of a xylanase or laccase did not significantly boost enzymatic hydrolysis. We concluded that similar hydrolysis patterns were observed with *Eucalyptus* that had been treated by steam or acid (or by their combined treatment with sodium chlorite or sodium carbonate), which may be attributable to the fact that steam explosion and acid pretreatments both result in lignin redistribution and removal of hemicellulose that increases cellulose accessibility (Donaldson and Vaidya, 2017). Furthermore, the glucan saccharification yield was also determined, which presented a different picture compared to the data for reducing sugar release. The saccharification potential of the untreated sample, which was 19.1% glucan conversion, remained consistent for sodium chlorite and sodium carbonate pretreatment (19%). However, the saccharification decreased slightly for steam + sodium carbonate (18.3%), acid (18.2%) and acid + sodium carbonate (17.4%), whereas a more significant decrease was observed for acid + sodium chlorite (15.5%) and steam + sodium chlorite (15.2%). Steam-explosion was the only pretreatment that showed an increase in saccharification yield (22.2%), indicating that steam explosion was the most effective pretreatment method (although the improvement wasn't significantly higher). When comparing the reducing sugars released to the saccharification yield, it was evident that enzymatic hydrolysis failed to release a large fraction of the available sugars, indicating that the readily available substrate was all that was released. However, it is difficult to ascertain whether the efficiency of the pretreatment or the enzymatic mixture limited the overall yield, since the enzyme mixture was specifically formulated for the untreated sample. It is important to note though, that the ratio of cellulase to cellulose was not the same for these substrates, i.e. the substrates that had been exposed to steam explosion or acid + delignification with sodium chlorite had approximately 33% more glucan than the untreated and steam exploded biomass. Therefore, the mg protein/g glucan will be less than that of untreated and steam exploded substrates, which may explain why the yield didn't increase and yet the activity of reducing sugars did.

Since the previous study allowed us to gain a better perspective of important cellulose structural features that were responsible for biomass recalcitrance, we wanted to determine how these factors could potentially have influenced enzymatic saccharification. When interrogating the results from Chapter 5 and Chapter 6, various conclusions were formulated with regards to biomass recalcitrance and enzymatic hydrolysis. The results revealed that a relationship between the S/G ratio and enzymatic saccharification existed and that a lower S/G ratio resulted in higher crystallinity, which led to a reduction in the glucose saccharification yield. An increase in cellulose crystallinity seemed to have a negative effect on enzymatic hydrolysis, which may have been attributable to the removal of more

amorphous cellulosic layers. The removal of these easily digested amorphous layers could cause a hindrance to enzymatic hydrolysis, since the substrate would be more crystalline in nature. Thus, cellulose accessibility, cellulose crystallinity and the changes in the lignin S/G ratio played an important role in the enzymatic activity of *Eucalpytus.*

The last experimental chapter of this study focused on understanding the adsorption-desorption characteristics of a cellulase mixture (CelMix) on various lignocellulosic components to better understand enzyme-substrate interactions. The primary objective of this chapter was to develop two recycling strategies to recover enzymes associated with the insoluble solid residue after hydrolysis of steam pretreated *Eucalyptus*. An evaluation on the recycling performance of two different approaches - recycling the entire un-hydrolysed solid residue (no desorption) and recycling the desorbed enzymes (via alkaline elution) for three consecutive rounds of hydrolysis showed that both approaches produced good recycling efficiencies (> 95% of initial hydrolysis yield was retained after 3 cycles) and reduced enzyme loadings by 50% and 40%, respectively, in successive hydrolysis cycles. These results revealed that it was possible to recover and recycle the insoluble solid substrate associated enzymes after hydrolysis of steam pretreated *Eucalyptus*. Therefore, this method presents a simple and effective way of improving the economic feasibility of biofuel production.

In conclusion, this study has contributed to expanding our knowledge of and providing new insights into factors relating to the biomass conversion process, including enzyme synergy, pretreatment method optimisation and enzyme recycling strategies for improving biomass conversion and its economic viability. Ultimately, the knowledge and information gained from this study can be used as a basis for the development of more efficient conversion technologies for new, competitive bio-refineries.

8.2. Scope for future research

It is well-known that biomass is a promising feedstock for the emerging renewable fuel industry, but achieving economic and environmental sustainability still remains a major challenge. In order to comprehensively understand the benefits of enzymatic biomass hydrolysis and the variables that affect the efficiency of the process, several issues must be addressed. Although this study provided a better understanding on enzyme synergism for biomass hydrolysis and how the chemical and structural features of biomass (with and without pretreatment) affect enzyme interactions, certain challenges remain. Thus, certain improvements to this process are still required for its efficient commercialisation. Recommendations to address some of these challenges are suggested below.

As previously discussed, the contribution of enzyme costs to the economics of lignocellulosic biofuel production is a major bottleneck in its commercialisation (Christopher *et al.,* 2015; Klein-Marcuschamer *et al.,* 2011). While purchasing the enzymes (from Novozymes, Danisco and DSM) is considered an easier option when it comes to performing enzyme studies, the manufacturing/formulation and transportation costs are extremely high; specifically when a designer enzyme cocktail is formulated using various enzymes from different sources (such as the formulated CelMix in this study). Therefore, we recommend that the Celmix is produced using an on-site strategy, as this may be more economical for the biomass saccharification process (Da Gama Ferreira *et al.,* 2018; Malgas, 2017). Although using a recombinant organism (i.e. *Aspergillus* sp.) for high levels of enzyme secretion, we need to take into account that fungal enzymes secrete mainly high levels of exo- and endo-cellulases, while only small quantities of glucosidase and hemicellulases are expressed (Malgas, 2017; Qing *et al.,* 2010). We, therefore, propose that a multienzyme preparation is produced from the co-cultivation of a cellulase-producing strain with a high-hemicellulase-producing microorganism – to allow for cheap enzyme production (Qadir *et al.,* 2018).

In this study, an optimal cellulase cockatil was designed to improve biomass saccharification. Although a xylanase and laccase was added to the mixture, no improvements to the saccharification of *Eucalyptus* were observed. However, the hemicellulases or lignin modifying enzymes and their synergistic interactions with cellulases were not investgated in this study. Thus, it would be very interesting to study the synergism between cellulases and xylanases and/or laccases or ligninases, much more extensively. Performing a thorough study of the hydrolysis modes of different xylanases, laccases or ligninanses (i.e. of different GH families, specificities and sources), could potentially assist our understanding of their functions and activities (inter-/intramolecular), thus assisting the selection of appropriate enzymes to develop an effective multienzyme cocktail. Furthermore, adding auxillary enzymes such as acetyl xylan esterases, LPMOs, or swollenins and expansins to the substrate before and after pretreatment may open new insights into the role of these enzymes and their synergistic behaviour with hydrolytic enzymes.

The protein loading of 6.875 mg/g biomass used in this study achieved approximately 18 - 25% glucose saccharification. Although this study was a fundamental study to gain an understanding of enzyme interactions and the factors that influence these interactions, we recommend that future studies should assess the effect of protein loading on *Eucalyptus* enzymatic hydrolysis, as well as perform time-course analysis studies to assess the hydrolysis profiles of untreated and pretreated *Eucalyptus* samples. This would also allow for a better understanding of the protein loading required for optimal saccharification

(100% yield). Moreover, the evaluation of the enzyme cocktail's performance was performed at 2% (w/v) substrate loading, but future studies should assess its performance at industry standards of up to 20% (w/v) biomass loadings.

Another challenge that restricts the cost effective production of cellulosic fuels is biomass recalcitrance. Although an aim of this study was to obtain a better understanding of the factors that induce biomass recalcitrance, much more extensive research on this topic is required, as many aspects of cellulose structure and cellulose matrix interactions are not well understood. Thus, many thought-provoking questions regarding cell wall polymers remain to be answered. Future studies should investigate different, novel pretreatments, and specifically optimise the pretreatments for *Eucalyptus* (i.e. temperature, residence time and severity of the pretreatments). Additionally, future studies could investigate how the Glycomic Code could be inserted in the context of the enzymatic breakdown of lignocellulosic substrates such as *Eucalyptus*. During this, studies on how pointrons (polysaccharide motifs that are recalcitrant to hydrolysis) and pexons (polysaccharide motifs that available for enzymatic attack) should be used to identify an enzyme cocktail action model (Buckeridge and Souza, 2014) could be conducted. Altogether, the combination of various techniques to characterise cell wall structural organisation provides an approach to examine the interactions between cellulose and other cell wall polysachharides. Additional techniques, such as atomic force microscopy (AFM), surface-enhanced and tip-enhanced Raman spectroscopies, and transmission electron microscopy (TEM) may contribute even further to our knowledge and our understanding of biomass recalcitrance, and how it influences enzyme synergism, and ultimately biomass degradation.

A side effect of pretreatment is the formation of lignocellulose-derived by-products that have an inhibitory effect on the enzymatic and process performance which results in decreased fermentable sugar yields (Jönsson and Martín, 2016). This study did not investigate the compounds released during pretreatment and their effect on enzymatic hydrolysis of *Eucalyptus.* Therefore, we recommend that future studies should look into the effects of these by-products on the enzymes.

Lastly, enzyme recycling was performed and the reusability of enzymes was achieved in this study. However, this was a lab-scale approach where the enzymes were only recycled in three (3) consecutive hydrolysis rounds. Moreover, high solid loadings (industrial conditions) were not used in this study, thus, we were unable to confidently confirm the adverse effects of lignin build-up on cellulase performance after additional hydrolysis/recycling cycles. Thus, we recommend that future studies

should perform this study under industrial conditions (higher enzyme and substrate concentrations) for proving the concept of enzyme recycling.

References

Abo, N., Gao, M., Wang, Y., Wu, C., Ma, H., Wang, Q. (2019). Lignocellulosic biomass for bioethanol on pretretament, hydrolysis and fermentation processes. Reviews of Environmental Health. 34(1): 57-64.

Adsul, M., Sandhu, S.K., Singhania, R.R., Gupta, R., Puti, A.K. (2020). Designing a cellulolytic enzyme cocktail for the efficient and economical conversion of lignocellulosic biomass to biofuels. Enzyme and Microbial Technology. 133: 109442.

Ahorsu, R., Medina, F., Constanti, M. (2018). Significance and challenges of biomass as a suitable feedstock for bioenergy and biochemical production: a review. Energies. 11: 3366.

Alcántara, MÁ., Dobruchowska, J., Azadi, P., García, B.D., Molina-Heredia, F.P., Reyes-Sosa, F.M. (2016). Recalcitrant carbohydrates after enzymatic hydrolysis of pretreated lignocellulosic biomass. Biotechnology for Biofuels. 9(207).

Alkaswaari, M., Eriksson, T., Borjessin, J., Wingeren, A., Galbe, M., Tjerneld, F., Zacchi, G. (2003). The effect of Tween-20 on simultaneous saccharification and fermentation of softwood to ethanol. Enzyme and Microbial Technology. 33(1): 71-78.

Alvira, P., Tomas-Pejo, E., Ballesteros, M., Negro, M.J. (2010). Pretreatment technologies for efficient bioethanol production process based on enzymatic hydrolysis - a review. Bioresource Technology. 101: 4851-4861.

Andersen, N., Johansen, K.S., Michelsen, M., Stenby, E.H., Krogh, K.B.R.M., Olsson, L. (2008). Hydrolysis of cellulose using mono-component enzymes shows synergy during hydrolysis of phosphoric acid swollen cellulose (PASC), but competition on Avicel. Enzyme and Microbial Technology. 42(4): 362-370.

Anderson, E.M., Stone, M.L., Katahira, R., Reed, M., Muchero, W., Ramirez, J., Beckham, G.T., Roman-Leshkov, Y. (2019). Difference in S/G ratio in natural poplar variants do not predict catalytic depolymerization monomer yields. Nature Communications. 10(2033).

Andlar, M., Rezic, T., Mardetko, N., Kracher, D., Ludwig, R., Santek, B. (2018). Lignocellulose degradation: An overview of fungi and fungal enzymes involved in lignocellulose degradation. Engineering in Life Sciences. 18: 1-11.

Antov, E., Schlembach, I., Regestein, L., Rosenbaum, M.A., Buchs, J. (2017). Process relevant screening of cellulolytic organisms for consolidated bioprocessing. Biotechnology for Biofuels. 10(106).

Anwar, Z., Gulfraz, M., Irshad. (2014). Agro-industrial lignocellulosic biomass a key to unlock the future bio-energy: A brief review. Journal of Radiation Research and Applied Sciences. 7(2): 163-173.

Arai, T., Araki, R., Tanaka, A., Karita, S., Sakka, K., Ohmiya, K. (2003). Characterization of a cellulase containing a family 30 carbohydrate-binding module (CBM) derived from *Clostridium thermocellum* CelJ: importance of the CBM to cellulose hydrolysis. Journal of Bacteriology. 185(2): 504-512.

Arantes, V. and Saddler, J.N. (2010). Access to cellulose limits the efficiency of enzymatic hydrolysis: the role of amorphogenesis. Biotechnology for Biofuels. 3(4).

Arfi, Y., Shamshoum, A., Rogachev, I., Peleg, Y., Bayer, E.A. (2014). Integration of bacterial lytic polysaccharide monooxygenases into designer cellulosomes promotes enhanced cellulose degradation. Proceedings of the National Academy of Sciences. 111(25): 9109-9114.

Arora, D.S. and Sharma, R.K. (2010). Ligninolytic fungal laccases and their biotechnological applications. Applied Biochemistry and Biotechnology. 160: 1760-1788.

Aspeborg, H., Coutinho, P.M., Wang, Y., Brummer III, H., Henrissat, B. (2012). Evolution, substrate specificity and subfamily classification of glycoside hydrolase family 5 (GH5). BMC Evolutionary Biology. 12(186).

Auxenfans, T., Cronier, D., Chabbert, B., Paes, G. (2017). Understanding the structural and chemical changes of plant biomass following steam explosion pretreatment. Biotechnology for Biofuels 10: 36.

Badino, S.F., Christensen, S.J., Kari, J., Windahl, M.S., Hvidt, S., Borch, K., Westh, P. (2017). Exo-exo synergy between Cel6A and Cel7A from *Hypocrea jecorina:* role of carbohydrate binding module and the endo-lytic character of the enzymes. Biotechnology and Bioengineering. 114(8): 1639-1647.

Baig, K.S., Turcotte, G., Doan, H. (2016). Adsorption of cellulose enzymes on lignocellulosic materials and influencing factors: A review. International Journal of Waste Resources 6(3).

Balan, V. (2014). Current challenges in commercially producing biofuels from lignocellulosic biomass. Biotechnology. 2014: 1-31.

Bali, G., Meng, X., Deneff, J.I., Sun, Q., Ragauskas, A.J. (2014). The effect of alkaline pretreatment methods on cellulose structure and accessibility. ChemSuschem. 8(2): 275-279.

Barr, B. K., Hsieh, Y. L., Ganem, B., Wilson, D. B. (1996). Identification of two functionally different classes of exocellulases. Biochemistry. 35: 586- 592.

Basit, A. and Akhtar, W. (2018). Truncation of the pocessive Cel5A of *Thermotoga maritima* in soluble expression and several fold increase in activity. Biotechnology and Bioengineering. 115(7): 1675-1684.

Batish, D.R., Singh, H.P., Kohli, R.K., Kaur, S. (2008). *Eucalyptus* essential oil as a natural pesticide. Forest Ecology and Management. 256 (12): 2166-2174.

Bayer, E.A., Chanzy, H., Lamed, R., Shoham, Y. (1998). Cellulose, cellulases and cellulosomes. Current Opinion in Structural Biology. 8: 548-557.

Bayer, E.A., Lamed, R., Himmel, M.E. (2007). The potential of cellulases and cellulosomes for cellulosic waste management. Current Opinion in Biotechnology. 18: 237-245.

Beg, Q.K., Kapoor, M., Mahajan, L., Hoondal, G.S. (2001). Microbial xylanases and their industrial applications: a review. Applied Microbiology and Biotechnology. 56: 326–338.

Benko, Z., Siika-aho, M., Viikari, L., Reczey, K. (2008). Evaluation of the role of xyloglucanase in the enzymatic hydrolysis of lignocellulosic substrates. Enzyme and Microbial Technology. 43(2): 109-114

Bernardinelli, O.D., Lima, M.A., Rezende, C.A., Polikarpov, I., deAzevedo, E.R. (2015). Quantitative (13)C MultiCP solid-state NMR as a tool for evaluation of cellulose crystallinity index measured directly inside sugarcane biomass. Biotechnology for Biofuels. 8: 110.

Berger, E., Zhang, D., Zverlov, V.V., Schwarz, W.H. (2007). Two noncellulosomal cellulases of *Clostridium thermocellum*, Cel9I and Cel48Y, hydrolyse crystalline cellulose synergistically. FEMS Microbiology Letters. 268: 194–201.

Beukes, N., Chan, H., Doi, R.H., Pletschke, B.I. (2008). Synergistic associations between *Clostridium cellulovorans* enzymes XynA, ManA and EngE against sugarcane bagasse. Enzyme and Microbial Technology. 42: 492-498.

Bhalla, A., Cai, C.M., Xu, F., Singh, S.K., Bansal, N., Phongpreecha, T., Dutta, T., Foster, C.E., Kumar, R., Simmons, B.A., Singh, S., Wyman, C.E., Hegg, E.L., Hodge, D.B. (2019). Performance

of three delignifying pretratments on hardwoods: hydrolysis yields, comprehensive mass balance, and lignin properties. Biotechnology for Biofuels. 12:213.

Bhat, M.K. and Bhat S. (1997). Cellulose degrading enzymes and their potential industrial applications. Biotechnology Advances. 15: 583-620.

Bhattacharya, A. and Pletschke, B.I. (2014). Magnetic cross-linked enzyme aggregates (CLEAs): A novel concept towards carrier free immobilization for lignocellulolytic enzymes. Enzyme and Microbial Technology. 61: 17-27.

Billard, H., Faraj, A., Ferreira, N.L., Blanquet, S.H. (2012). Optimization of a synthetic mixture of mahor *Trichoderma reesei* enzymes for the hydrolysis of steam-exploded wheat straw. Biotechnology for Biofuels. 5(1): 9.

Buckeridge, M.S. and De Souza, A.P. (2013). Breaking the 'Glycomic Code' of cell wall polysaccharides may improve second-generation bioenergy production from biomass. Bioenergy Research. 7: 1065-1073.

Bukhari, N.A., Kheang, L., Bakar, N.A., Jahim, H.M. (2018). Enhanced sugar recovery from oil palm trunk biomass by repeated enzymatic hydrolysis with surfactant addition. Malaysian Applied Biology Journal. 47(5): 165-172.

Bukhtojarov, F.E., Ustinov, B.B., Salanovich, T.N., Antonov, A.I., Gusakov, A.V., Okunev, O.N., Sinitsyn, A.P. (2004). Cellulase complex of the fungus *Chrysosporium lucknowense*: Isolation and characterisation of endoglucanases and cellobiohydrolases. Biochemistry. 69(5): 542-551.

Boer, H., Teeri, T.T., Koivula, A. (2003). Studied with wild-type and mutant *Trichoderma reesei* cellobiohydrolase Cel7A. The relationship between thermal stability and pH optimum. European Journal of Biochemistry. 270(5).

Boisset. C., Fraschini. C., Schulein, M., Henrissat. B., Chanzy, H. (2000). Imaging the enzymatic digestion of bacterial cellulose ribbons reveals the endo character of the cellobiohydrolase Cel6A *from Humicola insolens* and its mode of synergy with cellobiohydrolase Cel7A. Applied Environmental Microbiology. 66: 1444-1452.

Boraston, A.B., Chiu, P., Warren, R.A., Kilburn, D.G. (2000). Specificity and affinity by a family 17 carbohydrate-binding module from *Clostridium cellulovorans* cellulase 5A. Biocchemistry. 12(36): 11129-11136.

Borisova, A.S., Eneyskaya, E.V., Bobrow, K.S., Jana, S., Logachev, A., Poley, D.E., Lapidus, A.L., Ibatulin, F.M., Saleem, U., Sandgren, M., Kulminskaya, A., Staahlberg, J. (2015). Sequencing, biochemical characterization, crystal structure and molecular dynamics of cellobiohyrolase Cel7A from *Geotrichum candidum* 3C. The FEBS Journal. 282(23): 4515-4537.

Bothwell, M.K., Walker, L.P., Wilson, D.B., Irwin, D.C., Price, M. (1993). Synergism between pure *Thermomonospora fusca* and *Trichoderma reesei* cellulases. Biomass and Bioenergy. 4(4): 293-299.

Brás, J.L.A., Cartmell, A., Carvalho, A.L.M., Verze, G., Bayer, E.A., Vazana, Y., Correia, M.A.S., Prates, J.A.M., Ratnaparkhe, S., Boraston, A.B., Romao, M.J., Fontes, C.M.G.A., Gilbert, H.J. (2011). Structural insights into a unique cellulase fold and mechanism of cellulose hydrolysis. Proceedings of the National Academy of Sciences. 108(13): 5237-4242.

Bradford, M.M. (1976). A rapid and sensitive method for the quantitation of microgram quantities of protein utilizing the principle of protein-dye binding. Analytical Biochemistry. 72: 248-254.

Brennan, L. and Owende, P. (2010). Biofuels from microalgae- a review of echnologies for production, processing, and extractions of biofuels and co-products. Renewable and Sustainable Energy Reviews. 14: 557-77.

Bregado, J.L., Secchi, A.R., Tavares, F.W., De Sousa Rodrigues, D., Gambetta, R. (2019). Amorphous paracrystalline structures from native srystalline cellulose: a molecular dynamics protocol. Fluid Phase Equilibra. 491: 56-76.

Brienzo, M., Fikizolo, S., Benjamin, Y., Tyhoda, L., Gorgens, J. (2017). Influence of pretreatment severity on structural changes, lignin content and enzymatic hydrolysis of sugarcane bagasse samples. Renewable Energy. 104: 271-280.

Brodeur, G., Yau, E., Badal, K., Collier, J., Ramachandran, S. (2011). Chemical and physicochemical pretreatment of lignocellulosic biomass: a review. Enzyme Research. 2011: 787532.

Broeker, J., Mechelke, M., Baudrexl, M., Mennerich, D., Hornburg, D., Schwarz, W.H., Lebl, W., Zverlov, V.V (2018). The hemicellulose-degrading enzyme system of the thermophilic bacterium *Clostridium stercorarium:* comparative characterization and addition of new hemicellulolytic glycoside hydrolases. Biotechnology for Biofuels. 23(11): 229.

Brondi, M.G., Vasconcellos, V.M., Giordano, R.C., Farinas, C.S. (2019). Alternative low cost additives to improve saccharification of lignocellulosic biomass. Applied Biochemistry and Biotechnology. 187(2): 461-473.

Bronnenmeier, K, Ebenbichler, C., Staudenbauer, W.L. (1990). Seperation of the cellulolytic and xylanolytic enzymes of *Clostridium stercorarium*. Journal of Chromatography. 521: 301-310.

Bülbül, D. and Karakuş, E. (2013). Production and optimization of L-glutaminase fom *Hypocrea jecorina.* Preparative Biochemistry and Biotechnology. 43: 385-397.

Bura, R., Bothast, R.J., Mansfield, S.D., Saddler J.N. (2003). Optimization of SO_2-catalyzed steam pretreatment of corn fiber for ethanol production. Applied Biochemistry and Biotechnology. 106: 319-336.

Bura, R., Chandra, R., Saddler, J.N. (2009). Influence of xylan on the enzymatic hydrolysis of steam pretreated corn stover and hybrid poplar. Biotechnology Progress. 25(2): 315-321.

Busto, M.D., Ortega, N., Perez-Mateos, M. (1996). Location, kinetics and stability of cellulases induced in *Tricoderma reesei* cultures. Bioresource Technology. 57(2): 187-192.

Cetinkol, O.P., Smith-Moritz, A.M., Cheng, G., Lao, J., George, A., Hong, K., Henry, R., Simmons, B.A., Heazlewood, J.L., Holmes, B.M. (2012). Structural and chemical characterization of hardwood from tree species with applications as bioenergy feedstocks. Plos One. 7(12).

Chakdar, H., Kumar, M., Pandiyan, K., Singh, A., Nanjappan, K., Kashyap, P.L., Srivastava, A.K. (2016). Bacterial xylanases: biology to biotechnology. 3 Biotech. 6(2): 150.

Chandel, A.K., Garlapatib, V.K., Singh, A.K., Antunesa, F.A.F., Silvério da Silva, S. (2018). The path forward for lignocellulose biorefineries: Bottlenecks, solutions and perspectives on commercialization. Bioresource Technology. 264: 370-381.

Chandra, R., Ewanick, S., Hsieh, C., Saddler, J.N. (2008). The characterization of pretreated lignocellulosic substrates prior to enzymatic hydrolysis, part 1: a modified Simons' staining technique. Biotechnology Progress 24(5): 1178–1185.

Chang, K.L., Chen, X.M., Han, Y.J., Potprommanee, L., Liu, J.Y., Liao, Y.L., Ning, X.A., Sun, S.Y., Huang, Q. (2017). Impact of surfactant type for ionic liquid pretreatment on enhancing delignification of rice straw. Bioresource Technology. 227: 388-392.

Chang, K.L., Han, Y.J., Wang, Z., Chen, X.M., Leu, S.Y., Liu, J., Peng, Y.P., Liao, Y.L., Potprommannee, L. (2017). The effect of surfactant-assisted ultrasound-ionic liquid pretreatment on the structure and fermentable sugar production of water hyacinth. Bioesource Technology. 237: 27-30.

Chen, X., Shekiro, J., Franden, M.A., Wang, W., Zhang, M., Kuhn, E., Johnson, D.K., Tucker, M.P. (2012). The impacts of de-acetylation prior to dilute acid pretreatment on the bioethanol process. Biotechnology for Biofuels. 5(8).

Chen, L., Drake, M.R., Resch, M.G., Greene, E.R., Himmel, M.E., Chaffey. P.K., Beckham, G.T., Tan, Z. (2014). Specificity of *O*-glycosylation in enhancing the stability and cellulose binding affinity of Family 1 carbohydrate-binding module. Proceedings of the National Academy of Sciences. 111(21): 7612-7617.

Chen, Y., Yan, Z., Liang, L., Ran, M., Wu, T., Wang, B., Zou, X., Zhao, M., Fang, G., Shen, K. (2020). Comparative evaluation of organic acid pretreatment of *Eucalyptus* for kraft dissolving pulp production. Materials. 12:361.

Cheng, X.Y., Huang, W.J., Hu, S.C., Zhang, H.L., Wang, H. Zhang, J.X., Lin, H.H., Chen, Y.Z., Zou, Q., Ji, Z.L. (2012). A global characterization and identification of multifunctional enzymes. Plos One. 7(6).

Cherubini, F., Jungmeier, G., Weillisch, M., Wile, T,m Skiadas, I., Van Ree, R., De Jong, E. (2009). Toward a common classification approach for biorefinery systems. Biofuels, Bioproducts and Biorefining. DOI: 10.1002/bbb

Cherubini, F. (2010). The biorefinery concept: using biomass instead of oil for producing energy and chemicals. Energy Conversion and Management. 5: 1412-1421.

Chokhawala, H.A., Roche, C.M., Kim, T-W., Atreta, M.E., Vegesna, N., Dana, C.M., Blanch, H.W., Clark, D.S. (2015). Mutagenesis of *Trichoderma reesei* endoglucanase I: impact of expression host on activity and stability at elevated temperatures. BMC Biotechnology. 15(11).

Chiarello, L.M., Ramos, C.E.A., Neves, P.V., Ramos, L.R. (2016). Production of cellulosic ethanol from steam-exploded *Eucalyptus urograndisi* and sugarcane bagasse at high solid loadings and low enzyme loadings. Sustainable Chemcial Processes. 4(15).

Choudhary, J.M.S., Nain, L., Arora, A. (2014). Enhanced saccharification of steam retreated rice straw by commercial cellulase supplemented with xylanase. Journal of Bioprocessing and Biotechniques. 4(7): 1-6.

Christopher, L.P., Kumar, H., Zambare, V.P. (2015). Enzymatic biodiesel: challenges and opportunities. Applied Energy. 119: 497-520.

Cocinero, E. J., Gamblin, D. P., Davis, B. G., Simons, J. (2009). The building blocks of cellulose: the intrinsic conformational structures of cellobiose, its epimer, lactose, and their singly hydrated complexes. Journal of the American Chemical Society. 131: 11117–11123.

Collins, T., Gerday, C., Feller, G. (2006). Xylanases, xylanase families and extremophilic xylanases. FEMS Microbiology Reviews. 29(1): 3-23.

Colom, X., Carrillo, F., Nogue, F., Garriga, P. (2003). Structural analysis of photodegraded wood by means of FTIR spectroscopy. Polymer Degradation and Stability. 80: 543-549.

Coniglio, R.O., Fonseca, M.I., Villalba, L.L., Zapata, P.D. (2017). Screening of new secretory cellulases from different supernatants of white rot fungi from Misiones, Argentina. Mycology. 8(1).

Converse, A.O. and Optekar, J.D. (1993). A synergistickinetics model for enzymatic cellulose hydrolysis compared to degree-of-synergism experimental results. Biotechnology and Bioengineering. 42(1): 145-148.

Crous, P.W., Verkley, G, J.M., Groenewald, J.Z. (2006). *Eucalyptus* microfungi known from culture. 1. *Cladoriella* and *Fulvoflamma* genera nova, with notes on some other poorly known taxa. Studies in Mycology. 55: 53-63.

Cross, R. (2001). The preparation of biological material for electron microscopy part 3: The preparation of material for scanning electron microscopy (SEM). Rhodes University Press.

Cruz, A.F. (2013). Mannan-degrading enzyme system. In: Fungal enzymes. CRC Press, Boca Raron, pp 233-257.

Da Silva, V.D.T., De Souza Coto, A.L., De Carvalho Souza, R., Neves, M.B.S., Gomes, E., Rodriguez, G.O.B. (2016). Effect of pH, temperature, and chemicals on the endoglucanases and β-glucosidases from the thermophilic fungus *Myceliophthora heterothallica* F.2.1.4. obtained by solid-state and submerged cultivation. Biochemistry Research International. 1-9.

Dashtban, M., Schraft, H. and Qin, W. (2009). Fungal bioconversion of lignocellulosic residues; opportunities and perspectives. Biological Sciences. 5(6): 578-595.

Davison, B.H., Drescher, S.R., Tuskan, G.A., Davis, M.F., Nghiem, N.P. (2006). Variation of S/G ratio and lignin content in *Populus* family influences the release of xylose by dilute acid hydrolysis. Applied Biochemistry and Biotechnology 129-132: 427-435.

De Bhowick, G., Sarmah, A.K., Sen, R. (2018). Lignocellulose biorefinery as a model for sustainable development of biofuels and value-added products. Bioresource Technology. 247: 1144-1154.

Decker, C.H., Visser, J., Schreier, P. (2001). β-Glucosidase multiplicity from *Aspergillus tubingensis* CBS 643.92: Purification and characterization of four β-glucosidases and their differentiation with respect to substrate specificity, glucose inhibition and acid tolerance. Applied Microbiology and Biotechnology. 55: 157-163.

Deb, P., Talukdar, S.A., Mohsina, K., Sarker, P.K., Sayem, S.M.A. (2013). Production and partial characterization of extracellular amylase enzyme from *Bacillus amyloliquefaciens* P-001. Genetics in Medicine. 154(2).

Den Haan, R., van Zyl, J.M., Harms, T.M., van Zyl, W.H. (2013). Modelling the minimum enzymatic requirements for optimal cellulose conversion. Environmental Research Letters. 8(2): 1-11.

Deng, Z., Xia, A., Liao, Q., Zhu, X, Huang, Y., Fu. (2019). Laccase pretreatment of wheat straw: effects of the physicohemical characteristics and the kinestics of enzymatic hydrolysis. Biotechnology for Biofuels. 12: 159.

Dimarogona, M., Topakas, E., Christakopoulos, P. (2012). Cellulose degradation by oxidative znymes. Computational and Structural Biotechnology Journal. 2(3)

Din, N., Damude, H.G., Gilkes, N.R, Miller, R.C., Warren, R.A.J., Kilburn, D.G. (1994). C1– Cx revisited: intramolecular synergism in a cellulase. Proceedings of the National Academy of Sciences. 91: 11383-11387

Dobrev, G. and Zhekova, Y. (2012). Biosynthesis, purification and characterization of endoglucanase from a xylanase producing strain *Aspergillus niger* B03. Brazilian Journal of Microbiology. 43(1): 70–77.

Donaldson, L. and Vaidya, A. (2017). Visualising recalcitrance by colocalisation of cellulase, lignin and cellulose in pretreated pine biomass using fluorescence microscopy. Scientific Reports. 7: 44386.

Donohoe, B.S., Decker, S.R., Tucker, M.P., Himmel, M.E., Vinzant, T.B. (2008). Visualizing lignin coalescence and migration through maize cell walls following thermochemical pretreatment. Biotechnology and Bioengineering. 101: 913-925.

Du, R., Li, X., Tantai, X., Liu Z, Yang J., Qi, W., He, Z. (2012). Controlled adsorption of cellulase onto pretreated corncob by pH adjustment. Cellulose 19: 371-380.

Du, J., Lang, J., Gao, X., Liu, G., Qui,Y. (2020). Optimization of an artificial cellulase cocktail for high-solids enzymatic hydrolysis of cellulosic materials with different pretreatment methods. 295: 122272.

Duan, C.J., Feng, Y.L., Cao, Q.L., Huang, M.Y., Feng, J.X. (2016). Identification of a novel family of carbohydrate-binding modules with broad ligand specificity. Scientific Reports. 6: 19392.

El-Tayeb, O., Mohammed, F., Hashem, A., Abdullah, M. (2007). Optimization of the industrial production of alpha amylase in Egypt. IV. Fermentor production and characterization of the enzyme of two strains of *Bacillus subtilis and Bacillus amyloliquefaciens.* African Journal of Biotechnology. 7(24): 4521-4536.

Erriksson, T., Karlsson, J., Tjerland, F. (2002). Mechanism of surfactant effect in enzymatic hydrolysis of lignocellulose. Enzyme and Microbial Tecnology. 31(2): 353-364.

Esteves, B., Marques, A.V., Domigos, I., Pereira, H. (2013). Chemical changes of heat-treated pine and *Eucalypt* wood monitored by FTIR. Cencia Technologia. 15(2): 245-258.

Fägerstam, L.G. and Pettersson, L.G. (1980). The 1,4-β-glucan cellobiohydrolases of *Trichoderma reesei* QM414 a new type of cellulolytic synergism. FEBS Letters. 119(1).

Fang, H., Zhao, R., Li, C., Zhao, C. (2019). Simultaneous enhancement of the beta-eo synergism and exo-exo synergism in *Trichoderma reesei* cellulases to increase the cellulose degradability capability. Microbial Cell Factories. 18(9).

Feng, L. and Chen, Z. (2008). Research progress on dissolution and functional modification of cellulose in ionic liquids. Journal of Molecular Liquids. 142: 1-5.

Fierobe, H.P., Gaudin, A., Belaich, M., Faure, E., Bagnara, C., Baty, D., Belaich, J.P. (1991). Characterization of endoglucanase A from *Clostridium cellulolyticum.* Journal of Bacteriology. 173(24): 7956-7962.

Filiatrault-Chastel, C., Navarro, D., Haon, M., Grisel, S., Herpoel-Gimbert, I., Chevret, D., Fanuel, M., Henrissat, B., Heiss-Blanquet, S., Margeot, A., Berrin, J.G. (2019). AA16, a new lytic polysaccharide monooxygenase family identified in fungal secretomes. Biotechnology for Biofuels. 12: 55.

Florencio, C., Badino, A.C., Farinas, C.S. (2019). Addition of soybean protein improves saccharification and ethanol production from hydrothermally pretreated sugarcane bagasse. BioEnergy Research. ttps://doi.org/10.1007/s12155-018-9956-6.

Forseberg, Z., Mackenzie, A.K., Sorlie, M., Rohr, A.K., Helland, R., Arvai, A.S., Vaaje-Kolstad, G., Eijsink, V.G.H. (2014). Structural and functional characterisation of a conserved pair of bacterial cellulose-oxidizing lytic polysaccharide monooxygenases. Proceedings of the National Academy of Sciences. 111(23).

Fujii, M., Mori, J., Himma, T., Taniguchi, M. (1995). Synergy between an endoglucanase and cellobiohydrolase from *Trichoderma koningii.* The Chemical Engineering Journal and the Biochemical Engineering Journal. 59(3): 315-319.

Qadir, F., Shariq, M., Ahmed, A., Sohail, M. (2018). Evaluation of a yeast co-culture for cellulase and xylanase production under solid state fermentation using multivariate approach. Industrial Crops and Products. 123(1): 407-415.

Gandolfi, S., Ottolina, G., Riva, S., Fantoni, G.P., Patel, I. (2013). Complete chemical analysis of carmagnola hemp hurd and structural feature of its components. BioResources. 8(2): 26412656.

Ganner, T., Bubner, P., Eibinger, M., Mayrhofer, C., Plank, H., Nidetzky, B. (2012). Dissecting and reconstructing synergism: *In situ* visualisation and cooperativity among cellulases. Biological Chemistry. 287(52): 43215-43222.

Garg, G., Singh, A., Kaur, A., Singh, R., Kaur, J., Mahajan, R. (2016). Microbial pectinases: an eco-friendly tool of nature for industries. 3 Biotech. 6(1): 47.

Gaudix-Montero, S. and Sankar, M. (2018). Review on catalytic cleavage of C-C inter-unit linkages in lignin model compounds: towards lignin depolymerisation. Topics in Catalysis. 61: 183-198.

Gasteiger, E., Hoogland, C., Gattiker, A., Davaud, S., Wilkins, MR., Appel, R.D., Bairoch, A. (2005). Protein identification and analysis tools on the ExPASy server (In) The Proteomics Protcols Handbook. 571-607.

George, J. and Sabapathi, S.N. (2015). Cellulose nanocrystals: synthesis, functional properties, and applications. Nanotechnology Science and Applications. 8: 45-54.

Gerber, L., Eliasson, M., Trygg, J., Moritz, T., Sundberg, B. (2012). Multivariate curve resolution provides a high-throughput data processing pipeline for pyrolysis-gas chromatography/mass spectrometry. Journal of Analytical and Applied Pyrolysis Impact Factor. 95: 95-100.

Gielen, D., Boshell, F., Saygin, D., Bazilian, M.D., Wagner, N., Gorini, R. (2019). The role of renewable energy in the global energy transformation. Energy Strategy Reviews. 24: 38-50.

Goedegebuur, F., Dankmeyer, L., Gualfetti, P., Karkehabadi, S., Hansson, H., Jana, S., Huynh, V., Kelemen, B.R., Kruithof, P., Larenas, E.A., Teunissen, P.J.M., Stahlberg, J., Payne, C.M., Mitchinson, C., Sandgren, M. (2017). Improving the thermal stability of cellobiohydrolase Cel7A from *Hypocrea jecorina* by directed evolution. Journal of Biological Chemistry. 292(42): 17418-17430.

Gomes, D., Rodrigues, A.C., Domingues, L., Gama, M. (2015). Cellulase recycling in biorefineries - is it possible? Applied Microbiology and Biotechnology. 99: 4131-4143.

Gonzalez, R., Treasure, T., Phillips, R., Jameel, H., Saloni, D., Abt, R., Wright. (2011). Converting *Eucalyptus* biomass into ethanol: Financial and sensitivity analysis in a co-current dilute acid process. Part II. Biomass and Bioenergy. 35: 767-772.

Goshadrou, A., Karimi, K., Taherzadeh, M.J. (2011). Bioethanol production from sweet sorghum bagasse by *Mucor hiemalis.* Industrial Crops and Products 34: 1219-1225.

Goshadrou, A. and Lefsrud, M. (2017). Synergistic surfactant-assisted [EMIM]OAc pretreatment of lignocellulosic waste for enhanced cellulose accessibility to cellulase. Carbohydrate Polymers. 166: 103-113.

Gow, L.A. and Wood, T.M. (1988). Breakdown of crystalline cellulose by synergistic action between cellulase components from *Clostridium thermocellum* and *Trichoderma koningii.* FEMS Microbiology Letters. 50: 247-252.

Granum, D.M., Schutt, T.C., Maupin, M. (2014). Computational evaluation of the dynamic fluctuations of peripheral loops enclosing the catalytic tunnel of a family 7 cellobiohydrolase. The Journal of Physical Chemistry. 118(20): 5340.

Grattapaglia, D., Vaillancourt, R.E., Sheperd, M., Thumma, B.R., Foley, W., Kulheim, C., Potts, B.M., Myburg, A.A. Progress in *Myrtaceae* genetics and genomics: *Eucalyptus* as the pivotal genus. Tree

Guimarães, B.G., Souchon, H., Lytle, B.L., David, W., Alzari, P.M. (2002). The crystal structure and catalytic mechanism of cellobiohydroalse CelS, the major enzymatic component of *Clostridium thermocellum* cellulosome. Journal of Molecular Biology. 320(3): 587-596.

Guo, D.G., Chen, F., Wheeler, J., Winder, J., Selman, S., Peterson, M, Dixon, R.A. (2001). Improvement of in-rumen digestibility of alfalfa forage by genetic manipulation of lignin *O*-methyltransferases. Transgenic Research. 10: 457-464.

Gupta, P.K., Choudhary, S., Chandrananthi, C, Eveline, J.S., Sushmitha, S.P. (2019). Fungal biodiversity producing cellulases involved in efficient cellulolysis. Mycodegradation of Lignocelluloses In: Fungal Biology. 23-33.

Gusakov, A.V., Salanovic, T.N., Antonov, A.I., Ustinov, B.B., Okunev, O.N., Burlingame, R., Emalfarb, M., Baez, M., Sinitsyn, A.P. (2007). Design of highly efficient cellulase mixture for enzymatic hydrolysis of cellulose. Biotechnology and Bioengineering. 97(5): 1028-1038.

Hall, M., Bansal, P., Lee, J.H., Realff, M.J., Bommarius, A.S. (2010). Cellulose crystallinity- a key predictor of the enzymatic hydrolysis rate. FEBS Journal. 277: 1571-1582.

Han , Y., Bai, Y., Zhang, J., Liu, D., Zhao, X. (2020). A comparison of different oxidative pretreatments on polysaccharide hydrolyzability and cell wall structure for interpreting the greatly improved enzymatic digestibility of sugarcane bagasse by delignification. Bioresources and Bioprocessing. 7(24).

Harjanpaa, V., Teleman, A., Koivula, A., Ruhonen, L., Teeri, T.T., Teleman, O., Drakenberg, T. (1996). Cello-oligosaccharide hydrolysis by cellobiohydrolase II from *Trichoderma reesei*: association and rate constants derived from an analysis of progress curves. European Journal of Biochemistry. 240: 584-591.

He, Y., Mouthier, T.M., Kabel, M.A. Dijkstra, J., Hendriks, Struik, P.C., Cone, J.W. (2018). Lignin composition is more important than content for maize stem cell wall degradation. Journal of the Science of Food and Agriculture. 98(1): 384-390.

Hendriks, A. T. W. M. and Zeeman, G. (2009). Pretreatments to enhance the digestibility of lignocellulosic biomass. Bioresource Technology. 100(1): 10-18.

Henrissat. B., Driguez. H., Viet. C., Schülein. M. (1985). Synergism of cellulases from *Trichoderma reese*i in the degradation of cellulose. Nature Biotechnology. 3(8): 722-726.

Henrissat, B. (1991). A classification of glycosyl hydrolases based on their amino acid sequences similarities. Biochemistry. 280: 309-316.

Herlet, J., Kornberger, P., Roessler, B., Glanz, J., Schwarz, W.H., Liebl, W., Zverlov, V.V. (2017). A new method to evaluate temperature vs. pH activity profiles for biotechnological relevant enzymes. Biotechnology for Biofuels. 10(234).

Hindi, S.S.Z. (2017). The interconvertibility of cellulose's allomorphs. International Journal of Innovative Research in Science, Engineering and Technology. 6(1).

Hofrichter, M. (2002). Review: lignin conversion by manganese peroxidase (MnP). Enzyme and Microbial Technology. 30: 454-466.

Hong, S.Y., Lee, J.S., Cho, K.M., Math, R.K., Kim, Y.H., Hong, S.J., Cho, S.J., Kim, H., Yun, H.D. (2007). Construction of the bifunctional enzyme cellulase-β-glucosidase from the hyperthermophilic bacterium *Thermotoga maritima.* Biotechnology Letters. 29(6): 931-936.

Horn, S.J., Vaaje-Kolstad, G., Westereng, B., Eijsink, V.G.H. (2012). Novel enzymes for the degradation of cellulose. Biotechnology for Biofuels. 5(45).

Howard, R.L., Abotsi, E., Jansen van Rensburg, E.L., Howard, S. (2002). Lignocellulose biotechnology: Issues of bioconversion and enzyme production. Biotechnology. 2(12): 602-619.

Hu, G., Heitmann, J.A., Rojas, O.J., Pawlak, J.J., Argyropoulos, D.S. (2010). Monitoring cellulase protein adsorption and recovery using SDS-PAGE. Industrial and Engineering Chemistry Research 49: 8333-8338.

Hu, J., Arantes, V., Saddler, J.N. (2011). The enhancement of enzymatic hydrolysis of lignocellulosic substrates by the addition of accessory enzymes such as a xylanase: is it an additive or synergistic effect? Biotechnology for Biofuels. 4(36).

Hu, J. (2013). The role of accessory enzymes in enhancing the effective hydrolysis of the cellulosic component of pretreated biomass. PhD thesis. University of British Columbia. Vancouver, Canada.

Hu, J., Gourlay, K., Arantes, V., Van Dyk, J.S., Pribowo, A., Saddler, J.N. (2015). The accessible surface area influences synergism during the hydrolysis of lignocellulosic substrates. ChemSusChem. DOI: 10.1002/cssc.201403335.

Hu, J., Gourlay, K., Arantes, V., Van Dyk, J.S., Pribowo, A., Saddler, J.N. (2015). The accessible surface influences synergism during the hydrolysis of lignocellulosic substrates. ChemSusChem. DOI: 10.1002/cssc.201403335.

Hu, J., Mok, Y.K., Saddler J.N. (2018). Can we reduce the cellulase enzyme loading required to achieve efficient lignocellulose deconstruction by only using the initially absorbed enzymes? ACS Sustainable Chemistry and Engineering 6: 6233-6239.

Huang, X., Kocaefe, D., Kocaefe, Y., Boluk, Y., Krause, C. (2013). Structural analysis of heat-treated birch (*Betule papyrifera*) surface during artificial weathering. Applied Surface Science. 264: 117-127.

Huang, C., Zhao, C., Xiong, L., Chen, X., Luo, M., Chen, X. (2018). Comparison of different pretreatments on the synergistic effect of cellulase and xylanase during the enzymatic hydrolysis of sugarcane bagasse. RSC Advances. 54.

Igarashi, K., Koivula, A., Wada, M., Kimura, S., Penttilä, M. Samejima, M. (2009). High speed atomic force microscopy visualises processive movement of *Trichoderma reesei*. Biological Chemistry. 284: 36186-36190.

Imai, T., Boisset, C., Samejima, M., Igarashi. K., Sugiyam, J. (1998). Unidirectional processive action of cellobiohydrolase Cel7A on *Valonia* cellulose microcrystals. FEBS Letters. 432(3): 113-116.

Irwin, D.C., Spezio, M., Walker, L.P., Wilson, D.B. (1993). Activity studies of eight purified cellulases: specificity, synergism, and binding domain effects. Biotechnology and Bioengineering. 42: 1002-1013.

Irwin, D.C., Zhang, S., Wilson, D.B. (2000). Cloning, expression and characterization of a family 48 exocellulase Cel48, from *Thermobifida fusca.* European Journal of Biochemistry. 267(16): 4988-4997.

Jalak, J., Kurašin, M., Teugjas, H., Väljamäe, P. (2012). Endo-exo synergism in cellulose hydrolysis revisited. Journal of Biological Chemistry. 287(34): 28802-15.

Jansson, Z.L. (2013). Characterisation of spruce xylan and its potential for strength improvement. PhD Thesis. Royal Institute of Technology, School of Chemical Science and Engineering, Department of Fiber and Polymer Technology, Division of Wood Chemistry and Pulp Technology. Stockholm, Sweden.

Jeihanipour, A., Karimi, K., Taherzadeh, M.J. (2010). Enhancement of ethanol and biogas production from high-crystalline cellulose by different modes of NMO pretreatment. Biotechnology and Bioengineering. 105: 469-476.

Jeoh, T., Wilson, D.B., Walker, L.P. (2006). Effect of cellulase mole fraction and cellulose recalcitrance on synergism in cellulose hydrolysis and binding. Biotechnology Progress. 22(1): 270-277.

Jeon, S.D., Yu, K.O., Kim, S.W., Han, S.O. (2012). The processive endoglucanase EngZ is active in crystalline cellulose degradation as a cellulosomal subunit of *Clostridium cellulovorans*. New Biotechnology. 29: 365–371.

Johansen, K.S. (2016). Lytic polysaccharide monooxygenases: the microbial power tool for lignocellulose degradation. Trends in Plant Sience. 21(11): 926-936.

Jönsson, L.J., Alriksson, B., Nilvebrandt, N.O. (2013). Bioconversion of lignocellulose: inhibitors and detoxification. Biotechnology for Biofuels. 6:16.

Jönsson, L.J. and Martin, C. (2016). Pretreatment of lignocellulose: formation of inhibitory by-products for minimising thir effects. Bioresource Technology. 199: 103-112.

Jørgensen, H., Kristensen, F.B., Felby, C. (2007). Enzymatic conversion into fermentable sugars: challenges and oppurtunities. Biofuels, Bioproducts and Biorefining. 1(2): 119-134.

Jørgensen, H. (2017). Enzyme recycling in lignocellulosic biorefineries. Biofuels, Bioproducts and Biorefining. 11(1): 150-167.

Josefsson, P., Henriksson, G., Wagberg, L. (2007). The physical action of cellulases revealed by a quartz crystal microbalance study using ultrathin cellulose films and pure cellulose. Biomacromolecules. 9: 249-254.

Jung, H.G. and Deetz, D.A. (1993). Cell wall lignification and degradation, in forage cell wall structure and digestibility. 315-346.

Junior, A.B., Borges, D.C., Tardioli, O.W., Farinas, C.S. (2014). Characterization of beta-glucosidase produced by *Aspergillus niger* under solid-state fermentation and partially purified using MANAE-Agarose. Biotechnology Research International. 2014: 317092.

Kallioinen, A., Puranen, T., Siika-aho, M. (2014). Mixtures of thermostable enzymes show high performance in biomass saccharification. Applied Biochemistry and Biotechnology. 73(5): 1038-1056.

Karlsson, J., Medve, J., Tjerneld, F. (1999. Hydrolysis of steam-pretreated lignocellulose – synergism and adsorption for cellobiohydrolases I and endoglucanase II of *Trichoderma reesei.* Applied Biochemistry and Biotechnology. 82: 243-258.

Karp, S.G., Woiciechowski, A.L., Soccol, V.T., Soccol, C.R. (2013). Pretreatment strategies for delignification of sugarcane bagasse: a review. Brazilian Archives of Biology and Technology. 56(4): 679-689.

Karp, E.M., Donohoe, B.S., O'Brien, P.N., Ciesielski, P.N., Mittal, A., Biddy, M.J., Beckham, G.T. (2014). Alkaline pretreatment of corn stover: bench-scale fractionation and steam characterization. ACS Sustainable Chemical Engineering. 2: 1481-1491.

Kersten, P. and Cullen, D. (2007). Extracellulase oxidative systems of the lignin-degrading *Basidiomycete phanerochaete chrysosporium*. Forestry, Genetics and Biology. 44. 77-87.

Kim, C.H. (1995). Characterization and substrate specificity of an endo-β-1,4-D-glucanase I (Avicelase I) from an extracellular multienzyme complex of *Bacillus circulans.* Applied and Environmental Microbiology. 61(3): 959-65.

Kim, T.H. and Lee, Y.Y. (2005). Pretreatment of corn stover by soaking in aqueous ammonia. Applied Biochemistry and Biotechnology. 124(1-3): 1119-1131.

Kim, S., Lee, D.S., Choi, I.S., Ahn, S.J., Kim, J.H., Bae, H.J. (2010). *Arabidopsis thaliana* Rubisco small subunit transit peptide increases the accumulation of *Thermotoga maritima* endoglucanase Cel5A in chloroplasts of transgenic tobacco plants. Transgenic Resources. 19: 489-497.

Kim, J.K., Yang, J., Park. S.Y., Yu, J.H., Kim, K.H. (2019). Cellulase recycling in high-solids enzymatic hydrolysis of pretreated empty fruit branches. Biotechnology for Biofuels. 12:138.

Kipper, K., Väljamäe, P., Johannsson, G. (2005). Processive action of cellobiohydrolase Cel7A from *Trichoderma reesei* is revealed as 'burst' kinetics on fluorescent polymeric model substrates. Biochemistry. 15(385): 527-535.

Klein-Marcuschamer, D., Oleskowicz-Popiel, P., Simmons, B.A., Blanch, H. (2011). The challenge of enzyme costs in the production of lignocellulosic biofuels. Biotechnology and Bioengineering. 109(4): 1083-1087.

Kleywegt, G.J., Zou, J.Y., Divne, C., Davie, G.J., Sinning, I., Stahlberg, J., Reinikainen, T., Srisodsuk, M., Teeri, T.T., Jones, T.A. (1997). The crystal structure of the catalytic core domain of endoglucanase I from *Trichoderma reesei* at 2.6 A resolution, and a comparison with related enzymes. Journal of Molecular Biology. 26(3): 383-397.

Kluts, I.N., Brinkman, M.L.J., de Jong, S.A., Junginger, H.M. (2017). Biomass resources: agriculture. Advances in Biochemical Engineering and Biotechnology. 13-26.

Klyosov, A. (1990). Trends in biochemistry and enzymology of cellulose degradation. Biochemistry. 29: 10577-10585.

Ko, J.K., Xiemenes, E., Kim, Y., Ladisch, M.R. (2015). Adsorption of enzyme onto lignis of liquid hot water pretreated hardwoods. Biotechnology and Bioengineering. 122(3): 447-456.

Kognole, A.A., Payne, C.M. (2018). Cellulose-specific Type B carbohydrate binding modules: understanding oligomeric and non-crystalline substrate recognition mechanisms. Biochemistry. 11(319).

Kostylev, M. and Wilson, D.B. (2012). Synergistic interactions in cellulose hydrolysis. Biofuels. 3: 61-70.

Kostylev, M., Wilson, D. (2014). A distinct model of synergism between a processive endocellulase (TfCel9A) and an exocellulases (TfCel48A) from *Thermobifida fusca*. Applied Environmental Microbiology. 80(1): 339.

Kristensen, J.N., Borjesson J., Bruun, M.H., Tjerned, F., Jorgensen J. (2007). Use of surface active additives on enzymatic wheat straw lignocellulose. Enzyme and Microbial Technology. 40(4): 888-895.

Kristensen, J., Felby, C., Jørgensen, H. (2009). Determining yields in high solids enzymatic hydrolysis of biomass. Applied Biochemistry and Biotechnology. 156: 127-132.

Kuhad, R.C., Gupta, R., Singh, A. (2011). Microbial cellulases and their industrial applications. Enzyme Research. 2011: 1-10.

Kumar, R. and Wyman, C. E. (2009). Effects of cellulase and xylanase enzymes on the deconstruction of solids from pretreatment of poplar by leading technologies. Biotechnology Progress. 25: 302-314.

Kumar, P., Barrett, D.M., Delwiche, M.J., Stroeve, P. (2009). Methods for pretreatment of lignocellulosic biomass for efficient hydrolysis and biofuel production. Industrial and Engineering Chemistry Research. 48: 3713-3729.

Kumar, R., Mago, G., Balan, V., Wyman, C. E. (2009). Physical and chemical characterizations of corn stover and poplar solids resulting from leading pretreatment technologies. Bioresource Technology 100: 3948-3962.

Kumar, A.K. and Sharma, S. (2017). Recent updates on different methods of pretreatment of lignocellulosic feedstocks: a review. Bioresources and Bioprocessing. 4(7).

Kurašin, M. and Väljamäe, P. (2011). Processivity of cellobiohydrolases is limited by the substrate. The Journal of Biological Chemistry. 286(1): 169-177.

Laemmli, U.K, Amos, L.A., Klug, A. (1976). Correlation between structural transformation and cleavage of the major head protein of T4 bacteriophage. Cell. 7(2): 191-20.

Lakhundi, S., Siddiqui, R., Khan, N.A. (2015). Cellulose degradation: a therapeutic strategy in the improved treatment of *Acanthamoeba* infections. Parasites Vectors. 8(23) (2015).

Lamed, R., Kenig, R., Morgenstern, E., Calzada, J.F., De Micheo, D., Bayer, E.A. (1991). Efficient cellulose solubilisation by a combined cellulosome-β-glucosidase system. Applied Biochemistry and Biotechnology. 27(2): 173-183.

Larue, K., Melgar, M., Martin, V.J.J. (2016). Directed evolution of a fungal β-glucosidase in *Saccaromyces cervisiae*. Biotechnology for Biofuels. 9(52).

Le Traon-Masson, M.P. and Pellerin, P. (1998). Purification and Characterization of Two β-D-Glucosidases from an Aspergillus Niger Enzyme Preparation: Affinity and Specificity Toward Glucosylated Compounds Characteristic of the Processing of Fruits. Enzyme and Microbial Technology. 22(5): 374-382.

Ledford, H. (2014). Brazil considers transgenic trees. Nature. 512(5): 357.

Lee, J. (1997). Biological conversion of lignocellulosic biomass to ethanol. Journal of Biotechnology. 56: 1-24.

Leis, B., Held, C., Bergkemper, F., Dennemarck, K., Steinbauer, R., Reiter, A., Mechelke, M., Moerch, M., Graubner, S., Liebl, W., Schwartz, W.H., Zverlov, V.V (2017). Comparative characterization of all cellulolosomal cellulases from *Clostridium thermocellum* reveals high diversity in endoglucanase product formation essential for complex activity. Biotechnology for Biofuels. 10:240.

Leghlimi, H., Meralhi, Z., Boukhalfa-Lezza, H., Copinet, E., Duchlron, F. (2013). Production and characterization of cellulolytic activities produced by *Trochoderma longibrachiatum* (GHL). African Journal of Biotechnology. 12(5): 465-475.

Li, L.L., McCorkle, S.R., Monchy, S., Taghavi, S., van der Lelie, D. (2009). Bioprospecting metagenomes: Glycosyl hydrolases for converting biomass. Biotechnology for Biofuels. 2(10).

Li, C.L., Knierim, B., Manisseri, C., Arora, R., Scheller, V., Auer, M., Vogel, K.P., Simmons, B.A., Singh, S. (2010). Comparison of dilute acid and ionic liquid pretreatment of switchgrass: biomass recalcitrance, delignification and enzymatic saccharification. Bioresource Technology. 101(13): 4900–4906.

Li, X., Xiemenes, E., Kim, Y., Slininger, M., Meilan, R., Ladisch, M., Chapple, C. (2010). Lignin monomer composition affects *Arabidopsis* cell-wall degradability after liquid hot water pretreatment. Biotechnology for Biofuels. 3: 27-33.

Li, C.H., Wang, H.R. & Yan, T.R., 2012. Cloning, purification, and characterization of a heat- and alkaline-stable endoglucanase B from *Aspergillus niger* BCRC31494. Molecules. 17(8): 9774–9789.

Li, J., Lin, J., Xiao, W., Gong, Y., Wang, M., Zhou, P., Liu, Z. (2013). Solvent extraction of antioxidants from steam exploded sugarcane bagasse and enzymatic convertibility of the solid fractions. Bioresource Technology. 130: 8-15.

Li, M., Cao, S., Meng, X., Studer, M., Wyman, C.E., Ragauskas, A.J., Pu, Y. (2017). The effect of liquid hot water pretreatment on the chemical-structural alteration and the reduced recalcitrance in poplar. Biotechnology for Biofuels. 10(237).

Lima, M.A., Lavorente, G.B., da Silva, H.K.P., Bragatto, J., Rezende, C.A., Bernardinelli, O.D., deAzevedo, E.R., Gomez, L.D., McQueen-Masom, S.J., Labate, C.A., Polikarpov, I. (2013). Effects of pretreatment on morphology chemical composition and enzymatic digestibility of *Eucalyptus* bark: a potentially valuable source of fermentable sugars for biofuel production- part 1. Biotechnology for Biofuels. 75(6).

Limayem, A. and Ricke, S.C. (2012). Lignocellulosic biomass for bioethanol production: Current perspectives, potential issues and future prospectives. Progress in Energy and Combustion Science. 38: 449-467.

Lin, X., Qiu, X.Q, Yuan, L., Li, Z., Lou, H.M., Zhou, M.S., Yang, D. (2015). Lignin-based polyoxyethylene ether enhanced enzymatic hydrolysis of lignocelluloses by dispersing cellulase aggregates. Bioresource Technology. 185: 165-170.

Lindedam, J., Haven, M.O., Chylenski, P., Jorgensen, H., Felby, C. (2013). Recycling cellulases for cellulosic ethanol at industrial relevant condition: Potential and temperature dependency at high solid processes. Bioresource Technology. 148: 180-188.

Liu, H., Zhu, J.Y., Fu, S.Y. (2010). Effect of lignin–metal complexation on enzymatic hydrolysis of cellulose. Journal of Agricultural and Food Chemistry. 58(12): 7233-7238.

Lombard, V., Golaconda, R.H. Drula, E., Coutinho, P.M., Henrissat, B. (2014). The carbohydrate-active enzyms database (CAZy) in 2013. Nucleic Acids Research. 42. (Database issue): D490-D495.

Lopez-Mondejaar, R., Zuhlke, D., Becher, D., Riedel, K., Baldrian. (2016). Cellulose and hemicellulose decomposition by forest soil bacteria proceeds by the action of structurally variable enzymatic systems. Scientific Reports. 6: 2279.

Lou, H., Zhu, J.Y., Lan, T.Q., Lai, H., Qiu, X. (2013). pH-induced lignin surface modification ro reduce nonspecific cellulase bidning and enhance enzymatic saccharification of lignocelluloses. ChemSusChem. 6: 919-927.

Lu, Y., Yang, B., Gregg, D., Saddler, J.N., Mansfield, S.D. (2002). Cellulase adsorption and an evaluation of enzyme recycle during hydrolysis of steam-exploded softwood residues. Biochemistry and Applied and Biotechnology. 98-100: 641-654.

Lupoi, J.S., Singh, S., Lee, D.J., Sheperd, M., Simmons, B.A., Henry, R.J. (2014). High-throughput prediction of *Eucalypt* lignin syringyl/guaiacyl content using multivariate analysis: a comparison between mid-infrared, near-infrared, and Raman spectroscopies for model development. Biotechnology for Biofuels. 7(93).

Lynd, L.R., Weimer, P.J., Van Zyl, W.J., Pretorius, T.S. (2002). Microbial cellulose utilization: Fundamentals and biotechnology. Microbiology and Molecular Biology Review. 66: 507-577.

Machado, D.L., Moreira, N., J., Da Pradella, J.G., Bonomi, A., Rabelo, S.C., da Costa, A.C. Adsoprtion charaacteristics of cellulase and β-glucosidase on Avicel, pretreated sugarcane bagasse, and lignin. Applied Biotechnology and Biochemistry. 62(5): 681-689.

MacKenzie, L.F., Sulzenbacher, G., Divne, C., Jones, T.A., Woldike, H.F., Schulein, M., Withers, S.G., Davies, G.J. (1998). Crystal structure of the family 7 endoglucanase 1 (Cel7B) from *Humicola insolens* at 2.2 A resolution and identification of the catalytic nucleophile by trappig of the covalent glycosyl-enzyme intermediate. Biochemistry. 15: 409-416.

Madadi, M., Penga, C., Abbas, A. (2017). Advances in genetic manipulation of lignocellulose to reduce biomass recalcitrance and enhance biofuel production in bioenergy crops. Plant Physiology and Biochemistry 5: 182.

Madaj, R., Kalinowska, H., Sobieck, E. (2017). Plant biomass degradation supported by non-enzymatic proteins. Biotechnology and Food Science. 81(1): 71-81.

Malgas, S., Van Dyk, S.J., Pletschke, B.I. (2015). β-mannanase (Man26A) and α-galactosidase (Aga27A) synergism - a key factor for the hydrolysis of galactomannan substrates. Enzyme and Microbial Technology. 70: 1-8.

Malgas, S. (2017). Formulation of an enzyme cocktail, HoloMix, using cellulolytic and xylanolytic enzyme core-sets for effective degradation of various pre-treated hardwoods. PhD Thesis. Department of Microbiology and Biochemistry, Rhodes University. Grahamstown, South Africa.

Malgas, S., Chandra, R., Van Dyk., J.S., Saddler, J.N., Pletschke, B.I. (2017). Formulation of an optimized synergistic enzyme cocktail, HoloMix, for effective degradation of various pretreated hardwoods. Bioresource Technology 245: 52-65.

Malgas, S., Minghe, V.M., Pletschke, B.I. (2019). The effect of hemicellulose on the binding and activity of cellobiohydrolase I, Cel7A, from *Trichoderma reesei* to cellulose. Cellulose. DOI: 10.1007/S10570-019-02848-5.

Malgas, S., Mkabayi, L., Mathibe, B., Thoresen, M., Mafa, M., Le Roes-Hill, M., Van Zyl, W.H., Pletschke, B.I. (2020). Enzymatic path to bioconversion of lignocellulosic biomass In: Recent Advances in Bioconversion of Lignocellulose to Biofuels and Value Added Chemicals within the Biorefinery Concept. Ximenes Ferreira Filho, E., Rios de Souza Moreira, L., de Aquino Ximenes, E. and Sanchez Farinas, C. (Editors). ISBN: 978-0-12-818223-9.

Mansfield, S.D., Kang, K.Y., Chapple, C. (2012). Design for deconstruction-poplar trees altered in cell wall delignification improve the efficacy of bioethanol production. New Pythtologist. 194: 91-101.

Martín, C., Galbe, M., Nilvebrant, N-O., Jönsson, L.J. (2002). Comparison of the fermentability of enzymatic hydrolysates of sugarcane bagasse pretreated by steam explosion using different impregnating agents. Applied Biochemistry and Biotechnology. 98-100: 699-716.

Martin-Sampedro, R., Revilla, E., Villar, J.C., Eugenio. M.E. (2014). Enhancement of enzymatic saccharification of *Eucalyptus globulus*: Steam explosion versus steam treatment. *Bioresource Technology.* 167: 186-191.

Matthew, G.M., Sukumaran, R.K, Rani, R., Singhania, R.R., Pandey, A. (2008). Progress in research on fungal cellulases for lignocellulose degradation. Journal of Scientific and Industrial Research. 67: 898-907.

Mehrotra, R. and Aneja, K. (1990). An introduction to mycology: New Age International.

Melati, R.B., Shimizu, F.L., Oliveira, G., Pagnocca, F.C., de Souza, W., Sant'Anna, C., Brienzo, M. (2019). Key factors affecting the recalcitrance and conversion process of biomass, Bioenergy Research. 12(1): 1-20.

Meng, X. and Ragauskas, A.J. (2017). Pseudo-lignin formation during dilute acid pretreatment for cellulosic ethanol. Recent Advances in Petrochemical Science. 1(1): 1-4.

Miao, C. and Hamad, W.Y. (2019). Critical insights into the reinforcement potential of cellulose nanocrystals in polymer nanocomposites. Curent Opinion in Solid State and Materials Science. 23(4): 100761.

Miller, G.I. (1959). Use of dinitrosalicylic acid reagent for the determination of reducing sugars. Analytical Chemistry. 72: 426-428.

Mittal, A., Katahira, R., Himmel, M.E., Johnson, D.K. (2011). Effects of alkaline or liquid-ammonia treatment on crystalline cellulose: changes in crystalline structure and effects on enzymatic digestibility. Biotechnology for Biofuels. 4(21).

Meyer, A.S., Rosgaard, L., Sorensen, H.R. (2009). The minimal enzyme cocktail concept for biomass processing. Cereal Science. 50: 337-344.

Mitra, P.P. and Loque, D. Histochemical staining of *Arabidopsis thaliana* secondary cell wall elements. Journal of Visualised Experiments. (87): e51381. DOI:10.3791/51381

Mohanram, S., Amat, S., Choudhary, J., Arora, A., Nain, L. (2013). Novel perspectives for evolving enzyme cocktails for lignocellulose hydrolysis in biorefineries. Sustainable Chemical Processes. 1(15).

Mohaptra, S., Mishra, C., Behera, S.S., Thatoi, H. (2017). Application of pretreatment, fermentation and molecular techniques for enhancing bioethanol production from grass biomass- A review. Renewable and Sustainable Energy Reviews. 78: 1007-1032.

Moilanen, U., Kellock, M., Varnai, A., Andberg, M., Viikari, L. (2014). Mechanisms of laccase-mediator treatments improving the enzymatic hydrolysis of pretreated spruce. Biotechnology for Biofuels. 7(1): 177.

Mood, S.H., Golfeshan, A.H., Tabatabaei, M., Abbasalizadeh, S., Ardjmand, M. (2013). Comparison of different ionic liquids pretreatment for barley straw enzymatic saccharification. 3 Biotech. 3(5): 399-406.

Moon, R.J., Martini, A., Nairn, J., Simonsen, J., Youngblood, J. (2011). Cellulose nanomaterials review: structure, properties and nanocomposites. Chemical Society Reviews. 40: 3941-3994.

Moraïs, S., Barak, Y., Caspi, J., Hadar, Y., Lamed, R., Shoham, Y., Wilson, D.B., Bayer, E.A. (2010). Cellulase-xylanase synergy in designer cellulosomes for enhanced degradation of a complex cellulosic substrate. Microbiology. 1(5).

Moreira, L.R.S and Filho, E.X.F. (2008). An overview of mannan structure and mannan degrading enzyme systems. Applied Microbiology and Biotechnology. 79: 165-178.

Mosier, N., Wyman C., Dale, B., Elander, R., Lee, Y.Y., Holtzapple, M., Ladisch, M. (2005). Features of promising technologies for pretreatment of lignocellulosic biomass. Bioresource Technology. 96(6): 673-686.

Murashima, K., Kosugi, A., Doi, R.H. (2003). Synergistic effects of cellulosomal xylanase and cellulases from *Clostridium cellulovorans* on plant cell wall degradation. Journal of Bacteriology. 185(5): 1518-1524.

Muthuvela, K.S., Rajarthinam, R., Kanagaraj, L.P., Ranganathan, R.V., Dhanasekaran, K., Manickam, N.K. (2019). Evaluation and characterization of novel sources of sustainable lignocellulosic resdiues for bioethanol production using ultrasound-assisted alkaline pretreatment. Waste Management. 87: 368-374.

Narasimha, G., Sridevi, A., Ramanjaneyuli, G., Reddy, B.RR. (2016). Purification and characterization of β-glucosidase from *Aspergillus niger*. International Journal of Food Properties. 19(3): 652-661.

Naumoff, D.G. (2011). Hierarchical classification of glycoside hydrolases. Biochemistry. 76(6): 622-635.

Neiva, D., Fernandes, L., Araujo, S., Lourenc, A., Gominho, J., Simoes, R., Pereira, H. (2015). Chemical composition and kraft pulping potential of 12 *Eucalypt* species. Industrial Crops and Product*s*. 66: 89-95.

Nerinckx., Desmet, T., Piens, K., Claeyssens, M. (2005). An elaboration on the *syn-anti* proton donor concept of glycoside hydrolases: electrostatic stabilisation of the transition state as a general strategy. FEBS Letters. 579(2): 302-312.

Nidetzky, B., Steiner, W., Hayn, M., and Claeyssens, M. (1994). Cellulose hydrolysis by the cellulases from *Trichoderma reesei*: a new model for synergistic interaction. Biochemistry. 298: 705-710.

Normark, M., Winestrand, S., Lestander, T.A., Jönnsson, L.J. (2014). Analysis, pretreatment and enzymatic saccharification of different fractions of Scots pine. BMC Biotechnology. 14: 20.

Novy, V., Nielsen, F., Seiboth, B., Nidetzky, B. (2019). The influence of feedstock characteristics on enzyme production in *Trichoderma reesei*: a review on productivity, gene regulation and secretion profiles. Biotechnology for Biofuels. 12(238).

Nutt. A., Sild, V., Pettersson, G., Johansson, G. (1998). Progress curves - a mean for functional classification of cellulases. Biochemistry. 258(1): 200–206.

Nusrat, A. and Rahman, S.R. (2007). Comparative studies on the production of extracellulase α-amylase by three mesophilic *Bacillus* isolates. Bangladesh Journal of Microbiology. 24(2): 129-132.4.

Nguyen, H.Q. and Quyen, D.I. (2010). Purification and properties of an endoglucanase from *Aspergillus oryzae* VTCC-F045. Australian Journal of Basic and Applied Sciences. 4(12): 6217-6222.

O'Brien, P. and Herschad, D. (1999). Catalytic promiscuity and the evolution of new enzymatic activities. Chemistry and Biology. 6(4): 91-105.

Ogunmolu, F.E., Jagadeesha, N.B.K., Kumar, R., Kumar, O., Gupta, D., Yazdani, S.S. (2017). Comparitive insights into the saccharification potentials of a realtively unexplored but robust *Penicillium funiculosom* glycoside hydrolase 7 cellobiohydrolase. Biotechnology for Biofuels. 10(71).

Olver, B., Van Dyk, J.S., Beukes, N., Pletschke, B.I. (2011). Synergy between EngE, XynaA and ManA from *Clostridium cellulovorans* on corn stalk, grass and pineapple pulp substrates. 3 Biotech. 1: 187-192.

Palonen, H., Tjerneld, F., Zacchi, G., Tenkanen, M. (2004). Adsorption of *Trichoderma reesei* CBH I and EG II and their catalytic domains on steam pretreated softwood and isolated lignin. Journal of Biotechnology. 107: 65-72.

Pan, X., Xie, D., Gilkes, N., Gregg, J.D., Saddler, N.J. (2005). Strategies to enhance the enzymatic hydrolysis of pretreated softwood with high residual lignin content. Applied Biochemistry and Biotechnology. 121–124, 1069-107.

Pandey, L. and Pitan, A.J. (2003). FTIR studies of the changes in 827 wood following decay by brown-rot and white-rot fungi. International Biodeterioration and Biodegradation. 52: 151-160.

Pareek, N., Gilgren, T., Jonsson, L.J. (2013). Adsorption of proteins in hydrolysis of lignocellulose on lignins and hemicelluloses. Bioresource Technology 148: 70-77.

Parsiegla, G., Juy, M., Reverbel-Leroy, C., Tardif, C., Belai, J-P., Driquez, H., Haser, R. (1998). The crystal structure of the processive endocellulase CelF of *Clostridium cellulolyticum* in complex with a thio-oligosaccharide inhibitor at 2.0 Å resolution. The EMBO Journal. 17(19): 5551-5562.

Payne, C.M.., Knott, B.C., Mayes, H.B., Hansson, H., Himmel, M.E., Sandgren, M., Stahlberg, J., Beckham, G.T. (2015). Fungal cellulases. Chemical Reviews. 115:1308–448.

Pawar, P.M.A., Derba-Maceluh, M.D., Chong, S.L., Gandla, M.L., Bashar, S.S., Sparrman, T., Ahvenainen, P., Hedenstrom, M., Ozpapucu, M., Ruggeberg M., Serimaa, R., Lawoko, M., Tenkanen, M., Jonsson, L.J., Mellerowicz, J. (2017). *In muro* deacetylation of xylan affects lignin poperties and improves saccharification of aspen wood. Biotechnology for Biofuels. 10(98).

Peciulyte, A., Anasontzis, G.E., Karlström, K., Larsson, P.T., Olsson, L. (2014). Morphology and enzyme production of *Trichoderma reesei* RUT C-30 are affected by the physical and structural characteristics of cellulosic substrates. Fungal Genetics and Biology. 72: 64-72.

Peciulyte, A., Karlstrom, K., Larsson, P.T., Olson, L. (2015). Impact of supramolecular structure of cellulose on the efficiency of enzymatic hydrolysis. Biotechnology for Biofuels. 8(56).

Pedrolli, D.B., Monteiro, A.C., Gomes, E., Carmona, E.C. (2009). Pectin and pectinases: production, characterization and industrial application of microbial pectinolytic enzymes. The Open Biotechnology Journal. 3: 9-18.

Petkowicz, C.L.O., Reicher. F., Chanzy. H., Taravel, F.R, Vuong, R. (2001). Linear mannan in the endosperm of *Schizolobium amazonicum*. Carbohydrate Polymers. 44: 107-112.

Phitsuwan, P., Permsriburasuk, C., Baramee, S., Teeravivattanakit, T., Ratankhanokchai, K. (2017). Structural analysis of alkaline pretreated rice straw for ethanol production. International Journal of Polymer Science. 2017: 1-9.

Pielhop, T., Amgarten, J., Von Rohr, P.R., Studer, M.H. (2016). Steam explosion pretreatment of softwood: the effect of the explosive decompression on enzymatic digestibility. Biotechnology for Biofuels. 9(152).

Pingali, S.V., O'Neill, H.M., McGaughey, J., Urban, V.S., Rempe, C.S., Petridis, L., Smith, J.C., Evans, B.R., Heller, W.T. (2011). Small angle neutron scattering reveals pH-dependant conformational changes in *Trichoderma reesei* cellobiohydrolase I: implications for enzymatic activity. Journal of Biological Chemistry. 16(37): 32801-32809.

Poornejad, N., Karimi, K., Behzad, T. (2013). Improvement of saccharification and ethanol production from rice straw by NMMO and [BMIM][OAc] pretreatments. Industrial Crops and Products. 41: 408-413.

Popescu, C.M., Popescu, M.C., Singurel, G., Vaile, C., Argyropoulos, D.S., Willfor, S. (2007). Spectral characterization of *Eucalyptus* wood. Applied Spectroscopy. 61(11): 1168-1177.

Pradham, M.P and Loque, D. (2014). Histochemical staining of *Arabidopsis taliana* secondary cell wall elements. Journal of Visual Experiments 87: 51381.

Pribowo, A., Arantes, V., Saddler, J.N. (2012). The adsorption and enzyme activity profiles of specific *Trichoderma reesei* cellulase/xylanase components when hydrolyzing steam pretreated corn stover. Enzyme and Microbial Technology. 50(3): 195-203.

Qi, B., Chen, X., Su, Y., Wan, Y. (2011). Enzyme adsorption and recycling during hydrolysis of wheat straw lignocellulose. Bioresource Technology. 102: 2881-2889.

Qing, Q., Yang, B., Wyman, C.E. (2010). Impact of surfactants on preatreatment of corn stover. Bioresource Technology. 101: 5941-5951.

Quay, D.H.X. et al., 2011. Overexpression, purification and characterization of the *Aspergillus niger* endoglucanase, EglA, in *Pichia pastoris*. African Journal of Biotechnology. 10(11): 2101–2111.

Quiroz-Castañeda, R.E. and Folch-Mallol, J.L. (2013). Hydrolysis of biomass mediated by cellulases for the production of sugars In: Sustainable degradation of lignocellulosic biomass: techniques, applications and commercialization; Chandel, A.K and da Silva, S.S. (Editors). ISBN: 978-953-51-1119-1.

Rahikainen, J.L., Martin-Sampedro, R., Heikkinen, H., Rocio, S., Marjama, K., Tamminen, T., Rojas, O.J., Kruus, K. (2013). Inhibitory effect of lignin during cellulose bioconversion: The effect of lignin chemistry on non-productive enzyme adsorption. Bioresource Technology. 133: 270-288.

Rajan, S.S., Yang., X., Collart, F., Yip, V.L., Withers, S.G., Varrot, A., Thompson, J., Davies, G.J, Anderson, W.F. (2004). Novel catalytic mechanism of glycoside hydrolysis based on the structure of an NAD^{+}/Mn^{2+}-dependent phospho-alpha-glucosidase from *Bacillus subtilis.* Structure. 12: 1619-1629.

Ralph, J., Lundquist, K., Brunow, G., Lu, F., Kim, H., Schatz, P.F (2004). Lignins: Natural polymers from oxidative coupling of 4-hydroxyphenylpropanoids. Phytochemistry Reviews 3:2960.

Ramadevi, P., Hegde, D.V., Varghese, M., Kamalakannan, R., Ganapathy, S.P., Gurumurthy, D.S., 2016. Evaluation of lignin syringyl/guaiacyl ratio in *Eucalyptus camaldulensis* across three diverse sites based on near infrared spectroscopic calibration and modelling with five *Eucalyptus* species and its impact on kraft pulp yield. Journal of Near Infrared Spectroscopy. 24: 529-536.

Ramos, L.P. The chemistry involved in the steam treatment of lignocellulosic materials. Química Nova. 26: 863-871.

Rauwerdink, A. and Kazlauskas, R.J. (2015). How the same core catalytic machinery catalyzes 17 different reactions: the serine-histidine-apartate catalytic triad of α/β-hydrolase fold enzymes. ACS Catalysis. 5(10): 6153-6176.

Rencoret, J., Gutiérrez, A., Nieto, L., Jiménez-Barbero, J., Faulds, CB., Kim, H., Ralph, J., Martínez, A.T., Del Río, J.C. (2011). Lignin composition and structure in young versus adult *Eucalyptus globulus* plants. Plant Physiology. 155(2): 667-682.

Reverbel-Leroy, C., Pages, S., Belaich, A., Belaich, J-P., Tardif, C. (1997). The processive endocellulase CelF, a major component of the *Clostridium cellulolyticum* cellulosome: purification and characterization of the recombinant form. Journal of Bacteriology. 179: 46–52.

Rico, A., Rencoret, J., del Rio, J.C., Martinez, A.T., Gutierrez, A. (2014). Pretreatment with laccase and a phenolic mediator degrades lignin and enhances saccharification of *Eucalyptus* feedstock. Biotechnology for Biofuels. 7(6).

Rodrigues, A.C., Felby, C., Gama M. (2014). Cellulase stability, adsorption/desorption profiles and recycling during successive cycles of hydrolysis and fermentation of wheat straw. Bioresource Technology 156: 164-16.

Romaní, A., Ruiz, H.A., Pereira, F.B., Teizeira, J.A., Domingues, L. (2014). Integrated approach for effective bioethanol production using whole slurry from auto-hydrolyzed *Eucalyptus globulus* wood at high-solid loadings. Fuel. 35: 482-491.

Rongpipi, S., Ye, D., Gomez, E.D., Gomez, E. (2019). Progress and oppurtunities in the characterization of cellulose - an important regulator of cell wall growth and mechanics. Frontiers in Plant Science. 1(9): 1894.

Rouches, E., Dignac, M.F., Carrere, H. (2016). Pyrolysis-GC-MS to assess the fungal pretreatment efficiency for wheat straw anaerobic digestion. Journal of Analytical and Applied Pyrolysis. 123: 409-418.

Sajith, S., Priji, P., Sreedevi, S., Benjamin, S. (2016). An overview on fungal cellulases with an industrial perspective. Journal of Nutrition and Food Science. 6: 461.

Sammond, D.W., Yarbrough, J.M., Mansfield, E., Bomble, Y.J., Hobdey, S.E., Decker, S.R., Taylor, L.E., Resch, M.G., Bozell, JJ., Himmel, M.E, Vinzant, T.B., Crowley, M.F. (2014). Predicting enzyme adsorption to lignin films by calculating enzyme surface hydrophobicity. Journal of Biological Chemistry. 289(30): 20960-20969.

Sanchez, C. (2009). Lignocellulosic residues: biodegradation and bioconversion by fungi. Biotechnology Advances. 27: 185-194.

Sangian, H.F., Pangau, J.R., Tamunuan, G.H., Zulnazri, Z. (2018). The structural analysis of the lignocellulose, Campaca timber (*Elmerrilllaovalis*) modified by the microwave. Chemical Engineering Transactions. 65.

Segato, F., Damasio, A.R.L., Gonçalves, T.A., Murakamia, M.T., Squina, F.M., Polizeli, M., Mort, A.J., Prade, R.A. (2012). Two structurally discrete GH7-cellobiohydrolases compete for the same cellulosic substrate fiber. Biotechnology for Biofuels. 5(21).

Selig, M.J., Knoshaug, E.P., Adney, W.S., Himmel, M.E., Decker, S.R. (2008). Synergistic enhancement of cellobiohydrolase performance on pretreated corn stover by addition of xylanase and esterase activities. Bioresource Technology. 99: 4997-5005.

Seo, D.H., Fujita, H., Sakoda, A. (2011). Effects of non-ionic surfactant, Tween 20, on adsorption/desorption of saccharification enzymes onto/from lignocelluloses and saccharification rate. Adsorption. 17(5): 813-822.

Sethi, S., Datta, A., Gupta, B.L., Gupta, S. (2013). Optimization of cellulase production from bacterial isolated from soil. Biotechnology. 2013: 1-7.

Shahzadi, T., Mehmood, S., Irshad, M., Anwar, Z., Afroz, A., Zeesgan, N., Rashid, U., Sughra, K. (2014). Advances in lignocellulosic biotechnology: A brief review on lignocellulosic biomass and cellulases. Advances in Bioscience and Biotechnology. 5: 246-251.

Shallom, D. and Shoham, Y. (2003). Microbial hemicellulases. Current Opinion in Microbiology. 6: 219-228.

Shang, Y., Su, R., Huang, R., Yang, Y., Qi, W., Li, Q., He, Z. (2014). Recycling cellulases by pH-triggered adsorption-desorption during the enzymatic hydrolysis of lignocellulosic biomass. Applied Microbiology and Biotechnology 98(12): 5765–5774.

Sharma, N., Rathore, M., Sharma, M. (2012). Microbial pectinases, sources, characterization and applications. Reviews in Environmental Science and Biotechnology. 12: 45-60.

Shoseyov, O., Shani, Z., Levy, I. (2006). Carbohydrate binding modules: biochemical properties and novel applications. Microbiology and Molecular Biology Reviews. 70(2): 283-295

Silva-Fernandes, T., Duarte, D., Carvalheiro, F., Marques, S., Loureiro-Dias, M.C., Fonseca, C., Girio, F. (2015). Biorefining strategy for maximal monosaccharide recovery from three different feedstocks: *Eucalyptus* residues, wheat straw and olive tree pruning. Bioresource Technology. 183, 203-212.

Simon, I., Glasser, L., Harold A. Scheraga, H. A., Manley, R. S. J. (1988). Structure of cellulose. 2. low-energy crystalline arrangements. Macromolecules. 21(4): 990-998.

Sims, R.E.H., Mabee, W., Saddler, J.N., Taylor, M. (2010). An overview of second generation biofuel technologies. Bioresource Technology. 101: 1570-1580.

Singh, G., Verma, A.K., Kumar, V. (2016). Catalytic properties, functional attributes and industrial applications of of β-glucosidases. 3 Biotech. 6(1): 3.

Singhania, R.R., Patel, A.K., Sukumaran, R.K., Larroche, C., Pandey, A. (2013). Role and significance of beta-glucosidases in the hydrolysis of cellulose for bioethanol production. Bioresource Technology. 12: 500-507.

Sipos B, Dienes D, Schleicher A, Perazzini R, Crestini C., Siika-aho, M., Reczey, K. (2010). Hydrolysis efficiency and enzyme adsorption on steam pretreated spruce in the presence of poly-(ethylene glycol). Enzyme and Microbial Technology. 47:84-90.

Siquera, G., Arantes, V., Saddler, J.J., Ferraz, A., Milagre, A.M.F. (2017). Limitation of cellulose accessibility and unproductive binding of cellulases by pretreated sugar cane bagasse lignin. Biotechnology for Biofuels. 10(176).

Sørensen, A., Lübeck, M., Lübeck, P.S., Ahring, B.K. (2013). Fungal βeta-glucosidases: a bottleneck in industrial use of lignocellulosic materials. Biomolecules. 3: 612-631.

Srivastava, N., Rathour, R., J, S., Pandey, K., Srivastava, M., Thakur, V,.K., Sengar, R.S., Gupta, V.K., Mazumder, P.B., Khan, A.F., Mishra, P.K. (2019). Microbial beta glucosidase enzymes: recent advances in biomass conversion for biofuels application. Biomolecules. 9(6): 220.

Stange Jr., R.R., Ralph, J., Peng, J., Sims, J.J., Midland, S.L. and McDonald, R.E. (2001). Acidolysis and hot water extraction provide new insights into the composition of the induced "lignin-like" material from squash fruit. Phytochemistry. 57: 1005-1011.

Studer, M.H., DeMartini, J.D., Davis, M.F., Sykes, R.W., Davidson, B., Keller, M., Tuskan, G.A., Wyman, C.E. (2011). Lignin in natural *Populus* variants affects sugar release. Proceedings of the National Academy of Sciences. 8(15): 6300-6305.

Sun, Y. and Cheng, J. (2002). Hydrolysis of lignocellulosic materials for ethanol production: a review. Bioresource Technology. 83: 1-11.

Sun, Y.C., Xu, J.K., Xu, F., Sun, R.C. (2013). Structural comparison and enhanced enzymatic hydrolysis of *Eucalyptus* cellulose via pretreatment with different ionic liquids and catalysts. Process Biochemistry. 48: 844-852.

Sun, Q., Foston, M., Meng, X., Sawada, D., Pingali, S.V., O'Neill, H.M., Li, H., Wyman, C.E., Langan, P., Ragauskas, A.J., Kumar, R. (2014). Effect of lignin content on the changes in popular cellulose ultrastructure during dilute acid pretreatment. Biotechnology Biofuels. 7(1): 150.

Sunna, A. and Antranikian, G. (1997). Xylanolytic enzymes from fungi and bacteria. Critical Reviews in Biotechnology. 17: 39-67.

Sweeney, M.D. and Xu, F. (2012). Biomass converting enzymes as Industrial Biocatalysts for Fuels and Chemicals: Recent Developments. Catalysts. 2(2): 244-263.

Tabka, M.G., Herpoel-Gimbert, I., Monod, F., Asther, M., Sigoillot, J.C. (2006). Enzymatic saccharification of wheat straw for bioethanol production by combined cellulase, xylanase and feruloyl esterase treatment. Enzyme and Microbial Technology. 39(4):897-902.

Taherzadeh, M.J., Karimi, K. (2008). Pretreatment of lignocellulosic wastes to improve ethanol and biogas production: a review. International Journal of Molecular Science. 9(9): 1621-1651.

Takashima, S., Iikura, H., Nakamura, A., Hidaka, M., Masaki, H., Uozumi, T. (1997). Comparison of gene structures and enzymatic properties between two endoglucanases from *Humicola grisea.* Biotechnology. 67(2): 85-97.

Takahashi, M., Takahashi, H., Nakano, Y., Konishi, T., Terauchi, R., Takedu, T. (2010). Characterization of a cellobiohydrolase (MoCel6A) produced by *Magnaporthe oryzae*. Applied and Environmental Microbiology. 76(19): 6583-6590.

Tang, Z., Li, P., Sun, R., Liu, M., Jin, W., Gou, L., Chen, H., Qu, Q., Bu, T., Li, C. (2018). Optimum mixture and synergy analysis of three main cellulases. International Journal of Agriculture and Biology. 20: 255-262.

Taylor, L.E., Knott, B.C., Baker, J.O., Alahuhta, P.M., Hobdey, S.E., Linger, V.V., Amore, A., Subramanian, V., Podkaminer, K., Xu, Q., VanderWall, T.A., Schuster, L.A., Chaudhari, Y.B., Adney, W.S., Crowley, M.F., Himmel, M.E., Decker, S.R., Beckham, G.T. (2018). Engineering enhanced cellobiohydrolase activity. Nature Communications. 9:1186.

Teeri, T. (1997). Crystalline cellulose degradation: new insight into the function of cellobiohydrolases. Trends in Biotechnology. 15: 160-167.

Thoresen, M., Malgas, S., Pletschke, B.I. (2020). Enzyme adsorption-desorption and evaluation of various cellulase recycling strategies for steam pre-treated *Eucalyptus* enzymatic degradation. Biomass Conversion and Biorefinery. DOI: 10.1007/s13399-020-00670-9.

Thygesen, A., Oddershede, J., Lilholt, H., Thomsen, A.B., Stahl, K. (2005). On the determination of crystallinity and cellulose content in plant fibres. Cellulose. 12(563).

Tomme, P., Van Tilbeurgh, Pettersson, G., Van Damme, J., Vandekerckhove, J., Knowles, J., Teeri, T., Claeyssens, M. (1988). Studies of the cellulolytic system of *Trichoderma reesei* QM 9414. The FEBS Journal. 170(3):575-81

Trabucco, G.M., Matos, D.A., Lee, S.J., Saathoff, A.J., Priest, H.D., Mockler, T.C., Sarath, G., Hazen, S. (2013). Functional characterization of cinnamyl alcohol dehydrogenase and caffeic acid O-methyltransferase in *Brachypodium distachyon*. BMC Biotechnology. 13(61).

Troncoso, E., Castillo, R., Valenzuela, R., Reyes, P., Freer, J., Norambuena, M., Rodriquez, J., Parra, C. (2017). Chemical and microstructural changes in *Eucalyptus globulus* fibers subjected to four different pretreatment and their influence on the enzymatic hydrolysis. Journal of the Chilean Chemical Society. 62(2).

Tu, M., Zhang, X., Paice, M., McFarlane, P., Saddler, J.N. (2009). The potential of enzyme recycling during the hydrolysis of a mixed softwood feedstock. Bioresource Technology. 100: 6407-6415.

Turon, X., Rojas, O.J., Deinhammer, R.S. (2008). Enzymatic kinetics of cellulose hydrolysis: A QCM-D study. Langmuir. 24: 3880-3887.

Vaaje-Kolstad, G., Forsberg, Z., Loose, J.S.M., Bissaro, B., Eijsink, V.G.H. (2017). Structural diversity of lytic polysachharide monooxygenases. Current Opinion in Structural Biology. 44: 67-76.

Valdivia, M., Galan, J.L., Laffarga, J., Ramos, J.L. Biofuels 2020: biorefineries on lignocellulosic materials. (2016). Microbial Biotechnnology. 9(5): 585-594.

Väljamäe, P., Sild, V., Pettersson, G., Johansson, G. (1998). The initial kinetics of hydrolysis by cellobiohydrolase 1 and 11 is consistent with a cellulose surface-erosion model. Biochemistry. 352, 469-475.

Väljamäe, P., Sild. V., Nutt. A., Pettersson. G., Johansson. G. (1999). Acid hydrolysis of bacterial cellulose reveals different modes of synergistic action between cellobiohydrolase I and endoglucanase. Biochemistry. 266(2): 327-334.

Väljamäe, P., Pettersson, G., Johansson, G. (2001). Mechanism of substrate inhibition in cellulose synergistic interaction. Biochemistry. 26(16): 4520-4526.

Van Dyk, J.S and Pletschke, B.I. (2012). A review of lignocellulose bioconversion using enzymatic hydrolysis and synergistic cooperation between enzymes - factors affecting enzymes, conversion and synergy. Biotechnology Advances. 30: 1458-1480.

Vandenbrink, J.P., Hilten, R.N., Das, K.C., Paterson, A.H., Feltus. F.A. (2012). Analysis of crystallinity index and hydrolysis rates in the bioenergy crop *Sorghum bicolor.* Bioenergy Resources. 5: 387-397.

Valentine, J., Clifton-Brown, J., Hastings, A., Robson, P., Allison, G., Smith, P. (2012). Food vs fuel: the use of land for lignocellulosic 'next generation' energy crops that minimize competition with primary food production. GCB Bioenergy. 4: 1-19.

Van Zyl, W.H., Lynd, L.R., Den Haan, R., McBride, J.E. (2007). Consolidated bioprocessing for bioethanol production using *Saccharomyces cerevisiae*. Advances in Biochemical Engineering and Biotechnology. 108: 205-235.

Van Zyl, W.H., Rose, S.H., Trollope, K., Gorgens, J.F. (2010). Fungal β-mannanases: mannan hydrolysis, heterologous production and biotechnological applications. Process Biochemistry. 45: 203-1213.

Varnai, A., Viikari, L., Marjamaa, K., Silka-aho, M. (2011). Adsorption of monocomponent enzymes in enzyme mixture analysed quantitatively during hydrolysis of lignocellulose substrates. Bioresource Technology. 102: 1220-1227.

Varrot, A., Schulein, M., Davies, G.J. (1999), Structural changes of the active site tunnel of *Humicola insolens* cellobiohydrolase, Cel6A, upon oligosaccharide binding. Journal of Biochemistry. 38: 8884–8891.

Vena , P.F., Garcia-ia-aparicio, M.P., Brienzo, M., Gorgens, F., Rypstra, T. (2013). Effect of alkaline hemicellulose extraction on kraft pulp fibers from *Eucalyptus grandis.* Journal of Wood Chemistry and Technology. 33: 157-173.

Vermaas, J.V., Petridis, L., Qi, X.H., Schulz, R., Lindner, D., Smith, J.C. (2015). Mechanism of lignin inhibition of enzymatic biomass deconstruction. Biotechnology for Biofuels. 8(127).

Viborg, A.H., Terrapon, N., Lombard, V., Michel, G., Czjzek, M., Henrissat, B., Brumer, H. (2019). A subfamily roadmap of the evolutionarily diverse glycoside hydrolase family 16 (GH16). Journal of Biological Chemistry. 1(44): 15793-15986.

Visser, E.M, Leal, T.F., de Almeida, M.N., Guimaraes, V.M. (2015). Increased enzymatic hydrolysis of sugarcane bagasse from enzyme recycling. Biotechnology for Biofuels. 8(5).

Voragen, A.G.J, Coenen, G.J., Verhoed, R.P. (2009). Pectin, a versatile polysaccharide present in plant cell walls. Structural Chemistry. 20(2): 263-275.

Voutilainen, S.P., Murray, P.G., Tuohy, M.G., Koivula, A. (2010). Expression of *Talaromyces emersonii* cellobiohydrolase Cel7A in *Saccharomyces cerevisiae* and rational mutagenesis to improve it thermostability and activity. Protein Engineering, Design and Selection. 23(2): 67-79.

Wagschal, K., Heng, C., Lee, C.C., Wong, D.W.S. (2009). Biochemical characterisation of a novel dual-function arabinofuranosidase/xylosidase isolated from a compost started mixture. Applied Microbiology and Biotechnology. 81: 855-863.

Wang, H., Squina, F., Segato, F., Mort, A., Lee, D., Pappana, K., Prade, R. (2011). High temperature enzymatic breakdown of cellulose. Applied and Environmental Microbiology. 77(15): 5199-5206.

Wang, W., Zhuang, X., Yuan, Z., Yu, Q., Qi, W., Wang, Q., Tan, X. (2012). Effect of structural changes on enzymatic hydrolysis of eucalyptus, sweet sorghum bagasse, and sugarcane bagasse after liquid hot water pretreatment. Bioresources. 7(2): 2469-2482.

Wang, W., Ji, S., Lee, I. (2013). Fast and efficient nanoshear hybrid alkaline pretreatment of corn stover for biofuel and materials production. Biomass Bioenergy. 51: 35-42.

Wang, C., Li, H., Li, M., Bian, J., Sun, R. (2017). Revealing the structure and distribution changes of *Eucalyptus* lignin during the hydrothermal and alkaline pretreatments. Scientific Reports. 7(1): 593.

Wang, Z., Hou, X., Sun, J., Li, M., Chen, Z., Gao, Z. (2018). Comparison of ultrasound-assisted ionic liquid and alkaline pretreatment of *Eucalyptus* for enhancing enzymatic saccharification. Bioresource Technology. 254: 145-150.

Wang, Z., Winestrand, S., Gillgren, T., Jonsson, L.G. (2019). Chemical and structural factors influencing enzymatic saccharification of wood from aspen, birch and spruce. Biomass Bioenergy. 109: 125-134.

Wang, H., Liu, Z., Hui, L., Ma, L., Zheng, X., Li, J., Zhang, Y. (2019). Understanding the structural changes of lignin in poplar following steam explosion pretreatment. Holzforschung. 74(3): 275-285.

Wei, W., Wu, S., Liu, L. (2012). Enzymatic saccharification of dilute acid pretreated *Eucalyptus* chips for fermentable sugar production. Bioresource Technology. 110: 302-307.

Weiss, N., Borjesson, J., Pedersen, L.S., Meyer, A.S. (2013). Enzymatic lignocellulose hydrolysis: Improved cellulase productivity by insoluble solids recycling. Biotechnology for Biofuels. 6(5).

Weng, J., Jia, L., Wang, Y., Sun, S., Tang, X., Zhou, Z., Kohse-Hoinghaus, K., Qi, F, (2013). Pyrolysis study of poplar biomass by tunable synchrotron vaccum ultraviolet photoionization mass spectrometry. Proceedings of the Combustion Institute. 34(2): 2347-2354.

Wolf, S., Mouille, G., Pelloux, J. (2009). Homogalacturonan methyl-esterficication and plant development. Molecular Plant. 2(5): 851-860.

Wood, T.M. and McCrae, S.I. (1979). Synergism between enzymes involved in the solubilisation of native cellulose. Advances in Chemistry. 181: 181-209.

Woodward, J., Lima, M., Lee, N.E. (1988). The role of cellulase concentration in determining the degree of synergism in the hydrolysis of microcrystalline cellulose. Biochemistry. 255: 895-899.

Woodward, J. (1991). Synergism in cellulase systems. Bioresource Technology. 36: 67–75.

Woon, J.S., Mackeen, M.M., Illias, R.M., Mahadi, N.M., Broughton, W.J., Murad, A.M.A., Bakar, F.D.A. (2017). Cellobiohydrolase B of *Aspergillus niger* over-expressed in *Pichia pastoris* stimulates hydrolysis of oil palm empty fruit bunches PeerJ. Doi: 10.7717/peerj.3909

Wu, Y., Jiang, L., Lin, Y., Qian, L., Xu, F., Lang, X., Fan, S., Zhao, Z., Li, H. (2019). Novel crude glycerol pretreatment for selective saccharification and sugarcane bagasse via fast pyrolysis. Bioresource Technology. 294.

Xia, W., Bai, Y., Cui, Y., Xu, X., Qian, L., Shi, P., Zhang, W., Luo, H., Zhan, X., Yao, B. (2016). Functional diversity of family 3 β-glucosidases from thermophilic cellulolytic fungus *Humicola insolens* Y1. Scientific Reports. 6: 27062.

Xiao, L.P., Lin, Z., Peng, W.X., Yuan, T.Q., Xu, F., Li, N.C., Tao, Q.S., Xiang, H., Sun, R.C. (2014). Unraveling the structural characteristics of lignin in hydrothermal pretreated fibers and manufactured binderless boards from *Eucalyptus grandis.* Sustainable Chemical Processes. 2(9).

Xiemenes, E., Kim, Y., Mosier, N., Dien, B., Ladisch, M. (2011). Deactivation of cellulases by phenols. Enzyme and Microbial Technology. 48, 54-60.

Xue, Y., Jameel, H., Park, S. (2011). Strategies to recycle enzymes and their impact on enzymatic hydrolysis for bioethanol production. Bioresources. 7(1).

Xu, N., Zhang, W., Ren, S., Liu, F., Zhao, C., Liao, H. Xu, Z., Huang. J., Qing, L., Tu, Y., Yu, B., Wang, Y., Jiang, J., Qin, Q., Peng, L. (2012). Hemicellulose negatively affect lignocellulose crystallinity for high biomass digestibility under NaOH and H_2SO_4 pretreatment in *Miscanthus*. Biotechnology for Biofuels. 5(58).

Yamabhai, M., Sak-Ubol, S., Srila, W., Haltrich, D. (2014). Mannan Biotechnology: from biofuels to health. Critical Reviews in Biotechnology. 1(11).

Yang, B., Dai, Z., Sing, S.Y., Wyman, C.E. (2011). Enzymatic hydrolysis of cellulosic biomass. Biofuels. 2(4): 421-450.

Yang, M., Zhang, K.D., Zhang, P.Y., Zhou, Z., Ma, Z.Q., Li, F.L. (2016). Synergistic cellulose hydrolysis dominated by a multi-modular processive endoglucanase from *Clostridium cellulosi*. Frontiers in Microbiology. 15(7): 932.

Yanfei, L., Sun, Z., Ge, X., Zhang, J. (2016). Effects of lignin and surfactant on adsorption and hydrolysis of cellulases on cellulose. Biotechnology for Biofuels. 9(20).

Ye, M., Sun, L., Yang, R., Wang, W., Qi, K. (2017). The optimization of fermentation conditions for producing cellulase of *Bacillus amyloliquefaciens* and its application in goose feed. Royal Society Open Science. 4(10).

Yoshida, M., Liu, Y., Uchida, S., Kawarada, K., Ukagami, Y., Chinose, H., Kaneko, S., Fukud, K. (2008). Effect of cellulose crystallinity, hemicellulose, and lignin on the enzymatic hydrolysis of *Miscanthus sinesis* to monosaccharides. Bioscience, Biotechnology and Biochemistry. 72(3): 805-881.

Yoshida, T. Amakura, Y., Yoshimura, M. (2010). Soma plant families of the Order Myrtales. International Journal of Molecular Sciences. 11: 79-106.

Yu, Q., Zhuang, X., Yuan, Z., Wang Q., Qi, W., Wang, W., Zhang, Y., Xu, J., Xu, H. (2010). Two-step liquid hot water pretreatment if *Eucalyptus grandis* to enhance sugar recovert and enzymatic digestibility of cellulose. Bioresource Technology. 101: 4895-4899.

Yu, Q., Zhuang, X., Wang, Q., Qi, W., Tan, X., Yuan, Z. (2012). Hydrolysis of sweet sorghum bagasse and *Eucalyptus* wood chips with liquid hot water. Bioresource Technology. 116: 220-225.

Yuan, Y., Zhai, R., Li, Y., Chen., Xin, M. (2018). Developing fast enzyme recycling strategy through elucidating enzyme adsorption kinetics on alkali and acid pretreated corn stover. Biotechnology for Biofuels. 11(316).

Zao, S.Y. and Shao, Y.Y. (2012). Synergistic effect between cellulase and xylanase acting on alkaline pretreated straw. Advanced Materials Research. 396-39: 106-1412.

Zeng, Y., Himmel, M.E., Ding, S.Y. (2017). Visualisizing chemical functionality in plant cell walls. Biotechnology for Biofuels. 10(264).

Zhang, Y.H. and Lynd L.R. (2004). Toward an aggregated understanding of enzymatic hydrolysis of cellulose. Noncomplexed cellulase systems. Biotechnology and Bioengineering. 88: 797–82.

Zhang, J., Tuomainen, P., Siika-Aho, M., Viikari, L. (2011). Comparison of the synergistic action of two thermostable xylanases from GH families 10 and 11 with thermostable cellulases in lignocellulose hydrolysis. Bioresource Technology. 102(19): 9090-9095.

Zhang, J., Siika-aho, M., Tenkanen, M., Viikari, L. (2011). The role of acetyl xylan esterase in the solubilisation of xylan and enzymatic hydrolysis of wheat straw and giant reed. Bioresource Technology. 4(60).

Zhang, X.Z. and Zhang, Y.H.P. (2013). Cellulases: characteristics, sources, production, and appplications In: Bioprocessing Technologies in Biorefinery for Sustainable Production of Fuels, Chemicals and Polymers. Yang, S.T., El-Enhasy, H., Thongchul, N. (Editors). ISBN: 9781118642047.

Zhang, H., Wei, W., Zhang, J., Huang, S., Xie, J. (2018). Enhancing enzymatic saccharification of sugarcane bagasse by combinatorial pretreatment of Tween 80. Biotechnology for Biofuels. 11(309).

Zhang, Y., Huang, M, Su, J., Hu, H., Yang, M., Huang, Z., Chen, D., Wu, J., Feng, Z. (2019). Overcoming biomass recalcitrance by synergistic pretreatment of mechanical activation and metal salt for enhancing enzymatic conversion of lignocellulose. Biotechnology for Biofuels. 12(12).

Zheng, F. and Ding, S.J. Processivity and enzymatic mode of a glycoside hydrolase family 5 endoglucanase from *Volvariella volvacea.* (2013). Applied and Environmental Microbiology 79: 989-96.

Zheng, Y., Zhang, S., Miao, S., Su, Z., Wang, P. (2013). Temperature sensitivity of cellulase adsorption on lignin and its impact on enzymatic hydrolysis of lignocellulosic biomass. Journal of Biotechnology. 166: 135-143.

Zhou, J., Wang, Y-H., Chu, J., Luo, L-Z., Zhuang, Y-P., Zhang, S.L. (2009). Optimization of cellulase mixture for efficient hydrolysis of steam-exploded corn stover by statistically designed experiments. Bioresource Technology. 100: 819-825.

Zhu, Z., Sathitsuksanoh, N., Zhang, Y.H.P. (2009). Direct quantitative determination of adsorbed cellulase on lignocellulosic biomass with its application to study cellulose desorption. Analyst. 134(11): 2267-2272.

Zoghlami, A. and Paës, G. (2019). Lignocellulosic biomass: understanding recalcitrance and predicting hydrolysis. Frontiers in Chemistry. 7(874).

Zverlov, V.V., Velikodvorskaya, G.A., Schwarz, W.H. (2003). Two new cellulosome components encoded downstream of celI in the genome of *Clostridium thermocellum*: the non-procesive endoglucanase CelN and the possibly structural protein CseP. Microbial. 149: 515-524.

Appendices:

Appendix 1: Reagents list

Appendix 2: Standard curves

2A: Protein standard curve

2B: Glucose standard curve

2C: p-Nitrophenyl standard curve

2D: GOPOD standard curve

2E: Remazol Brilliant Blue Royal (RBBR) standard curve

2F: Simons' Stain standard curve (Direct Orange)

Appendix 3: SDS-PAGE

Appendix 4: Enzyme Synergy

4A: Enzyme combinations for the cellulase cocktails (Chapter 4)

4B: Summary of the reducing sugars and glucose released after 24 h hydrolysis of Avicel by the synergistic action of cellulases from different GH families and microbial sources

Appendix 5: Pretreatment ad substrate characterisation

5A: Quantitative analysis and comparison between compositional analysis[a], S/G ratio[b], crystallinity index[c] and Simons' staining[d] of untreated and treated Eucalyptus samples

5B: Relative changes in Eucalyptus samples after various pretreatment methods by FTIR[a] and NMR[b]

Appendix 1: Reagents list

Name of Reagent	Supplier (Catalogue number)
Ammonium persulphate	Sigma Aldrich (Cat no A3678)
Acrylamide	Sigma (Cat. No. A8887)
Ammonium persulphate	Sigma Aldrich (Cat. No. A3678)
Avicel PH101	Fluka (11365)
Birchwood xylan	Fluka (Cat. No. 95588)
Bovine serum albumin (BSA)	Sigma (Cat. No. A7906)
Bradford reagent	Sigma (Cat. No. B6916)
Bromophenol blue	Sigma (Cat. No. B8026)
Carboxymethyl cellulose	Calbiochem (Cat. No. 217277)
Calcium carbonate	Merck (Cat. No. 1020660250)
Coomassie Brilliant Blue R250	Merck (Cat. No. 1.12553)
Citric acid	Merck (Cat. No. 1.00244)
3,5-Dinitrosalicylic acid	Sigma (Cat No. D0550)
Ethanol	Merck (Cat. No. 8.18700)
Glacial acetic acid	Merck (Cat. No. 1.00063)
Glycerol	Saarchem (Cat. No. 2676520
Glycine	Merck (Cat. No. 1.04169)
D-glucose	Saarchem (Cat. No. 2676020)
D-Mannose	Sigma (Cat. No. M2069)
D-Mannose, D-Fructose & D-Glucose kit	Megazyme (Cat. No. K-MANGL)
2-mercaptoethanol	Fluka (Cat. No. 63700)
Methanol	Merck (Cat. No. 8.22283)
N,N-methylenebisacrylamide	Sigma (Cat. No.M7279)

4-Nitrophenyl-β-D-glucopyranoside	Sigma (N1377)
p-Nitrophenol	Sigma (Cat. No. 42,575-3)
PeqGold protein marker II	peqLab (Cat. No. 27-2010)
Phenol	Sigma (Cat.No. P3653)
Phloroglucinol	Sigma (Cat. No. P3502)
Di-potassium hydrogen phosphate	Merck (1.05104.1000)
Di-sodium hydrogen orthophosphate	Saarchem (Cat. No. 5822860)
Ethanol	Merck (Cat. No. 8.18700)
Folin-Ciocalteu	Merck (1.09001.0500)
Glacial acetic acid	Merck (Cat. No. 1.00063)
D-Glucose	Saarchem (Cat. No. 2676020)
Glycerol	Saarchem (Cat. No. 2676520)
Glycine	Merck (Cat. No. 1.04169)
p-Nitrophenol	Sigma (Cat. No. 42,575-3)
Potassium sodium tartarate	Merck (1.08087.1000)
Sodium azide	Merck (Cat. No. 8.22335)
Sodium carbonate	Merck (Cat. No. 1.06392.0500)
Sodium dodecyl sulphate (SDS)	BDH 173iochemical (Cat. No. 301754)
Sodium hydroxide	Saarchem (Cat. No. 5823200)
Sodium metabisulfite	Sigma-Aldrich (Cat. No. 255556)
Sodium potassium tartrate	Merck (Cat. No. 1.08087)
Sodium sulphate	Saarchem (Cat. No. 5825200)
Sodium sulphite	Saarchem (Cat. No. 5825400)
Sulfuric acid	Merck (Cat. No.1120802500)
N,N,N',N'-tetramethylethylene diamine	Sigma Aldrich (Cat. No. T9281)
Tris (hydroxymethyl) aminomethane	Merck (Cat. No. 1.08382)

Tri-sodium citrate dehydrate	Merck (Cat. No. 1.06448)
D-Xylose	Sigma (Cat. No. K-XYLOSE)

Appendix 2: Standard Curves

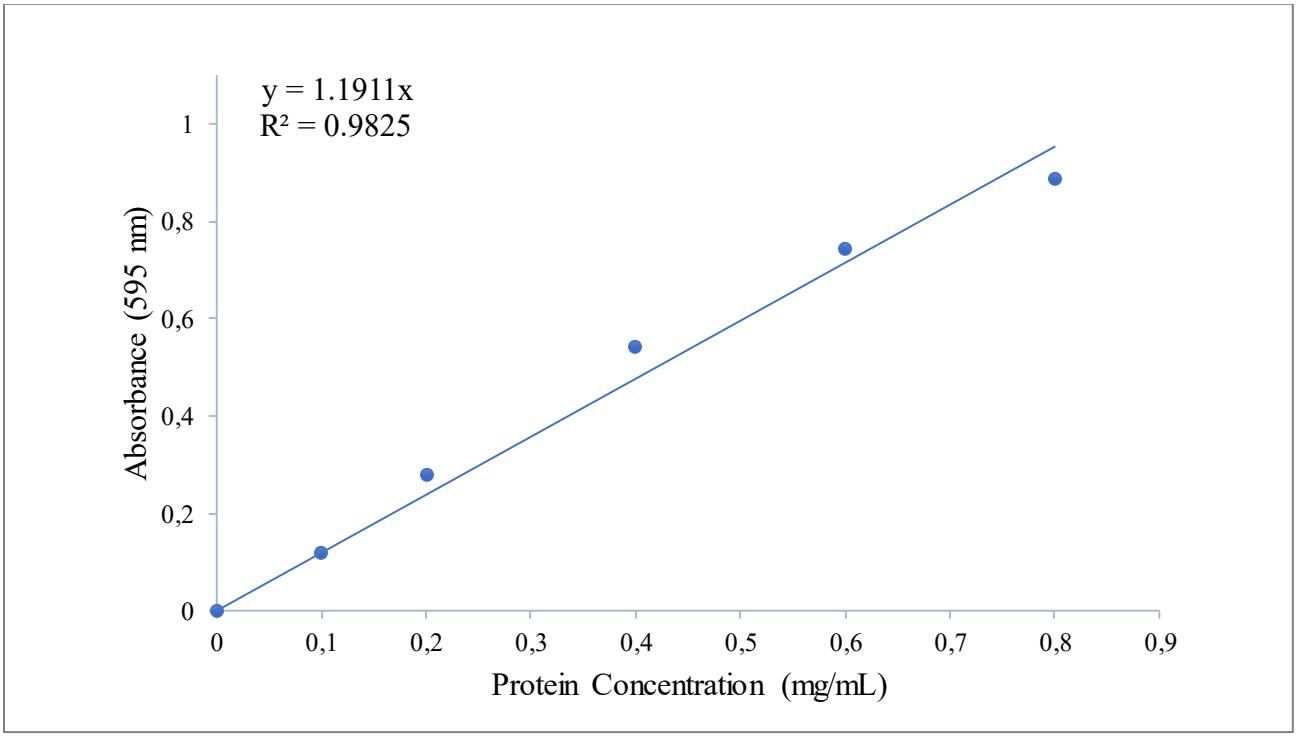

Figure 2A. Protein standard curve. 25 µL of protein sample was added to 230 µL Bradford reagent and incubated for 10 minutes at room temperature. Values are shown as the average (n=3, SD < 5%)

2B: Glucose standard curve

The composition of the DNS reagent were as follow:

2 g sodium hydroxide

2 g 3, 5 dinitrosalicylic acid (DNS)

40 g potassium sodium tartrate (Rochelle salt)

0.4 g phenol

0.1 g sodium metabisulfite

200 mL distilled water

A 2 % sodium hydroxide solution was made before the DNS was added. Once the DNS had dissolved, the other chemicals were added and the volume was made up to 200 mL.

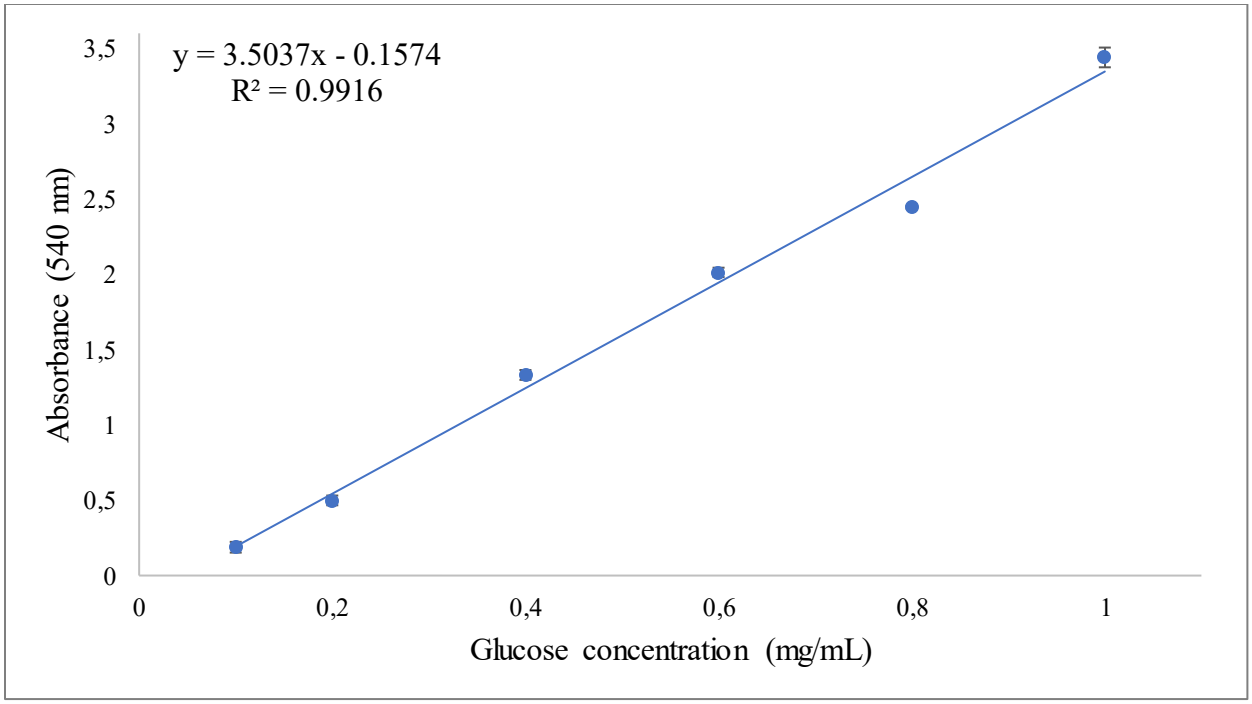

Figure 2B. Glucose standard curve. 150 µL of protein sample was added to 300 µL DNS reagent and incubated for 7 minutes at 100°C. Values are shown as the average (n=3, SD < 5%).

2C. GOPOD standard curve

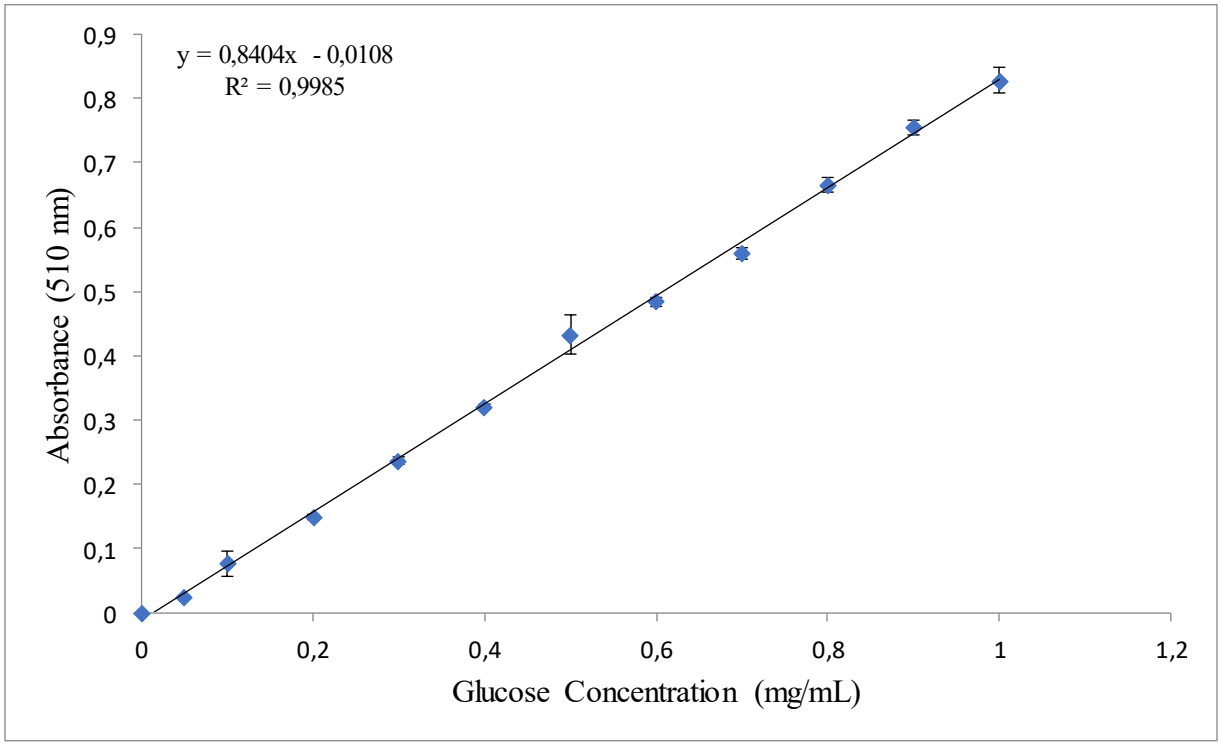

Figure 2C. *p*-nitrophenyl standard curve. Values are shown as the average (n=3, SD < 5%).

2D. *p*-Nitrophenyl standard curve

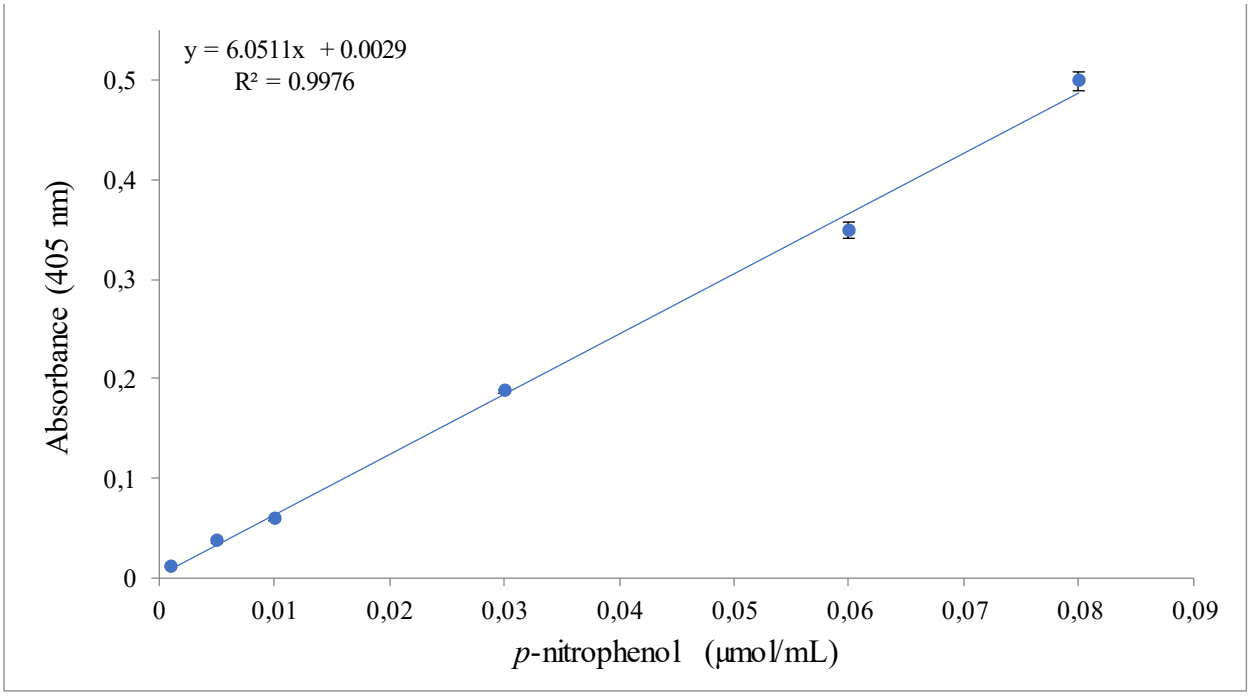

Figure 2D. *p*-nitrophenyl standard curve. Values are shown as the average (n=3, SD < 5%).

2E. RBBR standard curve

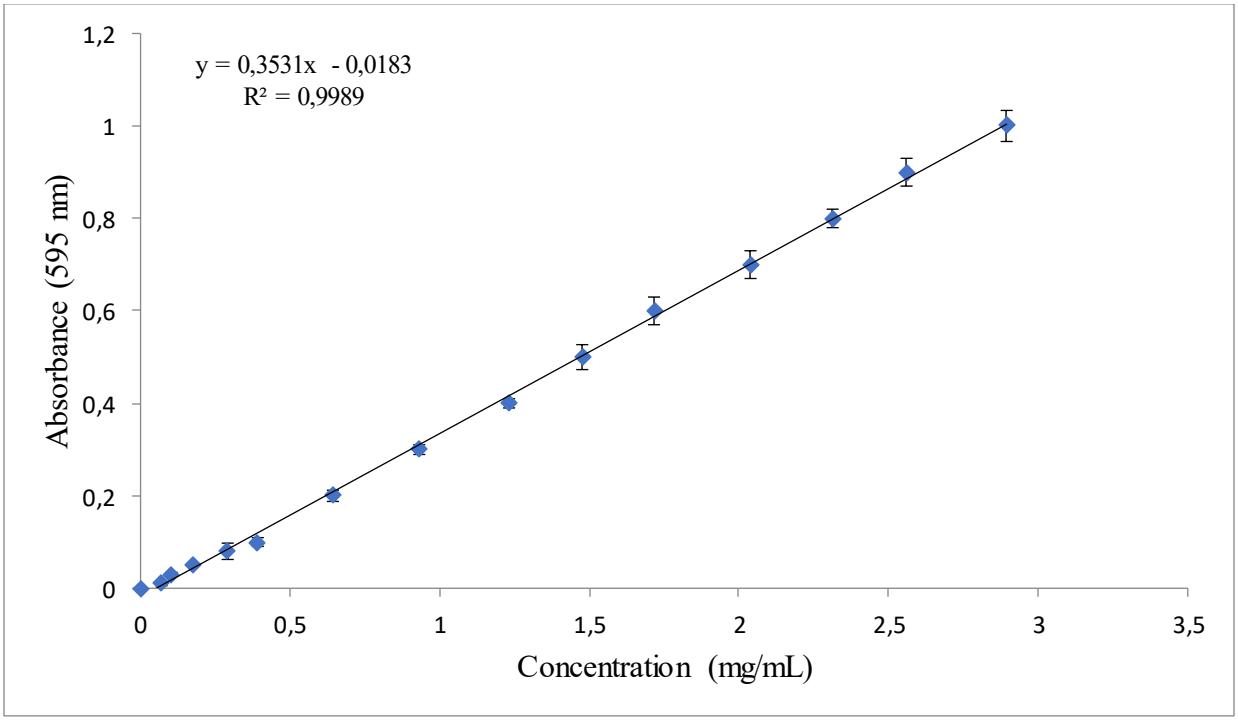

Figure 2E. RBR standard curve. Values are shown as the average (n=3, SD < 5%).

2F. Simons' stain standard curve

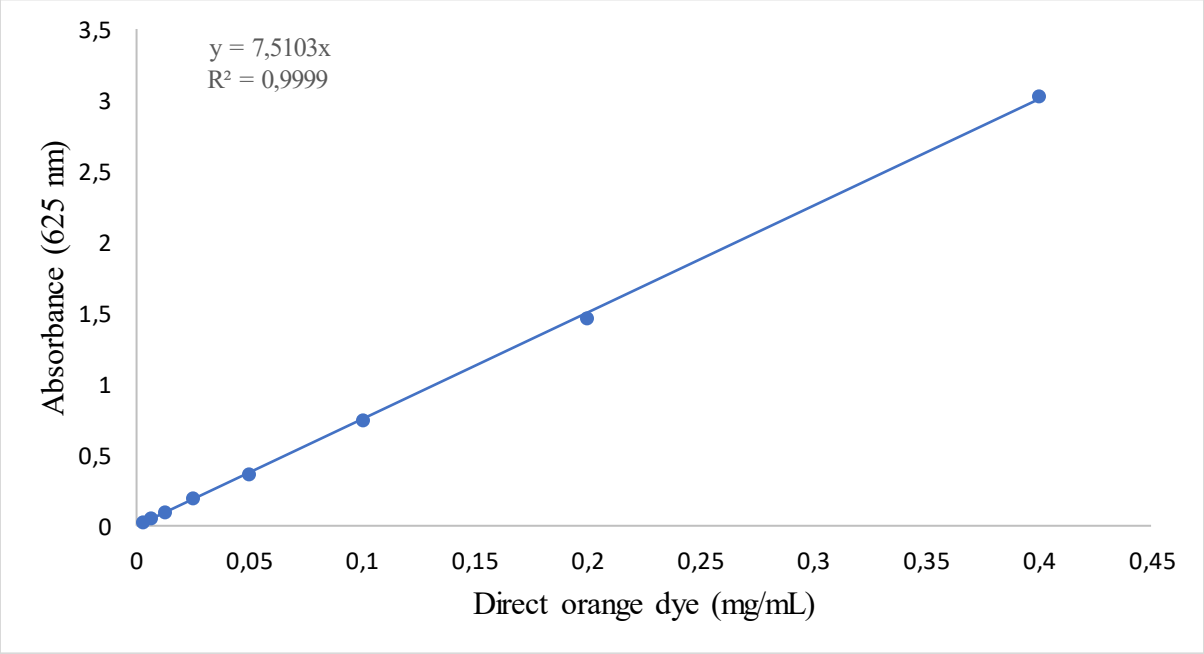

Figure 2E. RBR standard curve. Values are shown as the average (n=3, SD < 5%)

Appendix 3: SDS-PAGE

Sodium dodecyl sulphate polyacrylamide gel electrophoresis (SDS-PAGE) was performed (Laemmli, 1970) and modified according to the BioRad® Mini-Protean 3 Cell instruction manual. The solutions were prepared as follows:

1. 30% Acrylamide solution

29.8 g Acyrylamide

0.2 g Bis-Acrylamide

These chemicals were dissolved in 100 mL distilled water, wrapped in aluminum foil and stored at 4°C

2. 10 % (w/v) SDS stock solution

10 g SDS was dissolved in 10 mL distilled water

3. Stacking buffer (0.5 M Tris-HCl; pH 6.8)

6 g Tris (Hydroxymethyl) Aminomethane was dissolved in distilled water and HCl was added to adjust the pH to 6.8 before making the volume up to 100 mL. The buffer was stored at 4°C.

4. Resolving gel (1.5 M Tris-HCl; pH 8.8)

18.15g Tris (Hydroxymethyl) Aminomethane was dissolved in distilled water and HCl was added to adjust the pH to 8.8 before making the volume up to 100 mL. The buffer was stored at 4°C.

5. 10 x SDS running buffer

30.3 g Tris (Hydroxymethyl) Aminomethane

144 g glycine

10 g SDS

These chemicals were dissolved in 1 L distilled water and kept at room temperature.

6. 5 x SDS sample buffer

2.5 mL distilled water

1 mL 0.5 M Tris-HCl buffer (pH 6.8) 1 mL 10% SDS stock solution (w/v)

1 mL 1% bromophenol blue (w/v)

The sample buffer was kept at room temperature. β-mercaptoethanol (5 µL) was added to SDS sample buffer (95 µL), prior to preparing samples for electrophoresis. A volume of 3 µL of SDS sample buffer was added to 15 µL of protein samples and boiled for electrophoresis.

7. Coomassie Brilliant Blue protein staining solution

0.075% (w/v) Coomassie Brilliant Blue R250 was dissolved in 40% methanol and 0.7% glacial acetic acid.

8. Coomassie de-staining solution

45% methanol, 45% distilled water and 10% glacial acetic acid were mixed.

9. 10% Ammonium persulphate (APS) solution

0.1 g APS was dissolved in 1 mL distilled water. Samples were prepared prior to preparing the gel.

10. Preparation of gels

a) 10% resolving gel

4.04 mL distilled water

2.5 mL Tris-HCl buffer (pH 8.8)

3.3 mL acrylamide stock solution (30% w/v)

0.1 mL SDS stock solution (10% w/v)

0.1 mL APS solution (10% w/v)

0.05 mL TEMED.

b) 4% stacking gel

6.1 mL distilled water

2.5 mL Tris-HCl buffer (pH 6.8)

1.3 mL acrylamide stock solution (30% w/v)

0.1 mL SDS stock solution (10% w/v)

0.1 mL APS solution (10% w/v)

0.05 mL TEMED

Appendix 4A: Enzyme combinations

Table 4A: The various exo- and endo- combinations were used for the synergy studies

Cmix (CBH combination)	Enzymes used
A1	*Tl*Cel7A + microbial Cel6A
A2	*Tl*Cel7A + *Ct*Cel5A
B1	*Hj*Cel7A + microbial Cel6A
B2	*Hj*Cel7A + *Ct*Cel5A
C1	*Cs*Cel48A + microbial Cel6A
C2	*Cs*Cel48A + *Ct*Cel5A

Appendices:

Table 4B. Summary of the reducing sugars and glucose released after 24 h hydrolysis of Avicel by the synergistic action of cellulases from different GH families and microbial sources

		EG*Ba* (Cel5A)				**EG*Tm* (Cel5A)**				**EG*An* (Cel9,12,74)**				**EG*Tr* (Cel7B)**			
Cmix	**Cmix/Endo**	**RS (mg/mL)**	**Glu (mg/mL)**	**DS_{RS}**	**DS_{Glu}**	**RS (mg/mL)**	**Glu (mg/mL)**	**DS_{RS}**	**DS_{Glu}**	**RS (mg/mL)**	**Glu (mg/mL)**	**DS_{RS}**	**DS_{Glu}**	**RS (mg/mL)**	**Glu (mg/mL)**	**DS_{RS}**	**DS_{Glu}**
A1	0/100	0.18	0.228	-	-	0	0	-	-	1.16	1.1	-	-	0.45	0.465	-	-
	25/75	0.714	0.704	1.19	1.26	0.468	0.498	1.12	1.16	1.29	1.18	1.08	1.1	0.69	0.65	0.9	0.88
	50/50	0.95	0.901	1.3	0.28	0.6	0.644	1.09	1.09	1.27	1.13	1.15	1.31	0.8	0.82	0.95	0.99
	75/25	1.13	1.074	1.38	0.432	0.8	0.779	1.11	1.14	1.25	1.1	1.15	1.11	0.86	0.83	0.96	1
	100/0	0.842	0.849	-	-	0.842	0.849	-	-	0.842	0.849	-	-	0.842	0.849	-	-
A2	0/100	0.18	0.228	-	-	0	0	-	-	1.16	1.1	-	-	0.45	0.465	-	-
	25/75	0.798	0.754	1.33	1.39	0.504	0.495	1.26	1.2	1.43	1.345	1.19	1.29	0.702	0.69	0.92	0.95
	50/50	0.106	0.998	1.36	1.37	0.729	0.719	1.22	1.17	1.4	1.32	1.2	1.286	0.802	0.78	0.93	0.9
	75/25	0.121	0.112	1.47	1.41	0.886	0.815	1.23	1.22	1.32	1.31	1.19	1.27	0.846	0.82	0.92	0.94
	100/0	0.87	0.857	-	-	0.87	0.857	-	-	0.87	0.857	-	-	0.87	0.857	-	-
B1	0/100	0.18	0.228	-	-	0	0	-	-	1.16	1.1	-	-	0.45	0.465	-	-
	25/75	0.253	0.294	0.63	0.64	0.205	0.257	0.98	0.8	0.98	0.937	0.98	1	0.446	0.45	0.77	0.69
	50/50	0.31	0.347	0.641	0.641	0.295	0.326	0.94	0.8	0.88	0.84	1	0.99	0.434	0.45	0.72	0.67
	75/25	0.372	0.397	0.77	0.72	0.375	0.405	0.99	0.91	0.76	0.75	1	0.96	0.432	0.43	0.74	0.68
	100/0	0.397	0.414	-	-	0.397	0.414	-	-	0.397	0.414	-	-	0.397	0.414	-	-
B2	0/100	0.18	0.28			0	0			1.16	1.1	-	-	0.45	0.465	-	-

	25/75	0.282	0.339	0.72	0.72	0.23	0.283	0.98	0.87	1.04	1	1.03	0.95	0.56	0.53	0.98	0.82
	50/50	0.34	0.38	0.76	0.72	0.29	0.365	0.97	0.84	0.85	0.8	1.02	0.98	0.54	0.54	0.94	0.83
	75/25	0.37	0.44	0.88	0.82	0.335	0.38	0.99	0.88	0.69	0.66	0.97	0.86	0.512	0.52	0.94	0.85
	100/0	0.4	0.434	-	-	0.4	0.434	-	-	0.4	0.434	-	-	0.4	0.434	-	-
C1	0/100	0.18	0.228	-	-	0	0	-	-	1.16	1.1	-	-	0.45	0.465	-	-
	25/75	0.146	0.213	0.73	0.95	0	0.09	0	0.98	0.75	0.69	0.94	0.99	0.392	0.414	1.16	1
	50/50	0.136	0.198	0.76	0.93	0	0.127	0	1.23	0.45	0.4	0.65	0.78	0.361	0.379	1.18	1.05
	75/25	0.116	0.187	0.88	0.86	0.09	0.145	1.28	1.24	0.157	0.21	0.38	0.46	0.29	0.33	1.18	1.04
	100/0	0.1	0.153	-	-	0.1	0.153	-	-	0.1	0.153	-	-	0.1	0.153	-	-
C2	0/100	0.18	0.228	-	-	0	0	-	-	1.16	1.1	-	-	0.45	0.465	-	-
	25/75	0.14	0.186	0.7	0.85	0	0.06	0	0.78	0.79	0.71	1	1	0.405	0.406	1.09	0.99
	50/50	0.13	0.178	0.72	0.85	0	0.08	0	0.86	0.53	0.51	0.96	1	0.363	0.386	1.18	1.04
	75/25	0.1	0.162	0.83	0.8	0.065	0.128	1.2	1.23	0.25	0.3	0.58	0.66	0.285	0.306	1.17	1.06
	100/0	0.085	0.143	-	-	0.084	0.143	-	-	0.084	0.143	-	-	0.084	0.143	-	-

Appendix 5: Pretreatment ad substrate characterisation

Table 5A. Quantitative analysis and comparison between compositional analysis[a], S/G ratio[b], crystallinity index[c] and Simons' staining[d] of untreated and treated Eucalyptus samples.

	Untreated	**Sodium chlorite**	**Sodium carbonate**	**Steam explosion**	**Steam explosion + Sodium chlorite**	**Steam explosion + Sodium carbonate**	**Acid**	**Acid + Sodium chlorite**	**Acid + Sodium carbonate**
Chemical Composition[a]									
Klason lignin	24.7 ± 0.7	14.9 ± 2.3	24.2 ± 0.6	47.01 ± 1.7	19.3 ± 1.6	32.9 ± 0.8	36.9 ± 1.9	21.7 ± 0.5	30.4 ± 0.3
Ash	8.1 ± 0.3	6.6 ± 0.2	7.7 ± 0.7	15.6 ± 0.1.5	13.9 ± 0.4	12.1 ± 1.5	6.7 ± 0.3	11.1 ± 0.9	8.9 ± 0.1
Extractives	0.3	0.9	1.7	0.5	0.9	3.7	ND	0.1	0.3
Acid solubilised lignin	4.1 ± 0.2	7.8 ± 0.2	3.9 ± 0.1	1.4 ± 0.1	1.5 ± 0.1	1.5 ± 0.1	3.0 ± 0.1	3.3 ± 0.1	2.1 ± 0.1
Glucose	38.5 ± 1.4	48 ± 2.0	44 ± 2.7	48.9 ± 2.4	67.2±0.1	53.1 ± 1.4	50.7 ± 0.3	62.8 ± 1.2	54.9 ± 1.4
Xylose	10 ± 0.5	12.8 ± 0.5	11.9 ± 0.7	3.7 ± 0.1	1.8 ± 0.1	1.8 ± 0.1	2.6 ± 0.1	1.1 ± 0.1	1.7 ± 0.1
Mannose	0.5 ± 0.1	0.7 ± 0.1	0.6 ± 0.2	ND	ND	ND	0.4 ± 0.1	ND	0.3 ± 0.1
Arabinose	0.8 ± 0.1	0.3 ± 0.1	0.3 ± 0.1	ND	ND	ND	ND	ND	ND

Galactose	1.4 ± 0.1	1.6 ± 0.1	1.5 ± 0.1	0.2 ± 0.1	ND	0.2 ± 0.1	ND	ND	ND
Py-GC/MS[b]									
G Lignin	10.4 ± 1.5	7.4 ± 0.4	12.5 ± 0.2	10.3 ± 0.4	11.1 ± 0.4	12.8 ± 0.2	8.6 ± 1.0	2.9 ± 0.3	7.4 ± 0.5
S Lignin	19.7 ± 2.7	11.6 ± 0.9	30.7 ± 0.5	19.0 ± 0.9	15.5 ± 1.0	21.0 ± 0.6	13.3 ± 1.4	3.3±0.4	11.7 ± 0.1
H Lignin	1.0 ± 0.1	0.7 ± 0.1	1.0 ± 0.1	1.0 ± 0.1	1.4 ± 0.1	1.8 ± 0.1	0.9 ± 0.1	0.5±0.1	0.7 ± 0.1
G/S ratio	1.9 ± 0.1	1.7 ± 0.1	2.4 ± 0.1	1.8 ± 0.1	1.4 ± 0.1	1.6 ± 0.1	1.5 ± 0.1	1.1 ± 0.1	1.6 ± 0.1
XRD[c]									
*Cr*I (%)	74.44	72.77	68.61	77.19	87.85	80.59	77.91	87.85	75.24
Simon's Stain[d]									
Simons' stain (mg/g)	7.50	18.34	15.11	42.70	22.22	32.38	22.41	24.52	24.38

Appendices:

Table 5B. Relative changes in *Eucalyptus* samples after various pretreatment methods by FTIR[a] and NMR[b]

FTIR[a]										
Band Position (cm^{-1})	**Functionality**	**Untreated**	**Sodium chlorite**	**Sodium carbonate**	**Steam explosion**	**Steam explosion + Sodium chlorite**	**Steam explosion + Sodium carbonate**	**Acid**	**Acid + Sodium chlorite**	**Acid + Sodium carbonate**
3000-3600	O-H stretching of alcohols and carboxylic acids (breaking of C-H_2 bonds)	3335.12	3353.24	3328.65	3328.22	3346.62	3328.80	3337.02	3337.59	3335.92
2850-2970	C-H stretching	2909.74	2902.04	2909.74	Wide peak	Wide peak	Wide peak	Wide peak	Wide peak	Wide peak
1700-1750	C=O stretching of acetyl groups in hemicellulose	1733.92	1733.92	1733.92	ND	ND	ND	ND	1716.10	ND
1595	Benzene ring vibration (lignin)	1595.21	ND	1595.44	1597.51	1609.74	1594.55	1595.21	ND	1594.44
1500-1515	Benzene ring vibration (lignin)	1504.35	ND	1504.34	1513.20	1513.20	1504.35	1504.35	ND	1504.35
1460	C-H deformation (methoxyl deformation)	1456.14	ND	1456.14	1456.14	1456.14	1456.14	1456.15	ND	1456.66

1420 -1430	-CH_2 shear vibration in cellulose I	1425.49	ND	1425.49	1424.55	1425.49	1425.49	1425.49	1425.49	1425.49
1300- 1330	Lignin S + G units + OH (C-O stretching + bending OH, antisymmetric stretch vibration of acetyl ester groups)	1316.27	1317.27	1316.27	1316.27	1315.17	1316.64	1317.83	1316.41	1316.69
1218	C-N asymmetric stretching	1218.54	ND	1218.54	1218.54	ND	ND	1222.47	ND	1221.04
1161	C-O-C stretching at β-glycosidic linkages between sugars	1158.00	1159.44	1160	1158.00	1159.34	1159.34	1159.34	1159.34	1159.34
1105	C-O stretch or OH deformation of COOH	1105.55	1105.05	1106.05	1108.55	1106.05	1108.55	1106.05	1102.80	1106.05
1055	Asymmetric and symmetric C-C stretching mode	ND	ND	ND	1052.18	1052.18	1052.18	1052.18	1052.18	1052.18

980-1072	C-O-C deformation of polysaccharides	1029.69	1028.43	1029.69	1017.10	1018.19	1017.25	1017.19	1017.08	1017.31
NMR[b]										
^{13}C chemical shift (ppm)	**Chemical group**	**Untreated**	**Sodium Chlorite**	**Sodium Carbonate**	**Steam explosion**	**Steam explosion + Sodium chlorite**	**Steam explosion + Sodium carbonate**	**Acid**	**Acid + Sodium chlorite**	**Acid + Sodium carbonate**
32.5	Aliphatic lignin carbons not bound to oxygen	ND	ND	ND	Low intensity	Low intensity	Low intensity	Low intensity	ND	Low intensity
56.2	Aryl methoxyl carbons of lignin	56.2	Lower intensity	56.2	56.2	56.2	56.2	56.2	Lower intensity	56.2
62.5	C6 carbon of non-crystalline/amorphous cellulose, C6 carbon of hemicelluloses, $OC\gamma H_2$ carbons of lignin	62.5	Higher intensity	62.5	62.5	62.5	62.5	62.5	Higher intensity	62.5

64.8	C6 carbon of crystalline cellulose	64.8	64.8	ND	64.8	64.8	64.8	64.8	Higher intensity	64.8
72.5	C2, 3, 5 of cellulose, $OC\alpha H_2$ carbons of lignin	72.5	ND	ND	Higher intensity	Higher intensity	Higher intensity	Higher intensity	Higher intensity	Higher intensity
74.4	C2, 3, 5 of cellulose and hemicellulose	74.4	Higher intensity	Higher intensity	74.4	74.4	74.4	74.4	Higher intensity	74.4
83.5	C4 carbon of non-crystalline cellulose and hemicelluloses, $OC\beta H_2$ carbons of lignin	83.5	83.5	83.5	Lower intensity	Lower intensity	Lower intensity	Lower intensity	83.5	Lower intensity
87.9	C4 carbon of crystalline cellulose	87.9	87.9	Very low intensity	Higher intensity	Higher intensity	Higher intensity	Higher intensity	Higher intensity	Higher intensity
101.8	C1 carbon of hemicellulose	ND	ND	ND	ND	ND	ND	ND	ND	ND
105.0	C1 carbon of cellulose	105.0	105.0	Lower intensity	Higher intensity	Higher intensity	Higher intensity	Higher intensity	Higher intensity	Higher intensity
110.0-115.0	C2, 6 aromatic carbons of S lignin and C5,6	110.0-115.0	ND	ND	Higher intensity	Higher intensity	Higher intensity	Higher intensity	ND	Higher intensity

	aromatic carbons in G of lignin									
126.6	C2 of aromatic carbons in G lignin	ND	ND	ND	126.6	126.6	126.6	126.6	126.6	126.6
136.9	C1 and C4 aromatic carbons of S lignin	136.9	ND	136.9	136.9	136.9	136.9	136.9	ND	136.9
148.0	C3, 5 aromatic carbons of S lignin and C1,4 aromatic carbons of G in lignin	143	ND	ND	New peak (47 ppm)	New peak (47 ppm)	New peak (47 ppm)	New peak (47 ppm)	ND	New peak (47 ppm)
153.5	C3, 5 aromatic carbons of S in lignin	153.5	Lower intensity	153.5	Lower intensity	Lower intensity	Lower intensity	Lower intensity	Low intensity	Lower intensity
163.0-180.3	Carboxyl groups of lignin	ND	ND	ND	ND	ND	ND	ND	ND	ND
173.6	Carboxyl groups of hemicelluloses	173.6	173.6	ND	ND	ND	ND	ND	ND	ND

Alcántara *et al.,* 2016; Esteves *et al.,* 2013